UNIVERSITÀ DI PARMA

UNIVERSITA' DEGLI STUDI DI PARMA

DOTTORATO DI RICERCA IN SCIENZE DEL FARMACO, DELLE BIOMOLECOLE
E DEI PRODOTTI PER LA SALUTE
CICLO XXXI

DEVELOPMENT OF POLYSACCHARIDE NANOPARTICLES FOR THE NASAL ADMINISTRATION OF DRUGS FOR THE TREATMENT OF NEURODEGENERATIVE DISEASES

PhD Coordinator:
Chiar.mo Prof. MARCO MOR

PhD Supervisor:
Chiar.mo Prof. FABIO SONVICO

PhD Candidate:
ADRYANA ROCHA CLEMENTINO

Anni 2015/2018

To my parents,
Antonio e Marizulma

Acknowledgments

First and above all, I praise God, for providing me this opportunity and granting me the capacity to proceed successfully. I thank You to make all my dreams, Yours', all my problems Your problem, and all my life Your life. For taking care of me always and forever! *"Até aqui a mão ponderosa do Senhor nos ajudou [...] O que darei a ti Senhor, por todo bem que tens feito a mim?!".*

A special acknowledgment goes to my supervisor, professor Sonvico. I thank you immensely for your prompt availability since our first contact. For your admirable supervision, always giving me the best of your knowledge, attention and support. Thank you for trust on me, to be patient with me, to encourage me and embrace all my projects. Your competence and dedication inspired me. Work with you was a real pleasure.

I dedicate this work to my family, my parents Antonio and Marizulma, for all the love, affection and dedication. For all the sacrifices made to provide me all that I have. Thank you for always believe on me, support me and fight together with me for all my dreams. *Obrigada, papai e mamãe! Vocês são minha inspiração todos os dias. Amo vocês!*

To my sisters, for all you represent in my life! For always being there for me, for been my joy and giving me my best smiles! *Amo vocês!*

Special thanks to professor K. Dev, for kindly receiving me in his lab at Trinity College Dublin, providing me all the support to conclude this work. Also to the professor's Cantù, Dell'Favero and Dr. Pozzoli for their great partnership and constant availability.

To the Brazilian Government and the National Council for Scientific and Technological Development (CNPq) through the program Science without Border for the financial support of this research.

To the Laboratory of Pharmaceutical Technology in the person of professor Bettini, to openly receive me in this lab and provide us all the support in the realization of this work.

To professor Sergio Souza from University of Rio de Janeiro and Gaia Colombo from University of Ferrara for their support with animal experiments.

To all my friends and colleagues from University of Parma, that have been close to me during all this three years. I'll not name you all to avoid committing injustices, but I bring each one of you in my heart and I'm aware that you were an essential support in these years.

I could not forget to say thanks to my colleagues from Trinity to make my stay at Dublin so pleasurable! Thank you Sibylle (Sibelly), Luke, Trisha, Johnny, Kyle, Maria and Kapil. Thank you for making me fell at home!

A special thought to my friends Carol and Maida for sharing with me the life of a Brazilian foreign in Italy. To Gioia and Andrea, for all their care and support over these years.

Finally, a special and affective thanks to Jacopo, for his love, patience, sacrifices, support, encouragement and understanding in all difficulties. For sharing with me my dreams and never give up on us! *“O que será que meu Deus pensava, quando criou você! Acho que ele estava pensando em mim, porque me deu mais do que sonhei”! Amo você!*

Summary

GENERAL INTRODUCTION

1. General Introduction **1**

1.1. Neurodegenerative diseases epidemiology 1

1.2. Alzheimer disease pathogenesis 2

1.3. Simvastatin as potential AD therapeutic approach 3

References **6**

CHAPTER 1

SURFACE-MODIFIED NANOCARRIERS FOR NOSE-TO-BRAIN DELIVERY: FROM BIOADHESION TO TARGETING

Abstract **9**

1. Pharmaceutical Nanotechnologies for Nose-to-Brain Delivery **10**

2. Influence of Physicochemical Properties in Nanoparticles Nose-to-Brain Delivery **15**

3. Mucoadhesive Nanoparticles **20**

4. Beyond Bioadhesion: Mucus Penetrating and Penetration Enhancing Nanocarriers **30**

4.1. Mucus penetrating nanocarriers 30

4.2. Penetration enhancing nanocarriers 32

5. Targeting the Nasal Epithelium for Optimizing the Nose to Brain Delivery **36**

5.1. Lectin-modified nanocarriers 36

5.2. Cell penetrating peptides as surface ligands for targeted nanocarriers 39

5.3. Other targeting approaches 40

6. Future Perspectives of Nose-to-Brain Delivery with Nanocarriers **44**

References **46**

CHAPTER 2

THE NASAL DELIVERY OF NANOENCAPSULATED STATINS – AN APPROACH FOR BRAIN DELIVERY

Abstract **61**

1. Introduction **62**

2. Materials **65**

3. Methods **66**

3.1. Preparation of Simvastatin–Loaded Lecithin/Chitosan Nanoparticles 66

3.2. Physico-Chemical Characterization of Simvastatin–Loaded Lecithin/Chitosan Nanoparticles 66
3.3. Determination of Nanoparticle Structure and Interaction with a Nasal Mucus Model 69
3.4. In Vitro Drug Release from Lecithin/Chitosan Nanocapsules 70
3.5. Cytotoxicity Assay of Lecithin/Chitosan Simvastatin loaded nanoparticles 71
3.6. Gamma Scintigraphy Studies 71
4. Statistics 73
5. Results 74
5.1. Preparation and Physico-Chemical Characterization of Simvastatin Loaded Lecithin/Chitosan Nanoparticles 74
5.2. Nanoparticles Structure and Interaction with a Nasal Mucus Model 79
5.3. Simvastatin Release Studies 84
5.4. Cytotoxicity Studies 85
5.5. Gamma Scintigraphy Studies 87
6. Discussion 88
7. Conclusion 92
References 93

CHAPTER 3
MUCOADHESIVE AND BIODEGRADABLE HYBRID NANOPARTICLES FOR THE NASAL DELIVERY OF STATINS: ENZYME-TRIGGERED RELEASE AND MUCOSAL PERMEATION ENHANCEMENT
Abstract 99
1. Introduction 100
2. Materials 102
3. Methods 103
3.1. Simvastatin-Loaded Lecithin/Chitosan Nanoparticles 103
3.2. Nanoparticles *In Vitro* Drug Release 103
3.3. Nanoparticles Mucoadhesion on Excised Porcine Nasal Epithelium 104
3.4. Simvastatin Permeation Across RPMI2650 Nasal Cells 105
3.5. Simvastatin Transport Across Excised Rabbit Nasal Mucosa 105
4. Statistics 107
5. Results 108

5.1. Simvastatin-Loaded Lecithin/Chitosan Nanoparticles Physico-Chemical Characterization....108
5.2. Drug Release from Simvastatin-Loaded Lecithin/Chitosan Nanoparticles....108
5.3. Nanoparticles Mucoadhesion....111
5.4. Simvastatin *In Vitro* Permeation Across a Cellular Model of Nasal Epithelium....112
5.5. Simvastatin Transport Across Excised Rabbit Nasal Epithelium....114
6. Discussion....116
7. Conclusions....120
References....121

CHAPTER 4
DEVELOPMENT AND VALIDATION OF A RP - HPLC METHOD FOR THE SIMULTANEOUS DETECTION AND QUANTIFICATION OF SIMVASTATIN'S ISOFORMS AND COENZYME Q10 IN LECITHIN/ CHITOSAN NANOPARTICLES
Abstract....125
1. Introduction....126
2. Materials....128
2.1. Materials for Analytical Method Development....128
2.2. Materials for Nanoparticles Production and Characterization....128
2.3. Equipment and Chromatographic Conditions....128
3. Methods....130
3.1. Preparation of Simvastatin Hydroxyacid Isoform....130
3.2. Preparation of Stock and Working Solutions....131
3.3. Method Validation Protocol....131
3.4. Application of the Method....133
4. Statistics....135
5. Results and Discussion....136
5.1. Method Development and Optimization....136
5.2. Validation of the Method....137
5.3. Application of the Method....143
6. Conclusions....147
References....148

CHAPTER 5

HYBRID NANOPARTICLES REGULATE CYTOKYNE RELEASE AND PSYCHOSINE-INDUCED DEATH IN ASTROCYTES AND INHIBIT DEMYELINATION IN ORGANOTYPIC CEREBELLAR SLICES CULTURE

Abstract **150**

1. Introduction **150**

2. Materials and Methods **153**

2.1. Materials for nanoparticles production 153

2.2. Compounds and cell treatments 153

2.3. Nanoparticles preparation and characterization 154

2.4. Primary human astrocytes culture 154

2.5. Cell Viability 155

2.6. Human Astrocytes Immunocytochemistry 155

2.7. Pro-inflammatory IL-6 cytokine release from human astrocytes 156

2.8. Mouse organotypic cerebellar slice culture 157

2.9. Cerebellar Slices Immunocytochemistry 157

3. Statistics **158**

4. Results **159**

4.1. Hybrid lecithin/chitosan nanoparticles co-encapsulation of two potential neuro-protective compounds 159

4.2. Lecithin/chitosan nanoparticles loading simvastatin and coenzyme Q10 organize in a core-shell structure 160

4.3. SVT-CoQ10-LCN nanoparticles cytotoxicity on astrocytes 161

4.4. Effect of SVT/CoQ10 nanoparticles on psychosine-induced human astrocytes 163

4.5. Study of the mechanism by which nanoparticles prevent psychosine-induced astrocytes death 165

4.6. Nanoparticles effects on psychosine-induced changes in astrocytes morphology 166

4.7. Simvastatin and Coenzyme Q10 attenuat TNF-α/IL-17 A-induced release of the pro-inflammatory cytokine IL-6 from astrocytes 171

4.8. SVT/CoQ10-LCN nanoparticles effect on psychosine-induced demyelination in cerebellar slices culture: preliminary results 173

5. Discussion **176**

6. Conclusion **181**

References **182**

GENERAL CONCLUSION **188**

List of Symbols and Acronyms

ε	Epsilon
α	Alpha
β	Beta
ζ	zeta
N2B	Nose-to-brain
AD	Alzheimer Disease
Aβ	Amyloid beta
ApoE ε-4	Apo lipoprotein E allele ε-4
SVT	Simvastatin
SVA	Hydroxyl acid simvastatin isoform
CoQ10	Coenzyme Q10
LCN	Lecithin/ chitosan nanoparticles
Mai	Maisine™ 35-1: Glycerol/ glyceryl monolinoleate
Lab	Labrafac™ Lipophile WL 1349: Medium chain triglyceride
CapI	Capryol™ PGMC: Propylene glycol monocaprylate type I
CapII	Capryol™ 90: Propylene glycol monocaprylate type II
DLS	Dianamic light scattering
PALS	Phase analysis light scattering
D	Diameter
PDI	Polidispesity index
ζ Potential	Zeta Potential
NTA	Nanoparticles tracking analysis
STEM	Scanning transmission electron microscopy
SAXS	Small angle x-ray scattering
SANS	Small angle neuntron scattering
X g	Gravitational force
RPM	Rotations per minute
SNES	Simulated nasal electrolyte solution
BSA	Bovin serum albumin
LYS	Lysozyme

PLA2	Phospholipase A2
FBS	Fetal bovine serum
RPMI2650	Human nasal epithelial cell line
HPLC	High performance liquid chromatography
UV-vis	Ultraviolet - visible
RP	Reverse phase
EE%	Encapsulation efficiency in pecentual
DAE%	Drug association efficiency
RSD	Residual standard deviation
SD	Standard deviation
DAPI	4′,6-Diamidine-2′-phenylindole dihydrochloride
VMT	Vimentin
GFAP	Glyal fibrillary acidic protein
MBP	Myelin basic protein
TNF-α	Tumor necrosis factor alpha
IL-6	Interleukin 6
hIL-17	Human Interleukin 17
PSY	Psychosine

List of Figures

Chapter 1

FIGURE 1: (A) NASAL INNERVATION; (B) NOSE-TO-BRAIN PATHWAYS OF DRUG DELIVERY……12

FIGURE 2: DYNAMICS OF ALEXA-DEXTRAN IN BRAIN TISSUE FOLLOWING NASAL ADMINISTRATION OF HYDROPHOBIC (STR-CH2R4H2C) AND HYDROPHILIC (MPEG-PCL CH2R4H2C) SURFACE NANOCARRIERS.....19

FIGURE 3: SURFACE CHEMISTRY OF NANOPARTICLES AFFECTING MUCOADHESION……..……..22

FIGURE 4: FRACTION OF TOTAL RADIOACTIVITY RECOVERED PER ORGAN 90 MINUTES AFTER THE NASAL ADMINISTRATION IN RATS OF (A) ^{99M}TC-LABELED SIMVASTATIN-LOADED NANOPARTICLES; (B) ^{99M}TC-LABELED SIMVASTATIN SUSPENSION……..……..28

FIGURE 5: MAJOR MECHANISMS HINDERING PARTICLES FROM DIFFUSE THROUGH MUCUS……...30

FIGURE 6: DISTRIBUTION OF WGA-CONJUGATED QUANTUM DOTS-LOADED NANOPARTICLES IN VARIOUS ORGANS FOLLOWING INTRANASAL ADMINISTRATION 3 H AFTER DOSING…….....38

Chapter 2

FIGURE 1: PARTICLE SIZE DISTRIBUTION VS NANOPARTICLES CONCENTRATION AND INTENSITY OF SCATTERED LIGHT OBTAINED BY NTA……..77

FIGURE 2: STEM IMAGES……....79

FIGURE 3: SAXS INTENSITY SPECTRA OF LCN (BLACK LINE), LCN_MAILAB (BLUE LINE) AND SVT-LCN_MAILAB (RED LINE) NANOPARTICLES……..……80

FIGURE 4: SAXS INTENSITY SPECTRA OF SVT-LCN_MAILAB NANOPARTICLES DISPERSED IN ARTIFICIAL MUCUS……..82

FIGURE 5: SVT-LCN_MAILAB NANOPARTICLES INTERACTION WITH MUCUS PLUS LYSOZYME……..….83

FIGURE 6: SIMVASTATIN RELEASE PROFILE FROM SVT-LCN_MAILAB NANOPARTICLES (●) AND A CONTROL SIMVASTATIN SUSPENSION (○) IN SIMULATED NASAL FLUID WITH BSA 0.5% AT PH 6.5 AND 37°C……85

FIGURE 7: *IN VITRO* CYTOXICITY STUDIES ON HUMAN NASAL CELL LINE RPMI 2650 OF SIMVASTATIN (▲), SIMVASTATIN-LOADED NANOPARTICLES SVT-LCN_MAILAB (●), AND BLANK NANOPARTICLES LCN_MAILAB (○)……86

FIGURE 8: RADIOACTIVITY BIODISTRIBUTION IN WISTAR RATS 90 MINUTES AFTER THE NASAL INSTILLATION OF 20 µL (10 UL IN EACH NOSTRIL) OF ^{99M}TC LABELED SIMVASTATIN-LOADED NANOPARTICLES AND SIMVASTATIN SUSPENSION EXPRESSED AS PERCENTAGE OF THE DOSE PER ORGAN…….....87

Chapter 3

FIGURE 1: SIMVASTATIN SUSPENSION AND SVT-LCN NANOPARTICLES DRUG RELEASE IN SIMULATED NASAL ELECTROLYTE SOLUTION ……..……109

FIGURE 2: SVT-LCN NANOPARTICLES RELEASE IN SIMULATED NASAL ELECTROLYTE SOLUTION (SNES) PH 6.5, WITHOUT ENZYMES (●, SVT-LCN/SNES), WITH LYSOZYME (◆,SVT-LCN/LYS 0.5MG/ML) AND WITH LYSOZYME AND PHOSPHOLIPASE A2 (▲, SVT-LCN/LYS 0.5 MG/ML + PLA2 0.6 µG/ML) ....……110

FIGURE 3: SVT-LCN NANOPARTICLES RELEASE IN SOLO SNES (●, SVT-LCN/SNES), IN SIMULATED NASAL MUCUS (SNES PLUS PORCINE STOMACH MUCIN TYPE II AT 1%) (■, SVT-LCN/MUCUS 1%) AND IN SIMULATED NASAL MUCUS CONTAINING LYSOZYME AND PLA2 (▲, SVT-LCN/MUCUS 1% + LYS/PLA2). 111

FIGURE 4: *IN VITRO* MUCOADHESION OF SIMVASTATIN SUSPENSION (O) AND SIMVASTATIN-LOADED NANOPARTICLES (●, SVT-LCN). THE MUCOADHESION WAS EXPRESSED AS PERCENTAGE OF DRUG RETAINED ON THE MUCOSA AGAINST TIME .....……...……112

FIGURE 5: SIMVASTATIN TRANSPORT THROUGH RPMI2650 NASAL CELLS AFTER DEPOSITION OF SIMVASTATIN-SUSPENSION AND SIMVASTATIN-LOADED NANOPARTICLES, SVT-LCN.....113

FIGURE 6: DISTRIBUTION OF SIMVASTATIN RECOVERED AFTER TRANSPORT STUDIES OF SIMVASTATIN SUSPENSION AND LOADED INTO NANOPARTICLES (4H) ACROSS THE NASAL CELLS RPMI 2650 EPITHELIUM MODEL…….. 114

FIGURE 7: PROFILES OF SIMVASTATIN TRANSPORT ACROSS THE NASAL EPITHELIUM OF RABBIT OBTAINED FOR LOADED-NANOPARTICLES AND SIMVASTATIN SUSPENSION……115

Chapter 4

FIGURE 1: HPLC-UV CHROMATOGRAM OVERLAY OF STANDARD DILUENT (PINK LINE) AND HYDROXYL ACID SIMVASTATIN (SVA, BLUE LINE) AFTER SIMVASTATIN (SVT- LACTONE) HYDROLYSIS……...130

FIGURE 2: HPLC-UV CHROMATOGRAM SEPARATION OF 25 µG/ML STANDARD SOLUTION OF SVA, SVT (λ = 238) AND COQ10 (λ = 275)……137

FIGURE 3: CHROMATOGRAMS OVERLAY OF SVT/COQ10-NCL QUANTIFICATION (PINK LINE) AND STANDARD SOLUTION OF SVA, SVT AND COQ10 AT 25 µG/ML (BLUE LINE)……...145

Chapter 5

FIGURE 1: SANS INTENSITY SPECTRA OF SVT-LCN (BLACK LINE) AND SVT/COQ10-LCN (ORANGE LINE) NANOPARTICLES……...161

FIGURE 2: PSYCHOSINE-INDUCED CELL TOXICITY IN A DOSE-DEPENDED MANNER……...162

FIGURE 3: NANOPARTICLES ATTENUATE PSYCHOSINE-MEDIATED ASTROCYTES CELL DEATH……..164

FIGURE 4: NANOPARTICLES STRUCTURE IS INVOLVED ON THE REDUCTION OF PSYCHOSINE-MEDIATED ASTROCYTES CELL DEATH……165

FIGURE 5: PSYCHOSINE-INDUCED CHANGES IN VIMENTIN FROM HUMAN ASTROCYTES……168

FIGURE 6: PSYCHOSINE-INDUCED DECREASE IN VIMENTIN MARKER IN HUMAN ASTROCYTES IS PREVENTED BY SVT/COQ10 NANOPARTICLES……170

FIGURE 7: TNF-α AND IL-17 A INCREASES THE LEVEL OF IL-6 SECRETION IN HUMAN ASTROCYTES……. 172
FIGURE 8: TNF-α AND IL-17-INDUCED IL-6 SECRETION IN HUMAN ASTROCYTES IS ATTENUATED BY UNLOADED AND NANOPARTICLES-LOADED COMPOUNDS ……..173
FIGURE 9: SVT/COQ10-LCN NANOPARTICLES INHIBITS PSYCHOSINE-INDUCED DEMYELINATION ON CEREBELLAR SLICES……175

List of Tables

Chapter 1

TABLE 1: MUCOADHESIVE NANOCARRIERS STUDIES FOR NOSE-TO-BRAIN DELIVERY 29
TABLE 2: MUCUS-PENETRATING AND PENETRATION-ENHANCING NANOCARRIERS STUDIED FOR NOSE-TO-BRAIN DELIVERY. 35
TABLE 3: TARGETED NANOCARRIERS STUDIED FOR NOSE-TO-BRAIN DELIVERY 43

Chapter 2

TABLE 1: SIMVASTATIN-LOADED NANOPARTICLES PHYSICOCHEMICAL PROPERTIES AND ENCAPSULATION EFFICIENCY (N= 9 ± SD) 75
TABLE 2: PHYSICAL AND CHEMICAL STABILITY STUDY AT ROOM TEMPERATURE OF SIMVASTATIN-LOADED NANOPARTICLES (SVT-LCN_MAILAB)..... 76

Chapter 4

TABLE 1: CHROMATOGRAPHIC CONDITIONS OF MOBILE PHASE OF ANALYTICAL METHOD 129
TABLE 2: CHROMATOGRAPHIC PARAMETERS OF SYSTEM SUITABILITY 138
TABLE 3: LINEARITY OF THE SIX CONCENTRATION LEVELS OF SVA, SVT AND COQ10: LINEAR REGRESSIONS ARE Y = MX + Q. 139
TABLE 4: REPEATABILITY AND INTERMEDIATE PRECISION OF SVA, SVT AND COQ10 141
TABLE 5: RESOLUTION AND RECOVERY OF SVA, SVT AND COQ10 FOR EVALUATION OF METHOD ROBUSTNESS..... 142
TABLE 6: ACCURACY: RECOVERY AND RSD OF SVA, SVT AND COQ10 FROM SPIKED BLANK NANOPARTICLES. 143
TABLE 7: NANOPARTICLES QUANTIFICATION: DRUGS ASSOCIATION EFFICIENCY (AE%) AND ENCAPSULATION EFFICIENCY (EE%) 144

Chapter 5

TABLE 1: SIMVASTATIN/COENZYME Q10-LOADED NANOPARTICLES PHYSICOCHEMICAL PROPERTIES AND ENCAPSULATION EFFICIENCY (N= 6 ± SD)..... 160

GENERAL INTRODUCTION

1 General Introduction

1.1 Neurodegenerative Diseases Epidemiology

Dementias and others cognitive decline related diseases represent an enormous and growing burden on healthcare systems and economy. The World Health Organization (WHO) indicates that 50 million people currently suffer from dementia all over the world and anticipates that the number of affected patients could triple by 2050.[1] WHO also evidenced that in the last 20 years, the number of deaths related to neurodegenerative diseases increased by 114%, with 1.2 millions of notifications in 2015, attaining the seventh position among the top 10 leading causes of death worldwide. Moreover, it is estimated that the global impact of dementia on the economy will be 1 trillion dollars in 2018 and will rise to 2 trillion by 2030.

The increase in dementia prevalence is largely linked to the exponential increase of age-related neurodegenerative diseases such as Alzheimer's disease (AD), Parkinson's disease (PD) and amyotrophic lateral sclerosis (ALS). Together with the progressive growth of population life expectancy, the prevalence of these diseases has increased dramatically. However, the epidemiology, clinical signs and symptoms, laboratorial analysis, neuropathology and management differ greatly among these diseases.[2]

Alzheimer's disease is reported to be the major and most common cause of dementia accounting for 70% of the cases and affecting around 25 million people over the world.[3] The incidence rate of AD is close to 30% among people 85 years old. Risks increase steeply based on age, increasing from 0.5% in individuals between 65-69 years old to 6-8% for those 85 years' age and older.[2,4] Early onset AD is the most severe form of Alzheimer's disease and occurs in individuals younger than 65 years, although it is rare and generally comprise familial cases accounting for approximately 5-10% of total AD cases. AD incidence is generally higher in women and its clinical manifestation involves alterations in mood and behaviour, followed by memory loss, disorientation and aphasia in the late stage of the disease.[5] Great efforts have been made to elucidate more accurately AD physiopathogenesis. However, despite several hypotheses, the causes of AD are still unclear, and pathogenesis appear multifactorial. The identification of valid therapeutic targets is a high priority for the life sciences researchers to develop new strategies to better manage or cure this frightening disease.

1.2 Alzheimer Disease Pathogenesis

Alzheimer diseases is a progressive multifactorial neurodegenerative disorder involving several aetiopathogenic mechanisms. Since the discovery of AD, two principal hallmarks related to the disease have been: I) the extracellular deposits of amyloid-β (Aβ) in the form of senile plaques and II) the intracellular inclusions of hyperphosphorylated tau proteins in the form of neurofibrillary tangles (NFT).[6] For the last two decades, the amyloid cascade hypothesis, i.e., an impaired balance on Aβ clearance and/or production, has been the most commonly investigated cause of early onset of AD development. However, it is not completely clear whether this event can be etiologically extrapolated as the trigger of late-onset AD, the most prevalent form of the disease.[7] Moreover, although Aβ imbalance is a histopathological feature often present on AD, it is not the exclusive factor causing the disease development. The search upon mechanisms potentially involved in AD aetiology and providing alternative viewpoints beyond the amyloid cascade hypothesis is currently in the focus of the scientific community.

Altered cholesterol metabolism has been proposed as a key event in the pathogenesis of late onset Alzheimer.[8,9] Alterations in cholesterol homeostasis are linked to an imbalance between Aβ production/clearance and to a hyperphosphorylation of tau-protein. The cholesterol hypothesis is based upon several findings. The first important one was the discovery of a genetic variation in the major cholesterol transporter, i.e., apolipoprotein E allele ε-4 (ApoE ε-4), widely recognised a strong risk factor for the development of late-onset AD.[10] Indeed, ApoE transports cholesterol and other lipid components from astrocytes to the neurons to ensure neuronal metabolism, growth, repair and synaptogenesis. According to several studies the defective ApoE protein expressed by the ε-4 allele, which is regarded as the Aβ's chaperone, promotes the conversion of Aβ structure from an α helix to a β-pleated sheet folding. Furthermore, alterations in the intracellular trafficking and localization of amyloid protein precursor (APP) directly impacts on its processing to Aβ peptide. It has been suggested that the production of Aβ, through the proteolytic cleaving of APP could occur in the endocytic pathway.[11] A deep insight in the amyloidogenic pathway evidenced that APP trafficking is greatly affected by the cellular levels of cholesterol in neurons and astrocytes. Indeed, several findings indicate the connection of ApoE ε-4 allele in the stimulation of APP endocytosis, resulting in an increased processing in Aβ generation.[8]

Furthermore, the generation of free radicals with consequent oxidative damage and activation of inflammatory processes, associated with a severe immune response, have also

been evidenced during the development and progression of the late onset AD.[12] Recent preclinical studies observed that immune activation of glial and astrocytes cells not only accompanies AD pathologies, but also contributes to trigger the pathogenesis. Moreover, it has been postulated that immune processes may drive AD pathology independently from Aβ deposition, but sustaining increased levels of Aβ peptide could lead to the exacerbation of Alzheimer pathology and the establishment of a vicious cycle.[13] The strategy of reducing neuro-inflammation has attracted interest as an alternative therapeutic approach to tackle AD.

The five drugs currently available on the market, i.e. memantine, donepezil, rivastigmine, galantamine and tacrine offer only modest symptomatic benefits and do not have disease modifying effects. Despite the significant progresses in AD research, currently no effective treatment is available. As a matter of fact, the focus on the search for a single molecule able to manage all the various pathological aspects of the disease appears to be a major drawback in the development of an efficient AD therapy.[15]

1.3 Simvastatin as Potential AD Therapeutic Approach

Statins, 3-hydroxy-3-methylglutaryl coenzyme A (HMG-CoA) reductase inhibitors are the drugs of election to reduce cholesterol levels. From the statins currently available in the market, simvastatin results as the second most efficient to reduce blood cholesterol levels among the lipophilic group, i.e., atorvastatin > pravastatin > lovastatin > fluvastatin, but appears to be the most tolerable and safest.[16] Recently, the use of statins as a disease-modifying strategy in AD has elicited substantial interest. As aforementioned, the inhibition of brain cholesterol synthesis has been shown to reduce beta amyloid accumulation, interfering with the production of beta amyloid and its accumulation as extracellular plaques.[10] Moreover, parallel studies in large cohorts of patients reported a significant decrease in dementia incidence associated with patients under statins treatment.[17] However, early clinical studies in which simvastatin was administered orally to patients affected by Alzheimer' disease failed to show any significant improvement in cognitive memory or to delay the disease progression.[18] However, it is important to clarify that when administered orally, simvastatin is heavily submitted to hepatic metabolism and its hydrophilic metabolites are prevented from crossing the blood brain barrier (BBB). Since brain cholesterol is produced locally and in minimal quantities, it is likely that effects observed at the central nervous system (CNS) for orally administered simvastatin are poor, also due a lack in the

drug access to the cerebral parenchyma.

Nowadays, clinical evidences have suggested that some cholesterol-independent pleiotropic effects of statins are at play beyond the lipid-lowering actions. Pleiotropic effects of statins have been justified by the inhibition of the biosynthesis of isoprenoids intermediates (Rho, Ras, Rac, Rap and Ral) through the blocking the mevalonate pathway.[19] Thus, considering that isoprenoids affect a large variety of cellular processes and cellular functions, the reduction in protein isoprenylation due to statins could have a relevant number of beneficial effects. Indeed, many studies have shown the anti-inflammatory, antioxidant and immunomodulatory effects associated to simvastatin.

The multiple actions of simvastatin in the brain obtained through both cholesterol-dependent and cholesterol-independent pathways, could work synergistically against AD pathogenesis. Despite this clear potential, pleiotropic effects of statins have been generally associated with high drug dosing. This limitation appears as a direct consequence of the pharmacokinetics obtained after statins oral administration. In fact, the attainment of therapeutically relevant statin concentrations in the CNS after oral delivery appears very challenging.

The adoption of the two innovative strategies, i.e., the use of a novel and more efficient dosage form able to deliver simvastatin to the CNS and the exploitation of nose-to-brain transport to bypass the blood-brain barrier, could represents a winning approach to improve brain bioavailability of statins.

Thus, the overall scope of this thesis was the development of a nanoparticulate system suitable for the nasal delivery of simvastatin. For this purpose, hybrid nanoparticles composed of biodegradable materials, such as naturals polysaccharide and phospholipids, were designed to obtain: a) elevated simvastatin encapsulation efficiency; b) optimal physico-chemical properties able to promote simvastatin transport across nasal mucosa; c) increased brain bioavailability of simvastatin and d) biosafety, i.e. minimal or absent toxicity. Moreover, the preliminary investigation of potential therapeutic actions of the developed simvastatin-loaded nanoparticles formulation represent another key objective of this work.

In the first chapter of this thesis, nanomedicines designed for nose-to-brain delivery are discussed and critically evaluated in a detailed review.

The following chapters describe the experimental work carried out, and include:

- Development and characterization of simvastatin-loaded nanoparticles as a platform for nose-to-brain delivery of lipophilic statins.

- *In vitro* evaluation of simvastatin-loaded nanoparticles biopharmaceutical properties, including: *in vitro* drug release, nanoparticles interaction with simulated nasal mucus and physiological enzymes along with nanoparticles-mediated simvastatin enhanced permeability and transport across nasal epithelium models.

- Preliminary evaluation of simvastatin-loaded nanoparticles *in vivo* biodistribution following nasal administration.

- Preliminary *in vitro* and *ex vivo* investigation of loaded-nanoparticles pharmacological activity using a multimodal model of neurodegenerative processes involving human glial cells and mice brain tissue. In these experiments, the benefits from the co-encapsulation of simvastatin with another potential neuroprotective molecule, i.e., coenzyme Q10 was explored as well.

References

1. WHO. Towards a dementia plan: a WHO guide. (2018).

2. Erkkinen, M. G., Kim, M. O. & Geschwind, M. D. Clinical neurology and epidemiology of the major neurodegenerative diseases. Cold Spring Harb. Perspect. Biol. **10,** (2018).

3. WHO. WHO | Dementia: a public health priority. WHO (2012).

4. Mayeux, R. & Stern, Y. Epidemiology of Alzheimer disease. Cold Spring Harb. Perspect. Med. **2,** 1–18 (2012).

5. Ferri, C. P. et al. Global prevalence of dementia: A Delphi consensus study. Lancet **366,** 2112–2117 (2005).

6. Citron, M. Alzheimer's disease: Strategies for disease modification. Nature Reviews Drug Discovery **9,** 387–398 (2010).

7. Swerdlow, R. H. Pathogenesis of Alzheimer's disease. Clin. Interv. Aging **2,** 347–359 (2007).

8. Martins, I. J. et al. Cholesterol metabolism and transport in the pathogenesis of Alzheimer's disease. Journal of Neurochemistry **111,** 1275–1308 (2009).

9. Puglielli, L., Tanzi, R. E. & Kovacs, D. M. Alzheimer's disease: The cholesterol connection. Nature Neuroscience **6,** 345–351 (2003).

10. Bu, G. Apolipoprotein e and its receptors in Alzheimer's disease: Pathways, pathogenesis and therapy. Nature Reviews Neuroscience **10,** 333–344 (2009).

11. Marzolo, M. P. & Bu, G. Lipoprotein receptors and cholesterol in APP trafficking and proteolytic processing, implications for Alzheimer's disease. Seminars in Cell and Developmental Biology **20,** 191–200 (2009).

12. McGeer, P. L. & McGeer, E. G. NSAIDs and Alzheimer disease: Epidemiological, animal model and clinical studies. Neurobiology of Aging **28,** 639–647 (2007).

13. Heppner, F. L., Ransohoff, R. M. & Becher, B. Immune attack: The role of inflammation in Alzheimer disease. Nature Reviews Neuroscience **16,** 358–372 (2015).

14. Thambisetty, M. et al. Effect of complement CR1 on brain amyloid burden during aging and its modification by APOE genotype. Biol. Psychiatry **73,** 422–428 (2013).

15. De La Herrán-Arita, A. K. & García-García, F. Current and emerging options for the drug treatment of narcolepsy. Drugs **73,** 1771–1781 (2013).

16. Davies, J. T. et al. Current and emerging uses of statins in clinical therapeutics: A review. Lipid Insights **9,** 13–29 (2016).

17. Wolozin, B. Cholesterol and the Biology of Alzheimer's Disease. Neuron **41,** 7–10 (2004).

18. Sabbagh, M. n. & Sparks, d. L. Statins to treat Alzheimer's disease: An incomplete story. Expert Rev. Neurother. **12,** 27–30 (2012).

19. Sonvico, F., Zimetti, F., Pohlmann, A. R. & Guterres, S. S. Drug delivery to the brain: how can nanoencapsulated statins be used in the clinic? Ther. Deliv. **8,** 625–631 (2017).

CHAPTER 1

SURFACE-MODIFIED NANOCARRIERS FOR NOSE-TO BRAIN DELIVERY: FROM BIOADHESION TO TARGETING

Surface-Modified Nanocarriers for Nose-to-Brain Delivery: from Bioadhesion to Targeting

F. Sonvico[1,2], A. Clementino[1,2], F. Buttini[1,2], G. Colombo[3], S. Pescina[2], S. Guterres[4,5], A. Raffin Pohlmann[4,5], S. Nicoli [1,2]

[1] Interdipartmental Center for Innovation in Health Products, BIOPHARMANET TEC, University of Parma, Italy

[2] Food and Drug Department, University of Parma, Italy

[3] Department of Life Sciences and Biotechnology, University of Ferrara, Italy

[4] Programa de Pós-Graduação em Ciências Farmacêuticas, Universidade Federal do Rio Grande do Sul, Porto Alegre, Brazil

[5] Departamento de Química Orgânica, Instituto de Química, Universidade Federal do Rio Grande do Sul, Porto Alegre, Brazil

Published on March 2018, ***Pharmaceutics*** special issue

IF 3.7

Open access

Abstract

In the field of nasal delivery, one of the most fascinating applications is the delivery of drugs directly to the central nervous system avoiding the blood brain barrier. This approach would provide a series of benefits, such as the reduction of doses and the localization of potent drugs reducing their systemic side effects. Recently, clinical trials have been explored the nasal administration of insulin for the treatment of Alzheimer's disease, with promising results. The use of nanomedicines could provide further options for making nose-to-brain delivery reality. Apart from the selection of devices able for the deposition of the formulation in the upper part of the nose, the surface modification of these nanomedicines appears to constitute the key to optimize the delivery of drugs from the nasal cavity to the brain. In this review, the use in the design of nanomedicines of several approaches such as: surface electrostatic charges, mucoadhesive polymers, as well as targeting moieties directed towards specific proteins on the surface of nasal epithelial cells will be reported and critically evaluated for nose-to-brain delivery.

Keywords: Alzheimer's disease; CNS disorders; Parkinson's disease; mucoadhesion; mucus-penetrating particles; nanoparticles; neurodegenerative diseases; nose-to-brain delivery; pharmaceutical nanotechnology; targeting

1 Pharmaceutical Nanotechnologies for Nose-to-Brain Delivery

Among routes of drug administration that may represent an alternative to parenteral and oral administration, nasal delivery has without doubt received less attention compared to other administration routes such as pulmonary or transdermal delivery. Conventionally, nasal drug administration has been often associated to the treatment of minor local ailments such as rhinorrhea, nasal congestion, nasal infections and allergic or chronic rhinosinusitis[1]. However, nasal delivery shows a high number of clear advantages, such as ease of administration, non-invasiveness, good patient compliance, rapid onset of action, relatively large and permeable absorption surface, reduced enzymatic activity and avoidance of hepatic first-pass metabolism. Therefore, an increasing number of products exploiting the nose as site of administration for the systemic delivery of small and large molecules (including peptides, proteins and vaccines) are being developed and are reaching the market. That make nasal delivery one of the most versatile routes of administration with applications going from smoke cessation (nicotine, Nicotrol® NS, Pfizer, USA) to flu vaccination (live attenuated influenza vaccine, FluMist® Quadrivalent, Astra Zeneca, USA) from pain management (fentanyl, Intstanyl®, Takeda, Japan and Pecfent/Lazanda®, Archimedes Pharma Ltd., UK; butorphanol tartrate spray, Mylan Inc., USA) to postmenopausal ostheoporosis (salmon calcitonin, Fortical®, Upsher-Smith, USA) from the treatment of migrane (zolmitriptan, Zomig®, AstraZeneca, UK; sumatriptan, Imigran, GSK, UK and Onzetra™ Xsail™, Avanir Pharmaceuticals, USA) to that of endometriosis (nafarelin, Synarel®, Pfizer, USA) or prostate cancer (buserelin, Suprecur®, Sanofi-Aventis, France)[2].

Seemingly, however, the best is yet to come, as the nasal cavity offers a unique opportunity for the delivery of pharmaceutically active drugs to the central nervous system (CNS). Considering the increasing incidence of brain diseases associated with the aging population, achieving efficient drug delivery to the brain is one of the priorities of modern pharmaceutical sciences. However, brain delivery of drugs is a complex challenge, as CNS is protected by the blood brain barrier (BBB) and blood cerebrospinal fluid barrier (BCSFB), two formidable structures providing a selective brain permeability to circulating molecules. These physical, metabolic and transporter-regulated barriers tremendously limit the number of pharmacologically active substances able to gain access the CNS at therapeutic viable concentrations [3]. Several approaches have been proposed to improve brain delivery across BBB [3,4], including nanoparticulate drug carriers targeting specific transporters present on the BBB [5-7]. Unfortunately, the percentage of injected drug dose reaching the brain even with

BBB targeting or permeation enhancing strategies is below 5 %, typically less than 1%, with a 95-99% of the drug off-target and potentially responsible for systemic side effects. Furthermore, in the case of nanocarriers, the CNS chronic toxicity and immunogenicity of polymers, surfactants and other components has to be carefully evaluated, especially considering the prolonged treatments required for the notoriously difficult to treat CNS diseases [8].

An increasing number of studies suggest that intranasal drug delivery allows for brain delivery of both small and large molecules bypassing the BBB via the nerves present in the nasal cavity, i.e. the olfactory and trigeminal nerves. Particularly, the olfactory 'neuroepithelium', present exclusively in the nasal cavity, is the only part of the CNS that is in direct contact with the external environment and as a consequence a unique access port to the brain [9]. On the other side the trigeminal nerve has been demonstrated to be significantly involved in the nose-to-brain (N2B) delivery of certain substances, especially towards the posterior region of the brain [10,11]. As a consequence, drugs can reach the CNS following nasal administration via three main pathways, namely: A) the olfactory nerve pathway, which innervates the olfactory epithelium of the nasal mucosa and terminates in the olfactory bulb, B) the trigeminal nerve pathway, which innervates, through its ophthalmic and maxillary branches, both the respiratory and (to a lesser degree) the olfactory epithelium and terminates in the brainstem and olfactory bulb, respectively and C) the vascular pathway. Of these, the olfactory and trigeminal nerve pathways provide brain delivery either via a slow intracellular axonal transport (hours or even days) or fast perineural paracellular transport (minutes) from the sub-mucosal space to the cerebrospinal fluid (CSF) compartment [12,13]. The vascular pathway provides a secondary, indirect mechanism of delivery, whereby the drug is firstly absorbed into systemic circulation and subsequently transported to the brain across the BBB[14]. Figure 1 outlines the nasal innervation and the three brain-targeting pathways of nasal delivery.

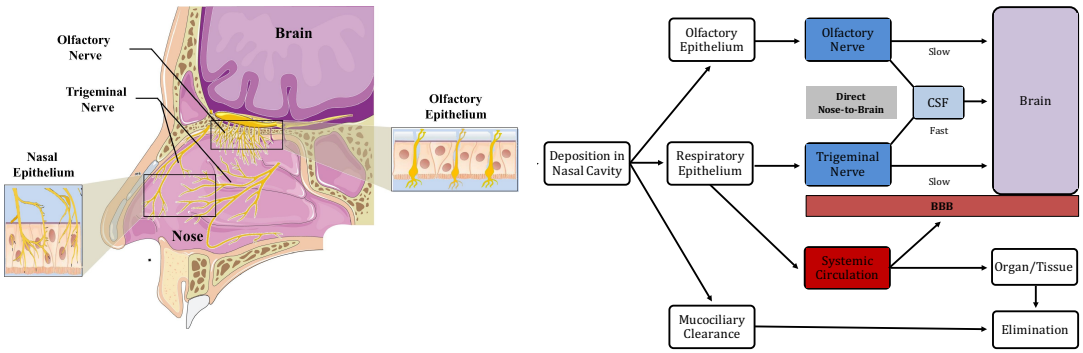

(a) **(b)**

Figure 1: (a**)** Nasal innervation; (b) Nose-to-brain pathways of drug delivery (modified from [15] and [16]).

Hence, nasal delivery has been proposed for the treatment of multiple central nervous system conditions, such as migraine [17], sleep disorders [18], viral infections [19], brain tumors [20,21], multiple sclerosis (MS) [22], schizophrenia [23], Parkinson's (PD) [24], Alzheimer's disease (AD) [25] and even for the treatment of obesity [26]. However, several limitations, such as small nasal cavity volume, limited amount of formulation that can be administered, poor olfactory region deposition from conventional nasal devices, short mucosal contact time due to the mucociliary clearance, poor bioavailability of hydrophilic and/or large molecules, mucosal irritation and lack of validated translational animal models [27], may affect the potential of the nose-to-brain transport, to the point that some authors around the mid 2000's doubted whether such approach could be exploited therapeutically in humans [28,29].

Since then, a number of nasal devices specifically able to deposit nasal formulation in the olfactory region of the nasal cavity, such as ViaNase atomizer (Kurve Technologies, USA), pressurized Precision Olfactory Device (Impel Neuropharma, USA) and the liquid and powder Exhalation Delivery Systems (OptiNose, USA), have been designed and are now available for new medicinal products development [30]. Preclinical studies in animals increasingly use specific indexes to quantify the efficiency of brain delivery following administration, such as nose-to-brain drug targeting efficiency (DTE, Equation 1) and direct transport percentage (DTP, Equation 2) [31]. Drug targeting efficiency index provides the exposure of the brain to the drug after nasal administration relative to that obtained by systemic administration:

$$DTE = \frac{\left({AUC_{Brain}}/{AUC_{Blood}}\right)_{IN}}{\left({AUC_{Brain}}/{AUC_{Blood}}\right)_{IV}} \cdot 100, \quad 1)$$

where AUC_{Brain} and AUC_{Blood} are the area under the concentration *vs.* time curves of the drug in the brain and in the circulation (blood, plasma or serum) after intranasal (IN) and intravenous (IV) administration. DTE values can range from 0 to + ∞, with values above 100% representing a more efficient brain targeting after IN administration, while those below 100% after IV administration. Direct transport percentage index calculates the estimated fraction of the dose reaching the brain via direct nose-to-brain pathways over the cumulative amount of drug reaching the brain after intranasal delivery:

$$DTP = \frac{B_{IN} - B_x}{B_{IN}} \cdot 100, \quad 2)$$

where B_{IN} is the brain AUC following intranasal administration, while B_x is the fraction of the same AUC due to the drug crossing the BBB from systemic circulation calculated according to Equation 3:

$$B_x = \frac{B_{IV}}{P_{IV}} \cdot P_{IN}, \quad 3)$$

where P_{IN} and P_{IV} are the blood AUC after intranasal and intravenous administration, respectively. DTP positive values up to 100 indicate a contribution of the direct nose-to-brain pathways to brain drug levels, while DTP equal to 0 (or even negative) indicate a preferential brain accumulation after IV administration of the drug. This quantitative preclinical pharmacokinetics data associated with pharmacodynamics results allows for the creation of advanced translational PK am PK-PD models able to predict CNS concentrations in humans[32].

Furthermore, some clinical trials on the brain delivery in humans of nasally delivered drugs, such as insulin for the treatment of Alzheimer's disease [33,34], oxytocin for autism [35], schizophrenia and major depressive disorder [36] and davunetide for mild cognitive impairment [37,38] and progressive supranuclear palsy [39], clearly demonstrate that the N2B delivery is by now considered a viable and promising clinical approach by several pharmaceutical companies [40].

Despite all these advancements, the delivery of drugs presenting unfavorable physico-chemical and biopharmaceutical characteristics such as rapid chemical or enzymatic degradation, poor solubility, low permeability and low potency requires a formulation able to promote the mechanisms of transport of the drug to the brain, without disrupting the structure and physiologic function of the nasal epithelium.

Pharmaceutical nanotechnologies appear as an ideal formulative strategy for the N2B delivery of these "problematic" substances, including peptide and proteins. In fact, nano-sized (1-1000 nm) drug delivery systems can:

- Protect the encapsulated drug from biological and/or chemical degradation;
- Increase apparent drug water-solubility;
- Enhance residence time at the site of absorption;
- Promote mucosal permeation and/or cellular internalization;
- Control the release kinetics of the encapsulated drug;
- Achieve targeted drug delivery through surface modification with specific ligands;
- Reduce drug distribution to non-target sites, minimizing systemic side effects.

All these features appear desirable for an efficient N2B delivery and are potentially critical to enable the therapeutic application of drugs that without a proper carrier would be unable to reach the CNS at concentrations sufficient to elicit a pharmacological response.

Therefore, almost all types of pharmaceutical nanocarriers have been studied for nose-to-brain delivery showing promising results, including nanocrystals[41,42], micelles [43,44], liposomes[45], solid lipid nanoparticles (SLN)[46,47], nanostructured lipid carriers (NLC)[48,49], polymeric nanoparticles[50-52], albumin nanoparticles[53], gelatin nanoparticles[53], dendrimers[54], mesoporous silica nanoparticles[55], nanoemulsions[56], just to cite some of the more common pharmaceutical nanocarriers.

In consequence of such an intense research activity in this field, several reviews have been published recently on the use of nanoparticles for the N2B delivery, covering both general [57-61] and specific disease [62,63] or vector-related topics [64-66]. Consequently, the present review does not aim to provide an exhaustive report on the various applications of nanoparticles administered nasally allowing for a direct drug delivery to the brain, but on the contrary, collect and appraise critically some facts and figures related to the leading strategies of nanoparticle design for nose-to-brain delivery. Particularly, the review will focus on nanoparticles physico-chemical characteristics and surface modification with

mucoadhesive, penetration enhancing or targeting moieties, able to affect and promote the brain delivery of therapeutically active substances.

2 Influence of Physicochemical Properties in Nanoparticles Nose-to-Brain Delivery

Many papers have described enhanced delivery to the brain after nasal administration of nanoencapsulated drugs in comparison with simple drug solutions. However, few studies draw attention on the precise mechanism through which nanoparticles enhance drug transport to the brain. Different scenarios can be depicted, from the simplest one, where the nanocarriers just interact with the mucus layer and release the drug in the mucus or at the mucus/epithelial cell interface, to the most "challenging" that see the crossing of the mucosal barrier, uptake by neurons and translocation of the drug-loaded nanoparticles along the axons of trigeminal and olfactory nerves to reach the brain, where the drug is delivered. In the middle, there is the possibility of nanoparticle uptake into the respiratory epithelium and/or through olfactory neuroepithelium, where the payload is released and then the drug diffuses along perineural spaces to achieve the CNS. It appears clear that the fate of particles depends upon the physicochemical characteristics of the nanoparticles themselves. Indeed, composition, size, superficial charge, shape and surface hydrophobicity/ hydrophilicity have an impact on nanocarrier interaction with the biological environment. In the case of nose-to-brain delivery, these features influence the interaction with the mucus, the uptake in the epithelial and neuroepithelial cells, the translocation to the brain by *diffusion* along the axons and the release kinetics of the drug. In this context, the elucidation of the role of physicochemical properties of NP is essential to be able to design both efficient and safe carriers.

To clarify the role of NP characteristics such as particle size, surface charge, hydrophobicity on their fate, some authors have studied nanoparticles transport either *in vitro* across olfactory cells monolayer, *ex vivo* across excised nasal mucosa, or *in vivo* on rat /mouse models.

In a recente paper Gartziandia *et al*. [67] have compared the permeability of nanoparticles having different physicochemical properties across rat olfactory mucosa primary cells monolayers. A fluorescent probe (DiR; 1-1'dioctadecyl-3,3,3',3' tetranethylindotricarbocyanine) was loaded to track the particles: previous studied demonstrated the absence of probe release in the transport buffer. The authors found

significant differences in nanoparticle permeation as a function of the constituting material: nanostructured lipid carriers (NLC) penetrate to a higher extent compared to PLGA nanoparticles having the same zeta potential (-23 mV). The change of the surface charge of NLC to positive by chitosan coating determined an almost 3 folds increase in the transcellular transport compared to the uncoated NLC. Finally, the surface functionalization using cell penetrating peptides (particularly Tat) further enhanced nanoparticle transport. While the role of chitosan can be explained considering an electrostatic interaction with the negatively charged cells, the different performance observed deserve further investigation before attributing it to nanoparticle constituents, i.e. polymeric *vs.* lipid particles. Indeed, the particles analyzed had different size (approx. 100 nm for NLC and 220 nm for PLGA) and different surfactants were used for their preparation: while NLC were made using polysorbate 80 and poloxamer (i.e. PEG moieties could be found on NP surface), PVA was used as surfactant for PLGA nanoparticles. This can contribute to the differences found considering the mucus-penetrating properties of PEG (see also section 4.1) and the mucoadhesive properties of PVA-coated particles, reported to interact with mucus constituents by hydrogen bonding and/or hydrophobic interactions [68].

Musumeci and collaborators [69] prepared PLGA, PLA and chitosan nanoparticles using tween 80 as surfactant and rhodamine as fluorescent probe. They found a higher uptake in olfactory unsheathing cells (extracted from rat pup's olfactory bulbs) for PLGA NP (132 nm, -15.8 mV) compared to chitosan (no surfactant, 181 nm, +34 mV) and PLA (152 nm, -30 mV) nanoparticles. In this case, the higher uptake of PLGA nanoparticles compared to the others has been explained by the authors with the lower absolute superficial charge, but the presence of PEG moieties on PLGA and PLA surface could have also contributed to the obtained result. It is however difficult to compare the data from the two previously cited studies since different cells were used, and it is known that the type and the physiological status of cell highly influence its behavior toward nanoparticle uptake [70].

Mistry *et al*. [71] adopted a more complex barrier, i.e. excised porcine olfactory epithelium mounted on Franz-type diffusion cells, to compare carboxylate-modified fluorescent polystyrene nanoparticles 20, 100 and 200 nm in size (ζ potential: approx. -42 mV) with surface-modified nanoparticles obtained using chitosan (48, 163 or 276 nm; ζ potential approx. +30 mV) or polysorbate 80 (ζ potential approx. – 21 mV) coating. None of the tested particles was found to cross the nasal epithelium after 90 minutes, but polysorbate 80-coated (PEGylated) particles penetrated deeper in the tissue compared to uncoated and chitosan-coated nanoparticles. On the other hand, the number of particles present at the epithelial surface was higher in case of chitosan coated particles, and histological images

suggest a localization within the mucus layer. No clear trend was found concerning the role of nanoparticle size on drug uptake into the tissue.

The same nanoparticles were also evaluated *in vivo* on a mice model [72]. A volume of 15 µl of formulation containing either 105 nm polystyrene nanoparticles (-42 V), 163 and 276 nm chitosan-coated NP (ζ potential +30 and +23 mV respectively) or 107 and 180 nm polysorbate 80 coated NP (ζ potential -21 and -24 mV respectively) were applied daily for 3 days. All the nanoparticles were found to be transported to some extent across the mucosa (both olfactory and respiratory) via a transcellular route. The presence of polysorbate 80 coating did not enhance tissue uptake when compared to the uncoated particles, despite the claimed mucus penetrating properties of PEG. The authors explained these results considering that the PEG chains were not covalently bound to the particles, and that a precise length and density of PEG chains is needed to obtain a relevant mucus penetrating effect [73,74]. A significant difference was found between 107 and 180 nm polysorbate 80 coated NP (ζ potential -21 and -24 mV respectively), and the lower accumulated amount found for bigger particles was attributed to a more difficult diffusion inside the mucus network. Chitosan-coated particles were mainly retained inside the mucus and lower amounts were recovered in the tissue for comparison to uncoated and polysorbate 80-coated nanoparticles. Despite the long application time (4 days) nanoparticles were never found in the olfactory bulb, regardless the size or the superficial properties.

Ahmad [75] studied the permanence of a nanoemulsion made with Labrafac® WL1349/ Labrafac® CC and Solutol® HS15 in the nasal cavity of rats from 0.5 to 16 hours after the application of 100 µl of formulation. Particularly, nanoemulsions with droplets of 80, 200, 500 and 900 nm (NE80, NE200, NE500 and NE 900) were compared. The droplets were tracked with environment-responsive probes giving a fluorescent signal when dispersed in the nanocarrier matrix that is quenched immediately after release. Results highlighted that the smaller the size, the higher was the retention in the nasal cavity. The even longer retention obtained with positively charged chitosan-coated nanodroplets (size 108 nm) was attributed to the interaction with the mucus and with the negatively charged epithelial membranes. Further evaluations were done with NE80, NE900 uncoated nanoemulsions and the chitosan-coated nanoemulsion 108 nm in size. After 1 h from the nasal instillation a large number of nanoemulsion droplets were present in the nasal mucosa, the highest signal was found for the chitosan-coated nanoemulsion, followed by NE80 and NE900 uncoated nanoemulsions. In the trigeminal nerve the translocation was size dependent being NE80>Chitosan coated>NE900. The accumulation in the brain (and in particular in the olfactory bulb) was also analyzed: only very minute numbers of NE droplets entered the brain

after 1 h, and these were only visualized in case of particles with small size (NE80 and 108 nm chitosan coated), in agreement with the *in vivo* results obtained by Mistry [72].

Diversely, a recent paper reported significant brain accumulation of PLGA nanoparticles after nasal administration in rats. The authors prepared rhodamine-loaded PLGA nanoparticles (surfactant: polysorbate 80, size 118 nm, ζ potential -26 mV) and chitosan-PLGA nanoparticles (213nm, +69 mV) and analyzed the brain distribution of fluorescence after 8, 24 or 48 h from the intranasal administration. The results evidenced that both positively and negatively charged particles could reach the brain and were localized mainly in the cytosol of the neural cells. Different localization (caudal vs rostral area) could be obtained by modifying the superficial charge. A different distribution as a function of the post-application time was also described, with a slower brain uptake for positive particles, attributed to both a mucus-nanoparticles interaction in the nasal cavity and to a different nose-to-brain pathway. The authors hypothesized that the slower translocation of positive particles is attributed to an intra-neuronal pathway (trigeminal nerve), while the extra-neuronal pathway, relying on bulk flow transport, was responsible for the negatively charged particles rapid transport. Despite the interesting results, no experimental evidence, except for the different timing of brain appearance, supported the hypothesis and the involvement of different (systemic) pathways could not be excluded.

A specific brain distribution as a function of the properties of the nanocarriers was also described by Kanazawa *et al.* [76] by using peptide-based carriers. They conjugate an arginine-rich oligopeptide (designed to have adhesiveness and transmissibility) with either a hydrophobic moiety (stearic acid) or with a hydrophilic one (PEG-PCL block copolymer) so as to obtain two stable nanomicellar formulations. An Alexa-dextran complex (MW 10,000 Da) was used as fluorescent probe to asses biodistribution. The stearate-peptide and PEG-PCL-peptide micelles were 100 and 50 nm in size and had a ζ potential of +20 and +15 mV respectively. After intranasal application in rats, the two carriers determined a much higher uptake in the nasal mucosa and in the brain if compared with Alexa-dextran alone. The hydrophobic stearate-peptide determined a markedly higher fluorescence in the nasal epithelium compared to the hydrophilic PEG-PCL-peptide, but a lower fluorescence in the trigeminal nerve. Additionally, when analyzing the intracerebral distribution pattern of Alexa (Figure 2) as a function of the time post-intranasal administration a significant difference between the two carriers can be appreciated: hydrophobic stearate-peptide shows a strong fluorescence in the forebrain after 15 minute, 30 minutes and 1 hour and no transport to the hindbrain is evident. On the contrary, upon PEG-PCL-peptide administration, a spreading of the fluorescence after 30 minute and 1 hour is evident, indicating a distribution of Alexa to the entire brain. This result, together with the higher trigeminal fluorescence, suggest that

PEG-PCL-peptide nanocarriers penetrate across the nasal mucosa and transport the probe to both the olfactory bulb (forebrain) and to the hindbrain via the olfactory and trigeminal nerves.

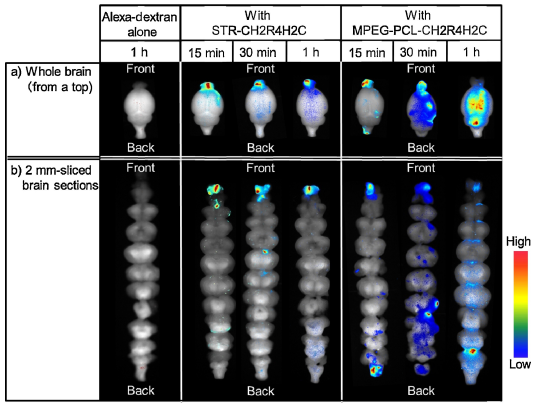

Figure 2: Dynamics of Alexa-dextran in brain tissue following NASAL administration of hydrophobic (STR-CH2R4H2C) and hydrophilic (MPEG-PCL CH2R4H2C) surface nanocarriers in: (a) Whole brain and (b) 2 mm-sliced brain sections (reprinted with permission from [76]).

Gabal *et al*. [77]e valuated the impact on N2B delivery of nanoparticle surface charge by preparing anionic and cationic NLC having very similar size (175 nm and 160 nm respectively), the same but opposite ζ potential (-34 and +34 mV respectively), containing the same amount of drug (ropinirole HCl, EE% 53 and 50 % respectively) and characterized by a very similar release kinetic in vitro. These nanoparticles were dispersed in a thermosensitive gel made of poloxamers (407 and 188) and HPMC and administered intranasally in albino rats. Animals were sacrificed 3 to 360 minutes after the intranasal application and drug levels were measured in plasma and brain to calculate the pharmacokinetic parameters. Overall, the result indicates that there is no significant difference between negative and positive nanoparticles and that both performed much better than a simple drug solution. However, it is not clear the effective contribution of the nanocarriers since the improved bioavailability appears mainly due to the increased residence time given by the gel and/or to the presence of a penetration enhancer (sodium deoxycolate) in the nanoparticle formulation. Indeed, the authors also compared the toxicity of anionic NLC, cationic NLC and the nanocarriers dispersed in the gel after 10 μl application

daily for 14 days in rats. The results highlighted the highest toxicity for cationic NLC, a lower toxicity for anionic NLC while no histopathological alteration was found for animals treated with gels loaded either with cationic or with anionic particles. The authors attributed this result to a direct protective mechanism of poloxamer 188 against oxidative stress and inflammation, however the hindered nanoparticles diffusion in the gel network and the consequent limited interaction between nanoparticles and tissue are to be considered the real reasons of the reduced toxicity evidenced.

The potential toxicity of nanoparticles on the mucosa and potentially to CNS structures is a critical aspect, related to the physicochemical properties, to be considered in nose-to-brain applications. In agreement with the above-mentioned results also other authors described a higher toxicity of positively charged nanoparticles: chitosan-coated nanoparticles applied in pH 6.0 citrate buffer had a size-dependent damaging effect on the excised porcine olfactory epithelium: 20 nm nanoparticles caused substantial tissue damage in comparison to 100 and 200 nm nanoparticles [71]. This effect can be partially attributed to the buffer used, but also to the high relative surface area, combined with the presence of the positive surface charge. However, it is worth mentioning that toxicity studies on animal models have evidenced a substantial safety of nanoparticles made or coated with chitosan [78] suggesting that *in vivo* the presence of a thicker mucus can reduce the toxic effect, probably by reducing the interaction between nanoparticles and epithelium.

Extensive nanotoxicological literature showed the capability of pollutant and metal nanoparticles to reach the brain parenchyma after nasal instillation or inhalation and, in some cases, to elicit toxic effect on the CNS [79-81]. A careful selection of the excipients used is thus mandatory and rapid and efficient biodegradation within the absorption tissue appears the best strategy to avoid unwanted accumulation and potential CNS toxicity of the innovative nanocarrier

3 Mucoadhesive Nanoparticles

One of the physiological factors having a significant impact on nasal delivery and on N2B transport is mucocilicary clearance. This physiological protection mechanism of the respiratory system allows for an efficient and rapid elimination of noxious substances, particulate and microorganisms trapped in the mucus layer (10-15 μm thick) during air intake (clearance $t_{1/2}$ 20 minutes in humans). However, this appreciably limits residence time of substances administered to the nasal cavity. As a consequence, traditional nasal

formulations exploited excipients able to increase viscosity and/or provide bioadhesion, such as hydrophilic polymers, to reduce mucociliary clearance, prolong formulation residence time, improve systemic bioavailability and reduce nasal absorption variability [82]. The mucus lining the nasal epithelium is secreted by goblet cells present in the epithelium itself and mainly by submucosal glands present in the lamina propria and it is composed of about 90-95% water, 2-5% mucins, 1% salts and variable amounts of cellular products and debris such as DNA, albumin, immunoglobulins, lysozyme, lactoferrin, and lipids [73,83]. Particularly, the highly-glycosylated proteins mucins (10-40 MDa) are the major determinant of mucus properties. These glycoproteins, because of their molecular weight, hydration, crosslinking and entanglement, confer to the nasal secretion viscosity and elasticity, typical of a non-Newtonian thixotropic gel. In addition, mucins present a high sialic acid and sulphate content, providing a strong negative charge to the polymer chains contributing the rigidity of their networks [73]. Mucoadhesion has been explained in the case of polymeric excipients with a combination of events necessary to explain the adhesion process: hydration of polymer chains, intimate contact with the mucus, diffusion and entanglement with mucin fibers, dynamic creation and disruption of labile bonds, such as disulfide bridges, electrostatic attractive forces, hydrophobic interactions, hydrogen and van der Waals bonds [84]. Several natural (gums, alginates, starch and gelatin), semisynthetic (cellulose derivatives, such as methyl-, hydroxylpropyl-, hydroxypropylmethyl- and carboxymethylcellulose) and fully synthetic polymers (polyacrylates, polymethacrylates, crospovidone) have been used to improve nasal delivery of drugs [83]. In the case of N2B transport, for example, chitosan and low molecular weight pectins were shown prolong residence time of nasal formulations on the olfactory region in man [85] and sodium hyaluronate was demonstrated to improve the brain delivery of high molecular weight hydrophilic model compound (fluorescein-labeled 4 kDa dextran) after nasal administration in rats [86].

When these polymers are present as constituents or surface-modifiers of nanocarriers the underlying adhesion mechanisms do not change, however the high surface-area-to-volume ratio provided by their size offers an extensive interface for more stable and prolonged interactions with mucus compared to larger structures. Besides, size below 500 nm allows nanoparticles to fit in the low viscosity aqueous spaces left in-between the mesh of the mucins network further enhancing the interaction with the mucus at molecular level. Finally, positive and hydrophobic surfaces may contribute to maximise nanoparticles adhesion towards the mucus, as a consequence of electrostatic attraction and hydrophobic interactions with mucins negatively charged and hydrophobic domains, respectively [84]. Some surface modifications, on the contrary, reduce mucoadhesion, a characteristic exploited by mucus penetrating nanocarriers as will be presented in next section of this review (Figure 3).

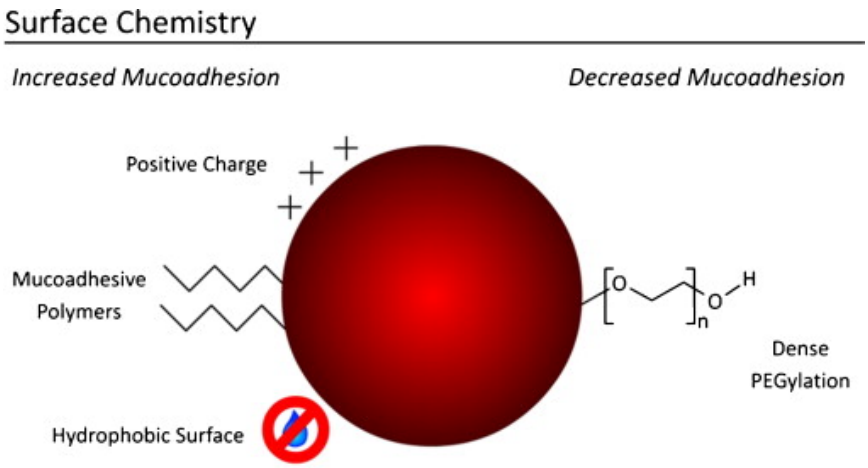

Figure 3: Surface chemistry of nanoparticles affecting mucoadhesion (modified with permission from [84]).

For the reasons explained above, mucoadhesive nanocarriers have been extensively studied for the N2B delivery of drugs.

Already in the year 2000, Betbeder and coworkers proposed Biovector™ nanoparticles for the nasal delivery of morphine to exploit the direct pathway between the olfactory mucosa and the CNS. These maltodextrin-based cationic nanoparticles surrounded by a phospholipid bilayer (average size 60 ± 15 nm) prolonged morphine antinociceptive activity when co-administered in mice in comparison to morphine solution. Interestingly, the result was not replicated when morphine was administered with a penetration enhancer such as sodium deoxycholate. Despite morphine was not actually encapsulated in the nanoparticles, it appears that nanoparticles improved specifically nose-to-brain transport of the opioid, while blood levels were not significantly affected. This is likely due to the interaction of positive nanoparticle with the nasal mucus layer that may have increased the formulation residence time and absorption from the olfactory region that is especially developed in mice [87].

In another approach, the group of Silvia Guterres and Adriana Pohlmann developed an amphiphilic methacrylic copolymer-functionalised poly(ε-caprolactone) nanocapsules as mucoadhesive system for the N2B delivery of the atypical antipsychotic drug, olanzapine [88].. Nanocapsules showed size and surface charge inversely proportional to pH, ranging from

324.3 to 235.2 nm and from +55 and +22.7 mV. Nanocampsules/mucin interaction was demonstrated by increase in particle size and reduction in nanoparticle concentration using Nanoparticle Tracking Analysis (NTA). The polymer mucoadhesion was tested both in terms of peak force and work of adhesion and of prolongation of olanzapine-loaded nanocapsules residence time on porcine nasal mucosa. *In vivo* studies performed in rats not only confirmed a 1.55 folds' higher accumulation of olanzapine in brain after the nasal administration mucaoadhesive nanoparticles in comparison to a control drug solution, but amphiphilic methacrylic copolymer-functionalised poly(ε-caprolactone) nanocapsules loaded with olanzapine outperformed controls (drug solution and blank nanocapsules) also in the pre-pulse inhibition model of cognitive impairment symptoms present in schizophrenia. Interestingly, the authors noted that the brain accumulation was higher than those reported in literature for olanzapine-loaded PLGA nanoparticles, attributing the improvement to the cationic mucoadhesive coating of the nanocapsules [88].

Notwithstanding the possibilities provided by new synthetic polymers, polysaccharides appears to have been amongst the most popular materials used to obtain mucoadhesive nanocarriers. Polysaccharides in fact appear to be an ideal choice to produce nanoparticles to be delivered nasally, not only because of their mucoadhesive properties, but also for many unique characteristics, such as biomimetic mucosal recognition, well-documented biocompatibility and biodegradability and ease of chemical modification with targeting moieties. In this respect, polysaccharides can be incorporated into pharmaceutical nanocarriers in three ways: by absorption to preformed nanoparticles, by copolymerization or covalent grafting leading to surface modification or by the production of entirely polysaccharide-based nanoparticles [89]. For example, albumin nanoparticles obtained by coacervation and thermal cross-linking, were prepared in presence of β-cyclodextrin derivatives to develop an innovative nasal drug delivery system for the anti-Alzheimer drug tacrine. The inclusion of β-cyclodextrin derivatives affected drug loading and modulated nanoparticle mucoadhesiveness. Finally, drug permeation behaviour across sheep nasal mucosa from tacrine-loaded nanoparticles modified with β-cyclodextrin derivatives was increased compared to nanoparticles based on albumin alone, but was lower than that obtained with tacrine solution. This can be explained considering the prolonged release of tacrine observed for nanoparticles [90].

Surface-engineered nanostructured lipid carriers coated with *Delonix regia* gum (DRG-NLC) as a natural mucoadhesive polymer were proposed for the efficient N2B delivery of ondansetron (OND), a centrally active drug used for the management of chemotherapy induced nausea and vomiting. The mucoadhesive formulation of OND was produced by high

pressure homogenization using glycerol monostearate and capryol 90, as solid and liquid lipids, while soybean lecithin and poloxamer 188 were used as stabilizers. The nanostructured lipid carriers were subsequently coated by dispersing OND loaded nanoparticles in a DRG 0.75% w/v aqueous solution. The optimal nanoparticles formulation showed average size 92 nm, polydispersity index (PDI) 0.36, negative surface charge (-11 mV) and moderate encapsulation efficiency (40% EE, 5.6% drug loading). Mucoadhesion was assessed *in vitro* determining a percentage of binding efficiency between DRG-NLC and mucin (72%). *In vivo* studies carried out in rats showed a brain targeting efficiency (DTE) of 506% and a direct transport percentage (DTP) of 97% for the intranasal administration of OND-loaded DRG-NLC using as a control the IV injection of a commercial OND IV formulation (Emeset®). This study, despite the remarkable results, lacked a nasal control (non-mucoadhesive formulation) and did not clarify what was the impact of the presence of free gum, of non-encapsulated drug, as well as of the processing of nanoparticles (freeze-drying) on the *in vivo* brain distribution results obtained after DRG-NLC nasal delivery [91].

Alginate nanoparticles were produced for the N2B delivery of venlafaxine, a serotonin and norepinephrine reuptake inhibitor, to treat depression. Alginate nanoparticles were prepared by ionotropic gelation with calcium ions and subsequent cross-linking with a polycation, i.e. low molecular weight chitosan glutamate. Optimized nanoparticles showed an average size slightly below 175 nm and positive surface charge (+37.4 mV), PDI 0.391, with a high encapsulation efficiency (81%) and a drug loading of nearly 27%. Mucoadhesion was not studied directly, but *ex vivo* permeation through porcine nasal mucosa was found to be more than double over 24 hours, when comparing the venlafaxine-loaded alginate nanoparticles to a simple drug solution. Forced swimming test and locomotor activity test were used as behavioral test to assess the efficacy of the nasal administration of the antidepressant nanoformulation using as controls the drug solution administered intranasally and a suspension obtained crushing commercial tablets administered orally. The alginate nanoparticle formulation performed better than the other formulations in the treatment of depressed animals, even if climbing and immobility parameters were not restored to levels of naive animals. It must be noted also that, considering the volume of nanoparticle suspension administered nasally (100 µl), an eventual inhalation or swallowing of part of the nanoformulation could not be excluded. This would eventually provide confounding effects to the final results. In any case, pharmacokinetics studies conducted using venlafaxine IV administration as reference and venlafaxine solution administered nasally as control, showed reduced blood levels and increased brain concentration for the antidepressant drug formulated in alginate nanoparticles. Particularly, DTE and DTP calculated for the venlafaxine-loaded nanocarrier were 426% and 76% respectively. An increase in absorption

as a consequence of reduced nasal mucociliary clearance, an enhanced mucosal permeation and the modulation of P-gp efflux transporters are some of the factors explaining the pharmacokinetics data [92]. It is remarkable however that the nanoparticle formulation increased the DTP value only from 63 to 76%, when compared to the nasal solution and that a significant part of the increase in the DTE is provided by BBB crossing of the drug after systemic absorption. This is not unexpected, considering that the antidepressant drug studied is already marketed as immediate and controlled release tablets and is able to cross the BBB. As such the real improvement of the N2B delivery will have to rest mostly on the reduction of systemic side effects of the drug.

Among the polysaccharides, chitosan, the glucosamine and N-acetyl glucosamine co-polymer obtained by the deacetylation of chitin, has been demonstrated to be one of the most promising and versatile materials for N2B delivery. In fact, chitosan not only is biocompatible, biodegradable, mucoadhesive and positively charged at nasal slightly acidic pH, but is also an efficient permeation enhancer able to transiently open the tight junctions of epithelial cells in mucosal tissues [78,93]. Interestingly this feature was demonstrated to be retained when chitosan was used as main constituent or surface coating for nanocarriers [84,94].

Wang and co-workers loaded estradiol in chitosan nanoparticles produced by ionotropic gelation for nasal administration in view of the treatment of Alzheimer's disease. Chitosan nanoparticles were obtained using tripolyphosphate anions (TPP) and chitosan with Mw 50,000 Da to obtain nanoparticles with particle size about 270 nm with positive surface charge (+25 mV). Encapsulation efficiency was around 60% (estradiol concentration 1.9 mg/ml). Smaller (below 100 nm) or larger (500 nm) nanoparticles could be obtained with Mw 6000 Da and 200,000 Da chitosan, respectively, but they were not considered suitable for the application. *In vivo* studies in rats showed a DTE of 320% and DTP of 68% by measuring estradiol concentration in cerebrospinal fluid (CSF) after IN or IV administration of the estradiol-loaded chitosan nanoparticles. The results were explained by the ability of chitosan nanoparticle to bind mucins and improvement of paracellular transport [95]. However, in these experiments nasal cavity was isolated from respiratory and gastrointestinal tracts, a surgical practice reducing the likeliness of interfering absorption from other organs but altering retention time and hence absorption from the nasal mucosa. In addition, paracellular transport is not expected to significantly affect the mucosal permeation of highly lipophilic steroid hormones as estradiol.

Similar chitosan nanoparticles obtained by ionotropic with TPP have been proposed by several authors for the for the N2B delivery of very different drugs: rivastigmine (size 164 nm, PDI 0.42, EE% 85; DTE 355%, DTP 71%) [96] and thymoquinone (size 103 nm, PDI 0.40,

EE%; DTE 3321% DTP 97%)[97] for AD, bromocriptine (size 161 nm, PDI 0.44, EE% 84; DTE 630%, DTP 84%) [98], ropinirole (size 171 nm, PDI 0.39, EE% 70; superior brain/blood ratio compared to IN solution in γ-scintigraphy studies) [99], rasagiline (size 151 nm, PDI 0.38, EE% 96; DTE 325%, DTP 69%) {Mittal:2016dm} and pramipexole (size 292 nm, PDI 0.29, EE% 93; superior to IN and oral solution in pharmacodynamics studies) [100] for PD, tapentadol (size 201 nm, PDI 0.20, EE%; DTE 321%, DTP 69%) for chronic pain management [101]. Despite the different physicochemical characteristics of the drugs studied results shared striking similarities.

Chitosan presents several desirable features but also some limitations, for example it is insoluble at physiologic pH and it is protonated only in acidic conditions, features potentially interfering with bioadhesion. Hence, several authors adopted nanocarriers based on chitosan derivatives. Trimethyl chitosan (TMC) for example is a water soluble permanently positively charged chitosan derivative and was used to encapsulate the analgesic neurotransmitter leucine-enkefaline (Leu-Enk) by ionotropic gelation. TMC nanoparticles (size 443 nm, PDI 0.32, EE% 78) were able to increase 35 times the permeability of the peptide across porcine nasal mucosa and produced a significant increase of the antinociceptive effect in mice after nasal administration during the hot plate and the acetic acid induced writhing tests [102]. Thiolated chitosan can increase mucoadhesive via the formation of covalent bonds, such as disulphide bridges, between the thiol groups and mucus glycoproteins [103]. Cyclobenzaprine (CB) and tizanidine (TZ), two central acting muscle relaxant used for pain management, were loaded into thiolated chitosan nanoparticles obtained by gelation with sodium alginate and showed enhanced permeation and reduced toxicity in the RPMI2650 cell model of human nasal epithelium, increase brain uptake (DTE 2461 and 8523% , DTP 96 and 99% for CB and TZ, respectively) and significantly enhanced antinociceptive activity for both drugs when compared to non-thiolated nanoparticles administered nasally [104,105]. In another study, in which the antidepressant selegiline HCl was encapsulated in thiolated chitosan nanoparticles (215 nm, EE% 70), authors claimed improved anti-inflammatory and neuroprotective effects for the thiolated polysaccharide itself. During *in vivo* experiments in depression-induced rats thiolated nanoparticles were found to be superior to control chitosan nanoparticles when administered at the same dose (10 mg/kg), while provided non-significant difference in pharmacodynamics effect compared to controls when dose administered was halved (5 mg/kg) [106]. In another research, Di Gioia and co-workers assessed the ability of chitosan derivative nanoparticles to deliver dopamine to the striatum. Glycol chitosan, a water-soluble derivative of chitosan, was used to manufacture nanoparticle by ionotropic gelation with TPP along with sulfobutylether-β-cyclodextrin to improve dopamine loading. When administered nasally as a single dose

nanoparticles did not modify brain levels of the neurotransmitter, but repeated intranasal administration significantly increased dopamine levels in the ipsilateral striatum [107].

It is worth mentioning that in almost all those promising studies, the nanocarriers improved the performance of drugs that already showed N2B transport when administered nasally with traditional formulations such as solutions.

In alternative formulation approaches chitosan is used as a surface modifier of carriers based on other materials. The water soluble antipsychotic chlorpromazine HCl was loaded into chitosan grafted PLGA nanoparticles in view of nasal treatment of schizophrenia to provide brain targeting and sustained release of drug, decrease the dose and administration frequency of dosing and reduce side effects. PLGA nanoparticles were prepared with a combined self-assembly/nanoprecipitation technique in presence of dextran sulphate followed by the grafting of the chitosan on PLGA nanoparticles surface. The selected formulation, presenting average size 464 nm (PDI 0.19) and 37% encapsulation efficiency showed good mucoadhesion on sheep nasal mucosa and provided a permeation of chlorpromazine of 9% over 4 hours, controlled by the release kinetics of the PLGA nanoparticles (40% release over 48 hours) [108]. Liposomes coated with a chitosan derivative were proposed for the nasal administration of ghrelin. Ghrelin is a centrally acting peptide hormone able to stimulate food intake and for this reason a potential drug for the treatment of cachexia the wasting pathologic syndrome associated to some chronic diseases, such as cancers, hearth or kidneys failure. Ghrelin loaded liposomes were prepared by the lipid film re-hydration/extrusion technique followed by coating with N([2-hydroxy-3-trimethylammonium]propyl) chitosan chloride (size 194 nm, PDI 0.19, EE% 56). The chitosan coated liposomes demonstrated to bind more efficiently mucin than simple anionic liposomes (63% *vs.* 40%) and improved permeation through a Calu-3 cell monolayer used as a model of the upper airways epithelial barrier (10.8% *vs.* 3.6% anionic liposome *vs*. 0% free peptide) [109]. Finally, Clementino and co-workers developed hybrid chitosan/lipid nanocapsules for the N2B delivery of simvastatin. Statins have in fact been indicated as potential neuroprotective drugs, in reason of their pleiotropic effects, i.e. anti-inflammatory, antioxidant and immunomodulatory actions [110,111]. The particles obtained by the self-assembly of a mixture of phospholipids and liquid lipids in presence of chitosan aqueous solution. The nanocapsules obtained not only showed small particle size (200 nm), positive surface charge and high encapsulation efficiency, but were shown to be efficiently biodegraded by enzymes present in nasal secretions such as lysozyme to provide a more efficient release of the drug at the deposition site on nasal mucosa. Gamma scintigraphy studies evidenced a significantly higher brain accumulation of the isotope (above 20% of the administered radioactivity) after

IN administration of simvastatin loaded nanocapsules in rats in comparison to the IN administration of a ^{99m}Tc-labelled suspension of the statin (Figure 4) [112].

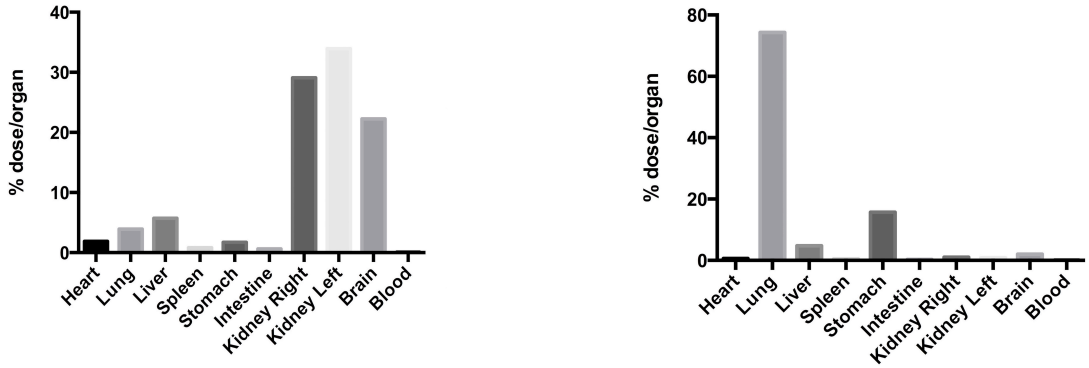

Figure 4: Fraction of total radioactivity recovered per organ 90 minutes after the nasal administration in rats of (a) ^{99m}Tc-labeled simvastatin-loaded nanoparticles**; (**b) ^{99m}Tc-labeled simvastatin suspension.

In recent years, several studies have proposed the inclusion of nanoformulations, often micro/nanoemulsions, lipid or polymer nanoparticles, within mucoadhesive gels (xantan gum, chitosan) [113,114] or *in situ* gelling preparations obtained with thermosensitive (poloxamers 407) [115], pH sensitive (Carbopol 934) [116] and ion sensitive (gellan gum) [117,118] polymers. Even if the approach is seemingly appealing (combination of nanoparticle encapsulation/protection within viscous medium able to prolong residence time), the gel matrix viscosity might result in hindered nanoparticles migration, poor interaction with the nasal mucosa as well as low drug release. In addition, the superiority over more traditional formulation solutions is open to question.

In summary, mucoadhesive nanoparticles have been one of the most explored platforms of the N2B delivery of drugs. Results are supporting in all cases a superiority of the mucoadhesive nanoformulation over simple solution administered nasally and/or intravenously, although too few studies focus on direct comparison with potential competing formulation approaches such as liquid or even solid formulations containing mucoadhesive or permeation enhancing excipients.

More extensive experimental details regarding mucoadhesive nanocarriers presented in this section can be found in Table 1.

Table 1: Mucoadhesive nanocarriers studies for nose-to-brain delivery

Nanocarrier	Drug	Application	size (nm)	PDI	potential (mV)	ΞE (%)	L (%)	Biodistribution	DTE	DTP	Ref.
Methacrylic-PCL Ncps	Olanzapine	Schizophrenia	254.9 ± 12.1	0.030	+22.0 ± 1.2	99.0	-	HPLC-UV	-	-	88
β CD Albumin	Tacrine	AD	177.4 ± 18.0	0.257	-10.0 ± 0.9	-	22.0	-	-	-	90
NPs *Delonix regia* gum NLC	Ondansetron	Nausea	92.0 ± 13.0	0.360	-11.5 ± 2.3	39.5	5.6	HPLC-UV	506.0	97.1	91
Alginate NPs	Venlafaxine	Depression	173.7 ± 2.5	0.391	+37.4 ± 1.7	81.3	26.7	CFM	425.8	76.5	92
Chitosan NPs	Estradiol	AD	269.3 ± 31.6	-	+25.4 ± 0.7	64.7	1.9	HPLC-Fluo	320.0	68.4	95
Chitosan NPs	Rivastigmine	AD	185.4 ± 8.4	0.391	+38.4 ± 2.8	85.3	43.4	CFM	355.0	71.8	96
Chitosan NPs	Thymoquinone	AD	172.4 ± 7.4	0.130	30.3 ± 2.1	63.3	31.2	γ Scintigraphy	3321	97.0	97
Chitosan NPs	Bromocriptine	PD	161.3 ± 4.7	0.440	+40.3 ± 2.7	84.2	37.8	γ Scintigraphy	533.0	84.2	98
Chitosan NPs	Ropinirole	PD	1773.7 ± 2.3	0.390	+32.7 ± 1.5	69.6	13.8	γ Scintigraphy	-	-	99
Chitosan NPs	Rasagiline	PD	151.1 ± 10.3	0.380	-	96.4		HPLC-UV	325.0	69.3	100
Chitosan NPs	Pramipexole	PD	292.5 ± 8.8	0.292	+14.0 ± 2.9	93.3	-	-	-	-	101
Chitosan NPs	Tapentadol	Chronic Pain	201.2 ± 1.5	0.201	+49.3 ± 1.2	63.5	17.3	HPLC-UV	321.0	68.9	102
Trimethylchitosan NPs	Leu-Enk	Chronic Pain	443.0 ± 23.0	0.317	+15.0 ± 2.0	78.3	14.0	-	-	-	102
Thiolated Chitosan NPs	Tizanidine	Muscular Pain	276.2 ± 13.9	-	+18.3 ± 1.4	75.6	-	γ Scintigraphy	3523	98.8	104,105
Thiolated Chitosan NPs	Cyclobenzaprine	Muscular Pain	272.1 ± 11.5	-	+20.9 ± 1.7	70.5	5.4	γ Scintigraphy	2471	96	106
Thiolated Chitosan NPs	Selegiline	Depression	215.0 ± 34.7	0.214	+ 17.1	70.0	-	-	-	-	106
GC SBE β CD NPs	Dopamine	PD	372.0 ± 81.0	0.260	+9.3 ± 1.3	54.5	-	FM	-	-	108
Chitosan-PLGA NPs	Chlorpromazine	Schizophrenia	463.9 ± 12.0	0.187	21.0 ± 2.0	36.7	4.6	-	-	-	108
Chitosan-coated Liposomes	Ghrelin	Cachexia	194.0 ± 6.1	0.198	+6.0 ± 0.4	56.1	-	-	-	-	109
Lecithin/Chitosan NPs	Simvastatin	AD	204.5 ± 15.4	0.098	+48.4 ± 4.1	98.5	-	γ Scintigraphy	-	-	112

Abbreviations: AD, Alzheimer's Disease; CFM, Confocal Fluorescence Microscopy; EE, Encapsulation Efficiency; GC SBE β CD NPs, Glycol Chitosan Sulfobutylether-β-cyclodextrin Nanoparticles; Leu-Enk, Leucine-Enkephalin; FM, Fluorescence Microscopy; NCL, Nanostructured Lipid Carriers; PCL Ncps, Poly(ε-caprolactone) Nanocapsules; PD, Parkinson's Disease.

4 Beyond Bioadhesion: Mucus Penetrating and Penetration Enhancing Nanocarriers

4.1 Mucus Penetrating Nanocarriers

The popular mucoadhesive approach has been in recent years challenged by the evidence of the multiple barrier properties provided by the presence of the mucus layer. For carrying out its physiologic function mucus acts as a dynamic semipermeable barrier via two major mechanisms working together: interaction filtering and size filtering (Figure 5) [119].

Interaction filtering occurs for molecules, supramolecular structures and particles independently from their size. This phenomenon limits diffusion in mucus via direct non-specific interactions, such as electrostatic, hydrogen and hydrophobic binding, with glycosylated, non-glycosylated regions of mucins as well as lipid components of mucus. These interactions has been evidenced for charged and/or hydrophilic molecules, lipophilic drugs, peptides and proteins [120].

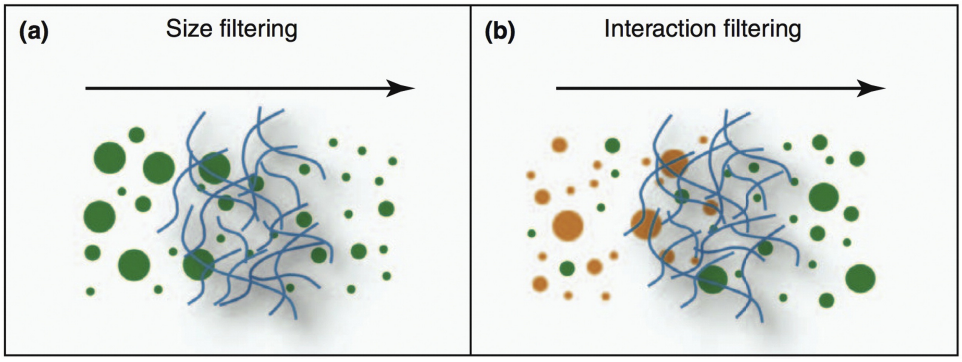

Figure 5: Major mechanisms hindering particles from diffuse through mucus: (a) Size filtering, only particles smaller than the mesh openings of the mucin fibers network are allowed to cross, whereas larger objects are blocked; (b) Interaction filtering, particles behaviour is different according to surface properties: particles (orange) interacting strongly with the components of the mucus gel are trapped, whereas particles (green) showing weak interactions are allowed to cross (reproduced with permission from [120]).

Mucus is a dense molecular network with a characteristic mesh spacing that prevents larger particles diffusion through the mucus. This mesh spacing has been reported to vary from 20 up to 200-500 nm from various authors [119,121].

Hence, it has been hypothesized that the use of nanocarriers with a sufficiently small size and coated with polymers that minimize interactions with mucins such as poly(ethylene) glycol (PEG) could increase mucus diffusivity and favour the close contact with the underlying epithelium. Interestingly, already in 2004 the group of Maria José Alonso observed that when fluorescent labelled PEG-PLA nanoparticles were administered intranasally in rats, the presence of PEG, smaller size (175 nm) and higher PEG coating density were the properties favouring the accumulation of particles within rat nasal mucosa [122]. Later, a group at John Hopkins University demonstrated using multiple particle tracking that 100 and 200 nm particles coated with high density of low Mw PEG (2 or 5 kDa) were able to rapidly penetrate human respiratory [123] and chronic rhinosinusitis mucus [124] and designed mucus penetrating PEG-PLGA nanoparticles [125,126]. However, those results were not replicated in experiments in which PEG-coated magnetic nanoparticles despite showing decreased adhesion to mucus components failed to penetrate through native respiratory mucus even in presence of a magnetic field [127].

Diazepam and midazolam, two benzodiazepines in use for the treatment of *status epilepticus*, were encapsulated in PLGA nanoparticles coated with poloxamers 407 (Pluronic® F127), a block co-polymer surfactant previously reported to enhance mucus penetration of nanoparticles [124]. In both research works optimal particles showed size below 200 nm, moderately negative surface charge (between -15 and -30 mV), controlled drug permeation kinetics across sheep nasal mucosa, direct brain transport (DTP around 60%)and superior brain targeting efficiency compared to drug solution after nasal administration in rats (235-260 % vs. 125-160% DTE) [51,128]. In these articles, however, the authors did not claim or study the mucus penetration of the produced particles.

Recently, Sekerdag and collaborators proposed lipid/PEG-PLGA nanoparticles as mucus penetrating carriers of farnesylthiosalicylic acid (FTA) for a non-invasive nose-to-brain treatment of glioblastoma. Nanoparticles produced (size 163 nm, PDI 0.19, surface charge -12 mV, EE% >95%) were demonstrated after nasal administration to significantly reduce tumour volume (55%) induced by implanting RG2 cells in rat brain as evidenced by MRI analysis. The antitumor effect obtained was comparable to that obtained by nanoparticles administered intravenously. The biodistribution studies evidenced that the percentage of the dose attaining the brain was 0.04% ID/g for both formulations, but in the case of the nasal administration the amount of the dose accumulating in liver and spleen was significantly

reduced, suggesting a superior safety profile for the nasal administration of the nanocarrier [129].

It is interesting to note that in some cases PEG-coated nanoparticles have been used as mucoadhesive carriers [130], but this is due to the fine tuning of the particle size and coating characteristic necessary to obtain particles able to slip through the mucus layer [131]. Furthermore, PEG coating has been associated with reduced interactions with epithelial cells and as a consequence reduced uptake, exactly for the same reasons related to mucus penetration, i.e. reduced interactions with proteins and biomolecules [132,133]. It appears clear that mucus penetrating particles have not been yet sufficiently studied in nose-to-brain delivery and that more robust studies must demonstrate the validity of the concept in terms of improved targeting of the CNS compared to other surface modification approaches.

4.2 Penetration Enhancing Nanocarriers

In alternative to mucus penetrating “stealth” particles, some authors have developed particles in which components can act as penetration enhancers. This classification is often superimposed to others (chitosan for example acts both as mucoadhesive and as penetration enhancer) but for this review penetration enhancing particles will be considered those having components, often surfactant, claimed to have the power to alter the barrier properties of nasal mucosa.

For example, zolmitriptan and sumatriptan, two selective serotonin agonists in use for the treatment of acute migraine, were encapsulated into micelles composed of PEG 400, benzyl alcohol, Vitamin E TPGS, Pluronic® F127 and Trascutol P®. In particular, Transcutol, i.e. diethylene glycol monoethyl ether, and Vitamin E TPGS were used to solubilize and enhance the absorption and of the drugs through the nasal mucosa [134]. The micelles exhibited size below 25 nm, significantly increased triptans delivery to the brain (up to 3-7% of the administered dose) compared to IN or IV drug solution and did not show evident sign of local toxicity also after prolonged nasal administration in comparison to controls (28 days) [135,136].

Olanzapine-loaded nanocubic vesicles, obtained by incorporating of the surface-active triblock copolymer poloxamer 188 (consisting of a hydrophobic polypropylene oxide block capped with hydrophilic polyethylene oxide moieties) in phosphatidylcholine bilayers, were compared to the corresponding liposomes in biodistribution studies in rats after nasal delivery. The nanocubic vesicles (size 363 nm, PDI 0.088, EE% 67) improved absolute bioavailability (37.9 *vs.* 14.9%) and DTE (100 *vs.* 80%) compared to the control liposomal

formulation. The improvement was attributed to the presence of poloxamers in the formulation imparting both higher elasticity and penetration enhancing properties to vesicles [137]. In this study, one of the few using LC-MS/MS to quantitate the drug in the biodistribution studies, the nanocarrier nasal delivery was not superior to the IV control in delivering the drug to the brain, as evidenced by the value of DTE. Also, in the work of Albdelrahman and co-workers elasticity of spanlastics nanovesicles was claimed to be the mechanism improving the N2B delivery of the antipsychotic drug risperidone. Spanlastics vesicles, produced by injecting a Span 60 and risperidone ethanol solution in a PVA aqueous solution (size 103 nm, PDI 0.34, EE% 64), exhibited relatively high Newtonian viscosity, improved permeation through *ex vivo* nasal sheep mucosa and improved brain accumulation of the drug in comparison to drug solution (DTE 469 *vs*. 217 %). However, DTP was superior for the nasal solution (55 *vs.* 79 %) as spanlastics significantly improved systemic absorption of the drug [138].

Gelatin nanostructured lipid carriers were used to deliver to the brain the neurotrophic factor, basic fibroblast growth factor (bFGF), suggested to protect dopaminergic neurons in Parkinson's disease, via the non-invasive nasal route. The gelatin nanoparticles were prepared by a water-in-water emulsion in presence of poloxamer 188 and phospholipids, crosslinking with glyceraldehyde following by freeze-drying (size 172 nm, PDI 0.210, ζ-potential -38 mV, EE% 87). The nasal administration of the gelatin NLC significantly increased exogenous bFGF in olfactory bulb and striatum without impacting the integrity to nasal mucosa. The surface modified nanocarriers outperformed control gelatine nanoparticles also in studies with hemiparkinsonian rats inducing functional recovery after IN nasal but not after IV administration. These was attributed to the presence of poloxamers 188 and its ability to reduce the barrier of mucus layer altering its viscosity and to enhance permeation by interacting and perturbing lipid membranes and/or modulating tight junctions [139]. Polysorbate 80 (Tween 80) was claimed to have similar effects in SLN loaded with rosmarinic acid obtained using glyceryl monostearate (GMS) and hydrogenated soy phosphatidylcholine. These particles were designed to manage symptom of Hungtingthon's disease. Tween 80 coated SLN improved behavioural abnormalities and attenuated the oxidative stress in 3-nitropropionic acid treated rats to greater extent that rosmarinic acid administered nasally or the same nanoparticles administered IV [140].

Fatty acids have been traditionally indicated as absorption promoting agents in nasal delivery [141]. Recently, zolmitriptan has been formulated in novasomes, i.e. nanovesicular fatty acid enriched structures. The optimized novasomes formulated with a combination of Span® 80, cholesterol and stearic acid (size 150 nm, PDI 0.48, ζ-potential -38 mV, EE% 93), showed an enhanced brain accumulation (C_{max} 1.27 % ID/g) with a direct transport

percentage of 99.2% when compared with the intravenous drug solution. The effects were attributed to the potential disruption of the nasal membrane and to the ability of these vesicles to “squeeze” themselves through the olfactory epithelium opening [142]. The actual contribution of this last mechanism to the nose-to-brain delivery is far from being supported by actual data demonstrating such ability to transfer across the nasal mucosa of elastic vesicles. Similarly, the occlusive effect claimed by other authors for nasally delivered alprazolam SLN appears highly unlikely [143].

In general, penetration enhancing nanocarriers studies lack of a fundamental control that is the one given by a traditional formulation of the same drug containing the penetration enhancer alone. Only demonstrating a superior nose-to-brain delivery over this formulation of the use of nanocarriers would be fully warranted.

More extensive experimental details regarding mucus-penetrating and penetration-enhancing nanocarriers presented in this section can be found in Table 2.

Table 2: Mucus-penetrating and penetration-enhancing nanocarriers studied for nose-to-brain delivery.

Nanocarrier	Drug	Application	size (nm)	PDI	ζ potential (mV)	EE (%)	DL (%)	Biodistribution	DTE	DTP	Ref.
Pluronic® F127-PLGA NPs	Diazepam	Epilepsy	183.2	<0.200	<-15	87.8	-	γ Scintigraphy	258.0	61.0	[88]
Pluronic® F127-PLGA NPs	Midalozam	Epilepsy	164.0 ± 4.5	0.099	-16.6 ± 2.5	87.4	5.3	γ Scintigraphy	234.7	-	[90]
Lipid/PEG-PLGA NPs TPGS	FTA	Glioblastoma	164.3 ± 10.3	0.192	-12.0 ± 1.3	97.7	3.5	HPLC-MS	-	-	[91]
TPGS Micelles	Zolmitriptan	Migraine	24.2 ± 0.7	0.064	-	-	-	γ Scintigraphy	-	-	[92]
TPGS Micelles	Sumatriptan	Migraine	23.1 ± 0.4	0.046	-	-	-	γ Scintigraphy	-	-	[95]
Polaxamer 188 Cubosomes	Olanzapine	Schizophrenia	363.0 ± 31.8	0.088	-	67.3	-	HPLC-MS/MS	100	-	[96]
Spanlastics	Risperidone	Schizophrenia	103.4	0.341	-45.92	63.9	-	HPLC-MS/MS	468.9	55.2	[97]
Gelatin NLC	bFGF	PD	172.0 ± 1.3	0.105	-27.6 ± 1.1	86.7	4.6	Western blot	-	-	[98]
Polysorbate 80 SLN	Rosmarinic acid	HD	149.2 ± 18.2	0.290	-38.27	61.9	-	HPLC-UV	-	-	[98]
Novasomes	Zolmitriptan	Migraine	149.9 ± 10.9	0.477	-55.6 ± 1.0	92.9	-	γ Scintigraphy	-	99.2	[98]

Abbreviations: bFGF, basic Fibroblast Growth Factor; EE, Encapsulation Efficiency; FTA, farnesylthiosalicylic acid; HD, Huntington's Disease; NLC, Nanostructured Lipid Carriers; PD, Parkinson's Disease; SLN, Solid Lipid Nanoparticles.

5 Targeting the Nasal Epithelium for Optimizing the Nose to Brain Delivery

Without doubt, one of the most fascinating aspects of the pharmaceutical nanotechnology is the so called “active” targeting of nanoparticles, i.e. the recognition of cells or tissues affected by the disease by means of surface ligands able to interact specifically with receptors and/or other biomolecules present on the biologic target. To deliver specifically the therapeutic dose of the drug where it should act, avoiding side effects and with optimal therapeutic efficacy has been the Grail Quest of pharmacotherapy since the dawn of modern pharmaceutical sciences.

As pointed out by an excellent paper by Alexander Florence, several obstacles (often underestimated or disregarded by scientist) are present *in vivo* for targeted nanocarriers (aggregation, drug early release from the carrier, uptake by reticuloendothelial system, delivery off-target, degradation) and those have actually hindered the successful translation of targeted approach of drug delivery systems to clinical settings [144].

In the case of nose-to-brain delivery the approach is interestingly not directed to the delivery of the particles themselves to a specific cell or receptor within the CNS, but to the interaction with cells of the nasal region more likely to favour the translocation to the brain, i.e. the olfactory epithelium. Several surface ligands have been proposed but two strategies emerge as the most studied in recent years: lectins and penetration peptides targeted nanocarriers.

5.1 Lectin-Modified Nanocarriers

Lectins are proteins or glycoproteins extracted from plants able to recognize and bind with high level of specificity glycan arrays of glycosylated lipids and proteins present on the surface of different cell types. For this reason, since 1988 they have been proposed as targeting ligands of drug delivery systems, initially in order to obtain absorption enhancement in the gastrointestinal tract [145]. However, the potential of lectins for nose-to-brain delivery has been demonstrated qualitatively and quantitatively in two seminal works by Broadwell and Balin [146] and Thorne *et al*. [147]. In those works, it has been demonstrated that wheat germ agglutinin (WGA) -horseradish peroxidase conjugate (62 kDa) can bind the cell surface of olfactory sensory cells, undergo adsorptive endocytosis and anterograde axonal transport and finally accumulate in the olfactory bulb to an extent (140 nM) more than 100 folds that

obtained by IV administration of the same conjugate and 700 folds the one attained by the enzyme not conjugated to WGA. In fact, WGA obtained from *Triticum vulgare* specifically bind to N-acetyl-D-glucosamine and sialic acid residues abundantly present in nasal structures. Consequently, WGA has been the most explored targeting ligand for nanocarriers for nose-to-brain delivery.

WGA was conjugated to PEG-PLA nanoparticles to obtain 85-90 nm targeted nanoparticles loaded with the fluorescent dye 6-coumarin. WGA targeted nanoparticles administered nasally improved both blood (1.4 folds) and brain (2 folds) concentrations of the fluorescent label when compared to plain PEG-PLA nanoparticles, without appreciable nasal ciliotoxicity [148]. Other studies in which WGA-conjugated PEG-PLA were radiolabelled with ^{125}I revealed that that nanoparticles after nasal administration in rats were rapidly (5-30 min) transported to the CNS via extracellular pathway along olfactory and especially trigeminal nerves, while cerebrospinal fluid appeared to contribute to a small extent to the process [149].

The same group from the Fudan University of Shanghai (PR China) incorporate vasoactive intestinal peptide (VIP), a neuroprotective peptide potentially useful in a number of neurodegenerative disorders including AD in WGA conjugated PEG-PLA nanoparticles (size 100-120 nm, EE% 70, drug loading% 1.4). In biodistribution studies, 30-50% of radioactively labelled VIP was found in the CNS and WGA-conjugated targeted improved brain targeting (5.66-7.71 folds increase) compared to non-targeted PLA nanoparticles (3.57-4.74 folds increase) and control VIP solution administered nasally in mice. Furthermore, in an *in vivo* model of cholinergic impairment, VIP loaded WGA-NP induced improvement in spatial memory of rats at lower doses compared to non-targeted nanoparticles (12.5 vs. 25 μg/kg) [150]. In a subsequent work, WGA-targeted PEG-PLA nanoparticles were loaded with quantum dots to develop specific brain imaging agents for CNS diseases. Once again, the brain targeting capacity of the WGA was demonstrated with a relative fluorescence intensity detected three hours after nasal administration in mice (40 mg/kg, 5 μl each nostril) that followed the order brain $\geq$ lung > liver > kidney > heart > spleen (Figure 6) [151].

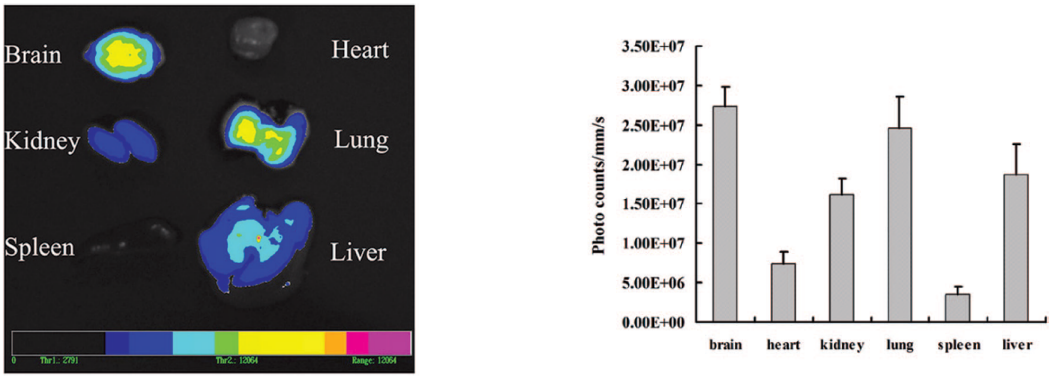

(**a**) (**b**)

Figure 6: Distribution of WGA-conjugated quantum dots-loaded nanoparticles in various organs following intranasal administration 3 h after dosing: (a) optical image (b) quantification of luminescence signals (adapted with permission from [151]. Copyright 2008 American Chemical Society).

PEG-PLA or PEG-PLGA nanoparticles were conjugated to other lectins, such as *Solanum tuberosum* lectin (STL), binding to N-acetylglucosamine [152], Ulex europeus agglutinin I (UEA I) and odorranalectin (OL), both binding to L-fucose largely present on the olfactory epithelium [153,154]. STL-functionalized PEG-PLGA nanoparticles loaded with haloperidol (size 132 nm, PDI 0.174, ζ-potential -14 mV, EE% 73, DL% 0.85) increased the brain tissue haloperidol concentrations after nasal administration by 1.5–3-fold compared to non-STL-functionalized particles and other routes of administration [155].

Since one of the major problems of lectins is their immunogenicity, OL, being the smallest peptide with lectin-like activity, was identified as a potential targeting ligand with reduced immunogenicity. OL-conjugated PEG-PLG nanoparticles were loaded with peptide urocortin reported to be able to restore nigrostriatal function in PD (size 115 nm, PDI 0.193, EE% 75, DL% 0.14). The *in vivo* studies in hemiparkinsonian rats not only evidenced a better improvement of the symptoms related to the dopaminergic lesion for OL-conjugated nanoparticles, as a consequence of a partial but not complete recovery of monoamine neurotransmitters levels [156].

Despite this recent advancement, the use of lectins still faces criticism related to the potential toxicity and immunogenicity, making mandatory a toxicological assessment of the targeted carrier both systemically and locally towards the nasal epithelial surface and the CNS [157].

5.2 Cell Penetrating Peptides as Surface Ligands for Targeted Nanocarriers

Cell penetrating peptides (CPPs) are short cationic sequences of amino acids able to cross cell membranes and translocate to intracellular space similarly to their model, i.e. the HIV transactivator of transcription (Tat) protein [158]. CPPs have been shown to be unspecific to cell-type and able to translocate various cargos (small molecules, proteins, nucleic acids, nanocarriers) across different biological barriers such as intestinal wall, BBB, skin [159].

These characteristics make CPP attractive as ligands for nose-to-brain delivery of nanocarriers. The conjugation of CPPs (Tat or Penetratin) to the surface of polymer and especially of lipid-based nanoparticles improved their ability to cross an *in vitro* primary rat olfactory cell monolayer model [67]. In another study, PEG-PLA nanoparticles were functionalized with low molecular weight protamine were found to accumulate in 16HBE14o- human bronchial epithelial cells more than unmodified cells and after loading with the fluorescence dye coumarin-6 and nasal administration to rats increased fluorescence signal in various brain structure more than two folds compared to unmodified particles [160]. In a similar set of experiments, micelles obtained using Tat conjugated to methoxy poly (ethylene glycol)-poly(ε-caprolactone) (mPEG-PCL) amphiphilic block copolymers and loaded with coumarin accumulated more than original micelles in C6 rat glioma cells and in rats bearing C6 tumours intracranially. In the latter *in vivo* experiment, it was found that no difference was present in fluorescence brain distribution 1h after nasal administration between micelles but after 4 hours while fluorescence signal decreased for unmodified micelles, it increased in animals treated with Tat conjugated mPEG-PCL micelles, probably due to their higher ability to penetrate intracellularly [161]. In subsequent works, the same group from Tokyo University of Pharmacy and Life Sciences loaded in the above-mentioned micelles with camptothecin in view of the treatment brain tumours and with small-interferin RNA (siRNA) for the suppression of genes influencing CNS disorders. Camptothecin-loaded Tat-mPEG-PCL micelles (size 88.5 nm, ζ-potential +10 mV, EE% 62) showed C6 higher cytotoxic effect on rat glioma cells *in vitro* compared to micelles not modified with the CPP and more interestingly, after nasal administration prolonged survival of rats bearing intracranial C6 glioma (including 1 long term survivor) compared to the control micelles and drug solution (1.2 mg/kg, once-a-day for one week) [162]. In the case of siRNA, the nucleic acid was condensed with Tat-mPEG-PCL to obtain polyplexes of 50-100 nm. Brain distribution studies after nasal administration, carried out loading Alexa-dextran 10 kDa as model of siRNA in micelles, evidenced an increase in brain accumulation in comparison to controls (IV Tat-

mPEG-PCL micelles or IN mPEG-PCL micelles) due to Tat-promoted permeation of the nasal mucosa and increased uptake within olfactory and trigeminal nerves [163].

Despite the impressing translocation abilities, CPPs have some drawbacks such as sequestration in endosomes, limited intracellular localization profiles and lack efficient transport to the cytoplasm [158]. These drawbacks have prompted the development of different delivery approaches. For example, the group of Paolo Giunchedi from University of Sassari designed a drug delivery system for the N2B delivery of the complex of the 29-amino-acid peptide derived from the rabiesvirus glycoprotein (RVG) with siRNA interfering with the expression of BACE1, the β secretase responsible for the processing of amyloid precursor protein in β amyloid peptide the main constituent of extracellular plaques hallmark of AD. The RVG-siRNA complex was loaded in SLN coated with chitosan and preliminary experiments showed an improved crossing of CaCo-2 cells monolayer by RVG-siRNA formulated in SLN and especially in chitosan-coated SLN, compared to the naked complex. In this approach, the mucoadhesive nanocarrier must protect the complex and help it cross the nasal mucosal barrier to allow interaction of RVG cell penetrating peptide with acetylcholine receptors located at the trigeminal nerve ending and olfactory bulb. This approach has to still be validated with *in vivo* experiments [164].

5.3 Other Targeting Approaches

Several other ligands have been indicated to be potentially useful to enhance nose-to-brain delivery and in this section some examples are provided of the most interesting approaches alternative to lectins and cell penetrating peptides.

One of the early approaches for targeted drug delivery suggested also for other administration routes has been the use of viral vectors. Frenken and Solomon adopted filamentous bacteriophages as vector for the nasal administration of anti-β amyloid (Aβ) antibodies designed for the monitoring of amyloid plaques of living AD patients. The bacteriophage f88 was genetically engineered to encode on its surface protein III a single-chain antibody constructed from variable sections of light and heavy chains of anti- Aβ IgM 508 antibody. After three daily nasal administration of the filamentous bacteriophage vector, amyloid plaques were successfully targeted and visualized fluorescent-labeled antiphage antibodies in the olfactory bulb and the hippocampus region of transgenic mice carrying a double mutation in the amyloid precursor protein (APP). The crossing of the nasal barrier was attributed to the linear structure of the phage, already demonstrated to provide penetration properties in various membranes, while the lack of spreading to other brain

sections suggested a transport via the olfactory neurons. The vector was proven to be inert and non-toxic, despite one of the possible drawbacks of viral vectors could be the trigger of immune defence mechanisms such as the activation of microglia scavenger cells [165]. Interestingly, the approach is the object of a filed patent application [166].

Lactoferrin (Lf), a natural iron-binding cationic glycoprotein of the transferrin family, has been used as targeting ligand on the surface of nanocarriers as Lf receptor has been demonstrated to be highly expressed on the surface of respiratory epithelial cells as well as on neurons and brain endothelial cells [167,168]. For this reason, lactoferrin modified PEG-PCL nanoparticles were developed to enable brain delivery following intranasal administration of the neuroprotective NAP peptide, a fragment of the activity-dependent neuroprotective protein. Nanoparticles were prepared using emulsion/solvent evaporation technique followed by conjugation with thiolated Lf (size 88 nm, PDI 0.22, ζ-potential -24 mV, EE% 48, DL% 0.62). The Lf targeted nanoparticles not only increased brain accumulation more than two folds compared to unmodified nanoparticles, but showed improved neuroprotection effects in an AD model, i.e. mice intracerebroventricularly co-injected with ibotenic acid and β-amyloid$_{1-40}$, as shown by behavioural experiments such as the Morris water maze task. This was found to be related to an amelioration of the disfunction cholinergic neurotransmission via a reduction in acetylcholinesterase activity and reduced depletion of choline acetyltransferase [169]. The same targeting strategy was successfully adopted for rotigotine-loaded PEG-PLGA nanoparticles for PD treatment [170] and for mPEG-PLA nanoparticles encapsulating α-asarone a drug extracted from the traditional Chinese medicine herb *Acorus tatarinowii* Schott and recently proposed for the treatment of epilepsy [171].

PEG-PLA nanoparticles loaded with the analgesic peptide α-cobrotoxin were modified with OX26 antibodies to target transferrin receptors present in the BBB after nasal administration (size 96 nm, PDI 0.11, ζ-potential -33 mV, EE% 82). Results showed that brain delivery of the peptide labelled with fluorescein isothiocyanate was enhanced by the intranasal delivery of nanoparticles in comparison to intramuscular administration and that the enhancement was more efficient in the case of antibody targeted nanoparticles. The peptide solution could hardly penetrate the brain. Despite this was attributed by the authors to an appreciable capacity of the nanoparticles to cross the BBB, the actual mechanism of transport hypothesized, i.e. intact nanoparticles crossing the nasal mucosa, entering capillaries and finally crossing untouched the BBB was not supported by experimental evidence [172].

Finally, in an interesting approach from the group of Rodney Ho of the University of Washington (USA) liposomes targeted with the integrin-targeting ligand Arg–Gly–Asp (RGD)

were coupled with a pressurized olfactory drug (POD) delivery device to improve nose-to-brain administration of the analgesic opioid fentanyl. RGD can increase binding and enhance permeability towards epithelial cells expressing $\alpha_v\beta_3$ integrins, thus fentanyl-loaded liposomes integrating the palmitoylated peptide (size 96 nm, PDI 0.11, EE% 80) were used to enhance residence time and absorption of the nasally administered fentanyl. The POD intranasal delivery device, is a new device able to achieve a preferential deposition of the aerosolized formulation on the olfactory tissue. Experiments demonstrated that RGD-conjugated liposomes could withstand the aerosolization with POD device without size change, phospholipid bilayer disruption or impairment of the targeting. Interestingly, when liposomes were administered to rats using POD device fentanyl plasma concentrations as well as those measured in the brain 5 minutes' post-administration were inferior (but not significantly different) to those obtained using free fentanyl. However, when the analgesic effect was measured, the fentanyl-loaded RGD liposomes provided a slightly slower onset of action and lower but more prolonged analgesic effect [173]. The decisions to combine the use of a device that is designed for an optimal deposition in human nasal cavity and the adoption of small animals for *in vivo* studies appears questionable. A larger animal model such as sheep appears more adapted to the test of nasal devices.

More details about targeted nanocarriers for nose-to-brain delivery are presented in Table 3.

Table 3: Targeted nanocarriers studied for nose-to-brain delivery

Nanocarrier	Drug	Application	size (nm)	PDI	ζ potential (mV)	EE (%)	DL (%)	Biodistribution	DTE	DTP	Ref.
WGA PEG-PLA NPs	VIP	AD	100-120	-	-	70.1	1.4	Radiolabeling(^{125}I)	-	-	[88]
WGA PEG-PLA NPs	Quantum Dots	Brain Imaging	95.3 ± 41.0	-	-22.7 ± 1.2	-	-	Luminescence	-	-	[90]
STL PEG-PLGA NPs	Haloperidol	Schizophrenia	132 ± 20	0.174	-14.4 ± 0.1	73.2	0.85	HPLC	-	-	[91]
OL PEG-PLGA NPs	Urocortin	PD	114.8 ± 5.6	0.193	-	75.5	0.14	Fluorescence imaging	-	-	[92]
Tat m PEG-PCL Micelles	Camptothecin	Giloma	88.5 ± 20.2	-	10.4 ± 2.8	62.5	-	-	-	-	[95]
Tat m PEG-PCL Micelles	siRNA	CNS Disorders	51.0	-	11.3	-	-	Fluorescence imaging	-	-	[96]
RVG SLN Chitosan	siRNA	AD	358.4 ± 25.9	0.028	10.5 ± 0.8	75.5	0.14	-	-	-	[97]
Lactoferrin PEG-PCL NPs	NAP	AD	88.4 ± 7.8	0.220	-23.6 ± 1.0	47.61	0.62	Fluorescence imaging	-	-	[98]
Lactoferrin PEG-PCL NPs	Rotigotine	PD	122.0 ± 19.3	0.194	-21.3 ± 2.2	92.6	~7	Fluorescence imaging	-	-	[98]
Lactoferrin PEG-PCL NPs	α-Asarone	Epilepsy	360.1 ± 3.7	0.165	-21.8 ± 1.0	86.3	7.3	UPLC-MS	261-734	>80	[98]
mAbOX26 PEG-PLA NPs	α-Cobrotoxin	Pain	96.2 ± 6.3	0.112	-33.4 ± 1.2	82.1	-	Fluorescence analysis	-	-	[98]
RGD Liposomes	Fentanyl	Pain	96.5 ± 6.1	-	-	~80	1.4	HPLC-MS	-	-	[98]

Abbreviations: AD, Alzheimer's Disease; EE, Encapsulation Efficiency; NAP, NAPVSIPQ peptide; OL, Odorranalectin; STL, *Solanum tuberosum* Lectin; PD, Parkinson's Disease; RVG, Rabiesvirus Glycoprotein; VIP, Vasoactive Intestinal Peptide.

6 Future Perspectives of Nose-to-Brain Delivery with Nanocarriers

Nose-to-brain delivery is a fascinating topic. In the quest to achieve a non-invasive, efficient, safe and potentially disruptive innovation in the field of treatment of CNS disorders and brain diseases, the application of nanocarriers appears an asset, with several advantages but also few risks to be addressed early-on in the medicinal product development. Despite the promising results with several drugs, different materials and targeting approaches, to our knowledge not even one is actively developed by a pharmaceutical company to transfer the technology from the laboratory to the clinical stage. Several reasons are behind the lack of translational research successes for nanomedicines, some of which are related to the manufacturing scale-up, safety and quality challenges related to these non-biological complex medicinal products in general. Some reasons are however to be pinpointed in some shortcomings of the scientific works that in several cases highlighted the potential overlooking the weak points of the approach or the more pertinent controls necessary to demonstrate superiority over "traditional" formulation approaches. Furthermore, too often the drugs selected are already able in some extent to cross the BBB and/or produce CNS pharmacological effects and for which nanoencapsulation improve the only performance. Nanomedicines, especially in the case of a sensitive application such as the therapy of CNS conditions, are not required to *improve* but to *enable* therapies that would not be possible without the application of nanoencapsulation [110,111].

For these reasons, in the planning of future nose-to-brain research protocols applying nanocarriers for the formulation of the drug, the rigorous and methodical pharmaceutical scientist should take in to account the following points to demonstrate the superiority of the designed nanomedicines and provide the data necessary for further development of a medicinal product:

- Select a potent drug with unfavorable physico-chemical characteristics for N2B;
- Design particles with biocompatible, biodegradable, GRAS materials;
- Adopt a robust, validated and up scalable fabrication method;
- Determine drug release from nanocarrier in biorelevant conditions;
- Establish early-on the safety and biodegradability pattern of the nanocarrier;
- If possible/advisable adopt particles with size 100-400 nm, as smaller particles are more likely to enter the CNS with consequent concerns related to the nanotoxicology of those materials;

- Develop bioanalytical methods able to detect the drug instead of fluorescent or radioactive labels in biodistribution studies, if possible;
- Develop methods allowing to track the particles in the tissues to differentiate free drug and nanomaterial biodistribution;
- Carry out the *in vivo* experiment perfusing the organs to eliminate blood from the analytical quantitation;
- Establish the pharmacokinetics of free and nanoencapsulated drug, applying multiple and relevant controls (IV and IN administered solutions or formulations including absorption promoting excipients);
- Determine relevant parameters such as drug targeting efficiency (DTE) and direct transport percentage (DTP);
- Establish the therapeutic proof of concept through pharmacodynamics studies in a disease model as close as possible to the human;
- Combine PK and PD data to critically predict the feasibility of the treatment in terms of drug dose, amount of formulation to be administered, posology etc.;
- Select the candidate for pre-clinical/clinical development.

In conclusion, nose-to-brain delivery evolved from a series of interesting observations looked upon with skepticism to a promising, although challenging, field of research. Nanomedicines appears to be a tool pivotal to enable the brain delivery of potent drug unable to cross the BBB and when used as such they will fulfill the potential demonstrated in the many scientific studies conducted so far.

References

1. Pozzoli M, Rogueda P, Zhu B, et al. Dry powder nasal drug delivery: challenges, opportunities and a study of the commercial Teijin Puvlizer Rhinocort device and formulation. *Drug Dev Ind Pharm*. 2016;42(10):1660-1668.

2. Pires A, Fortuna A, Alves G, Falcão A. Intranasal drug delivery: how, why and what for? *J Pharm Pharm Sci*. 2009;12(3):288-311.

3. Chen Y, Liu L. Modern methods for delivery of drugs across the blood-brain barrier. *Adv Drug Deliv Rev*. 2012;64(7):640-665.

4. Gabathuler R. Approaches to transport therapeutic drugs across the blood-brain barrier to treat brain diseases. *Neurobiology of Disease*. 2010;37(1):48-57.

5. Garcia-Garcia E, Gil S, Andrieux K, et al. A relevant in vitro rat model for the evaluation of blood-brain barrier translocation of nanoparticles. *Cell Mol Life Sci*. 2005;62(12):1400-1408.

6. Alam MI, Beg S, Samad A, et al. Strategy for effective brain drug delivery. *Eur J Pharm Sci*. 2010;40(5):385-403.

7. Wong HL, Wu XY, Bendayan R. Nanotechnological advances for the delivery of CNS therapeutics. *Adv Drug Deliv Rev*. 2012;64(7):686-700.

8. Costantino L, Boraschi D. Is there a clinical future for polymeric nanoparticles as brain-targeting drug delivery agents? *Drug Discov Today*. 2012;17(7-8):367-378.

9. Pardeshi CV, Belgamwar VS. Direct nose to brain drug delivery via integrated nerve pathways bypassing the blood-brain barrier: an excellent platform for brain targeting. *Expert Opin Drug Deliv*. 2013;10(7):957-972.

10. Thorne RG, Pronk GJ, Padmanabhan V, Frey WH. Delivery of insulin-like growth factor-I to the rat brain and spinal cord along olfactory and trigeminal pathways following intranasal administration. *Neuroscience*. 2004;127(2):481-496.

11. Chapman CD, Frey WH, Craft S, Danielyan L, Hallschmid M, Benedict C. Intranasal treatment of central nervous system dysfunction in humans. *Pharm Res*. 2013;30(10):2475-2484.

12. Illum L. Transport of drugs from the nasal cavity to the central nervous system. *Eur J Pharm Sci*. 2000;11(1):1-18.

13. Ying W. The nose may help the brain: intranasal drug delivery for treating neurological diseases. *Future Neurology*. 2008;3(1):1-4.

14. Dhuria SV. Intranasal delivery to the central nervous system: mechanisms and experimental considerations. *J Pharm Sci*. 2010;99(4):1654-1673.

15. Samaridou E, Alonso MJ. Nose-to-brain peptide delivery - The potential of nanotechnology. *Bioorganic & Medicinal Chemistry*. January 2017.

16. Comfort C, Garrastazu G, Pozzoli M, Sonvico F. Opportunities and Challenges for the Nasal Administration of Nanoemulsions. *Curr Top Med Chem*. 2015;15(4):356-368..

17. Cady R. A novel intranasal breath-powered delivery system for sumatriptan: a review of technology and clinical application of the investigational product AVP-825 in the treatment of migraine. *Expert Opin Drug Deliv*. 2015;12(9):1565-1577.

18. Yamada K, Hasegawa M, Kametani S, Ito S. Nose-to-brain delivery of TS-002, prostaglandin D2 analogue. *J Drug Target*. 2007;15(1):59-66.

19. Colombo G, Lorenzini L, Zironi E, et al. Brain distribution of ribavirin after intranasal administration. *Antiviral Res*. 2011;92(3):408-414.

20. Van Woensel M, Wauthoz N, Rosière R, et al. Formulations for intranasal delivery of pharmacological agents to combat brain disease: A new opportunity to tackle GBM? *Cancers (Basel)*. 2013;5(3):1020-1048.

21. Peterson A, Bansal A, Hofman F, Chen TC, Zada G. A systematic review of inhaled intranasal therapy for central nervous system neoplasms: An emerging therapeutic option. *J Neurooncol*. 2014;116(3):437-446.

22. Duchi S, Ovadia H, Touitou E. Nasal administration of drugs as a new non-invasive strategy for efficient treatment of multiple sclerosis. *J Neuroimmunol*. 2013;258(1-2):32-40.

23. Kulkarni JA, Avachat AM. Pharmacodynamic and pharmacokinetic investigation of cyclodextrin-mediated asenapine maleate in situ nasal gel for improved bioavailability. *Drug Dev Ind Pharm*. 2017;43(2):234-245.

24. Aly AE-E, Waszczak BL. Intranasal gene delivery for treating Parkinsons disease: Overcoming the blood-brain barrier. *Expert Opin Drug Deliv*. 2015;12(12):1923-1941.

25. Sood S, Jain K, Gowthamarajan K. Intranasal therapeutic strategies for management of Alzheimer's disease. *J Drug Target*. 2014;22(4):279-294.

26. Yuan D, Yi X, Zhao Y, et al. Intranasal delivery of N-terminal modified leptin-pluronic conjugate for treatment of obesity. *J Control Release*. 2017;263:172-184.

27. Arora P, Sharma S, Garg S. Permeability issues in nasal drug delivery. *Drug Discov Today*. 2002;7(18):967-975.

28. Merkus FWHM, van den Berg MP. Can Nasal Drug Delivery Bypass the??Blood-Brain Barrier? *Drugs in R & D*. 2007;8(3):133-144.

29. Illum L. Is nose-to-brain transport of drugs in man a reality? *J Pharm Pharmacol*. 2004;56(1):3-17.

30. Djupesland PG. Nasal drug delivery devices: characteristics and performance in a clinical perspective-a review. *Drug Deliv Transl Res*. 2012;3(1):42-62.

31. Kozlovskaya L, Stepensky D. Quantitative analysis of drug delivery to the brain via nasal route. *J Control Release*. 2014;189:133-140.

32. Ruigrok MJR, de Lange ECM. Emerging Insights for Translational Pharmacokinetic and Pharmacokinetic-Pharmacodynamic Studies: Towards Prediction of Nose-to-Brain Transport in Humans. *AAPS J*. 2015;17(3):493-505.

33. Reger MA, Watson GS, Green PS, et al. Intranasal insulin improves cognition and modulates beta-amyloid in early AD. *Neurology*. 2008;70(6):440-448.

34. Craft S, Claxton A, Baker LD, et al. Effects of Regular and Long-Acting Insulin on Cognition and Alzheimer's Disease Biomarkers: A Pilot Clinical Trial. *J Alzheimers Dis*. 2017;57(4):1325-1334.

35. Quintana DS, Westlye LT, Hope S, et al. Dose-dependent social-cognitive effects of intranasal oxytocin delivered with novel Breath Powered device in adults with autism spectrum disorder: a randomized placebo-controlled double-blind crossover trial. *Transl Psychiatry*. 2017;7(5):e1136.

36. Macdonald K, Feifel D. Helping oxytocin deliver: considerations in the development of oxytocin-based therapeutics for brain disorders. *Front Neurosci*. 2013;7:35.

37. Gozes I, Morimoto BH, Tiong J, et al. NAP: Research and development of a peptide derived from activity-dependent neuroprotective protein (ADNP). *CNS Drug Rev*. 2005;11(4):353-368.

38. Morimoto BH, Schmechel D, Hirman J, et al. A double-blind, placebo-controlled, ascending-dose, randomized study to evaluate the safety, tolerability and effects on cognition of AL-108 after 12 weeks of intranasal administration in subjects with mild cognitive impairment. *Dement Geriatr Cogn Disord*. 2013;35(5-6):325-336.

39. Boxer AL, Lang AE, Grossman M, et al. Davunetide in patients with progressive supranuclear palsy: a randomised, double-blind, placebo-controlled phase 2/3 trial. *Lancet Neurol*. 2014;13(7):676-685.

40. Landis MS, Boyden T, Pegg S. Nasal-to-CNS drug delivery: where are we now and where are we heading? An industrial perspective. *Ther Deliv*. 2012;3(2):195-208.

41. Kürti L, Gáspár R, Márki Á, et al. In vitro and in vivo characterization of meloxicam nanoparticles designed for nasal administration. *Eur J Pharm Sci*. 2013;50(1):86-92.

42. Bartos C, Ambrus R, Sipos P, et al. Study of sodium hyaluronate-based intranasal formulations containing micro- or nanosized meloxicam particles. *Int J Pharm*. 2015;491(1-2):198-207.

43. Abdelbary GA, Tadros MI. Brain targeting of olanzapine via intranasal delivery of core-shell difunctional block copolymer mixed nanomicellar carriers: In vitro characterization, ex vivo estimation of nasal toxicity and in vivo biodistribution studies. *Int J Pharm*. 2013;452(1-2):300-310.

44. Nour SA, Abdelmalak NS, Naguib MJ, Rashed HM, Ibrahim AB. Intranasal brain-targeted clonazepam polymeric micelles for immediate control of status epilepticus: in vitro optimization, ex vivo determination of cytotoxicity, in vivo biodistribution and pharmacodynamics studies. *Drug Deliv*. 2016;23(9):3681-3695.

45. Arumugam K, Subramanian GS, Mallayasamy SR, Averineni RK, Reddy MS, Udupa N. A study of rivastigmine liposomes for delivery into the brain through intranasal route. *Acta Pharm*. 2008;58(3):287-297.

46. Gupta S, Kesarla R, Chotai N, Misra A, Omri A. Systematic Approach for the Formulation and Optimization of Solid Lipid Nanoparticles of Efavirenz by High Pressure

Homogenization Using Design of Experiments for Brain Targeting and Enhanced Bioavailability. *Biomed Res Int*. 2017;2017(1):5984014-5984018. doi:10.1155/2017/5984014.

47. Fatouh AM, Elshafeey AH, Abdelbary A. Intranasal agomelatine solid lipid nanoparticles to enhance brain delivery: Formulation, optimization and in vivo pharmacokinetics. *Drug Des Devel Ther*. 2017;11:1815-1825. doi:10.2147/DDDT.S102500.

48. Alam T, Pandit J, Vohora D, Aqil M, Ali A, Sultana Y. Optimization of nanostructured lipid carriers of lamotrigine for brain delivery: in vitrocharacterization and in vivoefficacy in epilepsy. *Expert Opin Drug Deliv*. 2014;12(2):181-194. doi:10.1517/17425247.2014.945416.

49. Khan A, Imam SS, Aqil M, et al. Brain Targeting of Temozolomide via the Intranasal Route Using Lipid-Based Nanoparticles: Brain Pharmacokinetic and Scintigraphic Analyses. *Mol Pharm*. 2016;13(11):3773-3782. doi:10.1021/acs.molpharmaceut.6b00586.

50. Kubek MJ, Domb AJ, Veronesi MC. Attenuation of Kindled Seizures by Intranasal Delivery of Neuropeptide-Loaded Nanoparticles. *Neurotherapeutics*. 2009;6(2):359-371. doi:10.1016/j.nurt.2009.02.001.

51. Sharma D, Sharma RK, Sharma N, et al. Nose-To-Brain Delivery of PLGA-Diazepam Nanoparticles. *AAPS PharmSciTech*. 2015;16(5):1108-1121. doi:10.1208/s12249-015-0294-0.

52. Ahmad N, Ahmad I, Umar S, Iqbal Z, Samim M, Ahmad FJ. PNIPAM nanoparticles for targeted and enhanced nose-to-brain delivery of curcuminoids: UPLC/ESI-Q-ToF-MS/MS-based pharmacokinetics and pharmacodynamic evaluation in cerebral ischemia model. *Drug Deliv*. 2016;23(7):2095-2114. doi:10.3109/10717544.2014.941076.

53. Wong LR, Ho PC. Role of serum albumin as a nanoparticulate carrier for nose-to-brain delivery of R-flurbiprofen: implications for the treatment of Alzheimer's disease. *J Pharm Pharmacol*. 2018;70(1):59-69. doi:10.1111/jphp.12836.

54. Win-Shwe T-T, Sone H, Kurokawa Y, et al. Effects of PAMAM dendrimers in the mouse brain after a single intranasal instillation. *Toxicol Lett*. 2014;228(3):207-215. doi:10.1016/j.toxlet.2014.04.020.

55. Lungare S, Hallam K, Badhan RKS. Phytochemical-loaded mesoporous silica nanoparticles for nose-to-brain olfactory drug delivery. *Int J Pharm*. 2016;513(1-2):280-293. doi:10.1016/j.ijpharm.2016.09.042.

56. Mahajan HS, Mahajan MS, Nerkar PP, Agrawal A. Nanoemulsion-based intranasal drug delivery system of saquinavir mesylate for brain targeting. *Drug Deliv*. 2014;21(2):148-154. doi:10.3109/10717544.2013.838014.

57. Mistry A, Stolnik S, Illum L. Nanoparticles for direct nose-to-brain delivery of drugs. *Int J Pharm*. 2009;379(1):146-157. doi:10.1016/j.ijpharm.2009.06.019.

58. Kozlovskaya L, Stepensky D. Quantitative analysis of the brain-targeted delivery of drugs and model compounds using nano-delivery systems. *J Control Release*. 2013;171(1):17-23. doi:10.1016/j.jconrel.2013.06.028.

59. Md S, Mustafa G, Baboota S, Ali J. Nanoneurotherapeutics approach intended for direct nose to brain delivery. *Drug Dev Ind Pharm*. 2015;41(12):1922-1934. doi:10.3109/03639045.2015.1052081.

60. Pires PC, Santos AO. Nanosystems in nose-to-brain drug delivery_ A review of non-clinical brain targeting studies. 2018;270:89-100. doi:10.1016/j.jconrel.2017.11.047.

61. Feng Y, He H, Li F, Lu Y, Qi J, Wu W. An update on the role of nanovehicles in nose-to-brain drug delivery. *Drug Discov Today*. January 2018. doi:10.1016/j.drudis.2018.01.005.

62. Kulkarni AD, Vanjari YH, Sancheti KH, Belgamwar VS, Surana SJ, Pardeshi CV. Nanotechnology-mediated nose to brain drug delivery for Parkinson's disease: a mini review. *J Drug Target*. 2015;23(9):775-788. doi:10.3109/1061186X.2015.1020809.

63. Fonseca-Santos B, Gremião MPD, Chorilli M. Nanotechnology-based drug delivery systems for the treatment of Alzheimer's disease. *Int J Nanomedicine*. 2015;10:4981-5003. doi:10.2147/IJN.S87148.

64. Marianecci C, Rinaldi F, Hanieh PN, Paolino D, Marzio LD, Carafa M. Nose to Brain Delivery: New Trends in Amphiphile-Based "Soft" Nanocarriers. *Current Pharmaceutical Design*. 2015;21(36):5225-5232.

65. Kanazawa T. Brain delivery of small interfering ribonucleic acid and drugs through intranasal administration with nano-sized polymer micelles. *Med Devices (Auckl)*. 2015;8:57-64. doi:10.2147/MDER.S70856.

66. Selvaraj K, Gowthamarajan K, Karri VVSR. Nose to brain transport pathways an overview: potential of nanostructured lipid carriers in nose to brain targeting. *Artif Cells Nanomed Biotechnol*. 2017;7:1-8. doi:10.1080/21691401.2017.1420073.

67. Gartziandia O, Egusquiaguirre SP, Bianco J, et al. Nanoparticle transport across in vitro olfactory cell monolayers. *Int J Pharm*. 2016;499(1-2):81-89. doi:10.1016/j.ijpharm.2015.12.046.

68. Yang M, Lai SK, Yu T, et al. Nanoparticle penetration of human cervicovaginal mucus: the effect of polyvinyl alcohol. *J Control Release*. 2014;192:202-208. doi:10.1016/j.jconrel.2014.07.045.

69. Musumeci T, Pellitteri R, Spatuzza M, Puglisi G. Nose-to-brain delivery: Evaluation of polymeric nanoparticles on olfactory unsheathing cells uptake. *J Pharm Sci*. 2014;103(2):628-635. doi:10.1002/jps.23836.

70. Murali K, Kenesei K, Li Y, Demeter K, Környei Z, Madarász E. Uptake and bio-reactivity of polystyrene nanoparticles is affected by surface modifications, ageing and LPS adsorption: In vitro studies on neural tissue cells. *Nanoscale*. 2015;7(9):4199-4210. doi:10.1039/c4nr06849a.

71. Mistry A, Stolnik S, Illum L. Nose-to-Brain Delivery: Investigation of the Transport of Nanoparticles with Different Surface Characteristics and Sizes in Excised Porcine Olfactory Epithelium. *Mol Pharm*. 2015;12(8):2755-2766. doi:10.1021/acs.molpharmaceut.5b00088.

72. Mistry A, Glud SZ, Kjems J, et al. Effect of physicochemical properties on intranasal nanoparticle transit into murine olfactory epithelium. *J Drug Target*. 2009;17(7):543-552. doi:10.1080/10611860903055470.

73. Lai SK, Wang Y-Y, Hanes J. Mucus-penetrating nanoparticles for drug and gene delivery to mucosal tissues. *Adv Drug Deliv Rev*. 2009;61(2):158-171. doi:10.1016/j.addr.2008.11.002.

74. Xu Q, Ensign LM, Boylan NJ, et al. Impact of Surface Polyethylene Glycol (PEG) Density on Biodegradable Nanoparticle Transport in Mucus ex Vivo and Distribution in Vivo. *ACS Nano*. 2015;9(9):9217-9227. doi:10.1021/acsnano.5b03876.

75. Ahmad E, Feng Y, Qi J, et al. Evidence of nose-to-brain delivery of nanoemulsions: Cargoes but not vehicles. *Nanoscale*. 2017;9(3):1174-1183. doi:10.1039/c6nr07581a.

76. Kanazawa T, Kaneko M, Niide T, et al. Enhancement of nose-to-brain delivery of hydrophilic macromolecules with stearate- or polyethylene glycol-modified arginine-rich peptide. *Int J Pharm*. 2017;530(1-2):195-200. doi:10.1016/j.ijpharm.2017.07.077.

77. Gabal YM, Kamel AO, Sammour OA, Elshafeey AH. Effect of surface charge on the brain delivery of nanostructured lipid carriers in situ gels via the nasal route. *Int J Pharm*. 2014;473(1):442-457. doi:10.1016/j.ijpharm.2014.07.025.

78. Casettari L, Illum L. Chitosan in nasal delivery systems for therapeutic drugs. *J Control Release*. 2014;190C:189-200. doi:10.1016/j.jconrel.2014.05.003.

79. Lucchini RG, Dorman DC, Elder A, Veronesi B. Neurological impacts from inhalation of pollutants and the nose-brain connection. *NeuroToxicology*. 2012;33(4):838-841. doi:10.1016/j.neuro.2011.12.001.

80. Karmakar A, Zhang Q, Zhang Y. Neurotoxicity of nanoscale materials. *J Food Drug Anal*. 2014;22(1):147-160. doi:10.1016/j.jfda.2014.01.012.

81. Simkó M, Mattsson MO. Risks from accidental exposures to engineered nanoparticles and neurological health effects: A critical review. *Part Fibre Toxicol*. 2010;7:42. doi:10.1186/1743-8977-7-42.

82. Marttin E, Schipper NGM, Coos Verhoef J, Merkus FWHM. Nasal mucociliary clearance as a factor in nasal drug delivery. *Adv Drug Deliv Rev*. 1998;29(1-2):13-38. doi:10.1016/S0169-409X(97)00059-8.

83. Ugwoke MI, Agu RU, Verbeke N, Kinget R. Nasal mucoadhesive drug delivery: background, applications, trends and future perspectives. *Adv Drug Deliv Rev*. 2005;57(11):1640-1665. doi:10.1016/j.addr.2005.07.009.

84. Sosnik A, Neves das J, Sarmento B. Mucoadhesive polymers in the design of nano-drug delivery systems for administration by non-parenteral routes: A review. *Progress in Polymer Science*. 2014;39(12):2030-2075. doi:10.1016/j.progpolymsci.2014.07.010.

85. Charlton S, Jones NS, Davis SS, Illum L. Distribution and clearance of bioadhesive formulations from the olfactory region in man: effect of polymer type and nasal delivery device. *Eur J Pharm Sci*. 2007;30(3-4):295-302. doi:10.1016/j.ejps.2006.11.018.

86. Horvát S, Fehér A, Wolburg H, et al. Sodium hyaluronate as a mucoadhesive component in nasal formulation enhances delivery of molecules to brain tissue. *Eur J Pharm Biopharm*. 2009;72(1):252-259. doi:10.1016/j.ejpb.2008.10.009.

87. Betbeder D, Spérandio S, Latapie JP, et al. Biovector nanoparticles improve antinociceptive efficacy of nasal morphine. *Pharm Res*. 2000;17(6):743-748.

88. Fonseca FN, Betti AH, Carvalho FC, et al. Mucoadhesive amphiphilic methacrylic copolymer-functionalized poly(ε-caprolactone) nanocapsules for nose-to-brain delivery of olanzapine. *J Biomed Nanotechnol*. 2014;11(8):1472-1481. doi:10.1166/jbn.2015.2078.

89. Lemarchand C, Gref R, Couvreur P. Polysaccharide-decorated nanoparticles. *Eur J Pharm Biopharm*. 2004;58(2):327-341. doi:10.1016/j.ejpb.2004.02.016.

90. Luppi B, Bigucci F, Corace G, et al. Albumin nanoparticles carrying cyclodextrins for nasal delivery of the anti-Alzheimer drug tacrine. *Eur J Pharm Sci*. 2011;44(4):559-565. doi:10.1016/j.ejps.2011.10.002.

91. Devkar TB, Tekade AR, Khandelwal KR. Surface engineered nanostructured lipid carriers for efficient nose to brain delivery of ondansetron HCl using Delonix regia gum as a natural mucoadhesive polymer. *Colloids Surf B Biointerfaces*. 2014;122:143-150. doi:10.1016/j.colsurfb.2014.06.037.

92. Haque S, Md S, Fazil M, et al. Venlafaxine loaded chitosan NPs for brain targeting: pharmacokinetic and pharmacodynamic evaluation. *Carbohydr Polym*. 2012;89(1):72-79. doi:10.1016/j.carbpol.2012.02.051.

93. Deli MA. Potential use of tight junction modulators to reversibly open membranous barriers and improve drug delivery. *Biochim Biophys Acta*. 2009;1788(4):892-910. doi:10.1016/j.bbamem.2008.09.016.

94. Vllasaliu D, Exposito-Harris R, Heras A, et al. Tight junction modulation by chitosan nanoparticles: comparison with chitosan solution. *Int J Pharm*. 2010;400(1-2):183-193. doi:10.1016/j.ijpharm.2010.08.020.

95. Wang X, He H, Leng W, Tang X. Evaluation of brain-targeting for the nasal delivery of estradiol by the microdialysis method. *Int J Pharm*. 2006;317(1):40-46. doi:10.1016/j.ijpharm.2006.02.055.

96. Fazil M, Md S, Haque S, et al. Development and evaluation of rivastigmine loaded chitosan nanoparticles for brain targeting. *Eur J Pharm Sci*. 2012;47(1):6-15. doi:10.1016/j.ejps.2012.04.013.

97. Alam S, Khan ZI, Mustafa G, et al. Development and evaluation of thymoquinone-encapsulated chitosan nanoparticles for nose-to-brain targeting: a pharmacoscintigraphic study. *Int J Nanomedicine*. 2012;7:5705-5718. doi:10.2147/IJN.S35329.

98. Md S, Khan RA, Mustafa G, et al. Bromocriptine loaded chitosan nanoparticles intended for direct nose to brain delivery: Pharmacodynamic, Pharmacokinetic and Scintigraphy study in mice model. *Eur J Pharm Sci*. 2013;48(3):393-405. doi:10.1016/j.ejps.2012.12.007.

99. Jafarieh O, Md S, Ali M, et al. Design, characterization, and evaluation of intranasal delivery of ropinirole-loaded mucoadhesive nanoparticles for brain targeting. *Drug Dev Ind Pharm*. 2015;41(10):1674-1681. doi:10.3109/03639045.2014.991400.

100. Raj R, Wairkar S, Sridhar V, Gaud R. Pramipexole dihydrochloride loaded chitosan nanoparticles for nose to brain delivery: Development, characterization and in vivo anti-Parkinson activity. *Int J Biol Macromol*. 2017;109:27-35. doi:10.1016/j.ijbiomac.2017.12.056.

101. Javia A, Thakkar H. Intranasal delivery of tapentadol hydrochloride–loaded chitosan nanoparticles: formulation, characterisation and its in vivoevaluation. *J Microencapsul*. 2017;34(7):644-658. doi:10.1080/02652048.2017.1375038.

102. Kumar M, Pandey RS, Patra KC, et al. Evaluation of neuropeptide loaded trimethyl chitosan nanoparticles for nose to brain delivery. *Int J Biol Macromol*. 2013;61:189-195. doi:10.1016/j.ijbiomac.2013.06.041.

103. Shahnaz G, Vetter A, Barthelmes J, et al. Thiolated chitosan nanoparticles for the nasal administration of leuprolide: bioavailability and pharmacokinetic characterization. *Int J Pharm*. 2012;428(1-2):164-170. doi:10.1016/j.ijpharm.2012.02.044.

104. Patel D, Naik S, Misra A. Improved transnasal transport and brain uptake of tizanidine HCl-loaded thiolated chitosan nanoparticles for alleviation of pain. *J Pharm Sci*. 2012;101(2):690-706. doi:10.1002/jps.22780.

105. Patel D, Naik S, Chuttani K, Mathur R, Mishra AK, Misra A. Intranasal delivery of cyclobenzaprine hydrochloride-loaded thiolated chitosan nanoparticles for pain relief. *J Drug Target*. 2013;21(8):759-769. doi:10.3109/1061186X.2013.818676.

106. Singh D, Rashid M, Hallan SS, Mehra NK, Prakash A, Mishra N. Pharmacological evaluation of nasal delivery of selegiline hydrochloride-loaded thiolated chitosan nanoparticles for the treatment of depression. *Artif Cells Nanomed Biotechnol*. 2016;44(3):865-877. doi:10.3109/21691401.2014.998824.

107. Di Gioia S, Trapani A, Mandracchia D, et al. Intranasal delivery of dopamine to the striatum using glycol chitosan/sulfobutylether-β-cyclodextrin based nanoparticles. *Eur J Pharm Biopharm*. 2015;94:180-193. doi:10.1016/j.ejpb.2015.05.019.

108. Chalikwar SS, Mene BS, Pardeshi CV, Belgamwar VS, Surana SJ. Self-Assembled, Chitosan Grafted PLGA Nanoparticles for Intranasal Delivery: Design, Development and Ex VivoCharacterization. *Polym Plast Technol Eng*. 2013;52(4):368-380. doi:10.1080/03602559.2012.751999.

109. Salade L, Wauthoz N, Deleu M, et al. Development of coated liposomes loaded with ghrelin for nose-to-brain delivery for the treatment of cachexia. *Int J Nanomedicine*. 2017;12:8531-8543. doi:10.2147/IJN.S147650.

110. Romana B, Batger M, Prestidge C, Colombo G, Sonvico F. Expanding the Therapeutic Potential of Statins by Means of Nanotechnology Enabled Drug Delivery Systems. *Curr Top Med Chem*. 2014;14(9):1182-1193. doi:10.2174/1568026614666140329232252.

111. Sonvico F, Zimetti F, Pohlmann AR, Guterres SS. Drug delivery to the brain: how can nanoencapsulated statins be used in the clinic? *Ther Deliv*. 2017;8(8):625-631. doi:10.4155/tde-2017-0044.

112. Clementino A, Batger M, Garrastazu G, et al. The nasal delivery of nanoencapsulated statins - an approach for brain delivery. *Int J Nanomedicine*. 2016;11:6575-6590. doi:10.2147/IJN.S119033.

113. Kumar M, Misra A, Babbar AK, Mishra AK, Mishra P, Pathak K. Intranasal nanoemulsion based brain targeting drug delivery system of risperidone. *Int J Pharm*. 2008;358(1-2):285-291. doi:10.1016/j.ijpharm.2008.03.029.

114. Samia O, Hanan R, Kamal ET. Carbamazepine mucoadhesive nanoemulgel (MNEG) as brain targeting delivery system via the olfactory mucosa. *Drug Deliv*. 2012;19(1):58-67. doi:10.3109/10717544.2011.644349.

115. Perez AP, Mundiña-Weilenmann C, Romero EL, Morilla MJ. Increased brain radioactivity by intranasal P-labeled siRNA dendriplexes within in situ-forming mucoadhesive gels. *Int J Nanomedicine*. 2012;7:1373-1385. doi:10.2147/IJN.S28261.

116. Jain DS, Bajaj AN, Athawale RB, et al. Thermosensitive PLA based nanodispersion for targeting brain tumor via intranasal route. *Mater Sci Eng C Mater Biol Appl*. 2016;63:411-421. doi:10.1016/j.msec.2016.03.015.

117. Wavikar PR, Vavia PR. Rivastigmine-loaded in situ gelling nanostructured lipid carriers for nose to brain delivery. *J Liposome Res*. 2015;25(2):141-149. doi:10.3109/08982104.2014.954129.

118. Hao J, Zhao J, Zhang S, et al. Fabrication of an ionic-sensitive in situ gel loaded with resveratrol nanosuspensions intended for direct nose-to-brain delivery. *Colloids Surf B Biointerfaces*. 2016;147:376-386. doi:10.1016/j.colsurfb.2016.08.011.

119. Sigurdsson HH, Kirch J, Lehr C-M. Mucus as a barrier to lipophilic drugs. *Int J Pharm*. 2013;453(1):56-64. doi:10.1016/j.ijpharm.2013.05.040.

120. Lieleg O, Ribbeck K. Biological hydrogels as selective diffusion barriers. *Trends in Cell Biology*. 2011;21(9):543-551. doi:10.1016/j.tcb.2011.06.002.

121. Cone RA. Barrier properties of mucus. *Adv Drug Deliv Rev*. 2009;61(2):75-85. doi:10.1016/j.addr.2008.09.008.

122. Vila A, Gill H, McCallion O, Alonso MJ. Transport of PLA-PEG particles across the nasal mucosa: Effect of particle size and PEG coating density. *J Control Release*. 2004;98(2):231-244. doi:10.1016/j.jconrel.2004.04.026.

123. Schuster BS, Suk JS, Woodworth GF, Hanes J. Nanoparticle diffusion in respiratory mucus from humans without lung disease. *Biomaterials*. 2013;34(13):3439-3446. doi:10.1016/j.biomaterials.2013.01.064.

124. Lai SK, Suk JS, Pace A, et al. Drug carrier nanoparticles that penetrate human chronic rhinosinusitis mucus. *Biomaterials*. 2011;32(26):6285-6290. doi:10.1016/j.biomaterials.2011.05.008.

125. Mert O, Lai SK, Ensign L, et al. NANOMEDICINE. *J Control Release*. 2012;157(3):455-460. doi:10.1016/j.jconrel.2011.08.032.

126. Xu Q, Boylan NJ, Cai S, Miao B, Patel H, Hanes J. Scalable method to produce biodegradable nanoparticles that rapidly penetrate human mucus. *J Control Release*. 2013;170(2):279-286. doi:10.1016/j.jconrel.2013.05.035.

127. Kirch J, Schneider A, Abou B, et al. Optical tweezers reveal relationship between microstructure and nanoparticle penetration of pulmonary mucus. *Proc Natl Acad Sci USA*. 2012;109(45):18355-18360. doi:10.1073/pnas.1214066109.

128. Sharma D, Sharma RK, Bhatnagar A, et al. Nose to Brain Delivery of Midazolam Loaded PLGA Nanoparticles: In Vitro and In Vivo Investigations. *Curr Drug Deliv*. 2016;13(4):557-564.

129. Sekerdag E, Lüle S, Bozdağ Pehlivan S, et al. A potential non-invasive glioblastoma treatment: Nose-to-brain delivery of farnesylthiosalicylic acid incorporated hybrid nanoparticles. *J Control Release*. 2017;261:187-198. doi:10.1016/j.jconrel.2017.06.032.

130. Zhang Q-Z, Zha L-S, Zhang Y, et al. The brain targeting efficiency following nasally applied MPEG-PLA nanoparticles in rats. *J Drug Target*. 2006;14(5):281-290. doi:10.1080/10611860600721051.

131. Wang Y-Y, Lai SK, Suk JS, Pace A, Cone R, Hanes J. Addressing the PEG mucoadhesivity paradox to engineer nanoparticles that “slip” through the human mucus barrier. *Angew Chem Int Ed Engl*. 2008;47(50):9726-9729. doi:10.1002/anie.200803526.

132. Behrens I, Pena AIV, Alonso MJ, Kissel T. Comparative uptake studies of bioadhesive and non-bioadhesive nanoparticles in human intestinal cell lines and rats: the effect of mucus on particle adsorption and transport. *Pharm Res*. 2002;19(8):1185-1193.

133. Salmaso S, Caliceti P. Stealth properties to improve therapeutic efficacy of drug nanocarriers. *J Drug Deliv*. 2013;2013:374252. doi:10.1155/2013/374252.

134. Guo Y, Luo J, Tan S, Otieno BO, Zhang Z. The applications of Vitamin E TPGS in drug delivery. *Eur J Pharm Sci*. 2013;49(2):175-186. doi:10.1016/j.ejps.2013.02.006.

135. Jain R, Nabar S, Dandekar P, Patravale V. Micellar nanocarriers: potential nose-to-brain delivery of zolmitriptan as novel migraine therapy. *Pharm Res*. 2010;27(4):655-664. doi:10.1007/s11095-009-0041-x.

136. Jain R, Nabar S, Dandekar P, et al. Formulation and evaluation of novel micellar nanocarrier for nasal delivery of sumatriptan. *Nanomedicine (London, England)*. 2010;5(4):575-587. doi:10.2217/nnm.10.28.

137. Salama HA, Mahmoud AA, Kamel AO, Abdel Hady M, Awad GAS. Phospholipid based colloidal poloxamer-nanocubic vesicles for brain targeting via the nasal route. *Colloids Surf B Biointerfaces*. 2012;100:146-154. doi:10.1016/j.colsurfb.2012.05.010.

138. Abdelrahman FE, Elsayed I, Gad MK, Elshafeey AH, Mohamed MI. Response surface optimization, Ex vivo and In vivo investigation of nasal spanlastics for bioavailability enhancement and brain targeting of risperidone. *Int J Pharm*. 2017;530(1-2):1-11. doi:10.1016/j.ijpharm.2017.07.050.

139. Zhao Y-Z, Li X, Lu C-T, et al. Gelatin nanostructured lipid carriers-mediated intranasal delivery of basic fibroblast growth factor enhances functional recovery in hemiparkinsonian rats. *Nanomedicine*. 2014;10(4):755-764. doi:10.1016/j.nano.2013.10.009.

140. Bhatt R, Singh D, Prakash A, Mishra N. Development, characterization and nasal delivery of rosmarinic acid-loaded solid lipid nanoparticles for the effective management of Huntington's disease. *Drug Deliv*. 2015;22(7):931-939. doi:10.3109/10717544.2014.880860.

141. Illum L. Nasal drug delivery--possibilities, problems and solutions. *J Control Release*. 2003;87(1-3):187-198.

142. Abd-Elal RMA, Shamma RN, Rashed HM, Bendas ER. Trans-nasal zolmitriptan novasomes: in-vitro preparation, optimization and in-vivo evaluation of brain targeting efficiency. *Drug Deliv*. 2016;23(9):3374-3386. doi:10.1080/10717544.2016.1183721.

143. Singh AP, Saraf SK, Saraf SA. SLN approach for nose-to-brain delivery of alprazolam. *Drug Deliv Transl Res*. 2012;2(6):498-507. doi:10.1007/s13346-012-0110-2.

144. Ruenraroengsak P, Cook JM, Florence AT. Nanosystem drug targeting: Facing up to complex realities. *J Control Release*. 2010;141(3):265-276. doi:10.1016/j.jconrel.2009.10.032.

145. Bies C, Lehr C-M, Woodley JF. Lectin-mediated drug targeting: history and applications. *Adv Drug Deliv Rev*. 2004;56(4):425-435. doi:10.1016/j.addr.2003.10.030.

146. Broadwell RD, Balin BJ. Endocytic and exocytic pathways of the neuronal secretory process and trans synaptic transfer of wheat germ agglutinin-horseradish peroxidasein vivo. *J Comp Neurol*. 1985;242(4):632-650. doi:10.1002/cne.902420410.

147. Thorne RG, Emory CR, Ala TA, Frey WH. Quantitative analysis of the olfactory pathway for drug delivery to the brain. *Brain Res*. 1995;692(1-2):278-282.

148. Gao X, Tao W, Lu W, et al. Lectin-conjugated PEG-PLA nanoparticles: preparation and brain delivery after intranasal administration. *Biomaterials*. 2006;27(18):3482-3490. doi:10.1016/j.biomaterials.2006.01.038.

149. Liu Q, Shen Y, Chen J, et al. Nose-to-brain transport pathways of wheat germ agglutinin conjugated PEG-PLA nanoparticles. *Pharm Res*. 2012;29(2):546-558. doi:10.1007/s11095-011-0641-0.

150. Gao X, Wu B, Zhang Q, et al. Brain delivery of vasoactive intestinal peptide enhanced with the nanoparticles conjugated with wheat germ agglutinin following intranasal administration. *J Control Release*. 2007;121(3):156-167. doi:10.1016/j.jconrel.2007.05.026.

151. Gao X, Chen J, Chen J, Wu B, Chen H, Jiang X. Quantum Dots Bearing Lectin-Functionalized Nanoparticles as a Platform for In VivoBrain Imaging. *Bioconjug Chem*. 2008;19(11):2189-2195. doi:10.1021/bc8002698.

152. Chen J, Zhang C, Liu Q, et al. Solanum tuberosumlectin-conjugated PLGA nanoparticles for nose-to-brain delivery: in vivoand in vitroevaluations. *J Drug Target*. 2011;20(2):174-184. doi:10.3109/1061186X.2011.622396.

153. Gao X, Chen J, TAO W, et al. UEA I-bearing nanoparticles for brain delivery following intranasal administration. *Int J Pharm*. 2007;340(1-2):207-215. doi:10.1016/j.ijpharm.2007.03.039.

154. Wen Z, Yan Z, He R, et al. Brain targeting and toxicity study of odorranalectin-conjugated nanoparticles following intranasal administration. *Drug Deliv*. 2011;18(8):555-561. doi:10.3109/10717544.2011.596583.

155. Piazza J, Hoare T, Molinaro L, et al. Haloperidol-loaded intranasally administered lectin functionalized poly(ethylene glycol)–block-poly(d,l)-lactic-co-glycolic acid (PEG–PLGA)

nanoparticles for the treatment of schizophrenia. *Eur J Pharm Biopharm*. 2014;87(1):30-39. doi:10.1016/j.ejpb.2014.02.007.

156. Wen Z, Yan Z, Hu K, et al. Odorranalectin-conjugated nanoparticles: Preparation, brain delivery and pharmacodynamic study on Parkinson's disease following intranasal administration. *J Control Release*. 2011;151(2):131-138. doi:10.1016/j.jconrel.2011.02.022.

157. Liu Q, Shao X, Chen J, et al. In vivo toxicity and immunogenicity of wheat germ agglutinin conjugated poly(ethylene glycol)-poly(lactic acid) nanoparticles for intranasal delivery to the brain. *Toxicol Appl Pharmacol*. 2011;251(1):79-84. doi:10.1016/j.taap.2010.12.003.

158. Fonseca SB, Pereira MP, Kelley SO. Recent advances in the use of cell-penetrating peptides for medical and biological applications. *Adv Drug Deliv Rev*. 2009;61(11):953-964. doi:10.1016/j.addr.2009.06.001.

159. Lin T, Liu E, He H, et al. Nose-to-brain delivery of macromolecules mediated by cell-penetrating peptides. *Acta Pharm Sin B*. 2016;6(4):352-358. doi:10.1016/j.apsb.2016.04.001.

160. Xia H, Gao X, Gu G, et al. Low molecular weight protamine-functionalized nanoparticles for drug delivery to the brain after intranasal administration. *Biomaterials*. 2011;32(36):9888-9898. doi:10.1016/j.biomaterials.2011.09.004.

161. Kanazawa T, Taki H, Tanaka K, Takashima Y, Okada H. Cell-penetrating peptide-modified block copolymer micelles promote direct brain delivery via intranasal administration. *Pharm Res*. 2011;28(9):2130-2139. doi:10.1007/s11095-011-0440-7.

162. Taki H, Kanazawa T, Akiyama F, Takashima Y, Okada H. Intranasal Delivery of Camptothecin-Loaded Tat-Modified Nanomicells for Treatment of Intracranial Brain Tumors. *Pharmaceuticals*. 2012;5(12):1092-1102. doi:10.3390/ph5101092.

163. Kanazawa T, Akiyama F, Kakizaki S, Takashima Y, Seta Y. Delivery of siRNA to the brain using a combination of nose-to-brain delivery and cell-penetrating peptide-modified nano-micelles. *Biomaterials*. 2013;34(36):9220-9226. doi:10.1016/j.biomaterials.2013.08.036.

164. Rassu G, Soddu E, Posadino AM, et al. Nose-to-brain delivery of BACE1 siRNA loaded in solid lipid nanoparticles for Alzheimer's therapy. *Colloids Surf B Biointerfaces*. 2017;152:296-301. doi:10.1016/j.colsurfb.2017.01.031.

165. Frenkel D, Solomon B. Filamentous phage as vector-mediated antibody delivery to the brain. *Proc Natl Acad Sci USA*. 2002;99(8):5675-5679. doi:10.1073/pnas.072027199.

166. Janda KJ. Delivery of Active Proteins to the Central Nervous System Using Phage Vectors. THE SCRIPPS RESEARCH INSTITUTE, ed. 2008;(EP20050766655):A01N43/04AI; A61K31/70AI; A61K39/00AI; A61K39/38AI; C12N5/00AI; C12N5/02AI; C12N15/00AI; C12N15/09AI; C12N15/63AI; C12N15/70AI; C12N15/74AI.

167. Suzuki YA, Lopez V, Lönnerdal B. Mammalian lactoferrin receptors: Structure and function. *Cell Mol Life Sci*. 2005;62(22):2560-2575. doi:10.1007/s00018-005-5371-1.

168. Elfinger M, Maucksch C, Rudolph C. Characterization of lactoferrin as a targeting ligand for nonviral gene delivery to airway epithelial cells. *Biomaterials*. 2007;28(23):3448-3455. doi:10.1016/j.biomaterials.2007.04.011.

169. Liu Z, Jiang M, Kang T, et al. Lactoferrin-modified PEG-co-PCL nanoparticles for enhanced brain delivery of NAP peptide following intranasal administration. *Biomaterials*. 2013;34(15):3870-3881. doi:10.1016/j.biomaterials.2013.02.003.

170. Bi CC, Wang AP, Chu YC, et al. Intranasal delivery of rotigotine to the brain with lactoferrin-modified PEG-PLGA nanoparticles for Parkinson's disease treatment. *Int J Nanomedicine*. 2016;11:6547-6559. doi:10.2147/IJN.S120939.

171. Pan L, Zhou J, Ju F, Zhu H. Intranasal delivery of α-asarone to the brain with lactoferrin-modified mPEG-PLA nanoparticles prepared by premix membrane emulsification. *Drug Deliv Transl Res*. 2018;8(1):83-96. doi:10.1007/s13346-017-0438-8.

172. Liu L, Zhang X, Li W, et al. Transferrin receptor antibody-modified α-cobrotoxin-loaded nanoparticles enable drug delivery across the blood–brain barrier by intranasal administration. *J Nanopart Res*. 2013;15(11):1343. doi:10.1007/s11051-013-2059-6.

173. Hoekman JD, Srivastava P, Ho RJY. Aerosol-stable peptide-coated liposome nanoparticles: a proof-of-concept study with opioid fentanyl in enhancing analgesic effects and reducing plasma drug exposure. *J Pharm Sci*. 2014;103(8):2231-2239. doi:10.1002/jps.24022.

CHAPTER 2

THE NASAL DELIVERY OF NANOENCAPSULATED STATINS – AN APPROACH FOR BRAIN DELIVERY

The Nasal Delivery of Nanoencapsulated Statins – An Approach for Brain Delivery

Adryana Clementino,[1,2] Mellissa Batger,[3] Gabriela Garrastazu,[2,3] Michele Pozzoli,[3] Elena Del Favero,[4] Valeria Rondelli,[4] Bianca Gutfilen,[5] Thiago Barboza,[5] Maria B, Sukkar,[3] Sergio A.L. Souza,[5] Laura Cantù,[4] and Fabio Sonvico[1,3] *

[1] Department of Pharmacy, University of Parma, Parma (PR) Italy;

[2] Conselho Nacional do Desenvolvimento Cientifico e Tecnologico - CNPq, Brasilia, Brazil;

[3] Graduate School of Health - Pharmacy, University of Technology Sydney, Ultimo, NSW, Australia;

[4] Department of Medical Biotechnologies and Traslational Medicine, LITA, University of Milano, Segrate (MI), Italy;

[5] Laboratório de Marcação de Células e Moléculas, Departamento de Radiologia, Faculdade de Medicina, Universidade Federal do Rio de Janeiro, Rio de Janeiro, Brasil

Published on December 2016, ***International Journal of Nanomedicine***

IF 4.370

Open access

Abstract

Along with their cholesterol lowering effect, statins have shown a wide range of pleiotropic effects potentially beneficial to neurodegenerative diseases, but extremely elusive via the conventional oral administration. The purpose of the present study was to prepare and characterize the physico-chemical properties along the *in vivo* biodistribution of simvastatin-loaded lecithin/chitosan nanoparticles suitable for nasal administration in view of an improved delivery of statins to the brain. Chitosan, lecithin and different oil excipients were used to prepare nanocapsules loaded with simvastatin. Particle size distribution, surface charge, structure, simvastatin loading and release and interaction with mucus of nanoparticles were determined. The nanoparticle nasal toxicity was evaluated *in vitro* using RPMI 2651 nasal cell lines. Finally, *in vivo* biodistribution was assessed by gamma scintigraphy via Tc99m labelling of the particles. Among particles produced, the batch SVT-LCN_MaiLab showed the best physico-chemical characteristics, with small diameter (200 nm), positive surface charge (+48 mV) and high encapsulation efficiency (98%). Size distribution was further confirmed by Nanoparticle Tracking Analysis and electron microscopy. The particles showed a relatively fast release of simvastatin *in vitro* (35.6 ± 4.2 % in six hours) in simulated nasal fluid. Blank nanoparticles did not show cytotoxicity, evidencing that the formulation is safe for nasal administration, while cytotoxicity of simvastatin loaded nanoparticles (IC_{50}) was found to be three times lower than the drug solution (9.92 vs 3.50 µM). In rats, radioactivity distribution evidenced a significantly higher radioactivity in brain after nasal delivery of simvastatin-loaded nanoparticles in comparison to the administration of a similar dose of simvastatin suspension. The simvastatin-loaded lecithin/chitosan nanocapsules developed present some of the most desiderated characteristics for mucosal delivery, i.e. small particle size, positive surface charge, long term stability, high encapsulation efficiency, mucoadhesion. However, they display two most exciting features. One is their biodegradability by enzymes present in the mucus layer, such as lysozyme. This indicates a new Trojan-horse strategy to enhance drug release in proximity of the nasal mucosa. Second is their ability to enhance the nose-to-brain transport as evidenced by preliminary gamma-scintigraphy studies.

Keywords: Nose-to-brain, Statins, Nanoparticles, Neurodegenerative, Gamma scintigraphy, Nasal delivery, Lysozyme, Biodegradable nanoparticles

1 Introduction

The 3-hydroxy-3-methylglutaryl coenzyme A (HMG-CoA) reductase inhibitors, or statins, are arguably among the biggest advances in cardiovascular care in the 20th century. Statins reduce cholesterol serum levels by reversibly inhibiting HMG-CoA reductase, an essential enzyme in cholesterol biosynthesis, promoting a decrement of the risk of serious cardiovascular events.[1,2] Along with their lipid lowering effects, statins have been credited of a range of outcomes or 'pleiotropic effects'.[3] The mechanisms by which pleiotropic outcomes occur are diverse and still not fully elucidated. Many of those effects are attributed to the inhibition of isoprenoid intermediates, i.e. farnesylpyrophosphate and geranylgeranylpyrophosphate (FPP and GGPP) and their downstream effects on intracellular signalling proteins Ras, Rho and Rac.[4] Pleiotropic effects of statins include anti-inflammatory, antioxidant, immunomodulatory and antithrombotic actions as well as the ability to stabilise atherosclerotic plaques and inhibit the proliferation of vascular smooth muscle.[5-7] Because of these pleiotropic effects, it is now believed that statins could be more widely employed in other diseases, such as rheumatoid arthritis, chronic obstructive pulmonary disease, cancer and neurodegenerative disorders. [8-11]

In the case of Alzheimer's disease, clinical research evidenced that an increase in brain cholesterol levels directly upregulate the production of β–amyloid protein, the major protein involved in the formation of senile plaques in the brain of Alzheimer's patients.[12,13] Moreover, the most widely recognised risk factor of late onset Alzheimer's is the genetic variation in a transporter of cholesterol called apolipoprotein E ε4 (ApoE ε4) supposedly altering the brain cholesterol homeostasis, leading to Alzheimer's disease development.[14,15] The inhibition of brain cholesterol synthesis has been shown to reduce beta amyloid accumulation, interfering with the production of beta amyloid and its accumulation as extracellular plaques.[16,17] These works suggest that the effects of statins in lowering the cholesterol levels may have a beneficial role on the pathogenesis of Alzheimer's disease. It has also been postulated that statin pleiotropic effects could provide further benefit to Alzheimer's patients via a modulation of the chronic inflammatory response, another key factor in neurodegenerative process.[18] However, generally these effects of statins are only seen at high therapeutic concentrations at the target organ, while they are difficult to observe when the conventional oral administration route is selected. In fact, statins undergo extensive first pass metabolism and their hydrophilic metabolites are prevented from crossing the blood brain barrier (BBB), the principal biological barrier protecting the central nervous system (CNS).[3]

In the last few decades, the nasal mucosa has been demonstrated to be a site for drug administration that could allow for fast and efficient absorption of drug molecules normally not suitable for oral administration.[19] More recently, the intranasal (IN) route has been increasingly investigated to deliver drugs to the brain aimed to the treatment of specific brain diseases, including neurological diseases, such as Parkinson's, schizophrenia, epilepsy and Alzheimer's.[20] Several researches suggest the "nose-to-brain" route to be one of the most important developments of pharmaceutical research in brain treatment, including: i) the potential to avoid gastrointestinal and hepatic first-pass metabolism; ii) the possibility of delivering drugs not suitable for oral administration, such as peptides and proteins; iii) most important, the transport of exogenous material directly from the nasal cavity to the brain, thus bypassing the BBB.[21,22] It is known that the unique physiology of the olfactory region within the nasal cavity can provide a direct route of administration to the CNS, through the main innervation of the nasal cavity, i.e., the olfactory and trigeminal nerves.[23] However, drug delivery via the nose is also limited by a number of factors such as the administration volume, the barrier of the nasal epithelium, the nasal metabolic activity and the presence of a protective mucus layer. Additionally, the amount of drug administered nasally that have been shown to be transported directly from nose to brain are very low, normally less than 0.1%. Hence, the system is not currently used in the clinical practice.[24]

The extent of the nose-to-brain drug absorption has been shown to be highly dependent on the drug formulation.[25] The strategy of administering drugs encapsulated in nanoparticles via the olfactory epithelium could potentially improve the direct CNS delivery. Nanoparticles can improve nose-to-brain drug delivery, since they are able to interact with the nasal epithelium enhancing the drug absorption, to protect the encapsulated drug from biological/chemical degradation, and to avoid the drug transport to the extracellular space by efflux proteins, such as P-glycoprotein (P-gp). This could potentially increase CNS availability of the drug. In addition, their small diameter potentially allows for transcellular transport of nanoparticles through olfactory neurones to the brain, via the various endocytic pathways of neuronal cells in the olfactory region.[21]

From a drug delivery perspective, the application of polymeric nanoparticles has proven to perform statistically better in delivering model drugs into CNS or in enhancing their pharmacological activity, as compared to a simple formulation of drug, when administered intranasally.[26,27] Colloid nanoparticles, composed of polysaccharides, such as chitosan, and phospholipids, have been proposed recently as a biocompatible, biodegradable and safe delivery system for poorly soluble drugs in order to overcome biological barriers.[28,29] Their chitosan surface layer in particular seem adapted for nasal delivery, due to the

polysaccharide mucoadhesive properties and its potential to increase epithelia permeability by interaction with the junctional complexes between cells.[30,31]

In the present study, a mucoadhesive formulation based on self-assembled lecithin/chitosan nanoparticles designed for intranasal administration was developed and optimized as a promising strategy for delivering simvastatin into the CNS. Desired features of this approach were high positive charge, small particle size and high drug content. In order to obtain these features, different oils were incorporated into lecithin/chitosan nanoparticles in order to optimize the formulation. Physical and chemical stability was assessed along with drug release in simulated nasal fluid. Nanoparticle structure and interaction with mucus with and without lysozyme were investigated as well. The *in vitro* nasal toxicity of the nanoparticles alone or loaded with simvastatin was evaluated in a human nasal cell line (RPMI 2651). Finally, a preliminary gamma-scintigraphy study of the biodistribution of simvastatin-loaded nanoparticles *in vivo* after intranasal instillation was carried out in rats.

2 Materials

Chitosan (Chitoclear FG, deacetylation degree 95%, viscosity 45 cP) was provided by Primex (Siglufjordur, Iceland) and used without further purification. Lecithin (Lipoid S45) was obtained from Lipoid AG (Ludwigshafen, Germany). Pharmaceutical-grade oils Maisine™ 35-1 (glycerol mono- linoleate), Labrafac™ Lipophile WL 1349 (medium-chain triglycerides, European Pharmacopoeia), Capryol™ PGMC (propylene glycol monocaprylate type I, National Formulary [NF]), and Capryol™ 90 (propylene glycol monocaprylate type II, NF), were a kind gift of Gattefossé (Saint-Priest, France). Simvastatin USP 99%, mucin from porcine stomach (type III), human lysozyme and bovine serum albumin (BSA) were supplied by Sigma-Aldrich (St Louis, MO, USA). Sartorius (Göttingen, Germany). Dialysis tubing cellulose (14,000 MWCO) was supplied by Sigma-Aldrich. Cell line RPMI 2650 (CCL-30) was purchased from American Type Culture Col- lection (ATCC) (Manassas, VA, USA). Minimum essential medium (MEM) and fetal bovine serum (FBS) were acquired from ThermoFisher Scientific (Waltham, MA, USA). Cell culture inserts and other culture plastics were from Corning Incorporated (Corning, NY, USA). All other chemicals were of analytical grade. Ultrapure and degassed ultrapure water (Purelab Flex; ELGA-Veolia LabWater, Windsor Court, UK) was used in all experiments.

3 Methods

3.1 Preparation of Simvastatin–Loaded Lecithin/Chitosan Nanoparticles

Simvastatin-loaded (SVT) LCNs were prepared as reported previously with slight modifications. In summary, 4 mL of an ethanol solution containing soybean lecithin (100 mg), simvastatin (50 mg) and different types of oils (Maisine [Mai], Labrafac [Lab], Capryol PGMC [Cap_I], and Capryol 90 [Cap_{II}]) in 1:1 binary combination (100+100 mg) was injected, at controlled ow rate (15 mL/min), into 50 mL of 0.01% (w/v) chitosan aqueous solution, under constant mechanical stirring at 15,000 rpm for 10 minutes (Ultraturrax TP 18/10 – 10N; IKA-Werke GmbH, Stauffer, Germany). The 0.01% chitosan aqueous solution was prepared from a 1% chitosan solution in 0.03 N HCl. Volume of organic phase and rate ow injection (15 mL/min) were controlled using a mechanical syringe pump coupled with a glass pipette (Model 200; KD Scientific, Holliston, MA, USA). Finally, ethanol phase was evaporated from the prepared colloidal suspension using a rotary evaporator (Heidolph WB/VV 2000; Schwabach, Germany) at the temperature of 40°C. Batches of LCNs loaded with simvastatin, without oil (SVT-LCNs) and with different oils (SVT-LCN_MaiLab, SVT-LCN_MaiCapI, SVT-LCN_LabCapI, and SVT-LCN_CapICapII), were produced to optimize the formulation for stability and simvastatin encapsulation. All batches were prepared in at least triplicate and stored at room temperature for up to 3 months.

3.2 Physico-Chemical Characterization of Simvastatin–Loaded Lecithin/Chitosan Nanoparticles

3.2.1 Determination of Nanoparticle Size and Surface Charge

The particle size and polydispersity index (PDI) of all nanoparticles were determined by dynamic light scattering (DLS) using Malvern Zetasizer Nano ZSP (Malvern Instruments Ltd., Malvern, UK).

For DLS measurements, the colloidal nanoparticle suspensions were diluted with distilled water filtered at 0.45 μm to avoid multiple scattering. The analysis was performed at 25°C and at a 90° scattering angle. Three measurements were performed for each sample,

in triplicate (n=9± standard deviation [SD]).

The surface charge of the nanoparticles was measured using phase analysis light scattering. The same samples were used for both size and zeta potential determination, with the same instrument. For each measurement, nanoparticles were diluted (1:3) with distilled water filtered at 0.45 μm to achieve a desired conductance (< 300 μS) without altering the surface charge properties of nanoparticles. Zeta potential values were presented as means of triplicate runs (six sub- runs) per sample (n=9± SD).

3.2.2 Nanoparticle Tracking Analysis

In order to further confirm the particle size distribution and have an evaluation of particle concentration in suspension, nanoparticles tracking analysis (NTA) experiment was conducted using NanoSight NS300 (Malvern Instruments Ltd.) equipped with a 480 nm laser light source, and a 20× magnification microscope was used to carry out the particle tracking analysis with a field of view of approximately 100×80×10 μm. The built-in sCMOS camera was used to record videos, and the particle tracking was analyzed by NTA 3.1 software. NTA tracks single particles in Brownian motion through the light they scatter. Videos of the particle's tracks, projected on the *x*–*y* plane, observed through a 20x microscope, were analyzed by the built-in NTA 3.1 software that locates and follows the center of each individual particle moving in the observation volume, determining the average distance moved by each particle in the *x* and *y* directions. This value is then converted into particle size on the basis of a variation of Stokes–Einstein equation taking into account that the motion is tracked in two dimensions:

$$\text{Equation 1:} \qquad \overline{(x,y)}^2 = \frac{4Tk_B}{3\pi\eta d_h}t$$

where k_B is the Boltzmann constant and $\overline{(x,y)}^2$ is the mean squared displacement of a particle during time t at temperature T, in a medium of viscosity η, with a hydrodynamic diameter of d_h.[32]

Furthermore, knowing the volume of the suspension and the dilution, the associated NTA software is capable to calculate an approximate concentration of the nanoparticles inside the colloidal suspension.[33]

Only SVT-LCN_MaiLab nanoparticles were analyzed by NTA. The nanoemulsion was highly diluted (1:630,000) with ultrapure water for allowing single particle tracking. After that, sample was drawn into 1 ml plastic syringe, which were used for full sample injection into the instrument sample chamber. The nanoparticles images were acquired using a video capture

mode of the sample for three times of 60 seconds' analysis, which were used for subsequent analysis. Measurement was carried out at a defined temperature (28-28.2°C) and viscosity (0.828-0.832cP). The results values were obtained as mean and standard deviation of three runs analysis.

3.2.3 Quantification of Simvastatin in LCNs

The simvastatin content in nanoparticles was measured by high-performance liquid chromatography (HPLC) system. The instrumentation consisted of ESA model 542 Autosampler (Chelmsford, MA, USA), ESA Model 584 pump (Chelmsford, MA, USA), Shimadzu SPD10A UV detector (Kyoto, Japan). A reverse phase C_{18} column (Luna, 250 X 3.0 mm, 5 µm Phenomenex, Torrance, CA, USA) was employed for chromatographic separation of both simvastatin's isoforms, i.e. lactone and hydroxyl acid form [34] with a mobile phase consisting of a mixture 65:35 v/v acetonitrile and 0.025M sodium dihydrogen phosphate buffer pH 4.5 and a flow rate of 0.8 ml/min. The UV-detector was set at 238 nm with a sample injection volume of 50 µl. In order to quantitatively convert simvastatin into its hydroxyl acid form, simvastatin was dissolved in ethanol and added to a 1.5 volumes of NaOH 1N and heated at 50°C for 2 hours. Next, the pH of the solution was adjusted at 7.2 with HCl and volume was placed with water to 10 ml of solution. Linearity of calibration curves for both simvastatin and its hydroxyl acid form was verified in the range 0.5 – 50 µg/ml (r=0.998 and r=0.999 respectively). Limit of detection and limit of quantification were 0.02 and 0.08 µg/ml for simvastatin and 0.06 and 0.18 µg/ml for simvastatin hydroxyl acid form.

The encapsulation efficiency (EE) of nanoparticles was determined by an indirect method; that is, the amount of precipitated and free simvastatin was quantified and subtracted from the total amount of the drug quantified in the total preparation, and all amounts were determined by HPLC, and then expressed as a percentage of the total drug in the preparation. The total amount of simvastatin in the formulations was quantified. Firstly, 100 µL of the preparation was dispersed in 10 mL of ethanol by sonication for 15 minutes (ultrasonic cleaner; VWR, Radnor, PA, USA) to extract the entire amount of drug. Then, the ethanol dispersion was heated at 60°C in a tightly closed container for 5 minutes to solubilize the drug content extracted from the nanoparticles and directly assayed for HPLC. For the quantification of precipitated and free simvastatin in the aqueous medium, colloidal suspensions were first centrifuged at 1,500× *g* for 10 minutes (Medifuge; Heraeus Sepatech Gmbh, Hanau, Germany) to separate the nanoparticles from any large precipitate. The pellet obtained for each sample was re-suspended with ethanol, submitted to a brief sonication

process to solubilize the drug and then analyzed by HPLC. An aliquot of 2 mL of supernatant obtained in the previous step was further centrifuged using Vivaspin® Centrifugal Concentrator (MWCO 30,000 Da; Sartorius) at 4,000× *g* for 10 minutes (Medifuge, Heraeus Sepatech Gmbh) to separate the dissolved and hence non-encapsulated simvastatin. The ultra-filtered solution was diluted with ethanol by the same method used for pellet quantification and analyzed by HPLC as well. All analyses were performed in triplicate (n=9 ± SD). EE of simvastatin was determined by using the following formula:

Equation 2:

$$EE\% = \frac{Total\ amount\ of\ simvastatin\ -(Precipitated\ simvastatin + Non-ecapsulated\ simvastatin)}{Total\ amount\ of\ simvastatin} * 100$$

3.2.4 Nanoparticle Imaging by STEM

The morphology of simvastatin raw material, SVT-LCNs nanospheres (without oily core), blank LCN_MaiLab nanocapsules and SVT-LCN_MaiLab nanocapsules, was observed by scanning transmission electron microscopy (STEM) using an EVO® electron microscope (ZEISS International, North Ryde, NSW, Australia) operating at an accelerating voltage of 30kV. A drop of sample solution was placed onto a 200 mesh copper grid coated with carbon (Agar Scientific, Stansted, UK) and air dried for 1 minute, after which excess solution was removed gently with filter paper. Subsequently, a drop of phosphotungstic acid 2% w/v was used as a staining agent and removed after 30 seconds. The images were obtained via inverse contrast imaging with magnification between 75,000 -150,000 times.

3.3 Determination of Nanoparticle Structure and Interaction with a Nasal Mucus Model

The internal structure of nanoparticles and the structural effects occurring upon their interaction with a model of nasal mucus, were investigated by Synchrotron Small Angle X-ray scattering (SAXS) technique. Experiments were performed at the ID02 high-brilliance beamline (ESRF, Grenoble, France). The x-ray beam cross section was 200 μm x 400 μm with λ =0.1 nm. All measurements were performed at T = 25°C. Samples were put in plastic

capillaries (KI-BEAM, ENKI s.r.l, Concesio, Italy) with 2 mm internal diameter, mounted horizontally onto a thermostated sample holder. The region of investigated momentum transfer, $q = (4\pi/\lambda) \sin(\theta)$, was $0.0116 < q < 6.43\ nm^{-1}$, where 2θ is the scattering angle. To prevent any radiation damage, several frames with very short exposure time (0.1 s) were acquired, then checked and averaged. After solvent subtraction, the measured SAXS profiles report the nanoparticles scattered radiation intensity as a function of the momentum transfer, q. SVT-LCN_MaiLab nanoparticles were prepared according to the above described protocol at a final concentration of 7.1 mg/ml. In order to assess the stability of SVT-LCN_MaiLab nanoparticles in the presence of artificial mucus and their interaction with lysozyme, SAXS analyses were performed also on nanoparticles dispersions in simulated nasal fluid (8.77 mg/ml sodium chloride, 2.98 mg/ml potassium chloride and 0.59 mg/ml calcium chloride dehydrate) at three different mucus concentrations 2%, 1% and 0.5% w/v, and the kinetics of interaction in presence of both mucus (0.5 %) and lysozyme (0.5 mg/ml) was followed within 8 hours.

3.4 *In Vitro* Drug Release from Lecithin/Chitosan Nanocapsules

In vitro release from SVT-LCN_MaiLab nanocapsules was studied using simulated nasal electrolytic solution (SNES) containing potassium, calcium and sodium at biologic human concentrations of the nasal fluid, as described by Castile and colleagues.[35] In order to obtain sink conditions during the release experiments, simvastatin solubility in SNES was increased by adding Bovine Serum Albumin (BSA) 0.5% w/v to the medium.

The test for *in vitro* release from SVT-LCN_MaiLab in the SNES- BSA 0.5% release medium at pH 6.5, was conducted using the dialysis bag technique (Dialysis tube membrane, MW cut-off 14000 KDa, Sigma-Aldrich). A volume 1 ml of the nanoemulsion was diluted with 1 ml of SNES at pH 6.5 and placed in the dialysis bags. The sealed bags were immersed into 100 ml of the release medium containing BSA 0.5% kept at 37°C and magnetically stirred at 100 rpm/min. At predetermined time points (0, 1, 2, 3, 4, 5, 6, 7 and 8 hours) 1.5 ml aliquots of the dissolution medium were taken and replaced with an equivalent amount of fresh release medium. Sample were analysed by HPLC to determine the released simvastatin. The same experiment was conducted using a 1 mg/ml simvastatin suspension in ultrapure water used as control. *In vitro* release studies were replicated three times for both simvastatin nanoparticles and simvastatin suspension.

3.5 Cytotoxicity Assay of Lecithin/Chitosan Simvastatin loaded nanoparticles

Cytotoxicity assays of simvastatin suspension, SVT-LCN_MaiLab, Blank-LCN_MaiLab were conducted using the human nasal septum carcinoma cell line RPMI 2650 (ATCC) and performing a MTT [3-(4,5-Dimethylthiazol-2-yl)-2,5-Diphenyltetrazolium Bromide] cytotoxicity assay. The RPMI 2650 cell line was cultured in a Minimum Essential Medium (MEM) containing 10% of fetal bovine serum (v/v) and 1% of non-essential amino acid solution and incubated at 37°C with 95% air humidity and 5% CO_2 atmosphere. Cells were seeded with an initial density of 50,000 cells per well and incubated for 24 hours to allow cell adhesion in 96 Well Cell Culture Cluster (Costar, Corning Incorporated, New York, USA). Different concentrations from 0–240 μM of simvastatin, SVT-LCN_MaiLab and Blank-LCN_MaiLab nanoparticles were prepared by direct dilution in cell culture medium. To prepare the raw simvastatin solution, DMSO was used as simvastatin solvent and diluted to low final concentration (<0.1%) to avoid toxicity effects of the solvent on the cell viability. The cells were treated with the formulations for 72h, followed by incubation in MTT reagent for 2h at 37°C. Next, the cells medium was removed and 120 μL of Dimethyl Sulfoxide (DMSO) was added to each well to dissolve the metabolism violet colored product. The plates were shacked for 15 min, the content was pipetted and transferred to new plates and the absorbance was measured at 570 nm using a micro plate reader (Spark 10 M, Tecan, Männedorf, Switzerland). Absorbance values were considered directly proportional to cell viability and percentage cell viability was calculated by comparison to control values obtained for untreated cells.

3.6 Gamma Scintigraphy Studies

3.6.1 Particles Labeling with ^{99m}TC

A preliminary experiment to evaluate the administration of simvastatin loaded nanoparticles was carried out in rats by gamma scintigraphy. SVT-LCN_MaiLab nanoparticles and a simvastatin suspension were both labeled with ^{99m}Tc based on previous experiences, in which anti-CD3 monoclonal antibody was successfully labelled. [36-38]

Briefly, 60μL simvastatin nanoparticles or simvastatin suspension (1 mg/ml) was incubated with 100 μL of $SnCl_2$ (0.6, 6 or 60 μg) (Sigma Aldrich) in 0.9% NaCl and incubated for 20

minutes at room temperature. Afterwards, 100µL (100 µCi) of ^{99m}Tc pertechnetate (CNEN/IPEN, São Paulo, Brazil) was added and the reaction was incubated for further 10 minutes at room temperature. The radiolabeling efficiency of the nanoparticle and the pharmaceutical was evaluated using thin-layer chromatography (TLC), which was carried out using Whatman paper No.1 and acetone as mobile phase. The radioactivity of the strips was quantified in a gamma counter (Wizard^2, PerkinElmer, Waltham, MA, USA). The nanoparticle and the simvastatin were both successfully labelled when using 6 µg of $SnCl_2$ reaching an average 94% labelling efficiency.

To quantify the TLC results, the distance traveled by the substance being considered is divided by the total distance traveled by the mobile phase. This is called the retention factor (Rf), in these experiments free ^{99m}Tc pertechnetate has a high Rf being transported with the mobile phase. When the particle labelling is carried out, the new radiopharmaceutical conjugate is not efficiently eluted by the mobile phase, that is Rf = 0. Efficient radiolabeling was considered for a signal at Rf=0 > 80%.

3.6.2 *In vivo* Biodistribution Study

All animal experiments were approved by the Ethics in Research Committee of University Hospital Clementino Fraga Filho (affiliated university Federal University of Rio de Janeiro, Rio de Janeiro, Brazil; [CECA/CCS/UFRJ 129/14]. All animals were handled in accordance with Brazilian guidelines for the care and use of animals for scientific and education purposes (Conselho Nacional de Controle de Experimentaçao Animal – CONCEA, 2016). Nine Wistar rats weighing 300-350 g obtained from the central vivarium were used. The animals had free access to a standard rat diet and tap water at all times during the studies. Three Wistar rat per group were placed individually in an induction chamber and anesthesia was induced with 1% isoflurane. Then, 10µl of the radiolabeled formulation, i.e. SVT-LCN_MaiLab, simvastatin suspension or a simple pertechnetate solution (TcO^{4-}), was instilled with a micropipette in each nostril of the animal. Ninety minutes' post-administration animals were sacrificed with a high dose of isoflurane (5%).]).

For quantitative biodistribution analysis, rats brain, heart, lungs, liver, kidneys, spleen and stomach were removed and weighed. The total radioactivity administered to each animal and the radioactivity present in each organ were measured in a gamma counter (Packard Cobra II Auto-Gamma Counter, PerkinElmer, Waltham, MA, USA). The percentage of the dose per organ (% dose/organ: each organ counts/total dose activityx100) and the instilled dose per gram of tissue (%gram/tissue: % dose/organ/mass in grams) were determined for each sample.

4 Statistics

All results were reported as mean and SD of at least three replicates, unless stated otherwise. Cytotoxicity IC_{50} values were calculated by using a nonlinear (sigmoidal, 4PL) fitting of each data set (Prism, Version 7.0a; GraphPad Software Inc., La Jolla, CA, USA). The differences between data were tested using Student's *t*-test (paired, two-tailed) considering significant differences with P 0.05. The results of the biodistribution assays were analysed using two-way analysis of variance, and a Tukey's multiple comparisons test was used to compare the groups. Differences were considered to be statistically significant at P 0.001 (Prism, Version 7.0a; GraphPad Software Inc.).

5 Results

5.1 Preparation and Physico-Chemical Characterization of Simvastatin Loaded Lecithin/Chitosan Nanoparticles

Simvastatin nanoparticles were formed via the electrostatic self-assembly of lecithin and chitosan. In previous papers, this system was shown to be adapted for the encapsulation of lipophilic drugs, but the loading efficiency was limited by the affinity of the drug for the phospholipid component of the nanosystem. [39,40]

In this study, to improve their loading capacity, nanoparticles were produced by adding to the formulation different oils based on literature solubility studies of simvastatin. Maisine, Labrafac, Capryol PGMC, and Capryol 90 were chosen, and formulated with lecithin/chitosan in binary combinations, at the maximum amount compatible with the production of stable nanoparticles. Preliminary experiments were carried out to determine the maximum amount of oils that could be used to produce stable nanoparticles (data not shown).

To select the optimal formulation, all nanoparticles prepared were characterized for size, PDI, zeta potential, drug-loading efficiency, and stability during 3-month storage at room temperature. Table 1 reports the average size, PDI, zeta potential, and drug-loading efficiency of SVT-LCNs produced without oil and with different oil combinations.

Table 1: Simvastatin-loaded Nanoparticles Physicochemical Properties and Encapsulation Efficiency (n= 9 ± SD)

Batch code	Oil ratio	Particle Size (nm)	ζ potential (mV)	PDI	EE (%)
LCN	-	146.7 ± 26.2	+57.26 ± 2.57	0.380 ± 0.025	-
SVT-LCN	-	272.0 ± 12.6	+34.43 ± 2.13	0.263 ± 0.040	22.60 ± 20.80
SVT-LCN_Mai	1:0	192.4 ± 22.5	+36.63 ± 2.25	0.120 ± 0.035	74.13 ± 6.04
SVT-LCN_Mai_2	2:0	184.9 ± 9.5	+45.30 ± 1.08	0.089 ± 0.004	86.90 ± 6.28
LCN_MaiLab	1:1	205.6 ± 10.2	+50.20 ± 2.17	0.129 ± 0.017	-
SVT-LCN_MaiLab	1:1	204.5 ± 15.4	+48.45 ± 4.09	0.098 ± 0.040	98.52 ± 1.33
SVT-LCN_Cap_ICap_{II}	1:1	280.4 ± 9.2	+20.17 ± 2.03	0.185 ± 0.045	88.78 ± 0.99
SVT-LCN_$MaiCap_I$	1:1	352.0 ± 33.9	+11.34 ± 3.21	0.223 ± 0.020	90.74 ± 0.87
SVT-LCN_$LabCap_I$	1:1	271.1 ± 8.1	+17.01 ± 2.98	0.154 ± 0.040	94.68 ±0 .65

Abbreviations: ζ potential, zeta potential; PDI, polydispersity index; EE, encapsulation efficiency; LCN, lecithin/chitosan nanoparticles; SVT, simvastatin; Mai, Maisine™; Lab, Labrafac™; CapI, Capryol PGMC™; CapII, Capryol 90™.

SVT-LCNs produced without oily excipients showed higher average size (around 270 nm) and smaller positive surface charge compared to blank nanoparticles (LCNs). Furthermore, substantial precipitation of simvastatin affected the EE of SVT-LCN. The EE was approximately 22%. In all the examined cases, the addition of oil significantly reduced the amount of drug precipitated during preparation of nanoparticles. This was consistent with an improved loading capacity provided by adding an oily core to nanoparticles, leading to a fourfold increase in EE. In preliminary studies carried out with only Maisine, it was observed that the EE of simvastatin was increasing with increasing oil concentration (Table 1 presents the data for LCN_Mai and LCN_Mai2). It was hypothesized that the combination of different types of oils could promote a further improvement in EE. In most cases, no significant improvement was obtained. It can be seen in Table 1 that the addition of the oil combinations CapICapII and LabCapI in formulations (SVT-LCN_CapICapII and SVT-LCN_LabCapI) did not result in a significant variation in the average size compared to SVT-LCNs or EE when compared to lecithin/chitosan Maisine-containing nanoparticles (SVT-LCN_Mai2). On the other hand, SVT- LCN_MaiCapI showed larger particle size (352 nm) but not a dramatic increase in loading capacity. All the oil-containing formulations evidenced a positive surface charge with values ranging from +11 to +48 mV. The preparations with higher particle sizes also showed reduced surface charge and higher PDI, with a potential negative effect on their long-term stability. In fact, SVT-LCN_CapICapII and SVT- LCN_MaiCapI preparations

evidenced precipitation or flocculation just few days after preparation. SVT-LCN_LabCapI was apparently stable over 1-month storage but displayed a slight phase separation over longer times.

On the other hand, the addition of the oil combination Maisine and Labrafac had a huge positive effect. In fact, simvastatin-loaded nanoparticles produced using Maisine and Labrafac (SVT-LCN_MaiLab) showed a significantly smaller particle size (204 nm), elevated positive surface charge (nearly 50 mV) and high drug-loading efficiency, encapsulating 98% of the total amount of simvastatin. Moreover, SVT-LCN_MaiLab were found to be monodispersed (PDI 0.1). In addition, the system remained chemically and physically stable at room temperature up to 3 months, as shown in Table 2. Therefore, the SVT-LCN_MaiLab formulation was selected for further experiments, as it presented small and narrow particle size distribution, positive and sufficiently high superficial charge and optimal drug entrapment efficiency.

Table 2: Physical and Chemical Stability Study at Room Temperature of Simvastatin-loaded Nanoparticles (SVT-LCN_MaiLab)

Storage Time (Months)	Particle size (nm)	ζ potential (mV)	PDI	EE (%)
0	204.5 ± 15.4	48.4 ± 4.1	0.098 ± 0.040	98.52 ± 1.33
1	205.5 ± 15.2	48.1 ± 3.2	0.166 ± 0.024	97.11 ± 1.25
3	201.9 ± 18.6	39.9 ± 2.5	0.131 ± 0.033	96.54 ± 1.13

Abbreviations: ζ potential, zeta potential; PDI, polydispersity index; EE, encapsulation efficiency

5.1.1 Nanoparticle Tracking Analysis

To confirm the particle-sizing data obtained by DLS, SVT-LCN_MaiLab particle size distribution and concentration were measured using NTA. NTA is a relatively new investigation technique that offers direct and real-time visualization, sizing, and counting of nanoparticles, allowing high-resolution particle size distributions to be obtained. [41] Results are shown in Figure 1. The particle size distribution showed a peak at 100 ± 4.6 nm, 90% of the particles being below 132.1 ± 13 nm, confirming the narrow size distribution of the nanoparticles. A smaller NTA average particle size in comparison with DLS results was

expected, due to the different weighting functions, the intensity scattered by particles for DLS, much larger for large particles, the number of particles for NTA. NTA provides complementary information for both DLS and microscopy. In fact, as it follows individual particles, it enhances the resolution of polydispersed particle population which is usually obtained by DLS. The technique still operates on a statistically significant number of particles, larger than for microscopy, although not accessing their morphology.[42]

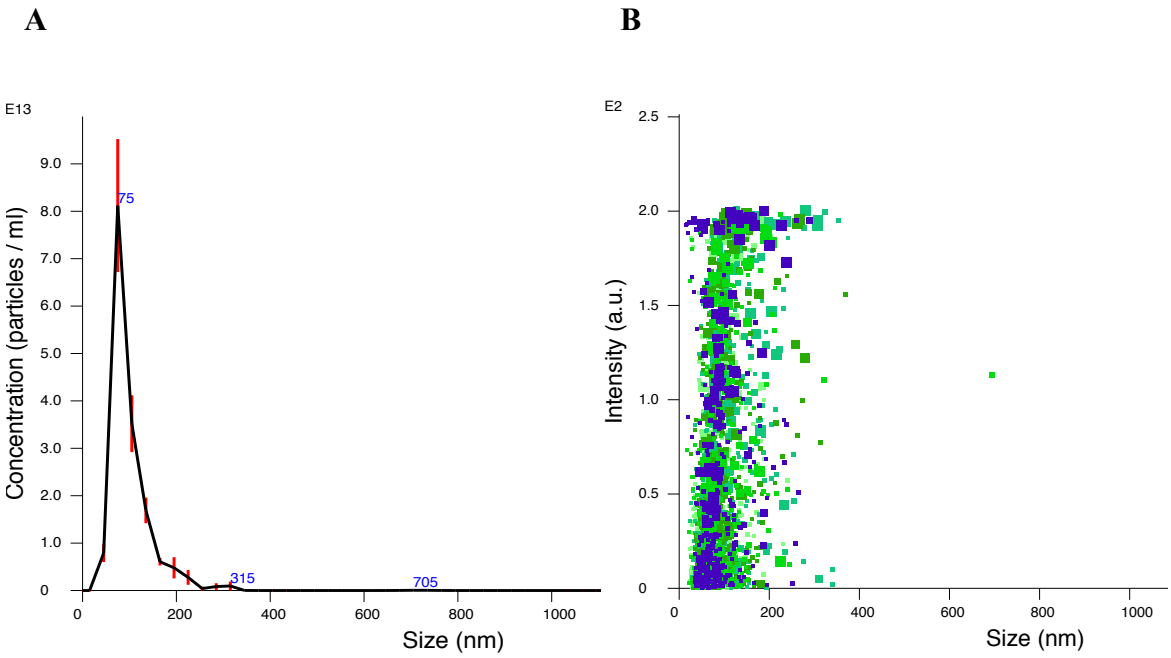

Figure 1: Particle size distribution vs nanoparticles concentration and intensity of scattered light obtained by NTA.

Notes: Particle size distribution is expressed as average and standard error of the mean of nanoparticle concentration (n=5) (**A**). Different colours and sizes of markers represent measures of particle size and scattered light intensity of single particles from the five independent experiments (**B**).

Abbreviation: NAT, nanoparticles tracking analysis.

NTA measurements also confirmed the stability of the lecithin/chitosan oil core nanoparticles prepared using Maisine and Labrafac combination, as similar results were

obtained for the same formulation stored for three months at room temperature (data not shown).

5.1.2 Nanoparticles Imaging by STEM

LCNs were further characterised by STEM (Figure 2). Simvastatin raw material, SVT-LCNs and SVT- prepared using Maisine and Labrafac are shown on Figure 2A-C, respectively. Simvastatin suspension was organized in agglomerates of individual elongated crystals few micrometers in size (Figure 2A). LCNs prepared without oil loaded with simvastatin produced spherical spongy particles in the range 100-500 nm, as shown in Figure 2B. Large simvastatin crystals were also observed within this formulation, because of low encapsulation efficacy and consistently with the extensive precipitation occurring during nanoparticle preparation. The incorporation of oils, i.e. Maisine and Labrafac, into the formulation of LCNs significantly improved nanoparticle morphology and size distribution. SVT-LCN_MaiLab (Figure 2C) appear as small almost perfectly spherical nanoparticles with narrow size distribution, 150-250 nm. Additionally, the increased EE of simvastatin following incorporation of oils in the formulation is confirmed by the absence of large simvastatin crystals.

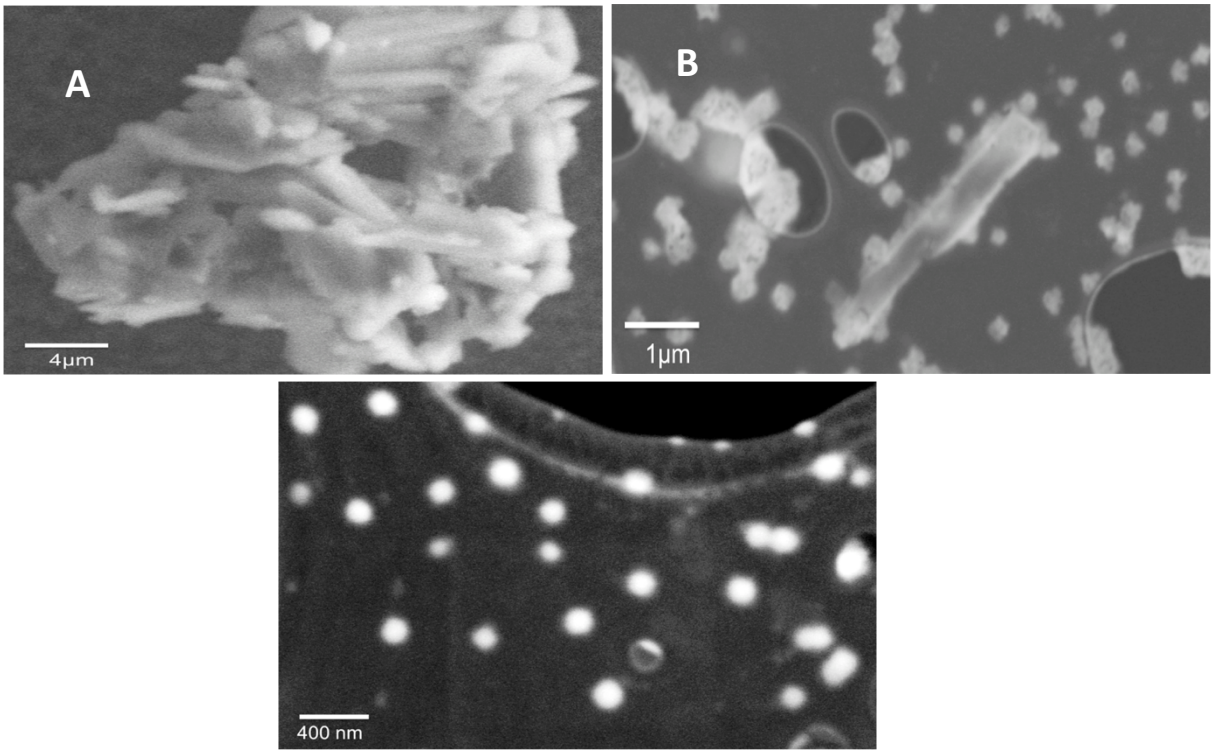

Figure 2: STEM images simvastatin crystals (A); simvastatin-loaded lecithin/chitosan nanoparticles (SVT-LCN) (B), and simvastatin-loaded lecithin/chitosan nanoparticles prepared using Maisine and Labrafac (SVT-LCN_MaiLab) (C).

5.2 Nanoparticles Structure and Interaction with a Nasal Mucus Model

To investigate the internal structure of nanoparticles, SAXS measurements were performed on blank and simvastatin-loaded nanoparticles. In Figure 3 we report the scattered X-ray intensity profiles for LCN, LCN_MaiLab and SVT-LCN_MaiLab nanoparticles.

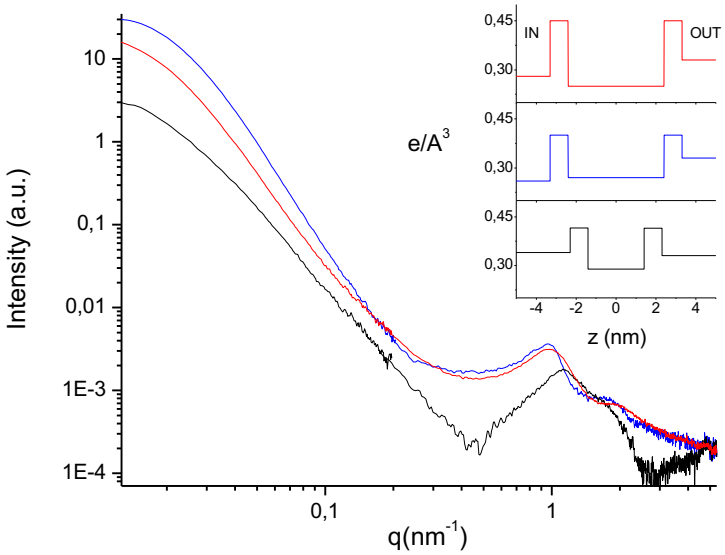

Figure 3: SAXS intensity spectra of LCN (black line), LCN_MaiLab (blue line) and SVT-LCN_MaiLab (red line) nanoparticles.

Notes: The corresponding electron density profiles (e/Å^3) across the bilayer are shown in the insert. IN is the core region, and OUT is the bulk solvent region and *z* is the distance from the centre of the bilayer. (e/Å^3) is the electron density for number of electrons/volume.

Abbreviations: SAXS, small-angle X-ray scattering; SVT-LCNs, simvastatin-loaded lecithin/chitosan nanoparticles; Mai, Maisine; Lab, Labrafac; *q*, momentum transfer.

Spectra were very different all over the investigated *q* region. Blank LCNs (bottom black line in Figure 3) showed the characteristic features of closed lamellar structures, such as vesicles, with low multilamellar layering as evidenced previously.[28] The structure peak at *q* = 1.13 nm^{-1}, corresponded to a characteristic interlamellar distance of 5.6 nm. In fact, the momentum transfer *q* was related to the characteristic scattering distance of supramolecular structures *d* by the equation:

Equation 3: $$D = \frac{2\pi}{q}$$

The obtained bilayer contrast profile is reported in the insert of Figure 3 (bottom black profile). The structural parameters are in agreement with typical values for

lipid/polysaccharide nanoparticles:[28] the overall size is 140 ± 20 nm, the hollow water core is surrounded by one or more lipid bilayers each 5 nm thick, the inter-layer regions containing water and chitosan.

Intensity spectra of LCN_MaiLab (blue line in Figure 3), clearly reveal the presence of an oil core that definitely changed the contrast of the inner region, the "IN" electron density being lower than the "OUT" (insert of Figure 3, central blue profile). The intensity decay in the low-q region is proportional to q^{-4}, as expected for globular particles with well-defined interfaces. The overall size of oil-containing particles is roughly 200 nm. The nanoparticle structure is core-shell type: the oil core is surrounded by a multilayer shell, as visible in the high q region of the spectra. The obtained profile of bilayers belonging to the shell shows that their structure is affected by the presence of the oil component, as reported in Figure 3. The internal hydrophobic region of the lamellae is thicker than for blank nanoparticles. Accordingly, the interlamellar peak appears at lower q-values (1 nm^1) corresponding to a characteristic distance of 6.3 nm, larger than for oil-free nanoparticles. Simvastatin-loaded nanoparticles (SVT-LCN_MaiLab) showed a structure quite similar to the unloaded ones. Interestingly simvastatin seems not only to be embedded in the oil core, but also to participate to the shell structure, lowering its electron density as compared to the unloaded nanoparticles.

To investigate the structural changes induced by the interaction of the nanoparticles with mucus, SAXS analyses were performed also on SVT-LCN_MaiLab nanoparticles dispersions in the presence of artificial mucus in simulated nasal fluid (2%, 1%, 0.5% w/v). Figure 4, left panel, reports the intensity spectrum of the nanoparticles in artificial mucus 0.5% together with that of the mucus itself. In the right panel, the spectrum obtained originally for the nanoparticles in simulated nasal fluid is compared to the one of the nanoparticles inside the mucus, after subtraction of the mucus contribution to the scattered intensity.

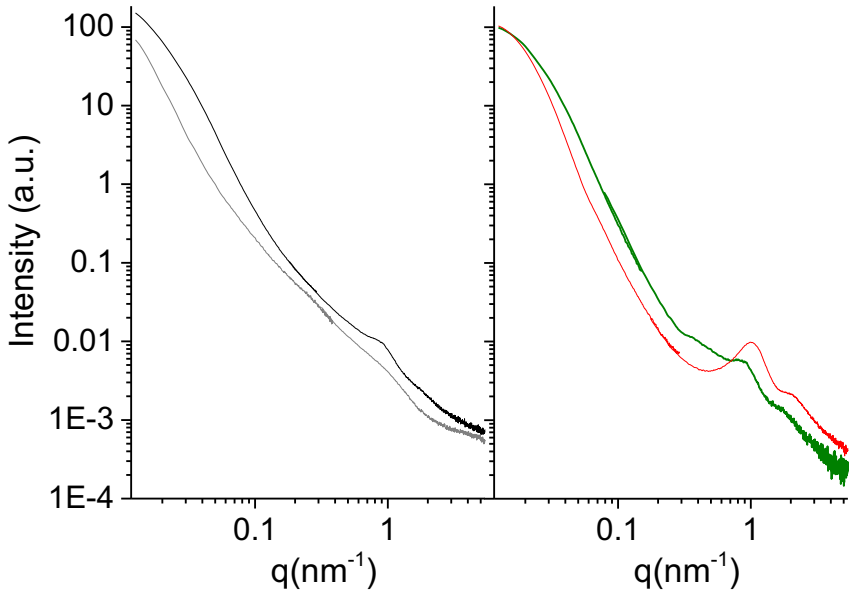

Figure 4: SAXS intensity spectra of SVT-LCN_MaiLab nanoparticles dispersed in artificial mucus.

Notes: Left panel: SVT-LCN_MaiLab in artificial mucus 0.5% (black line) and mucus 0.5% (gray line). Right panel: SVT-LCN_MaiLab nanoparticles before interaction with artificial mucus (red line) and in mucus, after mucus spectrum subtraction (green line).

Abbreviations: SAXS, small-angle X-ray scattering; SVT-LCNs, simvastatin-loaded lecithin/chitosan nanoparticles; Mai, Maisine; Lab, Labrafac; *q*, momentum transfer.

First, it was observed that in presence of mucus nanoparticles are still detected and keep the same core-shell structure. Differences are visible in the high q region of the spectra, corresponding to the local scale. The characteristic structure peak shifts to q = 0.89 nm^{-1}, corresponding to an interlamellar distance of 7 nm. The adjacent bilayers swell, as indicated by the interlamellar solvent layer increased thickness, showing that the particle is stretched by the presence of the mucus matrix. Meanwhile, the intensity of the structure peak is decreased, suggesting a peeling-off of layers from the multilayer shell. Moreover, an additional small peak at q = 0.38 nm^{-1} stems for polymer, chitosan and/or mucin, coordination, with correlation length of ~16.5 nm.

Finally, the effect and kinetics of the interaction upon addition of lysozyme to the mucus/nanoparticles system were tested, following its structural evolution within several hours. Lysozyme is a protein widely present in natural mucosal secretions, being one of the

most abundant antimicrobial factors that constitute the innate immunity.[43] Lysozyme at a physiological concentration (0.5 mg/ml)[44] was added in mucus plus SVT-LCN_MaiLab nanoparticles dispersion and subsequent SAXS spectra were acquired at different incubation times. The corresponding intensity spectra are reported in Figure 5. Experimental results revealed that lysozyme interacts with nanoparticles helping the peeling process of the multilayer shell. In fact, both the characteristic structure peak keeps on moving to lower q values, and the associated intensity decreases. After 6 h the effect was almost complete. In the first hours, the external layers of the shell progressively swell and peel off suggesting a specific biodegradation of the nanoparticles as a consequence of the interaction with the enzyme.

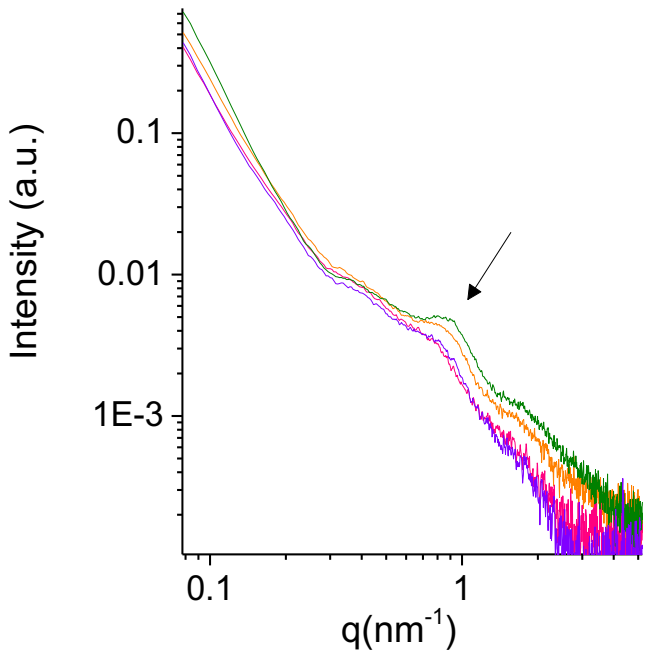

Figure 5: SVT-LCN_MaiLab nanoparticles interaction with mucus plus lysozyme.

Notes: SAXS intensity spectra of SVT-LCN_MaiLab nanoparticles in artificial mucus (0.5%) after mucus subtraction: without lysozyme (green line) and in interaction with lysozyme at different times: t = 0 h (orange line), t = 6 h (pink line), t = 8 h (violet line).

Abbreviations: SAXS, small-angle X-ray scattering; SVT-LCN, simvastatin-loaded lecithin/chitosan nanoparticles; Mai, Maisine; Lab, Labrafac; *q*, momentum transfer.

5.3 Simvastatin Release Studies

In vitro release testing is an important analytical tool, used to investigate and establish product behavior and stability during each step of the drug development.[45] The *in vitro* drug release was measured via the dialysis bag diffusion method one of the most commonly used dissolution methods used for testing nanoformulations designed for nasal drug delivery.[46-48] SVT-LCN_MaiLab were chosen for testing due to their optimal drug encapsulation efficiency and suitable physico-chemical features and a suspension of simvastatin was used as control. The simvastatin release profile from SVT-LCN_MaiLab can be seen in Figure 6. A simulated nasal fluid at pH 6.5, containing sodium, potassium and calcium salts, was used to simulate the nasal conditions. Due to the low solubility of simvastatin in aqueous solution, BSA was used to increase simvastatin solubility in the dissolution medium outside the dialysis bag to achieve sink conditions throughout the experiment. BSA was selected for being closer to physiological conditions in comparison to surfactants or co-solvents generally used to increase the solubility of poorly soluble drugs. The in vitro release tests were performed over 24 hours for SVT-LCN_MaiLab and simvastatin suspension. For the sus- pension, after an initial rapid release in the first hour, a plateau characterized by a very low dissolution rate was reached. This was not observed for the nanoparticle formulation. In fact, the nanoparticles kept releasing simvastatin at a constant release rate from the second hour to the end of the experiment. As shown in Figure 6, 40% of simvastatin was released from SVT-LCN_MaiLab nanoparticles within 8 hours, displaying a significantly faster release than the simvastatin suspension (21.17% simvastatin released after 8 hour).

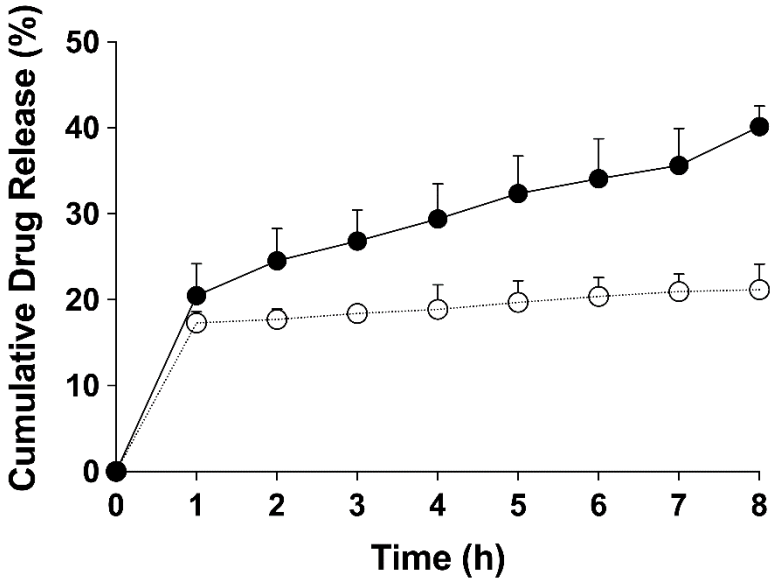

Figure 6: Simvastatin release profile from SVT-LCN_MaiLab nanoparticles (●) and a control simvastatin suspension (○) in simulated nasal fluid with BSA 0.5% at pH 6.5 and 37°C.

Abbreviations: BSA, bovine serum albumin; SVT-LCNs, simvastatin-loaded lecithin/chitosan nanoparticles; Mai, Maisine; Lab, Labrafac.

5.4 Cytotoxicity Studies

In the last few years, the human RPMI 2650 epidermoid carcinoma cells has been proposed as a suitable model of nasal mucosa for *in vitro* studies simulating nasal drug transport.[49] Recently, this nasal epithelial cell line has been grown in air-liquid interface conditions to develop an *in vitro* model of the nasal mucosa suitable for studies of deposition and permeation of nasally administered formulations. These cells appear a good choice also for *in vitro* cytotoxicity assay of a new formulation such as simvastatin-loaded lecithin/chitosan nanoparticles. For this purpose, RPMI 2650 cells were incubated for 72h with increasing concentrations of simvastatin solution, blank nanoparticles and simvastatin-loaded nanoparticles. The cells viability was recorded as percentage in comparison to untreated cells and plotted in Figure 7 against the simvastatin concentration. In the case of blank nanoparticles, this value corresponded to the equivalent amount of carrier nanoparticles.

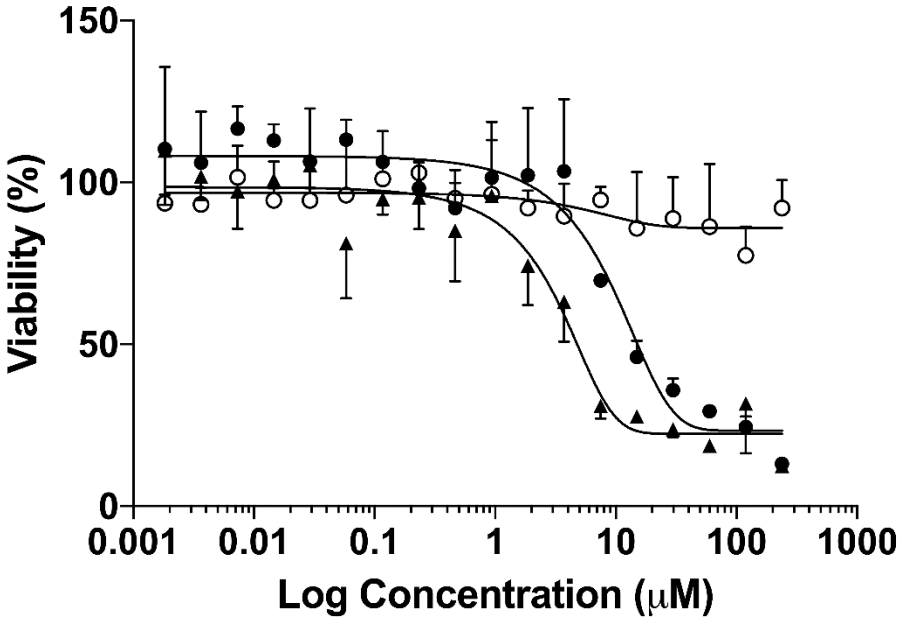

Figure 7: *In vitro* cytoxicity studies on human nasal cell line RPMI 2650 of simvastatin (▲), simvastatin-loaded nanoparticles SVT-LCN_MaiLab (●), and blank nanoparticles LCN_MaiLab (○).

Notes: Cell viability is plotted against the logarithm of simvastatin concentration.

Abbreviations: SVT-LCNs, simvastatin-loaded lecithin/chitosan nanoparticles; Mai, Maisine; Lab, Labrafac.

Blank particles did not show any cytotoxicity indicating that the carrier is suitable for nasal administration. Results show that cells viability remained around 100% also in the highest concentration, suggesting that our lecithin/chitosan nanoparticles containing oil are highly biocompatible.

Cytotoxicity of simvastatin and SVT-LCN_MaiLab nanoparticles shows up to be dose-dependent, as seen in the cells viability behaviour. For SVT-LCN_MaiLab nanoparticles IC_{50} was found to be 9.92 μM nearly three times that of pure simvastatin (3.50 μM), then displaying a reduced toxicity compared to the pure drug.

5.5 Gamma Scintigraphy Studies

A preliminary study of biodistribution in rats after nasal administration of ^{99m}Tc labelled nanoparticles was carried out by gamma scintigraphy which was compared to the administration of a radiolabelled suspension of simvastatin, used as controls. Figure 8 shows organ distribution of the radioactivity detected 90 minutes after the nasal instillation in each nostril of 10 µl nanoparticles or drug suspension. The two radioactivity distributions are very different. In the case of the drug suspension most of the radioactivity is found in the lung, followed by far by the stomach and the liver. Only a very limited amount of radioactivity is found in other organs or in the brain. On the contrary, after the nasal administration of nanoparticle formulation, a significant fraction of the radioactivity (more than 30%) was localized in the brain, followed by an accumulation in the kidneys comparable to the levels observed for controls. Other organs such as the liver, lung, heart, and stomach contained progressively decreasing amounts of radioactivity.

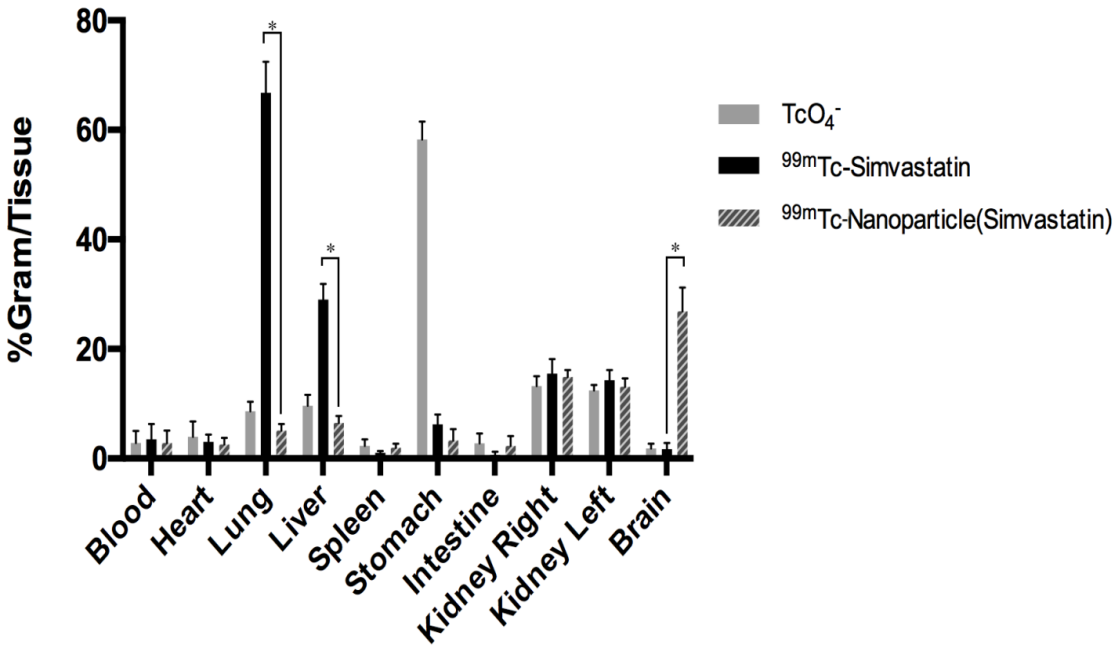

Figure 8: Radioactivity biodistribution in Wistar rats 90 minutes after the nasal instillation of 20 µL (10 µL in each nostril) of ^{99m}Tc-labeled simvastatin-loaded nanoparticles, simvastatin suspension, and pertechnetate (TcO^{4-}) expressed as percentage of administered dose (%D) per gram of tissue (n=3, *P<0.001).

6 Discussion

Administration of poorly soluble drugs intranasally for systemic and CNS therapeutic action can be extremely challenging due to the low volume of nasal secretions, the barrier provided by the mucus layer and the short time available for dissolution/absorption because of mucociliary clearance.[50,51]

It is considered that nanoparticles could improve the bioavailability of nasally administered substances.[52,53] Chitosan and lecithin have been used to produce nanoparticles and liposomes for many years.[54-56] The main advantages attributed to these components are their biocompatibility and biodegradability and in fact, liposomes are still by far the most successful nanomedicines on the market.[57] Recently, our research group proposed hybrid nanoparticles formed by the electrostatic interaction of these two components, i.e. the positively charged polysaccharide chitosan and the negatively charged phospholipids of soybean lecithin.[58,59] These nanoparticles were demonstrated to be extremely effective in the improvement of accumulation of corticosteroid drugs in skin layers and of the permeation of tamoxifen through the intestinal epithelium.[29,60,61]

Consequently, it has been hypothesized that this delivery system could be an interesting candidate for the nasal administration of lipophilic drugs, in particular for the nose-to-brain pathway. Simvastatin was selected as an ideal model drug as it has a sound rationale for its use in neurodegenerative diseases and could benefit from an alternative administration route, providing a direct access to the CNS.[62]

To efficiently load simvastatin into lecithin/chitosan nanoparticles efficiently was necessary the addition into the formulation of an oily component. Various pharmaceutical lipophilic solvents were selected based on simvastatin solubility data reported in the literature. In a systematic study of simvastatin solubility in oils and surfactants, Capryol PGMC and Capryol 90 were found to be the best solvents for simvastatin (~105 mg/ml), followed by other oily excipients, such as Maisine (~60 mg/ml) and Labrafac (~25 mg/ml).[63] Therefore, combinations of these oils were used in order to optimize simvastatin encapsulation efficiency in lecithin/chitosan nanoparticles. Nanoparticles with positive surface charge and a size of around 200-300 nm in size were obtained, showing a good simvastatin encapsulation efficiency and providing a 30-fold increase in simvastatin apparent solubility in water. Interestingly, the best formulation, containing the combination of glyceryl monolinoleate (Maisine) and medium-chain triglycerides (Labrafac), reached an apparent simvastatin solubility fivefold the one that could be expected extrapolating from the solubility of the drug in the two solvents and their respective amounts in the formulation, showing a

synergistic effect. This suggests an optimized accommodation of the simvastatin into the oily core of the particles surrounded by a lecithin/chitosan shell, as evidenced by the SAXS experiments. It could be hypothesized that Maisine, a lipid with slightly higher melting point than the others selected (Maisine is liquid at 40°C) can intimately mix with the molecules of Labrafac when heated, forming a semi-solid oil core when cooled down at room temperature, favouring simvastatin entrapping. In fact, LCN_MaiLab nanoparticles show the highest encapsulation efficiency of formulated drug, encapsulating it almost entirely.

Concerning the stability of the preparations, it has been previously reported that surface charge is a determinant parameter to stabilize nanoparticles. In particular, when the zeta potential exceeds 30 mV, nanoparticles are regarded as stable, their stability increasing along with net surface charge.[64] Blank nanoparticles displayed similar values of zeta potential, generally higher than their equivalent loaded nanoparticles (see Table 1). The surface charge of all lecithin/chitosan nanoparticles was highly positive, as expected for the presence of chitosan, a positive polysaccharide covering the surface of the nanoparticles, as reported previously. The introduction of simvastatin and of some of oils into lecithin/chitosan nanoparticles resulted in a decrease of their surface charge (SVT-LCN_$Cap_{I}Cap_{II}$, SVT-LCN_$MaiCap_{I}$ and SVT-LCN_$LabCap_{I}$). Being the simvastatin hydroxyl acid form capable to deprotonate to a negatively charged ion, this could lead to charge neutralisation and loading close to the external shell.

On the contrary, the addition of the oil combination Maisine plus Labrafac into lecithin/chitosan nanocapsules (SVT-LCN_MaiLab) did not result in an important reduction of the positive surface charge, in line with the already suggested efficient trapping of simvastatin in a solid lipid core. A similar behaviour can be observed also for SVT-LCN_Mai_2, supporting the effectiveness of this oil in embedding simvastatin inside the core, then conferring great stability to the nanoparticles system.

This core-shell organization evidenced by the nanoparticle structure investigation by SAXS, is maintained after interaction with mucus, where an interaction with the superficial shell is evidenced. This agrees with several previous studies that indicate mucoadhesion as an important feature of nasal preparations. In particular, this may provide a much higher residence time in the nasal cavity, pivotal to allow an enhancement of drug availability.[65]

For the *in vitro* release studies, a simulated nasal electrolyte solution containing BSA was preferred to surfactant solutions[47] or mixtures with organic solvents miscible with water[66], as a more physiologic dissolution medium. Generally, drug inclusion in nanoparticles is a strategy to prolong the release. Here, on the contrary, after a similar initial “burst” release, a faster release rate is evidenced for nanoparticles in comparison to a simple simvastatin suspension, likely resulting from the high surface area of nanoparticles and the

efficient dispersion of the drug in the nanoparticle core. This result is even more relevant as usually, apparent drug release in dialysis methods is hindered by the dialysis membrane itself, that poses an additional barrier to the diffusion of the drug to the receiver compartment.[67]

As already pointed-out, the major drawback affecting the nasal administration is the removal of the formulation through the mucocillary clearance, a mechanism that can reduce the bioavailability of poorly water-soluble drugs.[51] Hence fast absorption is required to achieve the needed therapeutic concentrations. The role of chitosan in promoting mucoadhesion and penetration is well known. Several studies suggest that chitosan nanoparticles are transported by transmucosal route with increased uptake when compared to other nanoparticles, thanks to chitosan mucoadhesivity.[68,69] However, it is doubtful that slow release nanoparticles would provide a significant improvement of intranasal drug delivery.[70] For this reason, the present system, both mucoadhesive and fast releasing as compared to a typical formulation for nasal administration of drugs, such as a suspension, could overcome limitation on delivery due to clearance. Moreover, previous studies have shown that chitosan/lecithin nanoparticles are highly susceptible to degradation by gastrointestinal enzymes, thus promoting drug release and drug permeation through intestinal epithelium via an enhanced paracellular transport.[29] This degradation is likely to occur also on the nasal mucosal surface. Degradation has been evidenced in presence of mucus and lysozyme, where a breakdown of the original particle structure occurs over time (see Figure 5). In fact, nasal secretions are rich in antibacterial peptides and proteins that are part of the innate immune defences of the body.[43] Among these proteins, one of the most abundant is lysozyme, an enzyme able to degrade proteoglycans of bacterial cell wall, but also able to degrade chitosan.[71] The degradation of the nanoparticles by endogenous enzymatic process constitutes a new approach for nasal delivery and could represent an interesting troyan-horse strategy for improving the nasal bioavailability of statins and other poorly soluble drugs.

Interestingly, despite some concerns have been raised in the literature on the biocompatibility of positively charged chitosan nanoparticles, the cytotoxicity studies carried out evidenced no apparent toxicity for the proposed drug nanocarriers. This is of course an important result, being safety a prerequisite to the exploitation of the formulation. In fact, the nasal epithelial layer represents one of the first body's defence lines, and materials harming the mucosal barrier constitute a potential health risk.[72] The cytotoxicity evidenced by simvastatin loaded nanoparticles is actually related to the statin itself. In fact, several recent studies have demonstrated the anticancer activity of statins in various cancer cells.[10,73,74]Since RPMI 2650 cells are derived from an epidermoidal carcinoma of the nasal

septum the cytotoxic activity detected is to be attributed to the drug released by nanoparticles or by the direct uptake of nanoparticles by the cells. As nanoparticles degradation and/or drug release is time dependent, SVT-LCN_MaiLab showed lower IC_{50} values than simvastatin.

In vivo preliminary studies were carried out to assess the potential of the formulation for the proposed nose-to-brain delivery of statins. Gamma scintigraphy was selected as a powerful and rapid method to evaluate the formulation biodistribution after nasal administration of the formulation in rodents.[75] A suspension of simvastatin was used as a control. It is worth pointing out that the radioactivity that is detected cannot be considered permanently bound to the particles or to the drug molecule. However, it appears clear that after the nasal instillation of the nanoparticle formulation, the radioactivity can be localized mainly in the kidneys and in the brain. This biodistribution implies a significant absorption of the radiolabel through the nasal mucosa, that accounts for the localization in the kidney where the radioisotope will be eliminated by filtration and an efficient transfer via the nose-to-brain pathway of around the 20% of the administered radioactivity dose. This is not observed for the control simvastatin suspension where the radioactivity mainly localizes in the lungs and GI tract of the animals, as often happens for rodents that are obligate nose breather. It can be hypothesized that the nanoparticle formulation is more effective both through chitosan-mediated mucoadhesion[76] and penetration enhancing via tight junctions opening[77], but most likely also as a consequence of mucosal biodegradation of the nanoparticle structure. Overall, these processes can favour the transmucosal absorption of the radioactivity, independently from the form it may assume: isotopes linked to entire nanoparticles, particle fragments, polysaccharide chains or free from linkage to any of nanoparticle structures.

7 Conclusion

Although some brain targeted nanoparticles loaded with statins have been proposed by some other authors, this is to our knowledge the first research proposing nanoparticles to be administered nasally to deliver statins to the brain. The particles were designed to optimize the loading of a lipophilic drug such as simvastatin and to provide multiple features helpful for nasal delivery, such as physical and chemical stability, biocompatibility, mucoadhesion and a rapid drug release. Furthermore, particles appear prone to a mucus specific biodegradation process that represent an innovative Trojan-horse strategy able to boost the permeation of the encapsulated drug. Preliminary *in vivo* gamma scintigraphy studies, showed an enhanced nose-to-brain transport of the radioactivity administered nasally for the simvastatin-loaded lecithin/chitosan nanoparticles but not for a more traditional formulation such as a suspension. Further *in vivo* studies are required to clarify if nanoparticles are taken up by nasal epithelium or just favour the drug absorption without crossing the mucosa and to investigate the pharmacokinetics and efficacy of the nanoformulated statin after administration via the nasal route.

References

1. Bonetti PO, Lerman LO, Napoli C, Lerman A. Statin effects beyond lipid lowering--are they clinically relevant? Eur Heart J. 2003;24(3):225-248. doi:10.1016/S0195-668X(02)00419-0.

2. Heart Protection Study Collaborative Group. MRC/BHF Heart Protection Study of cholesterol lowering with simvastatin in 20,536 high-risk individuals: a randomised placebo-controlled trial. The Lancet. 2002;360(9326):7-22. doi:10.1016/S0140-6736(02)09327-3.

3. Romana B, Batger M, Prestidge C, Colombo G, Sonvico F. Expanding the Therapeutic Potential of Statins by Means of Nanotechnology Enabled Drug Delivery Systems. Curr Top Med Chem. 2014;14(9):1182-1193. doi:10.2174/1568026614666140329232252.

4. Liao JK, Laufs U. Pleiotropic effects of statins. Annu Rev Pharmacol Toxicol. 2005;45:89-118. doi:10.1146/annurev.pharmtox.45.120403.095748.

5. Palinski W. Unraveling Pleiotropic Effects of Statins on Plaque Rupture. Arterioscler Thromb Vasc Biol. 2002;22(11):1745-1750. doi:10.1161/01.ATV.0000038754.39483.CD.

6. Blanco-Colio LM, Tuñón J, Martín-Ventura JL, Egido J. Anti-inflammatory and immunomodulatory effects of statins. Kidney Int. 2003;63(1):12-23. doi:10.1046/j.1523-1755.2003.00744.x.

7. Jain MK, Ridker PM. Anti-inflammatory effects of statins: clinical evidence and basic mechanisms. Nat Rev Drug Discov. 2005;4(12):977-987. doi:10.1038/nrd1901.

8. McCarey DW, McInnes IB, Madhok R, et al. Trial of Atorvastatin in Rheumatoid Arthritis (TARA): double-blind, randomised placebo-controlled trial. Lancet. 2004;363(9426):2015-2021. doi:10.1016/S0140-6736(04)16449-0.

9. Marin L, Colombo P, Bebawy M, Young PM, Traini D. Chronic obstructive pulmonary disease: patho-physiology, current methods of treatment and the potential for simvastatin in disease management. Expert Opin Drug Deliv. 2011;8(9):1205-1220. doi:10.1517/17425247.2011.588697.

10. Gopalan A, Yu W, Sanders BG, Kline K. Simvastatin inhibition of mevalonate pathway induces apoptosis in human breast cancer cells via activation of JNK/CHOP/DR5 signaling pathway. Cancer Lett. 2013;329(1):9-16. doi:10.1016/j.canlet.2012.08.031.

11. Wang Q, Yan J, Chen X, et al. Statins: Multiple neuroprotective mechanisms in neurodegenerative diseases. Exp Neurol. 2011;230(1):27-34. doi:10.1016/j.expneurol.2010.04.006.

12. Ghribi O, Larsen B, Schrag M, Herman MM. High cholesterol content in neurons increases BACE, β-amyloid, and phosphorylated tau levels in rabbit hippocampus. Exp Neurol. 2006;200(2):460-467. doi:10.1016/j.expneurol.2006.03.019.

13. Puglielli L, Tanzi RE, Kovacs DM. Alzheimer's disease: the cholesterol connection. Nat Neurosci. 2003;6(4):345-351. doi:10.1038/nn0403-345.

14. Bu G. Apolipoprotein E and its receptors in Alzheimer's disease: pathways,

pathogenesis and therapy. Nat Rev Neurosci. 2009;10(5):333-344. doi:10.1038/nrn2620.

15. Kivipelto M, Helkala EL, Laakso MP, et al. Apolipoprotein E epsilon4 allele, elevated midlife total cholesterol level, and high midlife systolic blood pressure are independent risk factors for late-life Alzheimer disease. Ann Intern Med. 2002;137(3):149.

16. Fassbender K, Simons M, Bergmann C, et al. Simvastatin strongly reduces levels of Alzheimer's disease beta -amyloid peptides Abeta 42 and Abeta 40 in vitro and in vivo. Proc Natl Acad Sci USA. 2001;98(10):5856-5861. doi:10.1073/pnas.081620098.

17. Ehehalt R, Keller P, Haass C, Thiele C, Simons K. Amyloidogenic processing of the Alzheimer beta-amyloid precursor protein depends on lipid rafts. J Cell Biol. 2003;160(1):113-123. doi:10.1083/jcb.200207113.

18. Wang Q, Yan J, Chen X, et al. Statins: multiple neuroprotective mechanisms in neurodegenerative diseases. Exp Neurol. 2011;230(1):27-34. doi:10.1016/j.expneurol.2010.04.006.

19. Pires A, Fortuna A, Alves G, Falcão A. Intranasal drug delivery: how, why and what for? J Pharm Pharm Sci. 2009;12(3):288-311.

20. Suman JD. Current understanding of nasal morphology and physiology as a drug delivery target. Drug Deliv and Transl Res. 2013;3(1):4-15. doi:10.1007/s13346-012-0121-z.

21. Mistry A, Glud SZ, Kjems J, et al. Effect of physicochemical properties on intranasal nanoparticle transit into murine olfactory epithelium. J Drug Target. 2009;17(7):543-552. doi:10.1080/10611860903055470.

22. Kozlovskaya L, Stepensky D. Quantitative analysis of drug delivery to the brain via nasal route. J Control Release. 2014;189:133-140. doi:10.1016/j.jconrel.2014.06.053.

23. Illum L. Transport of drugs from the nasal cavity to the central nervous system. Eur J Pharm Sci. 2000;11(1):1-18.

24. Illum L. Is nose-to-brain transport of drugs in man a reality? J Pharm Pharmacol. 2004;56(1):3-17. doi:10.1211/0022357022539.

25. Horvát S, Fehér A, Wolburg H, et al. Sodium hyaluronate as a mucoadhesive component in nasal formulation enhances delivery of molecules to brain tissue. Eur J Pharm Biopharm. 2009;72(1):252-259. doi:10.1016/j.ejpb.2008.10.009.

26. Zhang Q-Z, Zha L-S, Zhang Y, et al. The brain targeting efficiency following nasally applied MPEG-PLA nanoparticles in rats. J Drug Target. 2008;14(5):281-290. doi:10.1080/10611860600721051.

27. Betbeder D, Spérandio S, Latapie JP, et al. Biovector nanoparticles improve antinociceptive efficacy of nasal morphine. Pharm Res. 2000;17(6):743-748.

28. Gerelli Y, Di Bari MT, Deriu A, et al. Structure and organization of phospholipid/polysaccharide nanoparticles. J Phys: Condens Matter. 2008;20(10):104211. doi:10.1088/0953-8984/20/10/104211.

29. Barbieri S, Buttini F, Rossi A, et al. Ex vivo permeation of tamoxifen and its 4-OH metabolite through rat intestine from lecithin/chitosan nanoparticles. Int J Pharm. 2015;491(1-2):99-104. doi:10.1016/j.ijpharm.2015.06.021.

30. Takeuchi H, MATSUI Y, Yamamoto H, Kawashima Y. Mucoadhesive properties of carbopol or chitosan-coated liposomes and their effectiveness in the oral administration of calcitonin to rats. J Control Release. 2003;86(2-3):235-242.

31. Smith JM, Dornish M, Wood EJ. Involvement of protein kinase C in chitosan glutamate-mediated tight junction disruption. Biomaterials. 2005;26(16):3269-3276. doi:10.1016/j.biomaterials.2004.06.020.

32. Hole P, Sillence K, Hannell C, et al. Interlaboratory comparison of size measurements on nanoparticles using nanoparticle tracking analysis (NTA). J Nanopart Res. 2013;15:2101. doi:10.1007/s11051-013-2101-8.

33. Filipe V, Hawe A, Jiskoot W. Critical evaluation of Nanoparticle Tracking Analysis (NTA) by NanoSight for the measurement of nanoparticles and protein aggregates. Pharm Res. 2010;27(5):796-810. doi:10.1007/s11095-010-0073-2.

34. Yang D-J, Hwang LS. Study on the conversion of three natural statins from lactone forms to their corresponding hydroxy acid forms and their determination in Pu-Erh tea. J Chromatogr A. 2006;1119(1-2):277-284. doi:10.1016/j.chroma.2005.12.031.

35. Castile J, Cheng Y-H, Simmons B, Perelman M, Smith A, Watts P. Development of in vitro models to demonstrate the ability of PecSys®, an in situ nasal gelling technology, to reduce nasal run-off and drip. Drug Dev Ind Pharm. 2013;39(5):816-824. doi:10.3109/03639045.2012.707210.

36. Martins FPP, Gutfilen B, de Souza SAL, et al. Monitoring rheumatoid arthritis synovitis with 99mTc-anti-CD3. Br J Radiol. 2008;81(961):25-29. doi:10.1259/bjr/63780400.

37. Martins FPP, Souza SAL, Gonçalves RT, Fonseca LMB, Gutfilen B. Preliminary results of [99mTc]OKT3 scintigraphy to evaluate acute rejection in renal transplants. Transplant Proc. 2004;36(9):2664-2667. doi:10.1016/j.transproceed.2004.09.085.

38. Lopes FPPL, de Azevedo MNL, Marchiori E, da Fonseca LMB, de Souza SAL, Gutfilen B. Use of 99mTc-anti-CD3 scintigraphy in the differential diagnosis of rheumatic diseases. Rheumatology (Oxford). 2010;49(5):933-939. doi:10.1093/rheumatology/kep471.

39. Sonvico F, Cagnani A, Rossi A, et al. Formation of self-organized nanoparticles by lecithin/chitosan ionic interaction. Int J Pharm. 2006;324(1):67-73. doi:10.1016/j.ijpharm.2006.06.036.

40. Gerelli Y, Bari M, Barbieri S, et al. Flexibility and drug release features of lipid/saccharide nanoparticles. Soft Matter. 2010;6(3):685-691.

41. Wright M. Nanoparticle tracking analysis for the multiparameter characterization and counting of nanoparticle suspensions. Methods Mol Biol. 2012;906:511-524. doi:10.1007/978-1-61779-953-2_41.

42. Sokolova V, Ludwig A-K, Hornung S, et al. Characterisation of exosomes derived from human cells by nanoparticle tracking analysis and scanning electron microscopy. Colloids Surf B Biointerfaces. 2011;87(1):146-150. doi:10.1016/j.colsurfb.2011.05.013.

43. Travis SM, Singh PK, Welsh MJ. Antimicrobial peptides and proteins in the innate defense of the airway surface. Curr Opin Immunol. 2001;13(1):89-95.

44. Cole AM, Dewan P, Ganz T. Innate antimicrobial activity of nasal secretions. Infect Immun. 1999;67(7):3267-3275.

45. D'souza SS, Deluca PP. Methods to assess in vitro drug release from injectable polymeric particulate systems. Pharm Res. 2006;23(3):460-474. doi:10.1007/s11095-005-9397-8.

46. Chen KH, Di Sabatino M, Albertini B, Passerini N, Kett VL. The effect of polymer coatings on physicochemical properties of spray-dried liposomes for nasal delivery of BSA. Eur J Pharm Sci. 2013;50(3-4):312-322. doi:10.1016/j.ejps.2013.07.006.

47. Sood S, Jain K, Gowthamarajan K. Optimization of curcumin nanoemulsion for intranasal delivery using design of experiment and its toxicity assessment. Colloids Surf B Biointerfaces. 2014;113:330-337. doi:10.1016/j.colsurfb.2013.09.030.

48. Seju U, Kumar A, Sawant KK. Development and evaluation of olanzapine-loaded PLGA nanoparticles for nose-to-brain delivery: in vitro and in vivo studies. Acta Biomaterialia. 2011;7(12):4169-4176. doi:10.1016/j.actbio.2011.07.025.

49. Bai S, Yang T, Abbruscato TJ, Ahsan F. Evaluation of human nasal RPMI 2650 cells grown at an air-liquid interface as a model for nasal drug transport studies. J Pharm Sci. 2008;97(3):1165-1178. doi:10.1002/jps.21031.

50. Lochhead JJ, Thorne RG. Intranasal delivery of biologics to the central nervous system. Adv Drug Deliv Rev. 2012;64(7):614-628. doi:10.1016/j.addr.2011.11.002.

51. Sigurdsson HH, Kirch J, Lehr C-M. Mucus as a barrier to lipophilic drugs. Int J Pharm. 2013;453(1):56-64. doi:10.1016/j.ijpharm.2013.05.040.

52. Mistry A, Stolnik S, Illum L. Nanoparticles for direct nose-to-brain delivery of drugs. Int J Pharm. 2009;379(1):146-157. doi:10.1016/j.ijpharm.2009.06.019.

53. Kumar A, Pandey AN, Jain SK. Nasal-nanotechnology: revolution for efficient therapeutics delivery. Drug Deliv. September 2014:1-13. doi:10.3109/10717544.2014.920431.

54. Bernkop-Schnürch A, Dünnhaupt S. Chitosan-based drug delivery systems. Eur J Pharm Biopharm. 2012;81(3):463-469. doi:10.1016/j.ejpb.2012.04.007.

55. Akbarzadeh A, Rezaei-Sadabady R, Davaran S, et al. Liposome: classification, preparation, and applications. Nanoscale Res Lett. 2013;8(1):102. doi:10.1186/1556-276X-8-102.

56. Gabizon AA, Shmeeda H, Zalipsky S. Pros and cons of the liposome platform in cancer drug targeting. J Liposome Res. 2006;16(3):175-183. doi:10.1080/08982100600848769.

57. Barenholz Y. Doxil®--the first FDA-approved nano-drug: lessons learned. J Control Release. 2012;160(2):117-134. doi:10.1016/j.jconrel.2012.03.020.

58. Di Bari MT, Gerelli Y, Sonvico F, et al. Dynamics of lipid–saccharide nanoparticles by quasielastic neutron scattering. Chemical Physics. 2008;345(2-3):239-244. doi:10.1016/j.chemphys.2007.08.006.

59. Sonvico F, Di Bari MT, Bove L, Deriu A, Cavatorta F, Albanese G. Mean square

hydrogen fluctuations in chitosan/lecithin nanoparticles from elastic neutron scattering experiments. Physica B: Condensed Matter. 2006;385-386:725-727. doi:10.1016/j.physb.2006.06.034.

60. Senyiğit T, Sonvico F, Barbieri S, Ozer O, Santi P, Colombo P. Lecithin/chitosan nanoparticles of clobetasol-17-propionate capable of accumulation in pig skin. J Control Release. 2010;142(3):368-373. doi:10.1016/j.jconrel.2009.11.013.

61. Barbieri S, Sonvico F, Como C, et al. Lecithin/chitosan controlled release nanopreparations of tamoxifen citrate: loading, enzyme-trigger release and cell uptake. J Control Release. 2013;167(3):276-283. doi:10.1016/j.jconrel.2013.02.009.

62. Jiang Y, Li Y, Liu X. Intranasal delivery: circumventing the iron curtain to treat neurological disorders. Expert Opin Drug Deliv. 2015;12 (11):000-000. doi:10.1517/17425247.2015.1065812.

63. Karim FT, Kalam A, Anwar R, Miah MM, Rahman MS, Islam SMA. Preparation and evaluation of SEDDS of simvastatin by in vivo, in vitroand ex vivotechnique. Drug Dev Ind Pharm. 2014;41(8):1338-1342. doi:10.3109/03639045.2014.950271.

64. Müller RH, Jacobs C, Kayser O. Nanosuspensions as particulate drug formulations in therapy. Rationale for development and what we can expect for the future. Adv Drug Deliv Rev. 2001;47(1):3-19.

65. Casettari L, Illum L. Chitosan in nasal delivery systems for therapeutic drugs. J Control Release. 2014;190C:189-200. doi:10.1016/j.jconrel.2014.05.003.

66. Dalpiaz A, Ferraro L, Perrone D, et al. Brain uptake of a Zidovudine prodrug after nasal administration of solid lipid microparticles. Mol Pharm. 2014;11(5):1550-1561. doi:10.1021/mp400735c.

67. Modi S, Anderson BD. Determination of Drug Release Kinetics from Nanoparticles: Overcoming Pitfalls of the Dynamic Dialysis Method. Mol Pharm. 2013;10(8):3076-3089. doi:10.1021/mp400154a.

68. Artursson P, Lindmark T, Davis SS, Illum L. Effect of chitosan on the permeability of monolayers of intestinal epithelial cells (Caco-2). Pharm Res. 1994;11(9):1358-1361.

69. Prego C, García M, Torres D, Alonso MJ. Transmucosal macromolecular drug delivery. J Control Release. 2005;101(1-3):151-162. doi:10.1016/j.jconrel.2004.07.030.

70. Illum L. Nanoparticulate systems for nasal delivery of drugs: a real improvement over simple systems? J Pharm Sci. 2007;96(3):473-483. doi:10.1002/jps.20718.

71. Nordtveit RJ, Vårum KM, Smidsrød O. Degradation of partially N-acetylated chitosans with hen egg white and human lysozyme. Carbohydr Polym. 1996;29(2):163-167. doi:10.1016/0144-8617(96)00003-3.

72. Ekelund K, Östh K, Påhlstorp C, Björk E, Ulvenlund S, Johansson F. Correlation between epithelial toxicity and surfactant structure as derived from the effects of polyethyleneoxide surfactants on caco-2 cell monolayers and pig nasal mucosa. J Pharm Sci. 2005;94(4):730-744. doi:10.1002/jps.20283.

73. Wu H, Jiang H, Lu D, et al. Effect of simvastatin on glioma cell proliferation, migration,

and apoptosis. Neurosurgery. 2009;65(6):1087–96–discussion1096–7. doi:10.1227/01.NEU.0000360130.52812.1D.

74. Ali H, Shirode AB, Sylvester PW, Nazzal S. Preparation, characterization, and anticancer effects of simvastatin-tocotrienol lipid nanoparticles. Int J Pharm. 2010;389(1-2):223-231. doi:10.1016/j.ijpharm.2010.01.018.

75. Alam S, Khan ZI, Mustafa G, et al. Development and evaluation of thymoquinone-encapsulated chitosan nanoparticles for nose-to-brain targeting: a pharmacoscintigraphic study. Int J Nanomedicine. 2012;7:5705-5718. doi:10.2147/IJN.S35329.

76. Jogani VV, Shah PJ, Mishra AK, Misra AR. Intranasal mucoadhesive microemulsion of tacrine to improve brain targeting. Alzheimer Dis Assoc Disord. 2008;22(2):116-124. doi:10.1097/WAD.0b013e318157205b.

77. Vllasaliu D, Exposito-Harris R, Heras A, et al. Tight junction modulation by chitosan nanoparticles: comparison with chitosan solution. Int J Pharm. 2010;400(1-2):183-193. doi:10.1016/j.ijpharm.2010.08.020.

CHAPTER 3

MUCOADHESIVE AND BIODEGRADABLE HYBRID NANOPARTICLES FOR THE NASAL DELIVERY OF STATINS: ENZYME-TRIGGERED RELEASE AND MUCOSAL PERMEATION ENHANCEMENT

Mucoadhesive and Biodegradable Hybrid Nanoparticles for the Nasal Delivery of Statins: Enzyme-Triggered Release and Mucosal Permeation Enhancement

Adapted from **Respiratory Drug Delivery 2018** conference paper

April 2018

Abstract

The nasal delivery has been indicated as one of the most interesting alternative routes for brain delivery of drugs, since it is able to bypass the crossing of the blood brain barrier (BBB). The use of nanoparticles constitutes a promising approach for the transport of therapeutics across the nasal epithelium. However, the delivery of therapeutically relevant amounts of drugs exploiting the nasal route is strongly dependent on the permeation enhancement provided by nanoparticles drug carriers. In this work, we evaluated nanoparticle interaction and transport across the nasal epithelium. Hybrid lecithin/chitosan nanoparticles encapsulating simvastatin, presenting an average size of 200 nm and positive surface charge, were studied for their mucoadhesion and drug transport across the nasal epithelium. Drug release studies were also performed in conditions simulating those found in the nasal cavity to investigate nanoparticles delivery performance following nasal administration. Chitosan-coated nanoparticles showed good mucoadhesion on pig nasal mucosa, potentially providing an increased residence time into the nasal cavity compared to non-encapsulated statin. However, nanoparticles after interaction with a simulated nasal mucus showed a decreased simvastatin release and/or the drug could not diffuse trough the mucus network. Nevertheless, the effect of lysozyme and phospholipase A2, two antibacterial enzymes present in the nasal secretions, was able promote drug release as a consequence of nanoparticles composition. Indeed, an enzymatic triggered-release was observed in the presence of enzymes, increasing in 5-fold simvastatin release from lecithin/chitosan nanoparticles. Even in the presence of the simulated mucus, simvastatin release nanoparticles increased 3-fold in presence of the enzymes. Moreover, compared to the free drug material, chitosan-coated hybrid nanoparticles enhanced simvastatin permeation across a cellular model of nasal epithelium and excised rabbit nasal mucosa. Hence, mucoadhesive, biodegradable and permeation enhancing hybrid lecithin/chitosan nanoparticles represent an innovative strategy to efficiently delivery drugs exploiting the nasal route.

KEYWORDS: lecithin/chitosan nanoparticles, enzymatic degradation, mucus, RPMI2650 cell line, statins.

1 Introduction

The nasal delivery has been indicated as one of the most interesting alternative routes for brain drug delivery, being able to avoid systemic drug degradation and to bypass blood brain barrier (BBB).[1] Moreover, the non-invasive intranasal administration may offer additional advantages for patient compliance and better adherence in the case of chronic therapies. However, the extent of the nasal drug absorption is highly dependent on the formulation and on its residence time on the nasal mucosa.[2] Consequently, the ability to deliver therapeutically relevant amounts of drugs directly from the nose to the brain strictly depends on the composition and physico-chemical properties of drug delivery systems.[3]

Lecithin/chitosan nanoparticles (LCNs) have been proposed as a delivery system for hydrophobic drugs through mucosal tissues.[4–6] The chitosan surface layer characterizing their structure appears suitable for nasal delivery, promoting mucoadhesion and enhancing epithelial permeability. However, it is doubtful if slow drug-release nanoparticles would provide a significant improvement of nose-to-brain delivery.[7] Conversely, rapidly biodegraded nanoparticles could improve brain targeting and bioavailability of lipophilic drugs, providing prompt drug release and absorption across the nasal mucosal surface.

In this work, simvastatin was used as a model poorly soluble drug. Moreover, statins are claimed to possess pleiotropic effects beyond cholesterol lowering, such as anti-inflammatory, antioxidant and immunomodulatory effects, but those have proved to be quite elusive in the case of oral administration.[8] Nasal delivery, avoiding hepatic first-pass metabolism, could represent a way to maximize statins pleiotropic effects. More importantly, the efficient delivery of statins to the cerebral parenchyma could be beneficial for the management of several neurodegenerative disorders. In fact, statins pleotropic effects are particularly attractive for the early treatment of Alzheimer's disease (AD).[9] Increasing evidences demonstrate an involvement of cholesterol in the upregulation of β-amyloid protein production, accumulation and deposition in brain parenchyma. In addition to the lipid lowering effects, it has also been postulated that simvastatin could provide benefit to Alzheimer's patients via a modulation of the chronic inflammatory response, an important pathophysiological aspect of neurodegeneration in AD.[10]

Simvastatin-loaded lecithin/chitosan nanoparticles production and characterization has been described in a previous work. [11] The nanoparticles designed presents several features desirable for the nose-to-brain delivery of simvastatin such as, small particles size, narrow size distribution, high positive surface charge, high encapsulation efficiency and prolonged stability. The most interesting properties however, were nanoparticles

biocompatibility, prompt drug release and high brain accumulation of radioactivity after nasal administration of ^{99m}Tc-labeled simvastatin-loaded nanoparticles in their first *in vivo* biodistribution study in rats.

Hence, in this work LCNs mucus interaction, drug release and transport across the nasal epithelium were evaluated, particularly to demonstrate how nanoparticles degradation by endogenous enzymes could represent a new strategy for the nasal delivery of statins.

2 Materials

Chitosan (Chitoclear FG), with de-acetylation degree of 95%, viscosity 103 mPas and molecular weight 152 KDa was provided by Primex (Primex, Siglufjordur, Iceland). Soybean lecithin (Lipoid® S45) was obtained from Lipoid AG (Ludwigshafen, Germany). Pharmaceutical grade oils Labrafac™ Lipophile WL 1349 (Medium Chain Triglycerides, EP) and Maisine™ 35-1 (Glycerol monolinoleate) were purchased from Gattefossé (Saint – Priest, France). Simvastatin USP 99% was provided by Polichimica (Bologna, Italy). Dialysis tubing cellulose acetate 14,000 Da molecular weight cut off (MWCO) was purchased from Sigma Aldrich (St.Louis, MO, USA). Partially purified mucin type II, from porcine stomach, was obtained by Sigma Aldrich (St.Louis, MO, USA). Human lysozyme and phospholipase A_2, extracted from porcine pancreas, were supplied by Sigma Aldrich (St. Louis, MO, USA). Human nasal septum carcinoma cell line RPMI 2650 (batch CCL-30) was purchased from American Type Culture collection (ATCC) (Manassas, VA, USA). Minimal essential medium (MEM), Fetal Bovine Serum (FBS) and non-essential aminoacids 10 x solution were provided by Life Technologies (ThermoFisher Scientific, Waltham, MA, EUA). All cell culture inserts and other culture plastics were purchased from Corning Incorporate Life Science (Corning, NY, USA). Ultrapure water (Purelab Flex, ELGA-Veolia LabWater, Italy) was used in all experiments. All other chemical reagents were from analytical grade.

3 Methods

3.1 Simvastatin-Loaded Lecithin/Chitosan Nanoparticles

Simvastatin-loaded nanoparticles were prepared through a self-emulsifying process involving lecithin, a negatively charged phospholipid and chitosan, a natural polysaccharide, according to the protocol previously reported in Chapter 2. Simvastatin-loaded lecithin/chitosan nanoparticles (SVT-LCN) were characterized for particles size, polydispersity index and surface zeta potential using a Malvern Zetasizer Nano ZSP (Malvern Instruments Ltd., Malvern, UK). Nanoparticles encapsulation efficiency (EE) was determined indirectly (Ultrafiltration using Vivaspin®2, MWCO 30,000, Sartorius, Gottingen, Germany) applying a high-performance liquid chromatography (HPLC) analytical method with a UV/Vis detector set at 238 nm.[11]

3.2 Nanoparticles *In Vitro* Drug Release

In vitro release experiments were conducted using vertical Franz type diffusion cells (0.6 cm^2 diffusional area) (Disa, Milan, Italy) assembled with a dialysis cellulose membrane (MWCO 14,000 Da, Sigma-Aldrich, St. Louis, MO, USA) separating the donor and receptor compartments. Receptor compartments were accurately filled with 4 ml of simulated nasal electrolyte solution (SNES)[12] pH 6.5, 8.77 mg/ml sodium chloride, 2.98 mg/ml potassium chloride and 0.59 mg/ml calcium chloride dehydrate, was used as release buffer to mimic physiological nasal secretions. Assembled Franz cells were maintained in a thermostated water bath at constant temperature (37 ± 0.2 °C) and under magnetic stirring (800 rpm) throughout the experiment (24 hours). SVT-LCN drug release was performed dispersing 25 µl of simvastatin formulations, i.e. SVT-LCN nanoparticles or simvastatin aqueous suspension, in a volume of 175µl of: I) SNES; II) an artificial nasal mucus (1% of porcine stomach mucin type II dispersed in SNES) [13]; III) SNES or artificial mucus containing 0.5 mg/ml of lysozyme and 0.6 µg/ml of phospholipase A_2 (Sigma Aldrich, St.Louis, MO, USA).

The experiments were performed at least in triplicate. At predetermined time points, aliquots of 500 µl were withdrawn from the receptor compartment and replaced with the same amount of fresh SNES medium, in order to maintain *sink* conditions. Collected samples were analysed by HPLC-UV for simvastatin content. At the end of the experiment, the

residual content of donor compartments and the dialysis membrane from each Franz cell were also assayed for simvastatin content to calculate the drug mass balance.

3.3 Nanoparticles Mucoadhesion on Excised Porcine Nasal Epithelium

The bioadhesive properties of chitosan-coated nanoparticles were determined by a previously reported method first introduced by Rao and Buri,[14] called the "continuous flow assay", to evaluate the extent of adherence/ retention of drug delivery technologies in the surface of a mucosal tissue subjected to a controlled gravitational force. [12] Experiments were carried out using a system consisting in a glass plate held by a polystyrene backing, facing upwards at 45° from vertical and a syringe pump (Model 200, KD Scientific, Holliston, MA, USA) which allows the percolation of a biological fluid at a constant flow rate.

Firstly, mucosa tissues were excised from the nasal septum of freshly sacrificed newborn piglets (provided by the Veterinary Medicine Department of the University of Parma) from which 6 mm diameter discs were punched out. Fresh piglet nasal mucosa containing 10 µl of SVT-LCN nanoparticles or simvastatin aqueous suspension on its surface was pasted on the glass plate and left for 5 minutes undisturbed, allowing samples interaction. Experiment was then started by washing the nasal mucosal surface with SNES at a constant flow rate (100 µl/min) for 20 min. The nozzle tip was positioned perpendicularly to the surface of the glass plate with 3 mm distance from the tissue to ensure an even distribution of the liquid over the subjected mucosal surface. Samples of the eluted washing SNES were collected every two minutes and assayed for simvastatin content by HPLC-UV. At the end of the experiment, the tissue was collected and homogenized with 1 ml of acetonitrile: 25 mM PBS buffer (65:35 v/v, pH 4.5) to extract and quantify the residual drug still present on mucosal surface. Results of the analysis were expressed as the residual simvastatin adhering to the nasal mucosa over time, expressed as percentage of the total quantity recovered (sum of the simvastatin amount recovered at the end of the experiment in the eluted SNES and form the homogenized tissue).

3.4 Simvastatin Permeation Across RPMI2650 Nasal Cells

In vitro permeation studies were performed against a cellular model of nasal mucosa, as previously developed.[15] Briefly, RPMI 2650 human nasal epithelial cell line (ATCC, Manassas, USA) were cultivated in Minimum Essential Medium enriched with 10% (v/v) of foetal bovine serum (FBS) and 1% (v/v) of non-essential amino acid solution (Life Tecnologies™, ThermoFisher, Waltham, MA, EUA), incubated at 37°C with 95% relative humidity and 5% CO_2 atmosphere. Snapwell® polyester membrane inserts (1.13 cm^2, 0.4 µm pore size, Corning Costar, Corning, NY, USA) were coated with 250 µl of 1 µg/ml collagen solution in PBS 24h prior to seeding to increase RPMI2650 cells adherence to the membrane. Cells were seeded onto collagen coated inserts with 200 µl of a cell suspension containing 2.5 x 10^6 cells/ml. 24 hours after seeding, the medium on the apical chamber was completely removed to switch cells to air-liquid interface (ALI) culture conditions, allowing cells to differentiate into a pseudo-stratified monolayer. Acceptor compartments were filled with 1.5 ml of cells culture medium and replaced 3 times *per* week.

Trans-epithelial electric resistance (TEER) measurements where recorded using a EVOM2 epithelial voltohmmeter (World Precision Instruments, Sarasota, FL, USA) to evaluate the monolayer integrity and suitability for the transport studies. Finally, 14 days after seeding, 250 µl of 1 mg/ml simvastatin-loaded nanoparticles or 1 mg/ml simvastatin suspension in HBSS used as control, were added on the cells surface to carry out permeation studies, in triplicate. Samples of 200 µl were sampled from the acceptor compartment every hour and analysed by HPLC-UV for simvastatin content. After 4 hours, the apical surface of cells epithelia was washed twice with HBSS to collect any remaining non-permeated drug. Thereafter, cells were scraped from SnapWell® inserts and lysed with CelLytic™ buffer (Invitrogen Corporation, Carlsbad, CA, USA) to extract and quantify the simvastatin inside the cells.

3.5 Simvastatin Transport Across Excised Rabbit Nasal Mucosa

To investigate nanoparticles permeation enhancement properties, rabbit nasal mucosa was selected as model permeation tissue.[16,17] Rabbit heads were supplied by a local slaughterhouse (Pola, I-Finale Emilia). Mucosal layers (average thickness around 100 µm) were excised from both sides of nasal septum within 2 hours from animal's death. The specimens removed were rinsed with SNES (pH 6.5) and immediately mounted on vertical

Franz cells (Vetrotecnica S.r.l, Padua, Italy; 0.58 cm^2 permeation area) with the mucosal side facing the donor compartment and serosal side facing the receptor.

To verify the proper cell assembly, as well as the mucosa integrity, the donor compartment was filled with 500 µl of SNES solution and left for 5 minutes undisturbed, checking that no liquid was transferred to the receptor due to an inappropriate cell mounting or lack of tissue integrity. After checking the mucosa integrity, the receptor chambers were then filled with 5 ml of SNES (pH 6.5). Assembled Franz cells were maintained in thermostatic water bath for 1 hour prior experiments to allow temperature equilibration at 37°C. Thereafter, SENES solution was removed from donor compartments and replaced with 1 ml of 1 mg/ml freshly prepared simvastatin-loaded nanoparticles formulation. Apical entrance of donor chamber was closed with Parafilm™ to prevent water evaporation. Simvastatin suspension (1 mg/ml) in SNES was used as control. Experiments were carried out for 4 hours, under constant magnetical stirring of receptor compartment (800 rpm) to avoid boundary saturation on the mucosal membrane. At predetermined time points (0, 60, 120, 180 and 240 minutes), aliquots of 500 µl were sampled from the receptor compartment and replaced with the same volume of preheated SNES solution.

At the end of the experiment, to calculate mass balance, donor samples were quantitatively collected and the compartment washed rigorously with SNES to gather all samples content weakly adhered to glass walls or the mucosal surface of the nasal tissue. Samples collected from donor were assayed for simvastatin content by dissolving 100 µl of the homogenate into 10 ml of acetonitrile: 25 mM PBS buffer (65:35 v/v, pH 4.5) and sonicating for 45 minutes (Ultrasonic cleaner; VWR, Radnor, PA, USA) to extract all the drug content from nanoparticles. Samples were filtered prior HPLC-UV analyses, to remove traces of precipitated proteins from the mucosal tissue. To extract and quantify the simvastatin content inside the mucosa, the same treatment described on **Section 3.3** was applied. Samples were kept at -20 °C until analysed. Data from simvastatin permeation were calculated by the following formula,

$$Pe = \frac{Q}{A}$$

where *Pe* is the permeability per unit of area, *Q* is the the total amount of drug transported (µg) and *A* is the diffusion area (cm^2).

4 Statistics

All results are reported as mean and standard deviation of at least 3 replicates, if not stated otherwise. All statistics analyses were performed using Prism Software Version 8.0a (Prism, Version 8.0a, GraphPad Software Inc., La Jolla, CA, USA). The differences between data were tested using One-Way ANOVA with post-hoc Bartlett's statistic, considering significant differences with * $p < 0.05$, *** $p < 0.001$ and **** $p < 0.0001$ (Prism, Version 8.0a, GraphPad Software Inc., La Jolla, CA, USA).

5 Results

5.1 Simvastatin-Loaded Lecithin/Chitosan Nanoparticles Physico-Chemical Characterization

Simvastatin-loaded nanoparticles were formed by the electrostatic self-assembly of lecithin and chitosan, as previously demonstrated.[4] In order to improve drug encapsulation efficiency, nanoparticles were produced with the addition of pharmaceutical grade oils to allow drug solubilization in the lipophilic core of the nanoparticles. As reported on Chapter 2, the addition of glycerol monolinoleate (Maisine™ 35-1) and medium-chain triglycerides (Labrafac™ WL 1349, Lab) oils improved nanoparticles properties, increasing nanoparticles loading capacity and long term stability. In fact, simvastatin-loaded LCN_MaiLab nanoparticles showed a small particle size (218 ± 12 nm), narrow size distribution (PDI 0.096 ± 0.032) and high positive surface charge (+44.3 ± 2.1 mV). High drug encapsulation efficiency was achieved with nanoparticles encapsulating 98% (± 1.16 %) of the total amount of simvastatin used in the preparation (1 mg/ml).

5.2 Drug Release from Simvastatin-Loaded Lecithin/Chitosan Nanoparticles

To investigate *in vitro* drug release, a simple electrolyte solution containing sodium, potassium and calcium salts at concentrations equivalent to those present in human nasal fluid , was used as release medium to simulate nasal secretions.[12] Release studies were performed using vertical Franz diffusion cells apparatus and a semi-permeable membrane to separate released drug from the drug encapsulated nanoparticles. Drug release profiles obtained for simvastatin-loaded nanoparticles and simvastatin suspension, in SNES, are presented in Figure 1.

While the dissolution of simvastatin suspension is quite slow in the first 7 hours of experiment, simvastatin release from nanoparticles occurred in a faster and progressive manner. In fact, 15.31% (± 1.06) of simvastatin was released from nanoparticles within 7 hours, versus 4.93 ± 0.57 % from simvastatin suspension. However, after 24 hours of experiment no significant difference was found between the amount of simvastatin released

from nanoparticles and from the suspension. Nevertheless, in both cases, only around 20% of drug content was released during 24 hours.

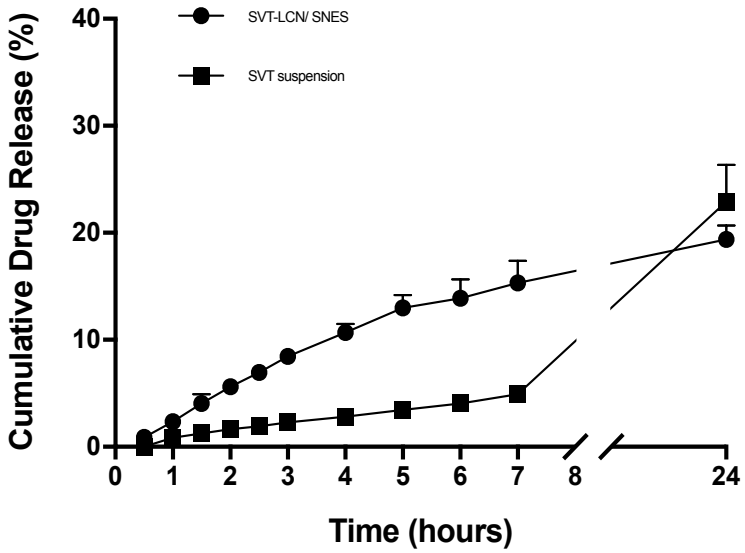

Figure 1: Simvastatin suspension and SVT-LCN nanoparticles drug release in simulated nasal electrolyte solution (SNES) pH 6.5 (n = 3, ± STD). Experiments were carried out in vertical Franz cells apparatus using cellulose dialysis membrane (MWCO 14,000).

In order to simulate more closely the physiological conditions of the nasal cavity, SNES containing mucus and/or two antibacterial enzymes present in nasal secretions, i.e. lysozyme and phospholipase A_2 (PLA2), was also used in nanoparticles drug release studies. [18]

While from SVT-LCN dispersed in only SNES simvastatin was released in a controlled manner, a different behavior was observed when enzymes were present in SNES, as shown in Figure 2. In fact, when lysozyme was added in the nanoparticles-SNES dispersion, the total drug release doubled, attaining 50% of simvastatin released in 24 hours. Interestingly, when both enzymes, lysozyme and PLA2 were added to SNES, almost all the encapsulated simvastatin was released (96.82 ± 2.62 %) within 24h.

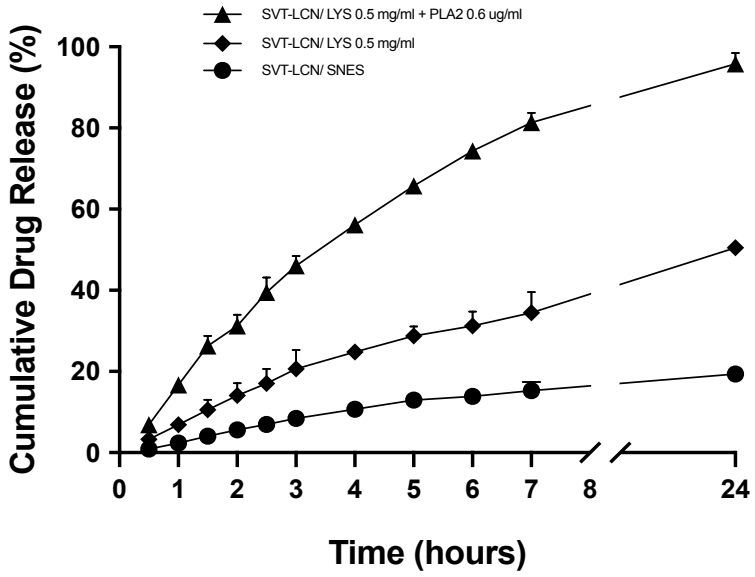

Figure 2: SVT-LCN nanoparticles release in simulated nasal electrolyte solution (SNES) pH 6.5, without enzymes (●, SVT-LCN/SNES), with lysozyme (◆, SVT-LCN/Lys 0.5mg/ml) and with lysozyme and phospholipase A2 (▲, SVT-LCN/Lys 0.5 mg/ml + PLA2 0.6 µg/ml). Experiments were carried out in triplicate (n = 3, ± STD), using vertical Franz cells apparatus using cellulose dialysis membrane (MWCO 14,000).

Finally, to understand how mucus could impact nanoparticles delivery following nasal administration, *in vitro* release studies were also performed using a simulated nasal mucus. Figure 3 illustrate that nanoparticles dispersed in the artificial mucus (1% porcine mucin) slowdown simvastatin release more than 2 times (19.40 ± 1.30 % vs 8.69 ± 2.63 %). However, when the enzymes were added to the simulated mucus, the total release ratio of simvastatin increased to 22%. These experiments corroborate with the hypothesis that hybrid phospholipid/polysaccharide nanoparticles are mucoadhesive systems prone to the biodegradation.

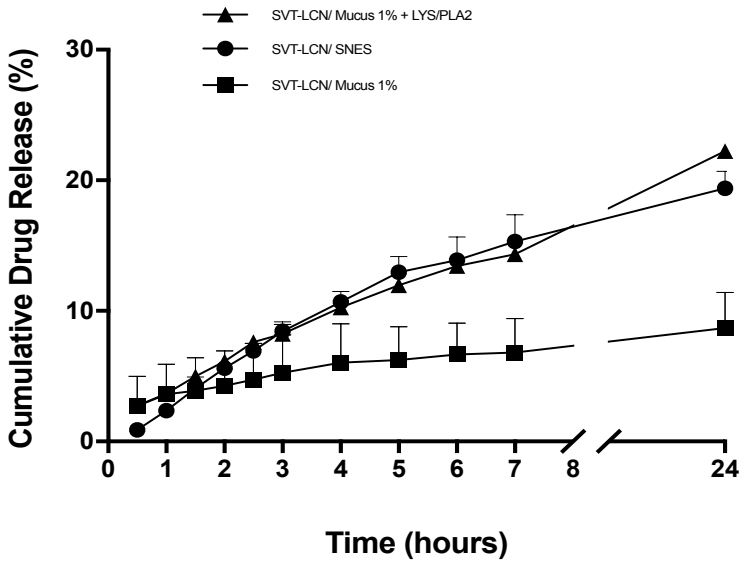

Figure 3: SVT-LCN nanoparticles release in solo SNES (●, SVT-LCN/SNES), in simulated nasal mucus (SNES plus porcine stomach mucin type II at 1%) (■, SVT-LCN/mucus 1%) and in simulated nasal mucus containing lysozyme and PLA2 (▲, SVT-LCN/mucus 1% + Lys/PLA2). Experiments were carried out at least in triplicate (n = 3, ± STD).

Taken together, data suggest that the presented hybrid chitosan-coated nanoparticles can interact with the mucus secretion; but, this interaction could prevent drug availability and consequently permeation through nasal epithelium. Nevertheless, their biodegradation by glycoside hydrolase and phospholipase enzymes naturally present in the nasal cavity, could represent a new strategy to overcome the mucus barrier.

5.3 Nanoparticles Mucoadhesion

To investigate how chitosan-coated nanoparticles affect residence time in the nasal cavity, a controlled gravitational force was applied to measure the bioadhesive strength between nanoparticulate formulation and the mucosal layer of a nasal tissue.[14] As shown in Figure 4, almost 77% of simvastatin content from a simple simvastatin suspension was washed out already within 2 minutes (33 ± 6.34% residual simvastatin on the mucosa), whereas 90% of simvastatin from nanoparticles formulation remained adhered at this time point. Experiments were prolonged up to 20 minutes, to simulate nasal mucociliary clearance removal of exogenous particles. At the end of the experiment, chitosan-coated simvastatin-

loaded nanoparticles showed a strong association with the nasal mucosa, resulting in more than 50% formulation still adhering to the mucosa at the end of the experiment. Instead, simvastatin was almost completely removed from the nasal tissue (only 11.67 ± 2.88 % adhered) after 20 minutes in the case raw material suspension. Thus, it is possible that chitosan-coated hybrid nanoparticles will be able to delay the nasal clearance of simvastatin, increasing formulation residence time in nasal cavity.

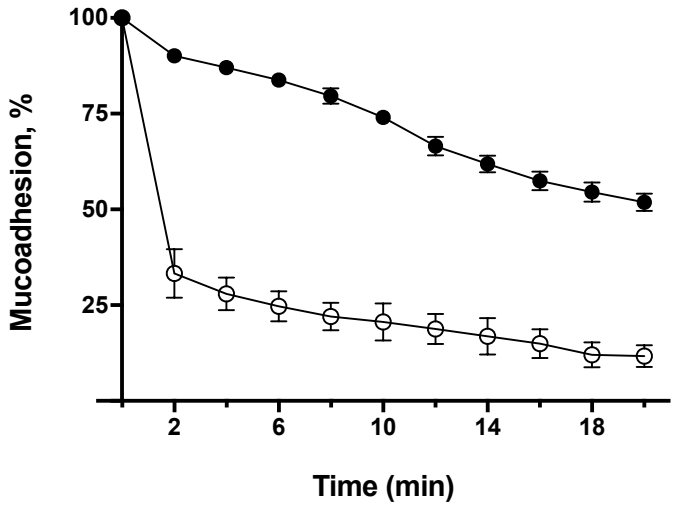

Figure 4*: In vitro* mucoadhesion of simvastatin suspension (○) and simvastatin-loaded nanoparticles (●, SVT-LCN). The mucoadhesion was expressed as percentage of drug retained on the mucosa against time (n = 3, ± STD).

5.4 Simvastatin *In Vitro* Permeation Across a Cellular Model of Nasal Epithelium

The permeability enhancement effects of SVT-LCN nanoparticles were studied assessing the simvastatin amount transported across a nasal mucosa model obtained using RPMI2650 cell line.[15] Figure 5 illustrates the percentage of drug permeated across nasal cell epithelial model after deposition of simvastatin suspension and simvastatin-loaded nanoparticles on cells surface. In the first hour, approximately 3 µg of simvastatin from SVT-LCN nanoparticles was transported, while only 0.25 µg of simvastatin was founded in the acceptor compartment of the drug suspension. After 4 hours of experiment, 9 µg of

simvastatin from nanoparticles permeated the nasal cells against 0.8 µg for simvastatin suspension (11-fold increase, $p < 0.0001$).

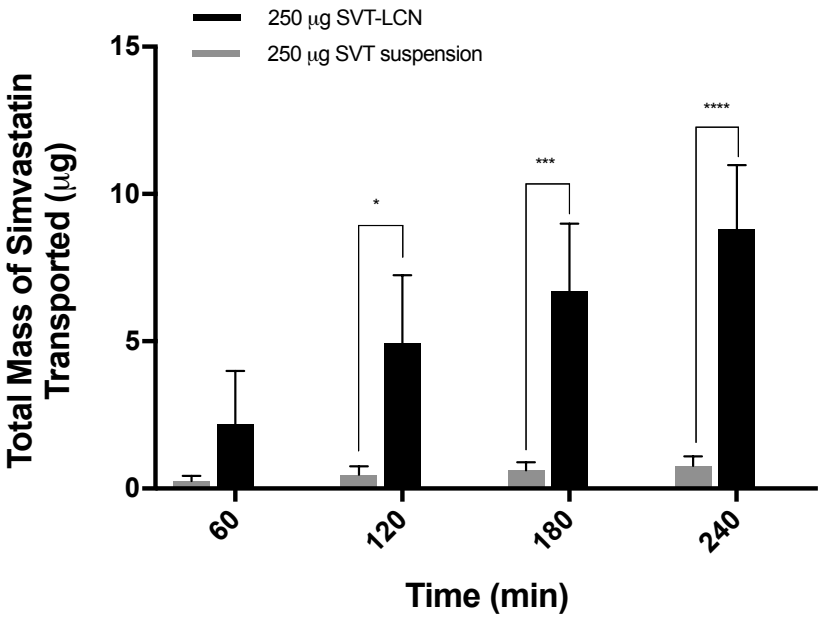

Figure 5: Simvastatin transport through RPMI2650 nasal cells after deposition of simvastatin-suspension and simvastatin-loaded nanoparticles, SVT-LCN (n = 3, ± STD). Permeability experiments were carried out on RPMI2650 cells grown in air-liquid interface conditions. TEER values were found to be around 120 Ω cm^2 before and after transport studies. Bartlett's statistics shown * $p < 0.05$, *** $p < 0.001$ and **** $p < 0.0001$

Importantly, it can be noticed a progressive increase in drug permeation for simvastatin-loaded nanoparticles, while the permeation of simvastatin as raw material occurred in a very slow rate, almost reaching a plateau. This suggests an enhanced drug permeability when lecithin/chitosan nanoparticles technology is applied.

Concerning the drug mass balance, as shown in Figure 6, after 4 hours of permeation, 84.42 ± 6.79 % and 72.94 ± 4.52 % of the drug remains on the surface of the cell for simvastatin suspension and nanoparticles, respectively. Also, around 14.94 ± 4.75 % of simvastatin from nanoparticles formulation and 11.03 ± 1.74 % from simvastatin suspension were found inside the cells, suggesting a higher binding of nanoparticles with the cells of the nasal mucosa, compared to the raw material.

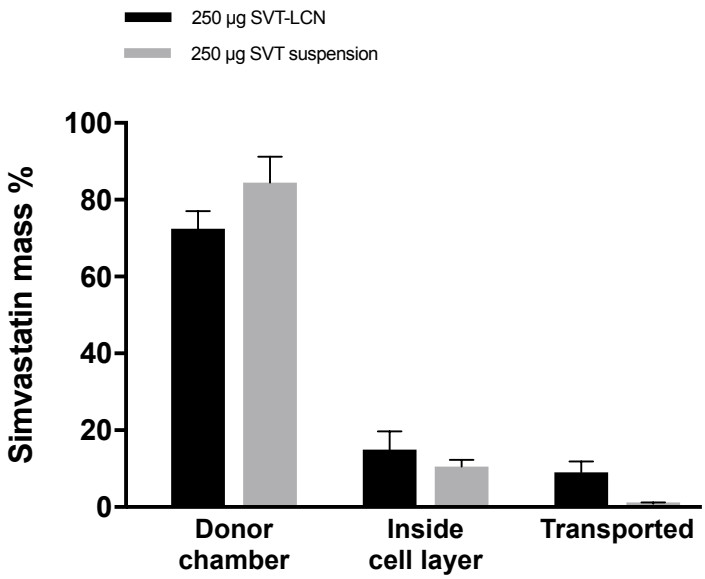

Figure 6: Distribution of simvastatin recovered after transport studies of simvastatin suspension and loaded into nanoparticles (4h) across the nasal cells RPMI 2650 epithelium model.

5.5 Simvastatin Transport Across Excised Rabbit Nasal Epithelium

To further evaluate nanoparticles permeation enhancement properties, simvastatin transport across the nasal epithelium was assessed using nasal mucosa tissues excised from rabbits. The experimental conditions were strictly controlled to keep nasal mucosae vital and in physiological conditions. All the experiments were completed in 4 hours to limit tissue damage and alteration. Simulated nasal fluid (SNES pH 6.5) was used as receptor medium.

Transport profiles obtained for simvastatin-loaded lecithin/chitosan nanoparticles in comparison with simvastatin suspension are presented in Figure 7. Increased simvastatin permeation across the nasal epithelium was obtained when the drug was nanoencapsulated compared to a simple suspension. In fact, already after the first hour, approximately 5 $\mu g*cm^{-2}$ of simvastatin from nanoparticle formulation were transported, while permeated from simvastatin suspension were below detection limit. After 4 hours, the cumulative amount of simvastatin permeated per unit area of tissue was 6.63 ± 0.38 $\mu g*cm^{-2}$ for the drug-loaded nanoparticles, about 50-times higher than the total amount permeated from simvastatin suspension ($p < 0.001$). Clearly, nanoparticles showed the capacity to enhance simvastatin

transport across rabbit nasal epithelium. Taking account, the total drug inside the mucosa, similar values were found for encapsulated and free simvastatin (0.29 ± 0.02 µg vs 0.22 ± 0.03 µg, respectively).

Taken together, these results assign to the lecithin/ chitosan nanoparticle structure a decisive role in simvastatin nasal absorption, although this process seems does not involve nanoparticles internalization and accumulation within nasal mucosa.

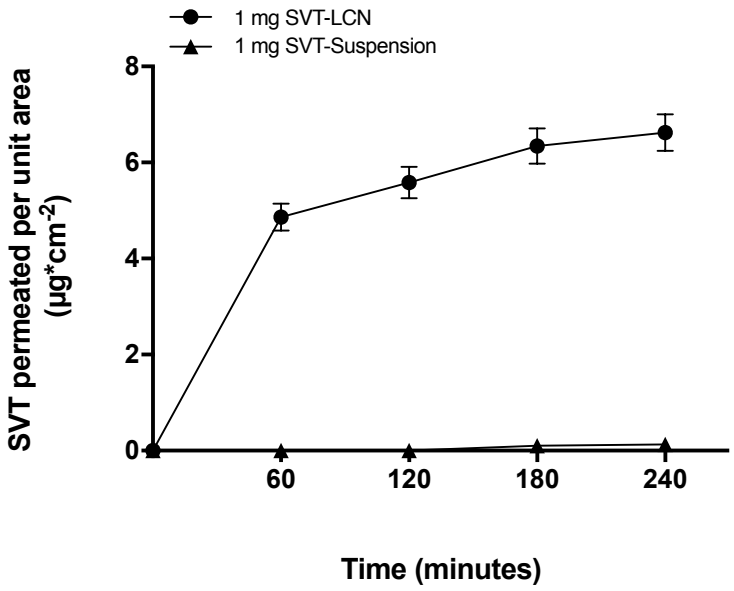

Figure 7: Profiles of simvastatin transport across the nasal epithelium of rabbit obtained for loaded-nanoparticles and simvastatin suspension (n = 3, ± STD).

6 Discussion

The nose represents an attractive alternative route for brain delivery of drugs. However, the complexity involving nasal anatomy and physiology can be very challenging for an efficient nose-to-brain administration of drugs. The use of nanoparticles represents a promising approach for the nose-to-brain transport of therapeutics across the nasal mucosa.[7] However, the delivery of therapeutically relevant amounts of drugs through this route is strongly dependent on the availability of nanoparticles drug carriers able to provide an improvement of drug targeting efficiency to the brain.[3] The major approaches to increase drug bioavailability of intranasally administered loaded-nanoparticles are: (i) the use of mucoadhesive polymers, increasing local drug residence time and (ii) the employment of permeation enhancers. [19]

In order to investigate lecithin/chitosan nanoparticles suitability for the nasal delivery of simvastatin, nanoparticles *in vitro* drug release was evaluated since it represents an important aspect in the development of nanomedicines.[20] Several conditions were tested to investigate nanoparticles performance in physiological environments simulating the nasal surface. For all *in vitro* release experiments a simulated nasal electrolyte solution (SNES) was selected as release medium to simulate nasal secretions.[12]

Comparing drug loaded nanoparticles with a simvastatin suspension, after an initial faster release rate evidenced for nanoparticles compared to the suspension up to 7 hours, simvastatin release substantially slowed down for nanoencapsulated simvastatin. In fact, drug released after 24 hours from nanoparticles was not significantly different from the amount released from a suspension. The decrease in the release-rate of the encapsulated simvastatin was attributed to the multilayered structure of nanoparticles hindering drug release of drug encapsulated in the inner core of the particle. In fact, the polymer on the nanoparticles surface acts as a drug release barrier; hence, the drug diffusion across the polymeric membrane becomes a determining factor in drug release.[20] Moreover, it has to be considered that all simvastatin is a lipophilic drug which has a higher tendency to partition in the oily core of nanoparticles and its release is hindered at oil-water interface due to its low drug aqueous solubility. Nevertheless, considering the mucociliary clearance effect on formulation residence time, the first hours of *in vitro* drug release experiments are the most important to determine drug availability from a nasal formulation. Within the first 3 hours, nanoparticles provided a 4-fold higher simvastatin release when compared to the free drug suspension. Anyway, it is important to highlight that within that time frame the amount of drug released is still relatively low (around 10%).

Considering nanoparticles composition, a potential action of enzymes naturally present in the nasal cavity toward hybrid lecithin/chitosan nanoparticles could trigger drug release. In a recent study, Barbieri and co-workers have shown the high susceptibility of similar lecithin/chitosan nanoparticles to biodegradation by gastrointestinal enzymes. The nanoparticle degradation was found to have an impact on promoting drug release and transport trough intestinal epithelium.[6] Lysozyme is the most abundant antibacterial protein of the nasal secretions.[18] In our case, biodegradation study employing lysozyme evidenced an improve in simvastatin release, doubling the amount of cumulative drug released by nanoparticles in SNES alone. Even if simvastatin release in the presence of lysozyme is enhanced, no more than 50% of drug content was released within 24 hours. Interestingly, the addition of a second enzyme, i.e., PLA A2, resulted in synergistic action providing a further improvement in drug release. In fact, PLA A2 is also an enzyme present in the nasal secretions and in presence of both enzymes almost the totality of the simvastatin loaded in nanoparticles was released within 7 hours (complete release was achieved after 24 hours of experiment). Simvastatin release from lecithin/chitosan nanoparticles is triggered by the enzymatic action upon nanoparticles structural components. In fact, as reported previously, lysozyme is capable to degrade chitosan,[5,21] while PLA2 catalyzes the hydrolysis of phospholipids, affecting the lipid components (in particular lecithin) of the nanoparticles.[22]

As aforementioned, the major drawback affecting availability of nasally administered lipophilic drugs is the mucus barrier.[23] Therefore, *in vitro* release studies were performed for SVT-LCN nanoparticles dispersed in simulated nasal artificial mucus. Decrease on the cumulative amount of simvastatin released suggest that the mucoadhesive interaction between nanoparticles and mucins, able to nanoparticles in the mucus network can hamper drug release. Additionally, the mucus layer is recognized as a barrier for the diffusion of poorly water soluble drugs, which interact with glycoproteins and lipids present in the mucus layer, leading to an overall reduced diffusion rate. The addition of enzymes, although to a lesser extent compared to nanoparticles in simple nasal fluid, is still able to promote drug release and diffusion towards the receptor compartment also in presence of a mucus barrier, confirming once again the enzyme-triggered release of simvastatin from hybrid lecithin/chitosan nanoparticles is working also in presence of the mucus barrier.

Moreover, it is important to emphasize that drug release experiments in the present work employed Franz cells vertical diffusion method. Despite *in vitro* experiments applying Franz has become one of the most adopted methods for researching and characterizing drug release, its process involves a static diffusion method.[24] If compared to the dynamic dialysis, another widely used method to perform *in vitro* drug release, a static diffusion method intrinsically does not facilitate the vertical diffusion of the drug released. Besides, synthetic

cellulose dialysis membrane employed to separate the released drug from loaded-nanoparticles, poses itself an additional barrier to the diffusion of the drug to the acceptor compartment.[25] All those considerations lead to the hypothesis that the released fractions of simvastatin could be even higher/ faster *in vivo* compared to the *in vitro* experiments.

Nanoparticles mucoadhesion experiments were carried out to predict more closely the ability of the simvastatin-loaded nanoformulation to improve residence time in the nasal cavity. Intranasal administration has shown serious limitations because of the incessant mucociliary clearance renewing the mucus layer from the nasal cavity surfaces.[23] Thus, simvastatin-loaded hybrid chitosan-coated nanoparticles applied on an excised porcine nasal tissue were exposed to the stress of a continuous washing and their mucoadhesion properties were evaluated in comparison with the simvastatin suspension. More than 50% of simvastatin loaded lecithin/chitosan nanoparticles remained strongly adhered to the mucosal tissue, while the drug suspension was almost completely removed after 20 minutes. Electrostatic interactions apparently play an important role in the mucoadhesion of chitosan-coated nanoparticles. In fact, chitosan amino groups confer to the nanoparticles a positively charged surface, while, the ionization at pH 5.5 to 6.5 of the sialic acid moieties present in the mucin glycoproteins confer to them an overall negative charge.[26] Thus, specific electrostatic interactions between chitosan-coated nanoparticles and mucins are considered responsible for the formulation mucoadhesion at the molecular level. Although electrostatic interaction is described as the major mechanisms involving the chitosan nanoparticles mucoadhesion, contributions from hydrogen bonding and hydrophobic effects have also been reported.[27]

Similarly, the role of chitosan in promoting penetration enhancement is well known,[28] however it can't be assumed that this is the only reason for the permeation enhancement of hybrid nanoparticles, since one of the main permeation limiting step across the nasal mucosa is simvastatin poor water solubility. In both transport studies performed, i.e., across the RPMI2650 cells nasal epithelium model and excised rabbit nasal mucosa, the amount of simvastatin permeated from the nanoparticle formulation in comparison with the transport of the free drug was significantly larger. In the case of transport across the RPMI2650 nasal cells, hybrid lecithin/chitosan nanoparticles increased the permeation of simvastatin by a factor larger than 10. For transport studies using the rabbit nasal mucosa, data were even more striking, as the only permeation observed was obtained with simvastatin loaded into nanoparticles. Interestingly, in both cases, the amount of simvastatin found within the cells and within the mucosa were similar for nanoencapsulated simvastatin and the drug suspension, suggesting that nanoparticles do not increase drug internalization and accumulation inside the epithelial nasal cells. Considering previous data of nanoparticles

biodegradation, it is plausive to assume that LCN-nanoparticles permeation enhancement is also supported by the biodegradation of the delivery system in the mucus barrier or intracellularly, providing a supplementary driving force to the drug diffusion across the mucosal barrier. In fact, in an elementary study of nasal transport of differently coated nanoparticles, Mistry and co-workers evidenced no transport of a fluorescent polystyrene latex nanoparticles coated with chitosan (C-PS) across porcine nasal epithelium.[3] Moreover, histological examinations of the nasal tissue evidenced that C-PS nanoparticles were manly localized in the apical edge of the olfactory epithelia, suggesting nanoparticles entrapment within the overlying mucus. In a recent study, Barbieri et al., investigated the permeation of tamoxifen across intestinal epithelium of rats using similar lecithin/chitosan nanoparticles.[6] Authors demonstrated that tamoxifen-loaded nanoparticles increased significantly the drug transport across rat intestinal wall when pancreatin or lipase enzymes were added to the donor chamber and the intimate contact between the nanoparticles and the intestinal tissue was maintained. In fact, when a semipermeable membrane was used to prevent nanoparticles contact with the mucosal tissue, the amount of drug transported from loaded-nanoparticles was similar as from the drug suspension. This suggests that nanoparticles are able improve drug permeation via an enhanced paracellular transport probably requiring nanoparticle degradation in close proximity of the mucosal epithelium.

Those results attribute to the structure of hybrid lecithin/chitosan nanoparticles a decisive role in enabling the transport of simvastatin across nasal barriers, exploiting nanoparticles local interaction and biodegradation to increased drug absorption and bioavailability, possibly providing a highly efficient drug delivery system for nose-to-brain delivery.

7 Conclusions

Considering results obtained for the free drug material, the encapsulation of simvastatin into lecithin/chitosan nanoparticles was shown to be beneficial for nasal delivery of lipophilic statins. Due the presence of chitosan, nanoparticles presented good mucoadhesion, which provided a prolonged contact of the formulation with the surface of porcine nasal epithelium. Furthermore, hybrid lecithin/chitosan nanoparticles enhanced *in vitro* transport of simvastatin across both, a RPMI2650 cells nasal epithelium model and excised rabbit nasal tissue. Besides, the capability to exploit nanoparticles biodegradation by antibacterial enzymes present in the nasal secretions to trigger drug release and, possibly, to promote drug permeation across mucosal surfaces, represents an innovative concept of controlled drug release for nanoparticles delivery carriers designed for nasal administration.

References

1. Illum, L. Transport of drugs from the nasal cavity to the central nervous system. *Eur. J. Pharm. Sci.* 11, 1–18 (2000).

2. Wu, H., Hu, K. & Jiang, X. From nose to brain: understanding transport capacity and transport rate of drugs. *Expert Opin. Drug Deliv.* 5, 1159–1168 (2008).

3. Mistry, A., Stolnik, S. & Illum, L. Nose-to-Brain Delivery: Investigation of the Transport of Nanoparticles with Different Surface Characteristics and Sizes in Excised Porcine Olfactory Epithelium. *Mol. Pharm.* 12, 2755–2766 (2015).

4. Sonvico, F. *et al.* Formation of self-organized nanoparticles by lecithin/chitosan ionic interaction. *Int. J. Pharm.* 324, 67–73 (2006).

5. Barbieri, S. *et al.* Lecithin/chitosan controlled release nanopreparations of tamoxifen citrate: Loading, enzyme-trigger release and cell uptake. *J. Control. Release* 167, 276–283 (2013).

6. Barbieri, S. *et al.* Ex vivo permeation of tamoxifen and its 4-OH metabolite through rat intestine from lecithin/chitosan nanoparticles. *Int. J. Pharm.* 491, 99–104 (2015).

7. Illum, L. Nanoparticulate systems for nasal delivery of drugs: A real improvement over simple systems? *Journal of Pharmaceutical Sciences* 96, 473–483 (2007).

8. Sonvico, F., Zimetti, F., Pohlmann, A. R. & Guterres, S. S. Drug delivery to the brain: how can nanoencapsulated statins be used in the clinic? *Ther. Deliv.* 8, 625–631 (2017).

9. McFarland, A. J. *et al.* Molecular mechanisms underlying the effects of statins in the central nervous system. *International Journal of Molecular Sciences* 15, 20607–20637 (2014).

10. Barone, E., Di Domenico, F. & Butterfield, D. A. Statins more than cholesterol lowering agents in Alzheimer disease: Their pleiotropic functions as potential therapeutic targets. *Biochem. Pharmacol.* 88, 605–616 (2014).

11. Clementino, A. *et al.* The nasal delivery of nanoencapsulated statins – An approach for brain delivery. *Int. J. Nanomedicine* 11, 6575–6590 (2016).

12. Castile, J. *et al.* Development of *in vitro* models to demonstrate the ability of PecSys®, an *in situ* nasal gelling technology, to reduce nasal run-off and drip. *Drug Dev. Ind. Pharm.* 39, 816–824 (2013).

13. Griffiths, P. C. *et al.* PGSE-NMR and SANS studies of the interaction of model polymer therapeutics with mucin. *Biomacromolecules* 11, 120–125 (2010).

14. Rao, K. V. R. & Buri, P. A novel in situ method to test polymers and coated microparticles for bioadhesion. *Int. J. Pharm.* 52, 265–270 (1989).

15. Pozzoli, M. *et al.* Application of RPMI 2650 nasal cell model to a 3D printed apparatus for the testing of drug deposition and permeation of nasal products. *Eur. J. Pharm. Biopharm.* 107, 223–233 (2016).

16. Bortolotti, F., Balducci, A. G., Sonvico, F., Russo, P. & Colombo, G. In vitro permeation of desmopressin across rabbit nasal mucosa from liquid nasal sprays: The enhancing effect of potassium sorbate. *Eur. J. Pharm. Sci.* 37, 36–42 (2009).

17. Russo, P. *et al.* Primary microparticles and agglomerates of morphine for nasal insufflation. *J. Pharm. Sci.* 95, 2553–2561 (2006).

18. Travis, S. M., Singh, P. K. & Welsh, M. J. Antimicrobial peptides and proteins in the innate defense of the airway surface. *Current Opinion in Immunology* 13, 89–95 (2001).

19. Ugwoke, M. I., Agu, R. U., Verbeke, N. & Kinget, R. Nasal mucoadhesive drug delivery: Background, applications, trends and future perspectives. *Adv. Drug Deliv. Rev.* 57, 1640–1665 (2005).

20. Aguilar, Z. P. Chapter 5 - Targeted Drug Delivery. in *Nanomaterials for Medical Applications* 181–234 (2013). doi:http://dx.doi.org/10.1016/B978-0-12-385089-8.00005-4

21. Nordtveit, R. J., Vårum, K. M. & Smidsrød, O. Degradation of partially N-acetylated chitosans with hen egg white and human lysozyme. *Carbohydr. Polym.* 29, 163–167 (1996).

22. Andresen, T. L., Thompson, D. H. & Kaasgaard, T. Enzyme-triggered nanomedicine: Drug release strategies in cancer therapy (Invited Review). *Molecular Membrane Biology* 27, 353–363 (2010).

23. Sigurdsson, H. H., Kirch, J. & Lehr, C. M. Mucus as a barrier to lipophilic drugs. *International Journal of Pharmaceutics* 453, 56–64 (2013).

24. Ng, S.-F., Rouse, J. J., Sanderson, F. D., Meidan, V. & Eccleston, G. M. Validation of a Static Franz Diffusion Cell System for In Vitro Permeation Studies. *AAPS PharmSciTech* 11, 1432–1441 (2010).

25. Modi, S. & Anderson, B. D. Determination of drug release kinetics from nanoparticles: Overcoming pitfalls of the dynamic dialysis method. *Mol. Pharm.* 10, 3076–3089 (2013).

26. He, P., Davis, S. S. & Illum, L. In vitro evaluation of the mucoadhesive properties of chitosan microspheres. *Int. J. Pharm.* 166, 75–88 (1998).

27. Sogias, I. A., Williams, A. C. & Khutoryanskiy, V. V. Why is chitosan mucoadhesive? *Biomacromolecules* 9, 1837–1842 (2008).

28. Smith, J. M., Dornish, M. & Wood, E. J. Involvement of protein kinase C in chitosan glutamate-mediated tight junction disruption. *Biomaterials* 26, 3269–3276 (2005).

CHAPTER 4

DEVELOPMENT AND VALIDATION OF A RP - HPLC METHOD FOR THE SIMULTANEOUS DETECTION AND QUANTIFICATION OF SIMVASTATIN'S ISOFORMS AND COENZYME Q10 IN LECITHIN/ CHITOSAN NANOPARTICLES

Development and Validation of A RP-HPLC Method for the Simultaneous Detection and Quantification of Simvastatin's Isoforms and Coenzyme Q10 in Lecithin/ Chitosan Nanoparticles

Adryana Clementino [1,2] Fabio Sonvico[1] *

[1]Food and Drug Department, University of Parma, Parma (PR) Italy

[2]Conselho Nacional do Desenvolvimento Cientifico e Tecnologico - CNPq, Brasilia, Brazil

Published on March 2018, ***Journal of Pharmaceutics and Biomedical Analysis***,
IF 3.255

Abstract

Hybrid nanocapsules constituted of phospholipids and polysaccharides have been proposed as colloidal systems for the delivery of drugs via non-parenteral administration routes, due their capacity of high drug loading, controlled drug release and targeted delivery to the specific organ. Moreover, nanoparticles systems offer the possibility of co-encapsulation of drugs in the same drug delivery system and, consequently, the simultaneous administration of compounds. Characterization of nanoparticles properties, specifically involves quantification of the active pharmaceutical ingredients and is pivotal in the development of innovative nanomedicines. Therefore, this study has proposed and validated a new RP-HPLC-UV method for the simultaneous determination of simvastatin and coenzyme Q10 in hybrid nanoparticles systems. A reversed phase (RP) C8 column and a gradient elution of water: methanol at flow rate of 1.5 ml/min was used. Simvastatin (SVT), simvastatin hydroxyacid isoform (SVA) and coenzyme Q10 were identified by dual wavelength-UV detection at 238 nm (statins) and 275 nm, respectively. The proposed method was selective and linear in the range of 0.5 – 25 μg/ml (r^2 > 0.999), precise, with values of relative standard deviation (RSD) lower than 2%, robust and accurate (recovery values of 100 ± 5 %), satisfying FDA guidelines. Furthermore, low detection (LOD < 0.2 μg/ml) and quantification limits (LOQ < 0.4 μg/ml) were suitable for the application of the method for the *in vitro* study of release kinetics of simvastatin and coenzyme Q10 co-encapsulated in lecithin/chitosan nanoparticles. The proposed method represents, to our knowledge, the only method for the simultaneous quantification of simvastatin, coenzyme Q10 and of the hydrolysed hydroxyacid isoform of the statin in nanoparticles.

Key words: RP-HPLC method, Simvastatin, Coenzyme Q10, Hybrid nanoparticles, Co-encapsulation, Chitosan

1 Introduction

Statins (3-hydroxy-3-methylglutaryl-coenzyme reductase inhibitors) are a class of lipid-lowering agents used as first-line therapy in the reduction of serum cholesterol concentrations. Preventing vascular deposition of cholesterol-laden plaques, statins reduce the morbidity and mortality of cardiovascular diseases[1]. However, in the past decade, statins have been investigated not only for their cholesterol lowering effects, but also for a series of pleiotropic effects, that could make statins beneficial for a number of other diseases, such as rheumatoid arthritis, pulmonary obstructive disease, inflammatory bowel disease, cancer and neurodegenerative disorders. [2–5] However, it has been demonstrated that to obtain those pleiotropic effects high statins dosages are required. [6] This presents an issue as statins have been associated to severe adverse effects, including myopathy such as myositis and rhabdomyolysis. [7,8] Statin-associated muscle symptoms (SAMS) are generated possibly through lowering muscle tissue and serum levels of ubiquinone, also known as coenzyme Q10 (CoQ10), an important lipophilic substance integral in the mitochondrial respiratory process for the production of cellular energy. [9] In addition, a negative correlation has been reported between low levels of CoQ10 and the prevalence of Alzheimer's on patients. [10] From this point of view, the association of simvastatin (SVT), a commonly used lipophilic statin, with coenzyme Q10 could be beneficial in preventing the statins side effects and reinforcing the therapeutic application of this combination in the treatment of degenerative brain processes. [10,11]

Recently, nanoparticles have been proposed as an innovative formulation approach to improve the efficacy and reduce the toxicity of several potent drugs, such as chemotherapeutics, antivirals, biopharmaceuticals and many others poorly water soluble drugs. In addition, pharmaceutical nanotechnologies can be applied to obtain the co-delivery of multiple drugs. [12,13] In fact, nanoparticles systems offer several advantages for the simultaneous delivery of drugs over their free combinations. For instance, co-encapsulation of drugs into nanostructured sustained-release carriers enables the combined controlled delivery of the molecules and their selective co-targeting to tissues, avoiding the fast-clearing processes observed for the free drugs. In this way, nanoparticles increase *in vivo* efficacy and limit toxicities by reducing non-target exposure. [13] Among the different types of nanoparticle systems, biodegradable polymeric nanocapsules have elicited great interest in drug delivery applications, due their high biocompatibility. Particularly, hybrid nanoparticles composed of polysaccharides and lipids have been demonstrated to have a number of interesting biopharmaceutical properties for oral, topical and nasal delivery. [14–16] Hydrophobic

drugs can be efficiently encapsulated into this systems with high stability and narrow size distribution, characterized by an oily core stabilized with soybean lecithin and coated by the cationic polysaccharide chitosan. These features make lecithin/chitosan nanoparticles (LCN) an ideal candidate for the co-encapsulation of simvastatin and coenzyme Q10.

To develop and characterize simvastatin/coenzyme Q10-loaded lecithin/chitosan nanoparticles (SVT/CoQ10-LCN) fundamental parameters such as drugs content, encapsulation efficiency and drug release must be investigated. In particular, when developing nanoparticle formulations the establishment of a set of procedures for the drug extraction from the drug delivery system along with the analytical tools for the encapsulated drugs quantification is paramount. [17] Besides, controlled-release nanoparticles imply that small quantities of drugs should be quantified during *in vitro* release experiments, requiring a sufficiently sensitive analytical method for the determination of drug concentrations in the dissolution medium. Moreover, simvastatin, a lactone prodrug, undergoes a reversible enzymatic or non-enzymatic hydrolysis interconversion into its active β-δ-dihydroxyacid hydrophilic form. [18] Consequently, an analytical method for simvastatin should include also the determination of the hydroxyacid simvastatin form (SVA).

Among the analytical methods currently available, high performance chromatography (HPLC) coupled with ultraviolet detector (UV) represent one of the most common analytical methods used for the characterization of pharmaceuticals. HPLC-UV offers a quick, sensitive and accurate method to separate and identify drugs in combination or other analytes into pharmaceutical nanoparticles formulations. [17,19] Although many researches have investigated the association between simvastatin and coenzyme Q10 [9–11], no HPLC method for the simultaneous determination of SVT, SVA and CoQ10 have been developed and applicate for the quantification of any matrix sample, specially nanoparticles systems.

Hence, the overall objective of this work was the development and validation of a routine reversed-phase (RP) HPLC UV method for the quantification of SVT, SVA and coenzyme Q10 CoQ10 from a lecithin/chitosan nanoparticles drug delivery system. The method developed was also applied to the determination of the *in vitro* drug release of SVT/CoQ10 from nanoparticles.

2 Materials

2.1 Materials for Analytical Method Development

Methanol, acetonitrile and ethanol HPLC grade, were purchased from VWR Chemicals (Radnor, Pennsylvania, USA). Simvastatin was purchased from Polichimica S.R.L (Bologna, Italy). Coenzyme Q10 and phosphoric acid (H3PO4) was supplied from A.C.E.F. s.p.a. (Fiorenzuola D'Arda, Italy). For all experiments, ultrapure water (Purelab Flex; ELGA-Veolia LabWater, Windsor Court, UK) and distilled water filtered through cellulose acetate filters 0.45 μm (Sartorius, Gottingen, Germany) were used. All reagents when not specified, were from analytical grade.

2.2 Materials for Nanoparticles Production and Characterization

Chitosan with a deacetylation degree of 95%, viscosity 103 mPas and molecular weight 152 KDa was provided by Primex (Chitoclear FG, Siglufjordur, Island). Lecithin Lipoid S45 was purchased from Lipoid AG (Ludwigshafen, Germany). Maisine™35:1 (glycerol monolinoleate) and Labrafac™ Lipophile WL1349 (medium-chain triglycerides) were a kind gift from Gattefossé (Saint-Priest, France). Bovine serum albumin and dialysis tubing cellulose (14,000 MWCO) were supplied by Sigma-Aldrich (St Louis, MO, USA). Centrifugal filter devices (Vivaspin® 2; 30,000 molecular weight cut-off [MWCO], PES) were purchased by Sartorius (Göttingen, Germany).

2.3 Equipment and Chromatographic Conditions

A chromatographic system Agilent 1200 series (St. Claire, CA, USA), consisting in Agilent 1200 series UV-detector, auto-sampler, pump and a vacuum degasser unit was used. Detector signal processing was performed using Agilent ChemStation Rev B.03.02 software. Analyses were carried out using gradient method and a SymmetryShield™ Reverse Phase C8, 5μm, 3.9 x 150 mm column (Waters Corp., MA, USA) as stationary phase, maintained at 45 °C. Composition of the mobile phase was, Eluent A: distilled water (adjusted to pH 5.5) and eluent B: methanol. The gradient applied at a constant flow rate of 1.5 ml/min is

presented in Table 1. UV-detector was set at 238 nm for the detection of SVT and SVA and switched to 275 nm from 6 min to 10 min for the detection of CoQ10.

Table 1: Chromatographic conditions of mobile phase of analytical method

Time (min)	**Eluent A** (%)	**Eluent B** (%)	**Flow rate** (ml/min)
0.01	80	20	1.5
2.00	50	50	1.5
3.50	20	80	1.5
5.00	5	95	1.5
6.00	0	100	1.5
10.00	80	20	1.5

Eluent A: Distilled water pH 5.5, adjusted with 1.0 M H_3PO_4
Eluent B: Methanol

3 Methods

3.1 Preparation of Simvastatin Hydroxyacid Isoform

Hydroxyl acid simvastatin (SVA) was obtained from simvastatin (SVT) following the method we have previously described. [15] Briefly, to obtains the quantitative conversion of SVA from SVT, 41.6 mg of simvastatin powder were solubilized in 1 ml of ethanol; 1.5 ml of 1N NaOH were then added to the solution. The SVT solution, in a hermetically closed recipient, was heated for 2h at 50°C in a BM4 water-bath (Falcon Instruments, Treviglio, Italy). Then the solution was cooled down and its pH was adjusted to 7.2 with 0.1N HCl. Finally, the solution volume was adjusted with ultrapure water to 10 ml in a volumetric flask. The SVA solution was then immediately frozen and kept at -20°C until usage. To control the conversion of SVT into SVA, a diluted solution of the fresh sample was analysed on HPLC and 100% conversion of simvastatin to acid simvastatin was evidenced (Figure 1).

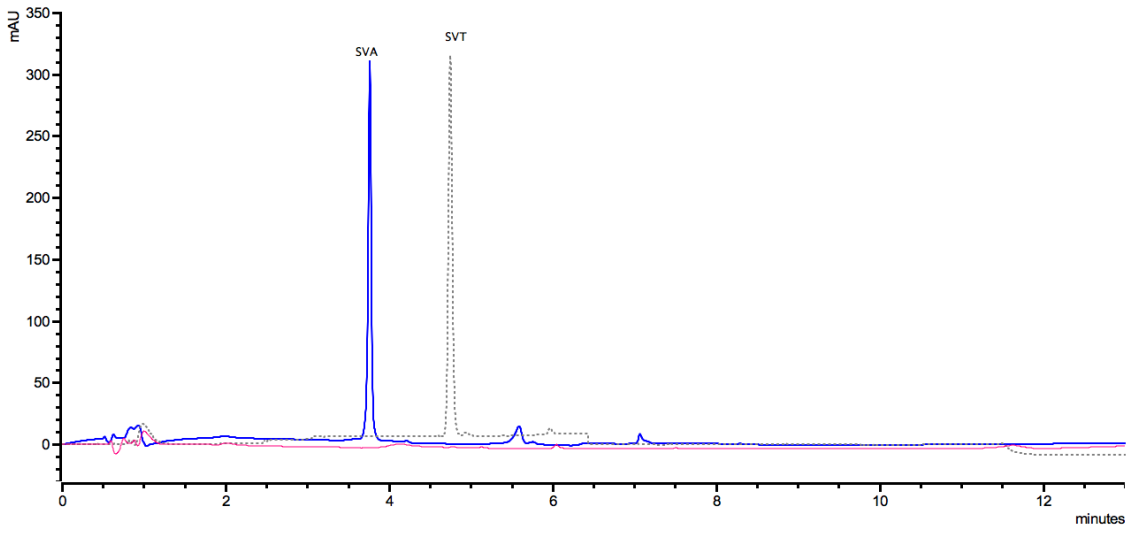

Figure 1: HPLC-UV chromatogram overlay of standard diluent (pink line) and hydroxyl acid simvastatin (SVA, blue line) after simvastatin (SVT- lactone) hydrolysis. No peak was detected on SVT retention time (~ 4.8 min, grey dotted; λ = 238).

3.2 Preparation of Stock and Working Solutions

The stock solutions of SVT, SVA and CoQ10 were prepared dissolving the three substances in appropriated solvents, each one individually. For SVT and SVA, stock solutions were prepared into a 10 ml volumetric flask, using acetonitrile: water 65:35, v/v mixture (pH 4.5, adjusted with 1.0 M H_3PO_4) at 1 mg/ml and 0.1 mg/ml, respectively. CoQ10 stock solution (0.1 mg/ml) was prepared by dissolving the coenzyme powder in ethanol, heated at 50°C into an amber glass vial hermetically closed. After cooling down the solution, it was adjusted to 50 ml in an amber glass volumetric flask using ethanol. The three stock solutions were mixed and diluted to obtain a working solution containing 25 μg/ml of each substance in a mixture of ethanol: acetonitrile: water (55:30:15, v/v/v, pH* 4.5 adjusted with 1.0 M H_3PO_4). Standard solutions used in the method validation were prepared by diluting the work solution in the same diluent mixture ethanol: acetonitrile: water (55:30:15, v/v/v, pH* 4.5) to obtain the following calibration curve concentrations range: 0.5, 1, 2, 5, 10 and 25 μg/ml. Stability of compounds in the standard diluent were investigated for over 24h at room temperature and three days in refrigerator (4°C) storage in amber glass vial, using the working solution. Recovery results of SVA, SVT and CoQ10 shown that compounds were stable during this period (Table 8), highlighting that diluent standard prevent the interconversion of both simvastatin isoforms and prevent the presence of degradation products.

3.3 Method Validation Protocol

3.3.1 Selectivity and System Suitability

To evaluate the method selectivity, diluent used for preparing standard solution, i.e. a mixture of ethanol: acetonitrile: water (55:30:15, v/v/v, pH* 4.5), pure and spiked with empty nanoparticles formulation was assessed for the presence of interfering peaks in the elution times corresponding to those of the analytes. Subsequently, the chromatographic separation of the three analytes was evaluated using the work solution (25 μg/ml SVA/SVT/CoQ10) to determine number of theoretical plates (N), analytes retention factor (K'), symmetry (α) and to calculate peaks resolution (*Rs*) and area repeatability (calculating relative standard deviation, RSD).

3.3.2 Detection and Quantification Limit

The determination of LOQ (limit of quantification) and LOD (limit of detection) for all analytes were calculated by considering the standard deviation of the response and the slope average of a specific calibration curve ranging from 0.25 to 25 µg/ml, using the following formulas:

$$LOQ = 10\sigma/S \qquad LOD = 3.3\sigma/S$$

where σ is the standard deviation of the response and S the slope of the calibration curve.

3.3.3 Linearity

Standard calibration solutions were prepared in the range of 0.5 to 25 µg/ml for SVA, SVT and CoQ10 by appropriate dilutions of work solution, as reported before. To access the linearity in the concentration range, samples were injected six times per concentration and peak area values were recorded to plot the detector response versus the analytes concentrations (Prism version 7.0, GraphPad software). Linearity of the calibration curve was calculated for each analyte, separately, applying linear regression using the least square method.

3.3.4 Precision

Precision was assessed in terms of repeatability (intra-day) and intermediate precision (inter-day). To assess method precision, we have evaluated the RSD of the concentration recovery by using the lowest, central and highest concentrations levels of calibration curve (0.5 – 2 – 25 µg/ml) for all analytes, in triplicate. Inter-day precision was assessed by analysing the same three concentrations on 3 different days. Mean recovery and RSD were calculated using six injections per sample.

3.3.5 Robustness

ICH Q2 [20] defines robustness of a method as a measure of its capability to remain unaffected by small, but deliberate variations in the method parameters. In our method, robustness was carried out by significant changes in three main chromatographic parameters: column temperature (± 2 °C), mobile phase flow rate (reduced of 0.2 ml/min)

and Eluent A pH (± 0.3 pH units). For each condition, analyses were carried out on the work solution (25 µg/ml SVA/SVT/CoQ10) in triplicate, and recovery, peaks resolution and peaks asymmetry were evaluated in comparison with standard conditions.

3.3.6 Accuracy

Accuracy was determined by assessing the percentage recovery of known concentrations of analytes spiked with nanoparticle formulation excipients. Pre-analysed standards at three levels of concentration (0.5 – 2 – 25 µg/ml) were spiked with 10 µl of empty nanoparticle formulation, simulating the amount of excipients that is present on the nanoparticles encapsulation efficiency assay (see also section 2.6.2). The experiment was conducted in triplicate and percentage recoveries and RSD were calculated for all analytes.

3.4 Application of the Method

3.4.1 Nanoparticle Preparation

Lecithin/chitosan nanoparticles loaded with simvastatin and CoQ10 (LCN-SVT/CoQ10) were prepared by self-assembly method, as previously reported. [15,21] Prior to nanoparticle preparation, a 1% w/v chitosan solution was prepared by diluting chitosan powder in 0.1N HCL solution under magnetic stirring (Arex CerAITop™ Hot Plate Stirrer, Velp®, USA), overnight. To prepare SVT/CoQ10-LCN nanoparticles, briefly, 100 mg of CoQ10 and 50 mg of SVT were dispersed into 4 ml of an ethanol solution of lecithin (2.5%), containing 200 mg of Labrafac™ and Maisine™ oils (1:1 w/w). To solubilize the drugs, specially CoQ10, ethanol solution was pre-heated at 50°C, under constant stirring. Sub-sequentially, the solution of simvastatin and coenzyme was injected, using a glass pipette, into 50 ml of an aqueous solution of 0.01% w/v chitosan under constant agitation (magnetic stirrer, 300 rpm) and temperature (50 °C). Freshly prepared nanoparticle suspension was kept under the constant conditions of stirring and temperature until the complete evaporation of ethanol from the system (2h). Finally, nanoparticles were characterized for particle size and polydispersity index (PDI) by dynamic light scattering (DLS) and nanoparticle zeta potential by electrophoresis mobility using a Brookhaven ZetaPALS Instrument (Brookhaven Instruments, Holtsville, NY, USA).

3.4.2 Nanoparticle Encapsulation Efficiency

To evaluate nanoparticles entrapment capacity for simvastatin and coenzyme Q10, an indirect quantification method has been used. This approach consists in the determination of the non-encapsulated or precipitated drugs and their subtraction from the total amount of drugs quantified in the formulation. To quantify the total amount of simvastatin (considering the sum of both isoforms) and coenzyme Q10 in the formulation, 100 µl of nanoemulsion were dispersed into 10 ml of the standard diluent solution (i.e. ethanol: acetonitrile: water) and sonicated for 45 minutes (Ultrasonic cleaner; VWR, Radnor, PA, USA) to quantitatively extract the drugs from nanoparticles. Samples were filtered (regenerate cellulose filters 0.45 µm, Sartorius, Gottingen, Germany) and analysed by HPLC for SVT, SVA and CoQ10 content. To quantify the amount of free drugs, firstly, formulations were centrifuged at 1,500 x g (Medifuge, Gmbh, Hanau, Germany) for 10 minutes to separate any large crystals or nanoparticles agglomerate. Centrifuge tubes where washed with drugs diluent and analysed by following the same methodology applied above. Finally, 2 ml of the nanoemulsion supernatant obtained in the step before were ultra-filtered using Vivaspin® Centrifugal Concentrator (MWCO 30,000 Da; Sartorius, Gottingen, Germany) at 4,000 x g for 10 minutes and ultrafiltered samples were analysed on HPLC for dissolved non-encapsulated drugs. All quantifications were determined as concentration by HPLC and express as mass percentage of recovery (n=3 ± SD). Simvastatin and Coenzyme Q10 co-encapsulation efficiency (EE%) was calculated using the following formula:

$$\text{Eq. 1} \qquad EE\% = \frac{Total\ quantified\ amount\ of\ drugs - free\ drugs}{Total\ quantified\ amount\ of\ drugs}$$

3.4.3 In Vitro Drug Release Studies

In vitro release studies of simvastatin and CoQ10 from LCN-SVT/CoQ10 nanoparticles were carried out using the dialyses bag diffusion method. [22] A simulated nasal electrolyte solution (SNES) [23], containing 8.77 mg/ml sodium chloride, 2.98 mg/ml potassium chloride and 0.59 mg/ml calcium chloride dehydrate, was used as dissolution medium since nanoparticles are intended to nasal administration. Bovine serum albumin (BSA), generally used to increase solubility of poor water soluble drugs, was used at a concentration of 0.5%,

increasing two times simvastatin solubility in the aqueous medium. [15] A volume of 1 ml of formulation containing 1 mg/ml of simvastatin and 2 mg/ml of CoQ10 were dispersed into 1 ml of SNES pH 6.5 and placed in the dialysis tube membrane (MWCO 14,000 kDa, Sigma-Aldrich). The sealed bags were immersed into 100 ml of the receptor medium, containing 0.5% of BSA, kept at 37°C and magnetically stirred at 100 rpm. At predetermined time points (1, 2, 3, 4, 5, 6, 7 and 8 h), aliquots were withdrawn from the receptor and replaced with a fresh medium solution. Samples where pre-treated with perchloric acid to precipitate and remove albumin by centrifugation (21,380 x g, 10 min; Scilogex D3024 Micro-centrifuge, USA). The supernatant was mixed with the standard diluent solution (1:1 v/v) to ensure drugs solubilisation and total recovery of drugs released. *In vitro* release studies of LCN-SVT/CoQ10 nanoparticles were conducted in triplicate and analysed on HPLC for all drugs content.

4 Statistics

All results are reported as mean and standard deviation of at least 3 replicates, if not stated otherwise. Linearity test for homogeneity of variances was calculated by using COCHRAN test at the significance level of α = 0.05. All statistics analyses were performed using Prism Software Version 7.0a (Prism, Version 7.0a, GraphPad Software Inc., La Jolla, CA, USA). The differences between data were tested using One-Way ANOVA with post-hoc Tukey HSD test, considering significant differences with $p < 0.05$ (Prism, Version 7.0a, GraphPad Software Inc., La Jolla, CA, USA).

5 Results and Discussion

5.1 Method Development and Optimization

The proposed analytical methodology was developed in order to provide a simple, reproducible and rapid RP-HPLC-UV method for the simultaneous detection and quantification of simvastatin and coenzyme Q10 in biodegradable lecithin/chitosan nanoparticle systems.

During the development of the analytical procedure, several chromatographic parameters were investigated taking into consideration the two drugs, but also possible degradation products appearing during nanoparticle manufacturing and characterization. In particular, simvastatin is a prodrug and easily undergoes a reversible hydrolysis into its active hydroxyl acid form. For this reason, the determination of the simvastatin hydroxyl acid was included in the proposed analytical method.

Chromatographic conditions, such as composition, pH and flow rate of mobile phase, as well as the chromatographic column and temperature of analysis were investigated to obtain peaks with good separation, symmetry and shape, together with acceptable retention times. Moreover, different solvents and proportions were tested to ensure the solubility of all compounds and their extraction from the drug delivery system.

To optimize the peak shape and separation between compounds, a stationary RP- C8 (3.9x150 mm, 5μm; Symmetry shield, Waters Corp., MA, USA) chromatographic column was used. A water and methanol gradient (from 80:20 % v/v) was applied as mobile phase, while an ethanol: acetonitrile: water mixture (55:30:15 v/v/v, pH* 4.5, adjusted with H_3PO_4 1M) was used as standard diluent solution for samples. The mobile phase flow rate and composition (see Table 1) provides analytes elution with short retention times, good peaks symmetry and shape. To confer the desirable peaks shape, with reduced tailing, Eluent-A pH was adjusted at 5.5 using H_3PO_4 1M and the chromatographic column was thermostated at 45 °C. The use of dual wavelengths detection, at 238 nm and 275 nm, enabled an efficient simultaneous detection approach for both statins isoforms and coenzyme Q10, respectively. The previous analytical conditions provide the chromatogram reported in Figure 2. The simultaneous analysis of SVA, SVT and CoQ10, showed a good peaks separation and shape for all molecules within a total analysis time of 13 min. Retention times of SVA, SVT and CoQ10 were $\mathbf{t_R}$*SVA*= 3.84min, $\mathbf{t_R}$*SVT*= 4.75 and $\mathbf{t_R}$*CoQ10*= 8.72, respectively (Figure 2). This method for the simultaneous quantification of simvastatin isoforms and CoQ10 was discriminating and rapid, two desirable features for laboratorial routine.

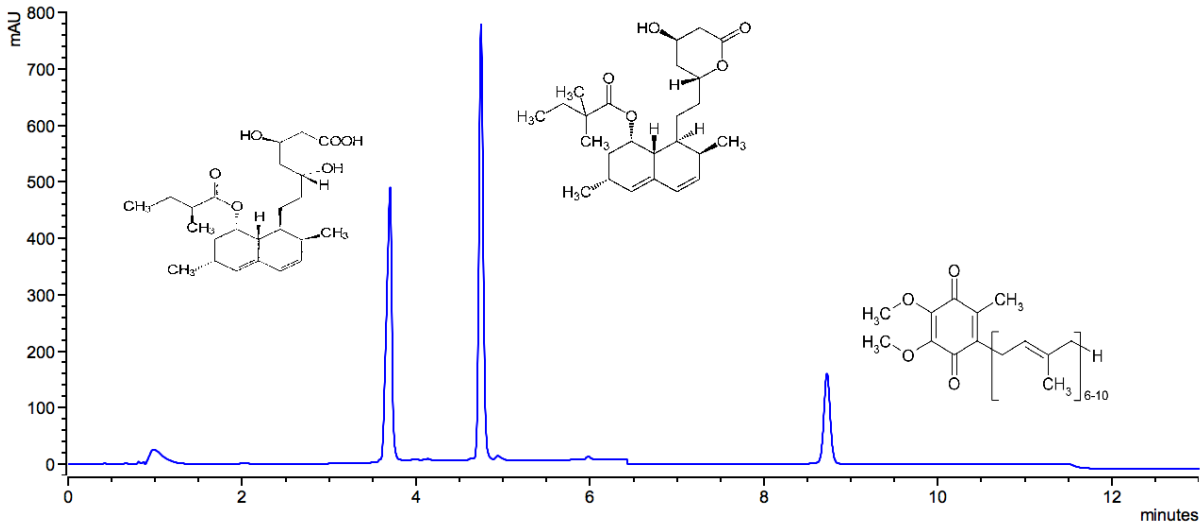

Figure 2: HPLC-UV chromatogram separation of 25 μg/ml standard solution of SVA, SVT (λ = 238) and CoQ10 (λ = 275).

5.2 Validation of the Method

The present method was developed and validated in accordance with the International Conference on Harmonization (ICH) guideline Q2 (R1),[20] determining the following parameters: selectivity/specificity, linearity, detection and quantification limits, repeatability and intermediate precision, robustness and accuracy. The method was then applied to the quantification of drug release from nanoparticles co-encapsulating simvastatin and coenzyme Q10.

5.2.1 Selectivity and System Suitability

The selectivity of the method was tested analysing the standard diluent solution by itself to show that no peaks interfere with analytes retention times during chromatographic separation. Standard diluent solution spiked with blank LCN nanoparticles was analysed as well for possible matrix-associated interferences.

The analysis of the three work solutions containing all the analytes (25 μg/ml) was also performed to verify if the method was suitable for the separation of SVT from its isoform SVA

and from CoQ10. The chromatograms of the standard diluent solution (Figure 1 A, Supplementary material) and of the standard diluent solution spiked with empty nanoparticles (Figure 1 B, Supplementary material) did not show any interfering peaks at the retention times of interest (for the analytes peaks and blank standard diluent solution overlay see chromatograms reported in Figure 2, Supplementary material). For system suitability, ICH Q2 (R1)[20] does not determine any criteria for the acceptance. Thus, following CDER-FDA guideline on "Validation of Chromatographic Method" acceptances criteria,[24] analytes retention factor (K' > 2), asymmetry (α > 0.75) and number of theoretical plates (N > 2000) were investigated. All obtained values were in accordance with required criteria, indicating the suitability of the analytical method (Table 2). Moreover, the system suitability of the developed method was also verified evaluating the separation between adjacent peaks, that showed high values of resolution (Rs > 2, FDA acceptance criteria), and the repeatability of peak area (RSD ≤ 1%), as reported on Table 2.

Table 2: Chromatographic parameters of system suitability

Analyte	*N*	*K'*	Peak area (RSD)	α *(mean)*	*Rs*
SVA	17698	3.27	0.66	0.99	10.48 $_{SVA/SVT}$
SVT	45969	4.28	0.59	0.89	36.33 $_{SVT/CoQ10}$
CoQ10	72244	8.69	0.45	0.91	-

Abbreviations: ***N***, number of theoretical plates; ***K'***, retention factor; **RSD**, residual standard deviation; ***α,*** symmetry; ***Rs***, resolution; SVA, hydroxide acid simvastatin; SVT, simvastatin (lactone); CoQ10, coenzyme Q10.

5.2.2 Detection (LOD) and Quantification Limits (LOQ)

The limit of detection and quantification represent the lowest concentration at which analytes can be identified (LOD) and quantified (LOQ) with precision and accuracy. [20] Specific calibration curves were built for LOD and LOQ determinations, with samples solutions containing SVA, SVT and CoQ10 in the concentration range from 0.25 to 25 µg/ml. LOD an LOQ values were separately calculated for each analyte using the slope and standard deviation of y-intercept from the linear regression (least square method) through the formula reported in section *2.5.3.* The following values of 0.10, 0.09 and 0.12 µg/ml were the

detection limits, while 0.30, 0.28 and 0.37 µg/ml the quantification limits for SVT, SVA and CoQ10, respectively.

5.2.3 Linearity

Linearity of the analytical method was assessed considering six concentrations levels in the range from 0.5 to 25 µg/ml for SVA, SVT and CoQ10 in mixture. Samples were analysed six times per concentration; peaks areas were recorded, analysed and results of the regression statistics are reported in Table 3. Since Cochran test evidenced no significant difference among the variance values of replicates at different concentration levels, calibration curves were elaborated using the linear regression model. A good linearity was stablished over the range considered (0.5-25 µg/ml) for all analytes, demonstrating the suitability for analysis. [20,24] The square of correlation coefficient (r^2) values over to the acceptance criteria (> 0.999) indicate a very high level of correlation between the concentration of analytes and peak area response provided by the detector. [20,25]

Table 3: Linearity of the six concentration levels of SVA, SVT and CoQ10: linear regressions are y = mx + q.

	SVA	**SVT**	**CoQ10**
Range (µg/ml)	0.5 - 25	0.5 - 25	0.5 - 25
Slope (m)	84.101	108.310	32.787
Standard error (m)	0.324	0.389	0.1561
Intercept (q)	14.490	15.960	4.443
Standard error (q)	3.186	3.867	1.534
Determination Coefficient (r^2)	0.9996	0.9997	0.9993
F value*	67245	77403	44075
C value (Cochran test) **	0.3150	0.3048	0.3357

* F (0.01; 1;35) = 12.90, $p < 0.0001$

** C (0.05; 6;6) = 0.4447

5.2.4 Precision

Repeatability expresses the precision of multiple sampling measurements under the same operating conditions over a short interval time, while intermediate precision expresses variations from the same laboratory under variable operation conditions, such as different days, analysts or equipment. [26] Precision of the method was determined at three different concentration levels of calibration curve: the lower (0.5 µg/ml), intermediate (2 µg/ml) and upper level (25 µg/ml). Repeatability of the method was demonstrated by the concentration recovery (100 ± < 2 %) and RSD (< 2%) for six repeated injections *per* sample, of the three samples replicates analysed in the same day (Table 4). Residual standard deviation of recovered concentrations lower than 2% for all analytes at the three concentration levels, in three alternated days, confirmed the intermediate precision (Table 4). The agreement between the experimental values of multiples analyses indicates the good precision of the method [24].

Table 4: Repeatability and Intermediate precision of SVA, SVT and CoQ**10**

Standard Solutions (µg/ml)	**Lower level** 0.5 µg/ml	**intermediate level** 2 µg/ml	**Up level** 25 µg/ml	**RSD lower level (%)**	**RSD Intermed. level (%)**	**RSD up level (%)**
Repeatability						
Recovered SVA (mean±SD)	0.50 ± 0.01	2.03 ± 0.01	25.07 ± 0.12	1.49	0.66	0.46
Recovered SVT (mean±SD)	0.50 ± 0.01	2.02 ± 0.01	25.09 ± 0.06	1.51	0.43	0.23
Recovered CoQ10 (mean±SD)	0.51 ± 0.00	2.00 ± 0.01	24.95 ± 0.03	0.47	0.34	0.11
Inter-day Precision						
Recovered SVA (mean±SD)	0.49 ± 0.01	2.04 ± 0.03	25.08 ± 0.08	1.30	1.33	0.32
Recovered SVT (mean±SD)	0.50 ± 0.01	2.08 ± 0.02	25.01 ± 0.13	1.51	0.87	0.50
Recovered CoQ10 (mean±SD)	0.51 ± 0.00	2.01 ± 0.02	25.03 ± 0.07	1.25	1.23	0.29

5.2.5 Robustness

A method is considered robust when no significant changes occurs after small, but deliberate variations on critical chromatographic parameters. [20] Even if the obtainment of a chromatogram with high resolution values between peaks (Figure 1, Table 2) confer by itself the required robustness to the method, [24] we introduced significant variations on the most important parameters for the chromatographic elution of multiples substances, i.e., temperature of the column (± 2 °C) and mobile phase: Eluent-A pH (± 0.3 units). As reported on Table 5, a good chromatographic separation between peaks was maintained after all parameters modifications, as no significant variation was observed on peaks resolution (One-Way ANOVA, $p > 0.05$). Moreover, a method is considered robust when average percentage recovery is around 100 (± 5%) and RSD is below 2%. [24] Percentage recovery for SVA, SVT and CoQ10 ranged from 97% to 101% and RSD values from 0.20 to 1.25% after modifications on temperature (43 and 47 °C) and mobile phase pH (5.2 and 5.8) parameters (Table 5). These variations are within the limits reported in the FDA guideline, supporting the robustness of the devolved method. However, it should be pointed out, that even if peaks are still resolved, the method recovery for SVA was reduced below 95% when the experimental conditions related to the mobile phase flow rate were modified.

Table 5: Resolution and Recovery of SVA, SVT and CoQ10 for evaluation of method robustness

Factor		*Rs* SVA/SVT	Rt SVT/CoQ10	Recovery ± RSD (SVA)	Recovery ± RSD (SVT)	Recovery ± RSD (CoQ10)
Flow **Temperature** **pH**	**1.5 ml/min** **45 °C** **5.5 units**	7.97	36.99	100.01 ± 1.08	100.00 ± 0.22	100.01 ± 0.69
Flow	1.3 ml/min	6.75	25.09	91.13 ± 2.72	101.09 ± 0.52	99.46 ± 0.76
Temperature	43°C	7.87	36.15	97.81 ± 0.30	99.91 ± 0.47	99.67 ± 0.41
Temperature	47°C	7.35	36.51	97.34 ± 0.60	98.91 ± 0.53	98.36 ± 0.72
pH	5.2	8.04	37.10	98.14 ± 1.23	100.14 ± 0.27	99.87 ± 0.78
pH	5.8	7.41	36.64	98.74 ± 1.25	100.19 ± 0.20	99.76 ± 0.44

5.2.6 Accuracy

According to ICH recommendations, to assess accuracy of the method for drugs formulation, studies are frequently performed by the addition of known amounts of drugs to the placebo, working at three concentration levels into the linear range of detection of the analyte. [20] Thus, accuracy of the method was assessed using the average recovery values of the lowest, intermediate and upper concentration levels of calibration curve (0.5, 2 and 25 µg/ml), covering the linear range of analytes. Blank matrix of empty nanoparticles spiked with the combined standard solutions of SVA, SVT and CoQ10 were analysed after three repeated injections for each sample, in triplicate. Accuracy analyses have been performed and expressed as percentage of concentration recoveries with their respective RSD (Table 6). For all analytes at the three concentration levels tested, recovery was within the 100 ± 1 % limit with RSD values lower than 2%. The method is accurate for the investigated drugs, as percentage recovery and RSD values obtained indicate an intimate concordance between theoretical and experimental results. [25]

Table 6: Accuracy: Recovery and RSD of SVA, SVT and CoQ10 from spiked blank nanoparticles

Standard Solutions	Recovery SVA (%)	Recovery SVT (%)	Recovery CoQ10 (%)	RSD SVA	RSD SVT	RSD CoQ10
Lower level 0.5 µg/ml	99.94	101.31	100.44	1.13	1.46	0.46
intermediate level 2 µg/ml	100.53	100.56	100.89	0.45	0.93	0.59
Upper level 25 µg/ml	101.1	100.02	100.34	0.54	0.32	0.24

5.3 Application of the Method

The present method was proposed to investigate simvastatin/ coenzyme Q10 co-encapsulation within lecithin/chitosan nanoparticles through a self-assembly manufacturing

process. Particularly, an analytical method able to simultaneously quantify the two drugs could be used to determine the *in vitro* drug release profiles from the nanoparticles. Nanoparticles as colloidal systems are being extensively investigated for the formulation and delivery of drugs, especially for their controlled release and targeting capacity. In this work, nanoparticles composed of a natural polysaccharide (chitosan) and phospholipids (lecithin) were developed for the co-encapsulation of simvastatin and coenzyme Q10 (SVT/CoQ10-LCN). Nanoparticle formulations were characterized for hydrodynamic particle diameter, particle size distribution and surface charge. SVT/CoQ10-LCN nanoparticles have an average diameter of 254 ± 20 nm, with narrow particles size distribution (PDI of 0.130 ± 0.042) and positive surface charge (+32.00 ± 1.09 mV), suggesting that chitosan, a positive polymer, is forming an external layer covering nanoparticles surface. [15]

Table 7: Nanoparticles quantification: Drugs association efficiency (AE%) and encapsulation efficiency (EE%)

SVT-CoQ10-LCN	TDR% ± RSD	EE% ± RSD
SVT	99.84 ± 0.20	99.77 ± 0.20
CoQ10	99.66 ± 0.18	99.57 ± 0.17

Abbreviations: TDR%, total drug recovered (%); **EE%,** encapsulation efficiency (%).

To determine simvastatin and coenzyme Q10 encapsulated in the nanoparticles, an indirect approach was used. Briefly, to assess encapsulated drug (EE%), the drug dissolved in the preparation medium, separated through ultrafiltration, was subtracted from the total content of drugs in the preparation, determined by direct analysis of a sample of the nanosuspension. The total drug content in the preparation was compared with the drug amount weighed, to evaluate the percentage recovery obtained (TDR%). Total drug recovery (TDR%) and encapsulation efficiency EE% with the respective value of SD and RSD are presented on Table 7. Total drug recovery data indicate that sample preparation efficiently extract drugs from the samples of nanodispersion (TDR% 100%, RSD < 2%). This result is important since the quantification of drugs in nanomedicine formulations is strictly dependent from the capacity of extraction and accurate drug recovery from the colloidal preparation. [17] Moreover, high EE% values were evidenced for both, simvastatin (SVT plus SVA) and CoQ10, with nanoparticles encapsulating up to 98% of the compounds. Particularly, the TDR and EE of total simvastatin were obtained considering the presence of both simvastatin

isoforms in freshly prepared formulations. This point reinforce that is necessary to use a method capable to effectively detect and quantify both, the statin drug and its hydroxyl acid isoform in pharmaceutical formulations, to account for the total content of the drug. Regarding HPLC analyses, no variations in the chromatogram were found for quantification of nanoparticle samples (Figure 3).

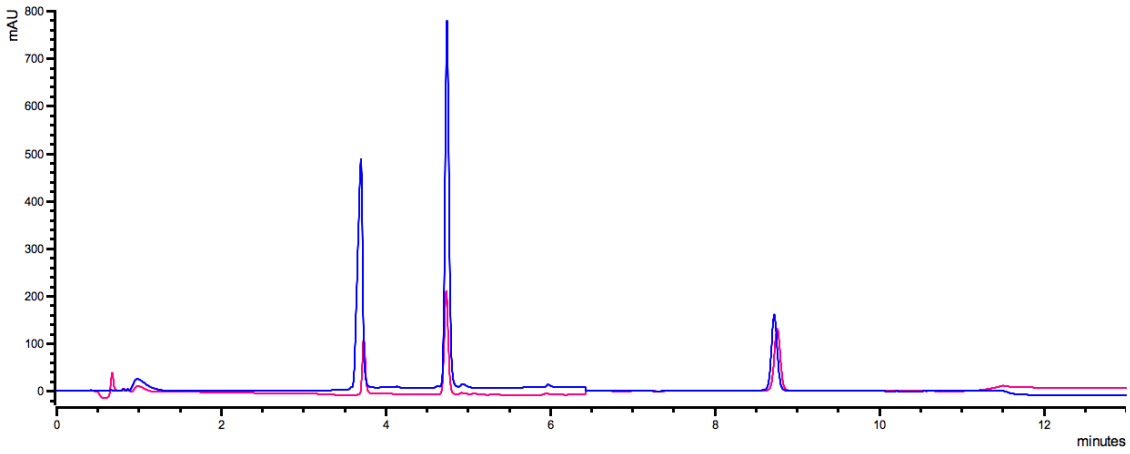

Figure 3: Chromatograms overlay of SVT/CoQ10-NCL quantification (pink line) and standard solution of SVA, SVT and CoQ10 at 25 μg/ml (blue **line)**

The *in vitro* release of simvastatin and coenzyme Q10 from LCN nanoparticles was performed in simulated nasal fluid at pH 6.5, as nanoparticles were designed for nasal administration. [23] Drugs release profiles are illustrated on Figure 4 showing a typical application of the proposed method. Simvastatin release profile is characterized by a continuous and progressive release of drug content from nanoparticles. After 8h of experiment, approximately 40% of total simvastatin (1 mg/ml) was released from the formulation. Release of coenzyme Q10, instead, shown a very slow but constant release, with a quite low (< 5%) release during the 8h of experiment. It has been hypothesized that for drugs encapsulated in the oil core of nanocapsules, such our LCN nanoparticles, drug release rate is affected by the partition coefficient of drugs between the hydrophobic phase and the release medium. [27] In the case of highly insoluble aqueous drugs, such as coenzyme Q10 (practically water insoluble) this phenomenon is reinforced when the release medium is

an simple electrolyte solution. [28] Moreover, when released from nanoparticles, the drugs need to diffuse through a cellulose acetate membrane of the dialysis bag to be released in the compartment where sampling occurs, providing, once again, a barrier to cross for the hydrophobic compounds [29,30]. Regarding chromatographic analyses, the method demonstrated to be selective and accurate, with recoveries of all investigated molecules (SVA = 26.34 ± 0.44 %, SVT = 73.86 ± 0.32 % and CoQ10 = 99.83 ± 0.77 %), within the required sensibility acceptance criteria.

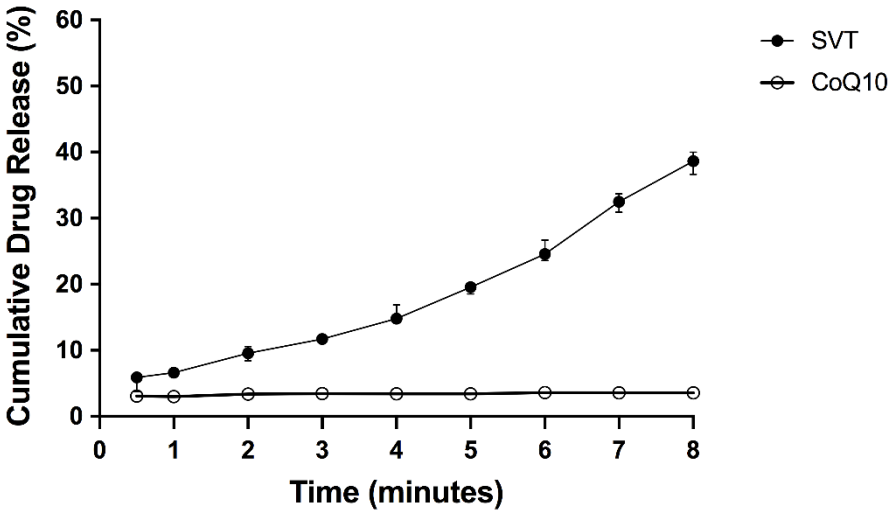

Figure 4 Simvastatin (●) and coenzyme Q10 (○) release profiles from lecithin/chitosan nanoparticles

6 Conclusions

Recently, the use of nanoparticles for the co-encapsulation of pharmaceutical products has attracted significant attention, increasing the need for efficient analytical methods for their characterization. To our knowledge, in this study, the first RP-HPLC method for the simultaneous quantification of simvastatin, the statin hydroxyacid form and coenzyme Q10 co-encapsulated into hybrid nanoparticles systems was developed and validated. The method was validated according to ICH Q2 and FDA guidelines for system suitability, linearity, limits of detection and quantification, intra-laboratory precision and recovery. Furthermore, it was demonstrated that the developed analytical method for simvastatin isoforms and coenzyme Q10 *in vitro* quantification can be applied to nanoparticle characterization for drug loading and to drug release experiments. Although the present work has focused on the characterization of hybrid lipid/polysaccharide nanoparticles, the proposed analytical method could be potentially valid for the quantification of simvastatin, simvastatin hydroxyl acid and coenzyme Q10 in other lipid-based pharmaceutical nanocarriers, such as liposomes, solid lipid nanoparticles, nanostructured lipid carriers or nanoemulsions.

References

1. Chou, R. *et al.* Statins for Prevention of Cardiovascular Disease in Adults. *Jama* **316,** 2008 (2016).

2. McCarey, D. W. *et al.* Trial of Atorvastatin in Rheumatoid Arthritis (TARA): Double-blind, randomised placebo-controlled trial. *Lancet* **363,** 2015–2021 (2004).

3. Marin, L. et al. Chronic obstructive pulmonary disease: patho-physiology, current methods of treatment and the potential for simvastatin in disease management. *Expert Opin. Drug Deliv.* **8,** 1205–1220 (2011).

4. Gopalan, A. et al. Simvastatin inhibition of mevalonate pathway induces apoptosis in human breast cancer cells via activation of JNK/CHOP/DR5 signaling pathway. *Cancer Lett.* **329,** 9–16 (2013).

5. Wang, Q. *et al.* Statins: Multiple neuroprotective mechanisms in neurodegenerative diseases. *Experimental Neurology* **230,** 27–34 (2011).

6. Sonvico, F., Zimetti, F., Pohlmann, A. R. & Guterres, S. S. Drug delivery to the brain: how can nanoencapsulated statins be used in the clinic? *Ther. Deliv.* **8,** 625–631 (2017).

7. Skottheim, I. B., Gedde-Dahl, A., Hejazifar, S., Hoel, K. & Åsberg, A. Statin induced myotoxicity: The lactone forms are more potent than the acid forms in human skeletal muscle cells in vitro. *Eur. J. Pharm. Sci.* (2008). doi:10.1016/j.ejps.2007.12.009

8. Schirris, T. J. J. *et al.* Statin-induced myopathy is associated with mitochondrial complex III inhibition. *Cell Metab.* **22,** 399–407 (2015).

9. Marcoff, L. & Thompson, P. D. The Role of Coenzyme Q10 in Statin-Associated Myopathy. A Systematic Review. *J. Am. Coll. Cardiol.* **49,** 2231–2237 (2007).

10. Yang, X., Dai, G., Li, G. & Yang, E. S. Coenzyme Q10 reduces beta-amyloid plaque in an APP/PS1 transgenic mouse model of Alzheimer's disease. *J. Mol. Neurosci.* **41,** 110–3 (2010).

11. Young, J. M. *et al.* Effect of Coenzyme Q10 Supplementation on Simvastatin-Induced Myalgia. *Am. J. Cardiol.* **100,** 1400–1403 (2007).

12. Hu, C. M. J. & Zhang, L. Nanoparticle-based combination therapy toward overcoming drug resistance in cancer. *Biochemical Pharmacology* **83,** 1104–1111 (2012).

13. Ma, L., Kohli, M. & Smith, a. Nanoparticles for combination drug therapy. *ACS Nano* **7,** 9518–9525 (2013).

14. Şenyiğit, T. *et al.* In vivo assessment of clobetasol propionate-loaded lecithin-chitosan nanoparticles for skin delivery. *Int. J. Mol. Sci.* **18,** (2017).

15. Clementino, A. *et al.* The nasal delivery of nanoencapsulated statins – An approach for brain delivery. *Int. J. Nanomedicine* **11,** 6575–6590 (2016).

16. Sonvico, F. *et al.* Mean square hydrogen fluctuations in chitosan/lecithin nanoparticles from elastic neutron scattering experiments. *Phys. B Condens. Matter* **385–386 I,** 725–727 (2006).

17. Fuster, J. *et al.* HPLC-UV method development and validation for the quantification of ropinirole in new PLGA multiparticulate systems: Microspheres and nanoparticles. *Int. J. Pharm.* **491,** 310–317 (2015).

18. Yang, D. J. & Hwang, L. S. Study on the conversion of three natural statins from lactone forms to their corresponding hydroxy acid forms and their determination in Pu-Erh tea. *J. Chromatogr. A* **1119,** 277–284 (2006).

19. Sarmento, B. et al. Development and validation of a rapid reversed-phase HPLC method for the determination of insulin from nanoparticulate systems. *Biomed. Chromatogr.* **20,** 898–903 (2006).

20. Ich. ICH Topic Q2 (R1) Validation of Analytical Procedures : Text and Methodology. *Int. Conf. Harmon.* **1994,** 17 (2005).

21. Barbieri, S. *et al.* Lecithin/chitosan controlled release nanopreparations of tamoxifen citrate: Loading, enzyme-trigger release and cell uptake. *J. Control. Release* **167,** 276–283 (2013).

22. Seju, U., Kumar, A. & Sawant, K. K. Development and evaluation of olanzapine-loaded PLGA nanoparticles for nose-to-brain delivery: In vitro and in vivo studies. *Acta Biomater.* **7,** 4169–4176 (2011).

23. Castile, J. *et al.* Development of *in vitro* models to demonstrate the ability of PecSys®, an *in situ* nasal gelling technology, to reduce nasal run-off and drip. *Drug Dev. Ind. Pharm.* **39,** 816–824 (2013).

24. Center for Drug Evaluation and Research, US Food and Drug Administration, U. *Reviwer Guidance, Validation of Chromatographic Methods*. (1994).

25. Shabir, G. A. Validation of high-performance liquid chromatography methods for pharmaceutical analysis: Understanding the differences and similarities between validation requirements of the US Food and Drug Administration, the US Pharmacopeia and the International Conf. in *Journal of Chromatography A* **987,** 57–66 (2003).

26. I, S. Mk. Validation of chromatographic methods. *Pharm. Technol.* **22,** 104–119 (1998).

27. Guterres, S. S. et al. Polymeric nanoparticles, nanospheres and nanocapsules, for cutaneous applications. *Drug Target Insights* **2,** 147–157 (2007).

28. Nepal, P. R., Han, H. K. & Choi, H. K. Enhancement of solubility and dissolution of Coenzyme Q10 using solid dispersion formulation. *Int. J. Pharm.* **383,** 147–153 (2010).

29. Modi, S. & Anderson, B. D. Determination of drug release kinetics from nanoparticles: Overcoming pitfalls of the dynamic dialysis method. *Mol. Pharm.* **10,** 3076–3089 (2013).

30. Wallace, S. J., Li, J., Nation, R. L. & Boyd, B. J. Drug release from nanomedicines: Selection of appropriate encapsulation and release methodology. *Drug Deliv. Transl. Res.***2,** 284–292 (2012).

CHAPTER 5

HYBRID NANOPARTICLES REGULATE CYTOKYNE RELEASE AND PSYCHOSINE-INDUCED DEATH IN ASTROCYTES AND INHIBIT DEMYELINATION IN ORGANOTYPIC CEREBELLAR SLICES CULTURE

Hybrid Nanoparticles Regulate Cytokine Release and Psychosine-Induced Death in Astrocytes and Inhibit Demyelination in Organotypic Cerebellar Slices Culture

Clementino A[1,2,3]., Velasco M[3]., Benech S[3]., Del Favero H[1]., Sonvico F[1] and Dev K[3].

[1]Food and Drug Department, University of Parma, Parma (PR) Italy

[2]Conselho Nacional do Desenvolvimento Cientifico e Tecnologico - CNPq, Brasilia, Brazil

[3]Trinity Biomedical Science Institute, Trinity College Dublin, Dublin, Ireland

To be submitted to ***International Journal of Neuroinflammation***

Abstract

Polymeric nanoparticles are being extensively investigated as an approach for brain delivering of drugs, especially for their controlled release and targeting capacity. The nose-to-brain administration of nanoparticles, bypassing the blood brain barrier (BBB) offer a promising strategy to delivery neuroprotective compounds direct to the central nervous system (CNS) parenchyma. Simvastatin (SVT) and coenzyme Q10 (CoQ10) are nowadays claimed for their potential role in the prevention of neurodegenerative diseases, involving statins pleiotropic effects like anti-inflammatory, anti-apoptotic and immunomodulatory properties and the strong anti-oxidant activity of coenzyme Q10. The purpose of this study was to evaluate nanoparticles loaded with SVT and CoQ10 in a preliminary *in vitro/ex vivo* multimodal model of neurodegenerative diseases. Biocompatible and biodegradable hybrid nanaoparticles were prepared by self-assembly technique of lipid and polysaccharide components, i.e. lecithin and chitosan. Nanoparticles physico-chemical properties, encapsulation efficiency and structure were determined. Anti-apoptosis and anti-inflammatory properties of the formulation were evaluated against an *in vitro* model of psychosine-induced astrocytes cellular toxicity. Finally, nanoparticles prevention of cerebellar demyelination was performed using the organotypic cerebellar slices culture excised from the brain of 10 days old mice. Nanoparticles were obtained with desirable features of small particles size (250 nm), positive surface charge (+ 36mV) and high encapsulation efficiency (> 99%). Nanoparticles size was further confirmed by SANS technique, highlighting particles core-shell structure. Astrocytes viability and inflammation studies evidenced a reduction of psychosine-induced toxicity and cytokines-induced IL-6 release when SVT and CoQ10 were associated in the nanoparticle formulation. Moreover, results evidenced that also blank nanoparticles inhibit almost completely psychosine-induced astrocytes death, suggesting an important role of nanoparticles composition and structure against psychosine toxic effects. In mice cerebellar slices, nanoparticles significantly prevented astrocytes activation (decreasing GFAP expression) and cerebellar demyelination (restoring MBP levels) caused by psychosine. Nanoparticles with desirable features for the nose-to-brain delivery of medicines presenting significant neuroprotection against aggressive brain injuries, as evidenced in this work, represent an innovative and promising approach for the treatment of several neurodegenerative diseases.

Keywords: hybrid nanoparticles, chitosan nanoparticles, astrocytes, psychosine, organotypic cerebellar slices.

1 Introduction

Despite significant advances have been made in brain research, delivery of drugs for the treatment of central nervous system (CNS) disorders remains a challenge. The major obstacle in delivering drugs to brain is the impervious nature of the blood brain barriers (BBB), which limits the access to CNS of a huge number of drugs, especially hydrophilic and large molecular weight compounds [1]. As a matter of fact, many potential neuroprotective agents have been abandoned as therapeutic brain levels of drugs are not achieved following the systemic administration. In other cases, invasive procedures have been adopted to promote the infusion of drugs directly into brain structures to obtain high cerebrospinal fluid (CSF) concentrations. Another invasive strategy adopted to enhance drugs delivery to CNS involves the infusion of hyperosmotic solutions to disturb the BBB permeability [2]. However, many of those approaches are either risky and ridden by side effects or clinically unacceptable. Non-invasive therapies with efficient brain targeting would favour patient compliance and treatment effectiveness, especially in the case of chronic neuropathology.

It has been proven that nanoparticles enable the brain delivery of a numerous variety of drugs, including anticancer, antivirus, anti-Alzheimer's, anti-schizophrenia drugs and several other molecules [3–6]. Pharmaceutical nanotechnology employs several strategies to facilitate drug delivery to the brain, involving non-invasive methods to cross the BBB or to bypass it. For instance, nanoparticles-mediated transport across the BBB involves:

I) Nanoparticles size and zeta potential:

a. *positively charged nanoparticles:* should be able to bind negatively charged endothelial cells membrane and cross the BBB by adsorption-mediate endocytosis [7].

II) Nanoparticles drug release in the endothelial cells of the BBB after uptake [8]

III) Receptor-mediate nanoparticles endocytosis and/or transcytosis:

a. *modification of nanoparticles surface with surfactants for the adsorption of plasmatic proteins*: a specific adsorption of apolipoproteins on the nanoparticles corona leads to an interaction with LDL receptors of the BBB [9];

b. *covalent nanoparticles conjugation with targeting ligands:* specific antibodies and peptides, like transferrin and lactoferrin are used to obtain a specific binding to BBB receptors [8].

Although many promising strategies to increase the drug transport of nanoparticles across the BBB have been proposed, it is important to highlight that systemic administration of nanoparticles carriers is still focus of the scientific community concern. In fact, the most efficient carries for brain delivery across the BBB still accumulate massively in other regions of the body, especially in vital organs like liver, spleen, lungs and kidneys, increasing the risk of undesirable toxicities [8].

Nasal delivery has been indicated as a possible and convenient alternative route for CNS drug delivery. In fact, the main innervation of the olfactory cavity, i.e., the olfactory nerve, represents the only part of the body where the CNS is in a direct contact with the environment [10]. Hence, the direct transport from the nose to the brain (nose-to-brain, N2B) could provide drugs access to the CNS, avoiding systemic administration and bypassing the BBB. Considering the main physiological barriers of the nasal route (mucus layer, mucociliary clearance and low percentage of dose <0.1% directly transported from nose to brain) [1], the strategy of applying drugs encapsulated into nanoparticles vectors to the olfactory region of the nose could improve the direct CNS delivery of many molecules, including biologics [11].

In the present work, we propose the formulation in hybrid nanoparticles of simvastatin and coenzyme Q10, two lipophilic molecules recently claimed for their potential neuroprotection in neurodegenerative diseases. Simvastatin (SVT), an HMG-CoA reductase inhibitor, is commonly used in the prevention of cardiovascular diseases, by inhibiting the cholesterol synthesis in the liver. However, statins have gained attention for their non-lipid lowering effects, also known as pleiotropic effects, involving anti-inflammatory, anti-apoptosis, anti-oxidant and immunomodulatory properties [7]. Those effects made statins attractive for many neurodegenerative brain diseases. However, low brain accumulation of simvastatin after systemic administration prevent its clinical application in CNS pathologies [12]. Moreover, elevated quantities of systemic circulating simvastatin are not beneficial due the well-known muscular toxicity of statins. In fact, the assumption of statins is correlated with many muscular dysfunctions, ranging from a simple myalgia to the sever rhabdomyolyses [13,14].

It has been suggested that an impaired ubiquinone (Coenzyme Q10) synthesis may be responsible for muscular statins side effect [15]. In this scenario, the employment of

coenzyme Q10 (CoQ10) co-formulated with simvastatin sounds as an interesting strategy. Moreover, CoQ10 antioxidant and anti-inflammatory properties may promote a synergic effect with simvastatin against inflammatory and oxidative processes involved in neurodegeneration processes [16,17]. Thus, in the present study a biocompatible and biodegradable formulation based on the self-assembly of lecithin and chitosan co-encapsulating simvastatin and coenzyme Q10 were developed as a promising strategy for the nose-to-brain delivery of neuroprotective compounds. The present work aimed to investigate whether the association of two compounds with antioxidant, anti-inflammatory and anti-apoptotic properties could be beneficial in the inhibition of neurodegenerative processes. Moreover, to investigate the role of nanoparticles on the formulation efficacy against cellular apoptosis, neuro-inflammation and cerebellar demyelination. In fact, neuro-inflammation, cellular apoptosis and demyelination are highlighted as the most common pathways of the onset, development and progression of neurodegenerative pathologies, including multiple sclerosis (MS), Krabbe's disease (KD) and Alzheimer disease (AD) [18–22].

Hence, to evaluate the simvastatin and coenzyme Q10 loaded-nanoparticles preliminary efficacy as multimodal approach against neurodegeneration, a multifunctional study involving astrocytes cells inflammation and death as well as demyelination processes on cerebellar slices induced by the toxic lipid metabolite galactosylsphingosine (psychosine) was carried out.

2 Materials and Methods

2.1 Materials for Nanoparticles Production

Chitosan with deacetylation degree of 95% and viscosity 45 cP was purchased from Primex (Chitoclear FG, Siglufjordur, Iceland). Lecithin Lipoid® S45 was supplied by Lipoid AG (Ludwigshafen, Germany). Pharmaceutical grade oil vehicles Maisine™ 35-1 (glyceryl monolinoleate) and Labrafac™ Lipophile WL 1349 (medium chain triglycerides) were a kind gift from Gattefossé (Saint-Priest, France). Simvastatin and deuterated water (D_2O) were provided by Sigma Aldrich (Steinheim, Germany), while coenzyme Q10 was supplied by A.C.E.F. S.p.A. (Fiorenzuola D'Arda, Italy). Ultrapure water (Purelab Flex; ELGA-Veolia LabWater, Windsor Court, UK) was used for nanoparticles production. All other reagents used for nanoparticles characterization were of analytical grade.

2.2 Compounds and Cell Treatments

Simvastatin (SVT) and coenzyme Q10 (CoQ10) raw material or encapsulated into lecithin/chitosan nanoparticles (SVT/CoQ10-LCN) were used at the concentrations of 10 μM, 1 μM and 0.1 μM upon dilution in cell culture medium (HyClone DMEM-F/12, Fisher Scientific, Waltham, MA, USA). SVT and CoQ10 stock solutions were prepared in ethanol. Psychosine (Psy) (Santa Cruz, Dallas, TX, USA) was prepared as a 10 mM stock solution diluted in dimethyl sulfoxide (DMSO, Sigma Aldrich, Schnelldorf, Germany) and stored at -20°C until usage. To avoid any cytotoxic effect, organic solvents concentrations during cell treatments were maintained below 0.01%. Human IL-6 Elisa Kit and standard L-17A cytokine were obtained from R&D Systems (Minneapolis, MN, USA), while standard human TNF-α cytokine was supplied by Peprotech (UK). Primary antibodies used were the following: anti-vimentin (sc-373717, Santa Cruz Biotech, Dallas, TX, USA), anti-GFAP (ab2109815, Millipore, USA) and anti-MBP (ab40390, Abcam, Cambridge, UK). Secondary antibodies used were: anti-chicken 633 (A21103, Invitrogen Alexa,), anti-rabbit 488 (A27034, Invitrogen Alexa Fluor, Thermo Fisher Scientific, Waltham, MA, USA) and anti-mouse Dylight 549 (715-505-020, Jackson ImmunoResearch, Ely, UK). For nuclear staining DAPI (4',6-Diamidino-2-Phenylindole, Dihydrochloride; 62248, Thermo Fisher Scientific, Waltham, MA, USA) was used.

2.3 Nanoparticles Preparation and Characterization

Hybrid lecithin/chitosan nanoparticles loaded with simvastatin and coenzyme Q10 (LCN-SVT/CoQ10) were prepared trough a self-emulsifying method, as previously reported [23,24]. Briefly, 20 mg of CoQ10 and 10 mg of SVT were dispersed into 0.8 ml of an ethanol solution of lecithin (2.5%), containing 20 mg of both Labrafac™ and Maisine™ oil vehicles. Then, the lecithin solution containing the compounds was injected into 10 ml of a 0.01% w/v chitosan aqueous solution under constant agitation (magnetic stirring300 rpm) and temperature (50 °C). Freshly prepared nanoparticle suspensions were kept in agitation and at the same temperature conditions for 10 min to allow the complete evaporation of ethanol from the system. Nanoparticles were characterized for particle size and polydispersity index (PDI) by dynamic light scattering (DLS) and nanoparticle zeta potential by electrophoresing mobility applying phase analysis light scattering (PALS) (Malvern Zetasizer Nano ZS, Malvern Instruments Ltd., Malvern, UK). Nanoparticle encapsulation efficiency (EE) was determined through an indirect method using both, centrifugation and ultrafiltration (Vivaspin® 2, MWCO 30KD, Sartorius, Germany) to separate nanoparticles from non-encapsulated drugs. Simvastatin and CoQ10 were simultaneously quantified applying a previously developed high performance liquid chromatography analytical method (HPLC; Agilent 1200 series, Agilent, St Claire, USA), coupled with a UV/Vis detector working in a dual wavelength mode (238 nm for SVT and 275 nm for CoQ10) [24]. The internal structure of nanoparticles was investigated by the small angle neutron scattering technique (SANS), exactly as reported before [23,25]. For these experiments, nanoparticles were produced using deuterated water (D_2O). Experiments were performed at the D33 beamline at the Institute Laue-Langevin (ILL, Grenoble, France).

2.4 Primary Human Astrocytes Culture

Human astrocytes derived from the cerebral cortex of fetal male at 21 weeks' gestation (11065, Sciencell Research Lab., Carlsbad, CA, USA) were cultured in DME-F/12 medium (Hyclone™ NAH9812) supplemented with 10% of foetal bovine serum (FBS, F7524, Sigma Aldrich, St. Louis, MO, USA), 1% penicillin/streptomycin (Sigma Aldrich, P4333) and 1% astrocytes growth supplement (1852, Sciencell Research Lab., Carlsbad, CA, US). Cells were cultured in T75 flasks incubated at 37°C, 95% humidity and 5% CO_2, changing the media every 3 days until 70% confluent and every day after 70% of confluence was reached. When 90% confluent, cells were split and platted in 24-well cell culture plates at 2.4 x 10^5

cells/ml density and grown for 48h to perform experiments. For all experiments, cells were serum starved from 3h to overnight (DME-F/12 incubation only) prior each treatment. Treatment details are indicated in the figure legends. Cells supernatant were used to quantify protein levels of pro-inflammatory cytokines, while attached cells were tested for viability and immunocytochemistry assay.

2.5 Cell Viability

Cytotoxicity of compounds as raw materials or drug-loaded nanoparticles, as well as astrocytes viability after psychosine treatments were performed using the MTT [3-(4,5-dimethylthiazol-2-yl)-2,5-diphenyltetrazolium bromide] assay. Briefly, cells were seeded at a density of 2.4 x 10^5 cells/ml in 24-well plates, grown for 48 hours until 70-90% confluent and serum starved for at least 3 hours prior to treatments. To determine the concentrations and treatment time at which compounds treatments did not affect astrocytes viability, cells were previously treated with drugs and nanoparticles at different concentrations (1.25, 2.5, 5, 10 and 20 µM) for 2, 4 and 6 h. Then, to investigate effect of compounds in reducing astrocytes death induced by psychosine, cells were treated with psychosine alone (10 µM, 15 µM and 20 µM) or supplemented with SVT, SVT/CoQ10, blank-LCN or SVT/CoQ10-LCN at 0.1 µM, 1 µM and 10 µM for 4 h. Prior to MTT incubation, representative images of cells in all treatment studies were taken using a CKX41 Olympus inverted microscope (Mason Technologies, Dublin, Ireland) at 10× magnification (n=4-6). Finally, after 4h of experiment, cells were incubated with fresh medium supplemented with MTT reagent at 5 mg/ml (Invitrogen™, Thermo Fisher Scientific, Waltham, MA, USA) for 3h at 37°C, followed by the addition of DMSO to each well to dissolve the violet-coloured metabolite. Plates were gently shaken for 15 min to homogenize the wells content and the absorbance's read at 540 nm (microplate reader, Labsystem Multiskan, LabX, Midland, ON, Can). Absorbance values were directly correlated with the cellular viability and percentage of cell viability for each treatment were calculated in comparison to control values obtained for untreated cells.

2.6 Human Astrocytes Immunocytochemistry

Immunocytochemistry of human astrocytes, as well as image analysis, were performed as previously reported [26–28], with slight modifications. To perform these experiments, cells were cultured and treated as appropriate in 24-well plates with sterile

glass coverslips added to the bottom of plates. Following the same treatment conditions described in the previous section, cells were firstly fixed in 4% of paraformaldehyde solution for 5 min on ice. After that, cells were washed twice with phosphate buffered saline (PBS), then permeabilized with 0.1% Triton™ X-100 in PBS (PBS-T) for 5 min at room temperature. Non-reactive sites were blocked overnight at 4°C using blocking buffer solution (BB; PBS supplemented with 1% of BSA and 0.1% of Triton x-100). Following, cells were incubated overnight at 4°C with primary mouse antibody anti-vimentin (1:800 dilution in BB), used to stain astrocytes cytoskeleton. After incubation with primary antibody, cells were washed twice with both, PBS and PBS-T, and incubated with secondary antibodies anti-mouse Dylight 549 (1:1000 dilution in BB) in the dark, at room temperature for an hour. For nuclear staining, cells were washed three times with PBS and incubated for 20 min, in the dark, with DAPI (1:500 dilution in BB). Cells were washed again with PBS and coverslips were finally mounted on a microscope slide (Clarity C361; Smith Scientific, Edenbridge, UK) with antifade reagent (S36936, ThermoFisher Scientific). Coverslips extremities were sealed with nail varnish and stored at 4°C until imaging. Staining and imaging of astrocytes treated with psychosine, nanoparticles and raw materials were performed in duplicate. Fluorescent imagines were acquired using an Olympus Bx51 upright fluorescent microscope (Olympus, Tokyo, Japan) at 20x resolution. Imagine acquisition settings were kept constant across all treatment and four imagines were taken for each condition to cover the whole coverslip. Image analysis of fluorescence were made using Image J software (ImageJ software version 1.51 (100), 2015, https://imagej.nih.gov/ij/).

2.7 Pro-inflammatory IL-6 Cytokine Release from Human Astrocytes

Primary human astrocytes, cultivated in 24-well plates as previously described, were serum starved overnight and treated with increasing concentrations of *h*TNF-α (10 ng/ml and 100 ng/ml) and 50 ng/ml of *h*IL-17 A, at increasing time points of 2h, 4h and 6h, to determine the stimulus *v*s response on the secretion IL-6 cytokine. In order to investigate the effect of SVT and CoQ10 raw compounds and loaded-nanoparticles on the production and release of the pro-inflammatory cytokine IL-6, human astrocytes were treated with 10 ng/ml of *h*TNF- α and 50ng/ml of *h*IL-17 A alone or supplemented with compounds at 0.1 µM, 1 µM and 10 µM and incubated for 6h at 37°C. Cells supernatant was removed and kept at -20°C until cytokine levels measurement. The amount of cytokine released in the culture media was

measured using an ELISA kit for human IL-6 according to the manufacturer's instructions (R&D Systems).

2.8 Mouse Organotypic Cerebellar Slice Culture

Organotypic slice cultures were isolated from the cerebellum of 10 days (P10) male C57Bl/6J mice in accordance with European guidelines and internal protocols approved by Trinity College Dublin ethical committee. Following previously published protocols [28–31], cerebellar tissues were dissected from P10 mice, following decapitation, and cut into 400 µm thick parasagittal slices using a McIlwain tissue chopper (Champeden Instruments Ltd., Loughborough, England). Individually separated slices were seeded on Milli-cell cell culture inserts (PICMORG50; Merck, Kenilworth, NJ, USA), at least 3 slices per well. Slices were grown using an air-liquid interface method, incubated at 35.5 °C and 5% CO_2 in a humidified incubator. From the day zero to four (D4), cerebellar slices were cultured in serum-based medium: 50% Opti- Mem (Invitrogen), 25% Hanks' buffered salt solution (HBSS) (Gibico®, Thermofisher, Waltham, MA, USA), 25% heat-inactivated horse serum and supplemented with 2 mM Glutamax, 28 mM D-glucose, 100 U/ml penicillin/streptomycin (Sigma) and 25 mM HEPES (Sigma). Next, slices were transferred to a serum free based medium: 98% Neurobasal-A and 2% B-27 (Invitrogen) medium, supplemented with 2 mM Glutamax, 28 mM D-glucose, 100U/ml penicillin/streptomycin and 25mM HEPES, until performing demyelination experiments. At 12 days of culture, cerebellar demyelination was induced with 1 µM of psychosine and/or SVT/CoQ10 raw materials and drug-loaded nanoparticles for 18h. Afterwards, cerebellar slices medium was removed and replaced for fresh medium alone (controls) or supplemented with SVT/CoQ10 raw material and nanoparticles for a further 30 h of continuous treatment.

2.9 Cerebellar Slices Immunocytochemistry

Cerebellar slices were processed for immunocytochemistry staining for MBP (myelin basic protein) and GFAP (glial fibrillary acid protein) following the protocol described by O'Sullivan and co-workers (2018) [26]. Slices were firstly washed twice in PBS and further fixed by incubation with increasing concentrations of paraformaldehyde (PFA, from 1% to 4%, 5 min each), to better preserve slices structure. Following, slices were washed twice with PBS

and incubated overnight with blocking buffer solution (PBS supplemented with 10% of BSA and 0.5% of Triton-X 100). Slices were then incubated for 24h at 4 °C with the primary antibodies (anti-GFAP and anti-MBP, diluted in PBS supplemented with 2% of BSA and 0.1% of Triton-X 100). After primary antibodies removal, slices were washed three times with PBS-T (PBS supplemented with 0.01% of Triton-X 100) and incubated for 2h at room temperature with secondary antibodies (anti-chicken 633 and anti-rabbit 488). Finally, slices were washed again three times with PBS and mounted on glass cover slides with antifade reagent. In this preliminary experiment, 3 slices were grown per condition of a single replication. Fluorescent imagines were acquired using an Olympus Bx51 upright fluorescent microscope (Olympus, Tokyo, Japan) at 10x magnification. Image acquisition settings were maintained constant across treatments. Image analysis of fluorescence were made using Image J software (ImageJ software).

3 Statistics

All graphical data are represented as mean and standard deviation (SD). One-Way ANOVA and Newman-Keuls multiple comparisons post-hoc test was performed to assess significant differences between treatment groups, considering significant at least with $p < 0.01$.

4 Results

4.1 Hybrid Lecithin/Chitosan Nanoparticles Co-Encapsulation of Two Potential Neuro-Protective Compounds

The strategy of administering drugs encapsulated into polymeric nanoparticles has proven, from animal and human studies, to perform statistically better in delivering drugs to the central nervous systems (CNS), in promoting brain-targeting and improving their pharmacological effect [1,32]. In this study, we selected the combination between biocompatible and biodegradables phospholipid (lecithin) and polysaccharide (chitosan) components to obtain nanoparticles suitable for the co-encapsulation of two compounds known for their anti-inflammatory, anti-apoptotic and anti-oxidant properties, i.e., simvastatin and coenzyme Q10 [16,33–36].

Nanoparticles were formed through an emulsification/self-assembly process driven by the electrostatic interaction between oppositely charged components, i.e. negative phospholipids and positive polysaccharide. Colloidal systems were characterized for their hydrodynamic particle diameter, particles size distribution and nanoparticles surface charge. Results reported in Table 1 showed that empty nanoparticles, formulated without the addition of active compounds, presented a particles size around 180 nm, with a narrow particle distribution (PDI 0.09) and a high nanoparticles surface charge of +45 mV. The introduction of simvastatin and CoQ10 into nanoparticles (SVT/CoQ10-LCN) increased the particle diameters (230 nm). However, the homogeneity (PDI 0.108) and stability (surface charge +39 mV) of the nanoemulsion were maintained. Nanoparticles have been also evaluated by their capacity to encapsulate two components in the same system. As presented in Table 1, almost the totality of both SVT (1 mg/ml) and CoQ10 (2 mg/ml), were encapsulated in the nanoparticles. These data showed that simvastatin and CoQ10 have been successfully encapsulated into lecithin/chitosan nanoparticles with desirable features for nasal drug delivery, such as small particles size, high surface charge and high drug content in a monodisperse colloidal system.

Table 1: Simvastatin/Coenzyme Q10-loaded Nanoparticles Physicochemical Properties and Encapsulation Efficiency (n= 6 ± SD)

Formulation	Particle Size (nm)	ζ potential (mV)	PDI	EE (%)
B-LCN	180.2 ± 09.2	+40.21 ± 1.09	0.094 ± 0.009	-
SVT/CoQ10-LCN	234.2 ± 12.2	+36.34 ± 2.87	0.114 ± 0.012	^{CoQ10}99.57 ± 0.97 ^{SVT}98.77 ± 1.20
PSY 20 µM in DEM-F/12	294.5 ± 33.4	-	0.262 ± 0.072	-
LCN 0.02 µl + Psy	733.1 ± 58.3	+3.20 ± 0.87	0.684 ± 0.082	-
LCN 0.2 µl + Psy	1046 ± 60.4	+1.09 ± 0.04	0.321 ± 0.056	-
LCN 2 µl + Psy	1191 ± 30.2	+0.69 ± 0.02	0.218 ± 0.048	-

Abbreviations: ζ potential = zeta potential; PDI = polydispersity index; EE = encapsulation efficiency

4.2 Lecithin/chitosan Nanoparticles Loading Simvastatin and Coenzyme Q10 Organize in a Core-Shell Structure

To understand nanoparticles physico-chemical properties, their interaction with the biological environment and their properties as drugs carrier, it is interesting to investigate nanoparticles structure. The internal structure of SVT/CoQ10-LCN nanoparticles was investigated using the small angle neutron scattering technique (SANS), as previously reported. Briefly, SANS profiles report nanoparticles' scattered radiation intensity as a function of the momentum transfer, *q*, which is correlated to the characteristic scattering distance of supramolecular structures *d,* through the following equation:

Eq. 1. $$d = \frac{4\pi}{q}$$

SANS intensity spectra presented on Figure 1 reveal a core-shell conformation of SVT/CoQ10-LCN nanoparticles, with chitosan covering particles surface. Specifically, fitting the correspondent spectrum (orange line) with standard methods [25,37], it is possible to evidence nanoparticles with defined oil-core of about 180-200 nm surrounded by a multi-

lamellar shell (lecithin bilayers and chitosan) with interlamellar distance around ~5.7 nm, as evidenced by the presence of a structure peak centred around q = 0.1 Å^{-1}.

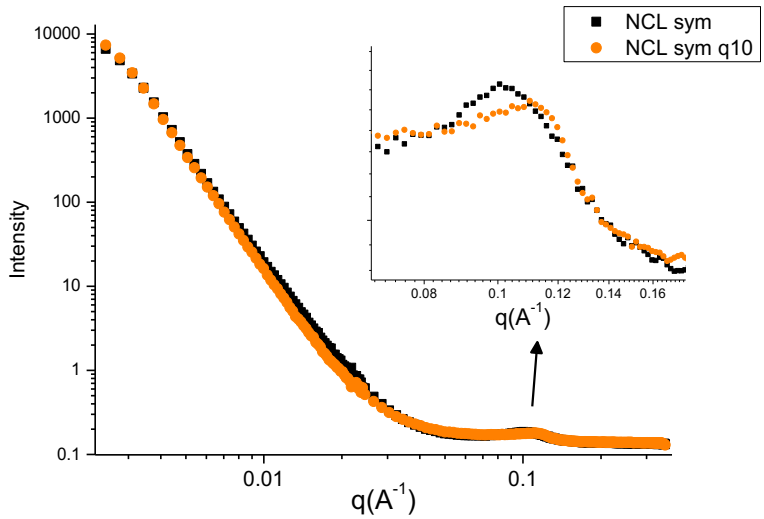

Figure 1: SANS intensity spectra of SVT-LCN (black line) and SVT/CoQ10-LCN (orange line) nanoparticles.

Notes: In the insert, the region of the multilamellar structure peak (around 0.1 Å^{-1}) is enlarged showing an increase in q values for the orange curve, highlighting a decrease in the multilayer's distance after the introduction of the second drug, i.e. coenzyme Q10, into nanoparticles core.

Nanoparticles overall size around 200 nm confirms DLS finds for particles diameter. Interesting, drugs appears to be loaded not only in the oil-core structure, but also in the hydrophobic layers of the shell, reducing the electronic intensity of loaded nanoparticles, compared to empty ones. Thus, suggesting a direct correlation of the drugs loading with the reduction of nanoparticles surface charge.

4.3 SVT-CoQ10-LCN Nanoparticles Cytotoxicity on Astrocytes

It has been reported that statins can affect the proliferation or induce cell death in cancer cells, airway smooth muscle cells and fibroblasts [38–41]. Also, there are in the literature reports expressing concerns on the biocompatibility of cationic nanoparticles [42–44]. To evaluate the effect on human astrocytes viability of all compounds and nanoformulations,

cells were incubated up to 6h with increasing concentrations of simvastatin solution, alone or in combination with CoQ10 and of SVT/CoQ10-loaded nanoparticles. The corresponding amount of empty nanoparticles were used as control and to assess the nanomaterial toxicity. Figure 2(B) reports the cellular viability of human astrocytes after 6h of incubation with increasing concentrations of SVT, SVT-CoQ10 and SVT/CoQ10-loaded nanoparticles. (astrocytes viability was not affected after 2 h and 4 h of incubation, data not shown). It is interesting to observe that empty and loaded nanoparticles did not shown any relevant toxic effect (viability ~ 100%) over all tested concentrations, suggesting that the nanocarrier system is safe for brain delivery.

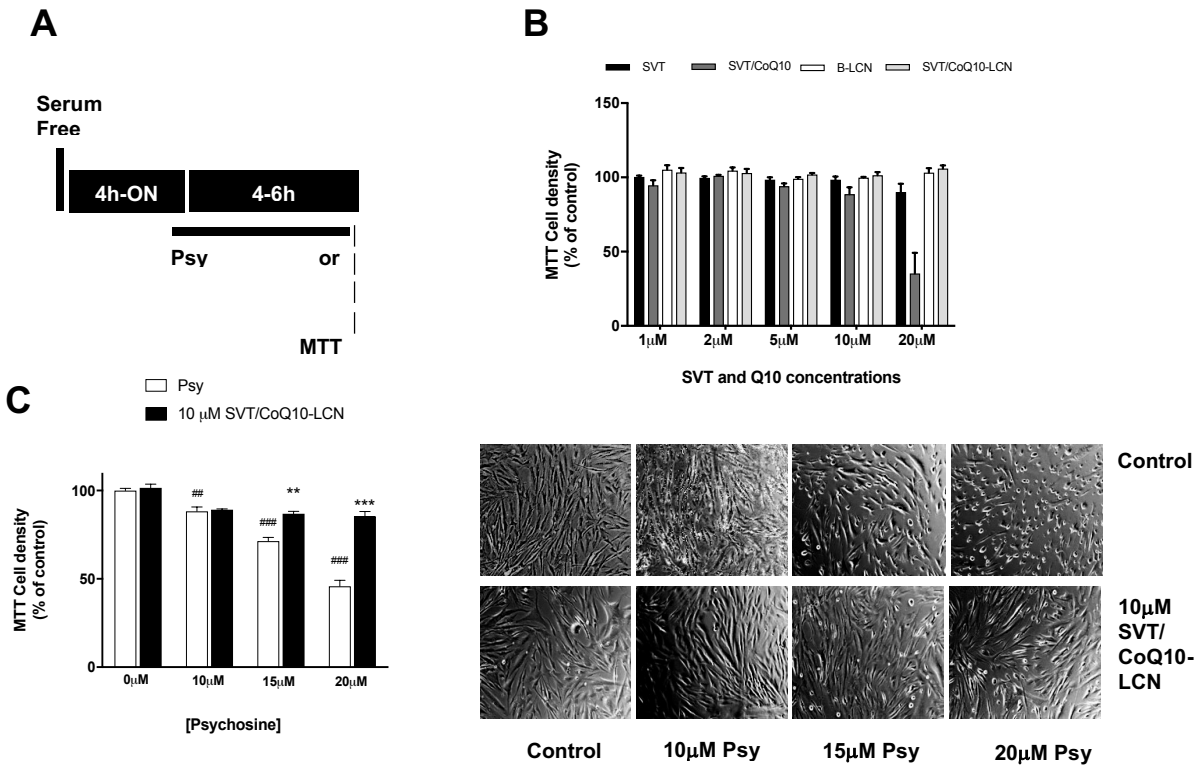

Figure 2: ***Psychosine-induced cell toxicity in a dose-depended manner.*** (A) Experimental diagram for treatments and analysis. (B) Human Astrocytes were seeded at $3.9x10^5$ cell/ml density and treated with unformulated compounds, empty and compounds-loaded nanoparticles for 6h at increasing concentrations for cytotoxicity assay. (C) Cells were treated with increasing concentrations of psychosine at 10μM, 15μM and 20μM for 4h ± 10μM of SVT/CoQ10 nanoparticles. Representative images indicate cell density of each treatment after 4h incubation. Concentration-dependent psychosine-induced cell death is attenuated by SVT/CQ10-LCN nanoparticles at 10μM. $^{###}p < 0.001$ compared to control, $^{***}p < 0.001$ compared with Psy.

While simvastatin raw material did not affect significantly the astrocytes viability even in the highest tested concentration (20 μM), while the combination with CoQ10 reduced human astrocytes number in a dose-dependent manner. In fact, at the maximum concentration (20 μM) of both compounds, astrocytes viability was around 35%. Thus, to avoid any toxic effect, the maximal concentration values used for SVT and CoQ10 in further tests was 10 μM.

4.4 Effect of SVT/CoQ10 Nanoparticles on Psychosine-Induced Human Astrocytes

Psychosine, a galactolipid molecule, is suspected to promote toxicity and cellular death of oligodendrocytes, one of the pathological mechanisms involved in neurological disorders, especially in Krebs's diseases [45–47]. However, previous studies demonstrated also several pathological pathways involving psychosine-induced cellular toxicity in human and mouse astrocytes [26,30,48]. Therefore, the ability of tested compounds and formulation to limit or prevent psychosine-induced cellular damages on astrocytes was investigated.

Human astrocytes were incubated with increasing concentrations of psychosine for 4h. Results confirmed previous findings showing a psychosine concentration-dependent reduction of astrocytes cells viability (10 μM, 88.2 ± 4.9 %; 15 μM, 71.3 ± 4.25 %; 20 μM, 45.7 ± 6.6% relatively to untreated controls). Figure 1(C) highlighted a significant drop in cell viability at 20μM within 4h of experiment. Notably, the simultaneous addition of 10μM of SVT/CoQ10-LCN nanoparticles significantly attenuates psychosine-induced cell death, preserving astrocytes viability to around 90% (Figure 1(C) and Figure 3(D)).

The psychosine-induced reduction of cells viability was also attenuated in the presence of non-encapsulated simvastatin and CoQ10. However, the effect of raw materials was found to be lower compared to the nanoparticles (Figure 3). Interestingly, a synergic effect was observed when combining simvastatin and CoQ10: while simvastatin reduced by 10.35 ± 1.06% (10 μM) the psychosine-induced cell death (Figure 3 (B)), incubation of both compounds increased reduction of psychosine toxicity in a dose-dependent manner (reduction of 10.05 ± 0.88% at 0.1 μM; 18.72 ± 0.6% at 1 μM and 20.46 ± 1.42 at 10 μM) (Figure 3 (C)). Nevertheless, the most significant result in terms of cell survival was obtained when both, SVT and CoQ10 where combined via the co-encapsulation into the nanoparticles. SVT/CoQ10 co-encapsulated into nanoparticles preserved not only the

cellular density (Figure 3 (D)), but also the astrocytes cellular shape against the structural damages caused by psychosine (Figure 3(A)).

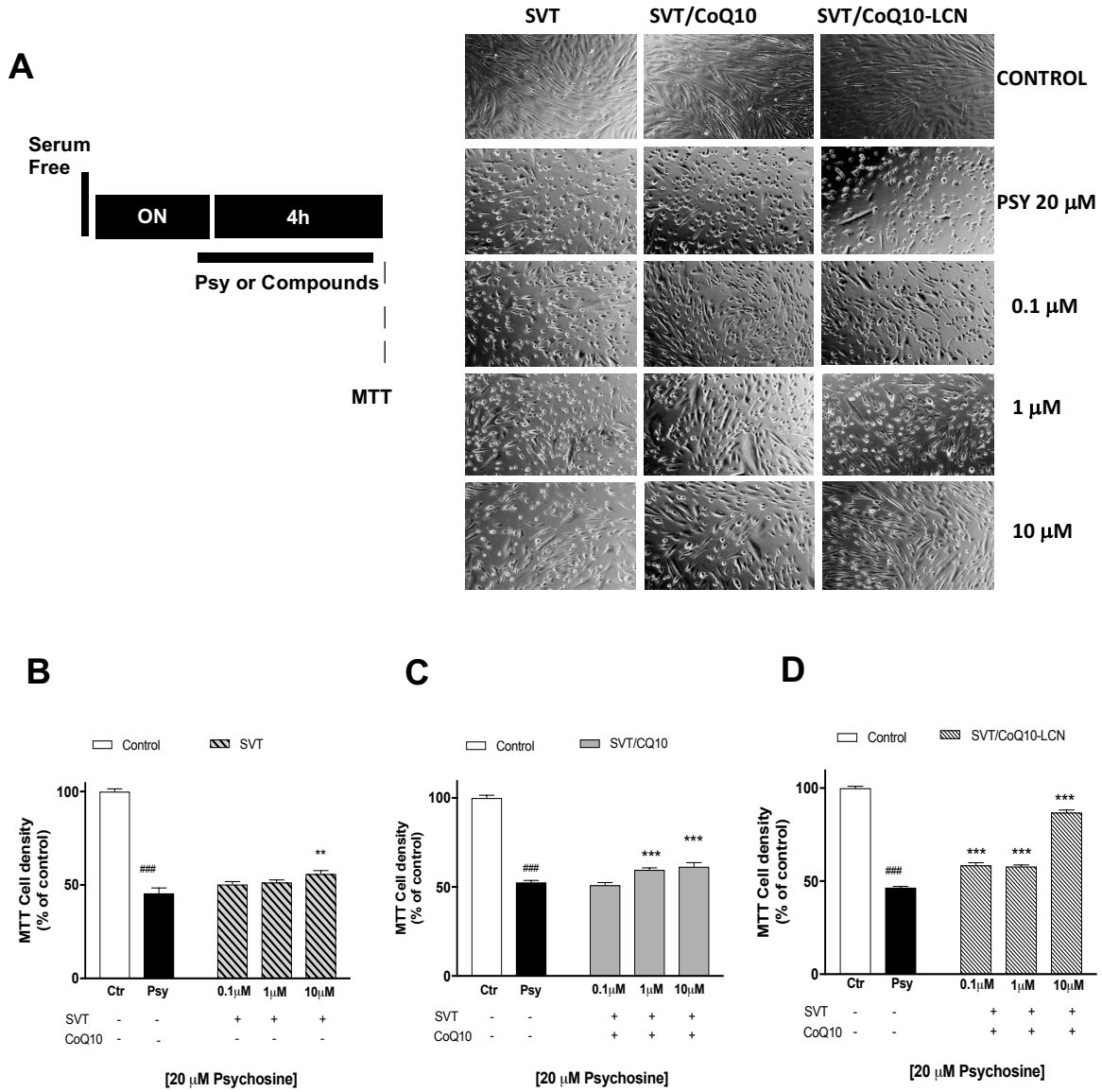

Figure 3: Nanoparticles attenuate psychosine-mediated astrocytes cell death. (A) Experimental diagram for treatments and analysis. Human astrocytes were seeded at $3.9x10^5$ density and treated for 4h with 20μM of psychosine±: simvastatin raw material (B), simvastatin plus CoQ10 raw material (C) and SVT/CoQ10-LCN nanoparticles (D) from 0.1μM to 10 μM. (C). Nanoparticles prevent almost completely the cell death induced by psychosine. Light microscopy images show cell density for each treatment after 4h incubation. Controls (Ctr) are shown as white bars. $^{###}p$, 0.001 compared to control $^{***}p < 0.001$ compared with Psy.

4.5 Study of The Mechanism by Which Nanoparticles Prevent Psychosine-Induced Astrocytes Death

To better understand the mechanism behind the results showing the astrocytes protection against psychosine-induced cell death when treated with SVT/CoQ10-LCN nanoparticles, the performance of blank nanoparticles was also evaluated as well. Astrocytes pre-treated with psychosine (20μM) were incubated for 4h with the correspondent volume of blank nanoparticles. Results showed up an effect for the blank carrier similar to the one obtained with those loaded with SVT and CoQ10 (Figure 4).

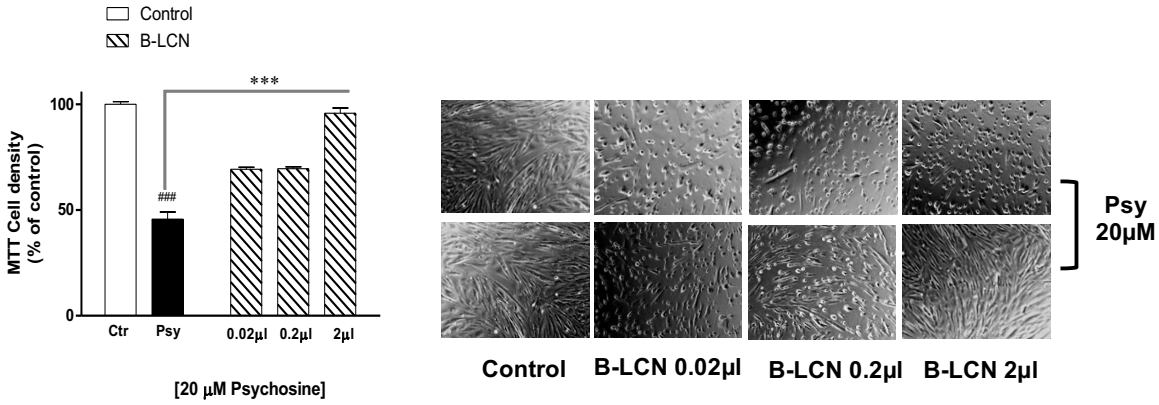

Figure 4: **Nanoparticles structure is involved on the reduction of psychosine-mediated astrocytes cell death.** Human astrocytes were seeded at $3.9x10^5$ density and treated for 4h with 20μM of psychosine ± blank nanoparticles using the same amount of formulation used for experiments with drug-loaded nanoparticles. Blank nanoparticles (B-LCN) prevent astrocytes apoptosis. Representative images showing cell densities after the treatment are presented. Control incubation is shown in white. ***$p < 0.001$ compared with Psy; ###$p < 0.001$ compared with untreated control.

It was than hypothesized that nanoparticles structure could be at the base of the inhibition of psychosine cytotoxicity. As mentioned previously hybrid nanoparticles used in this study are manly composed of lecithin, a natural phospholipid, with their external surface covered by chitosan, a cationic polysaccharide.

To understand the interaction between psychosine and nanoparticles, changes in the physico-chemical properties of nanoparticles in presence of psychosine were investigated using DLS measurements. Table 1 reports average particle diameter, particle size

distribution and zeta potential of lecithin/chitosan nanoparticles dispersed at increasing concentrations in cell culture medium with 20μM of psychosine. psychosine. When psychosine alone at 20μM was dispersed in DEM-F/12 medium, particles with an average diameter around 300 nm where found, with a relatively large particle size distribution (PDI 0.292).

Following, nanoparticles at 0.02 μl, 0.2 μl and 2 μl were dispersed in DME-F/12 serum free containing 20 μM of psychosine, to mimic conditions close to those occurring in the experiments with astrocytes. As shown in Table 1, there is a substantial increase of nanoparticles diameter in the presence of psychosine. Moreover, the increase in particles size is dependent on the number of particles available to interact: while in the smallest nanoparticles concentration the diameter is around 700 nm, in the highest amount the it increased to more than 1000 nm. Also, PDI values variate according to the ratio between nanoparticles and psychosine: increasing the number of particles available for interaction with psychosine, the homogeneity of the dispersion increases (PDI 0.673 with LCN at 0.02 μl; PDI 0.321 with LCN at 0.2 μl; PDI 0.218 with LCN at 2 μl).

Finally, psychosine caused also a reduction of nanoparticles zeta potential reducing the surface charge close to neutral values (+0.3 mV, Table 1). These data suggested that nanoparticles structural interactions with psychosine may represent the key factor for the inhibition of the *in vitro* effects of psychosine on astrocytes.

4.6 Nanoparticles Effects on Psychosine-Induced Changes in Astrocytes Morphology

To confirm the protective effect of nanoparticles on psychosine-induced astrocytes death, we investigated the effect of psychosine on the type III intermediate filament astrocytes marker vimentin. Vimentin marker is involved in the formation of astrocytes cytoskeleton and serves as an important signalling platform in situations linked to cellular stress [48].

Treatment of human astrocytes with psychosine 10μM for 4h induced a light reduction of vimentin expression (fluorescence reduced by 9%) (Figure 5). However, the alteration in number of astrocytes processes was not significant (1.78 ± 0.21 vs 2.14 ± 0.16 from control incubation), confirming MTT finds, where psychosine at 10 μM did not affect cells viability within 4h of incubation. Conversely, fluorescence levels of astrocytes cytoskeleton marker decreased significantly when cells were incubated with 15 μM and 20 μM of psychosine (reduction 68%; and 77%, respectively). Moreover, in both cases, the reduction of the

filament marker was particularly relevant when observing astrocytes processes (15 μM: 0.77 ± 0.06; 20 μM: 0.24 ± 0.08), suggesting an alteration in the cellular cytoskeleton. Once again, SVT/CoQ10-LCN nanoparticles (10 μM) significantly preserve astrocytes from psychosine damages, maintaining the basal levels of the filament marker (fluorescence around 100%) and the number of cellular processes per cell (Psy 20μM: 2.07 ± 0.10).

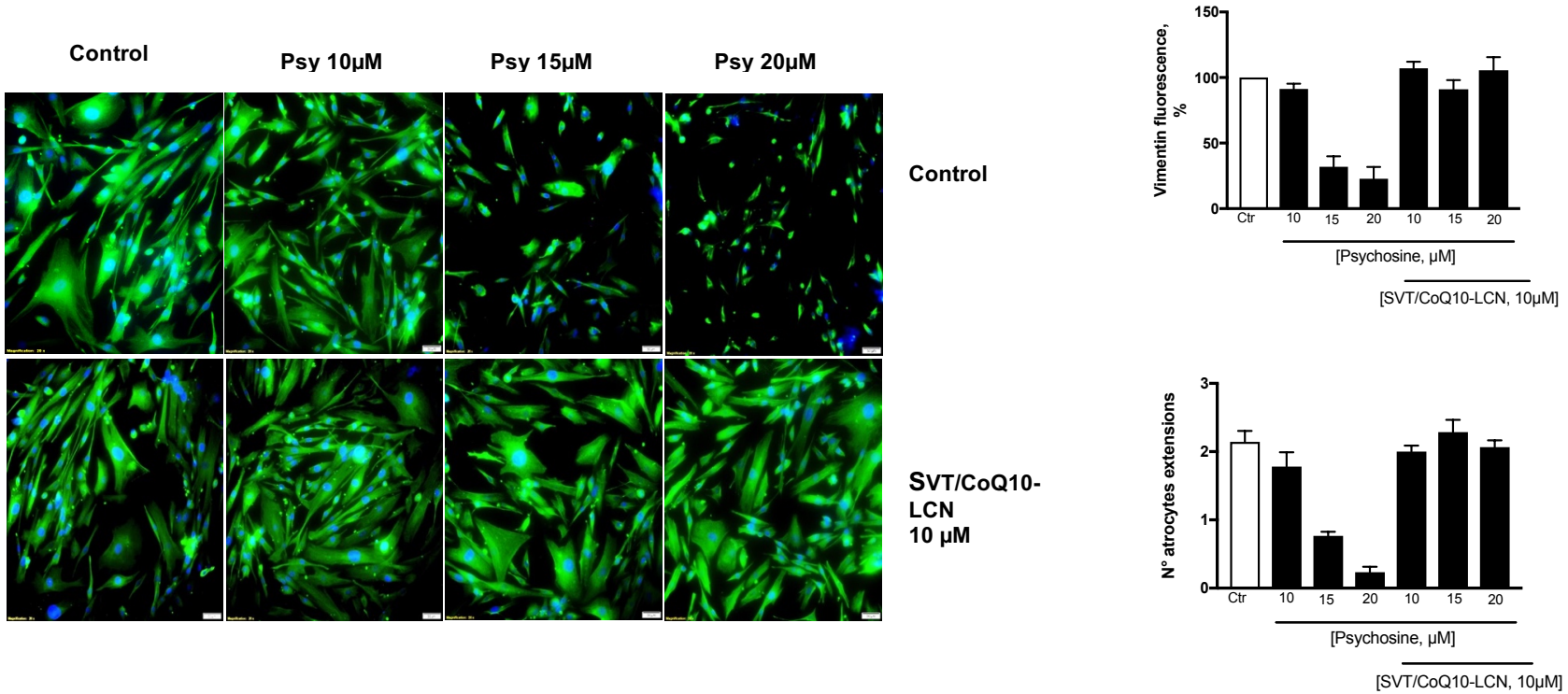

Figure 5: Psychosine-induced changes in vimentin from human astrocytes. Human astrocytes were seeded at $3.9x10^5$ density per well and grown for 36h. Serum preserved cells were treated for 4h with 10 µM, 15 µM and 20 µM of psychosine ± SVT/CoQ10-LCN nanoparticles at 10 µM. Representative fluorescent imagines with a 20x magnification are displaying DAPI (blue) and vimentin (green) under treatment conditions as indicated on the figure. A 50 µM concentric circle from cell nucleus was drawn and the number of astrocytes extensions beyond was counted. 30 cells were counted to each condition. Fluorescence analysis was recorded using ImageJ software and expressed as percentage in a direct comparison to untreated cells control.

To compare free drugs with drug-loaded nanoparticles, cells were incubated for 4h with psychosine (20μM) alone or supplemented with 10μM of SVT/CoQ10 raw material or SVT/CoQ10-nanoparticles (Figure 6). Again, fluorescence levels of vimentin marker decreased significantly in the presence of psychosine (reduced by 62%). While simvastatin co-treatment as free drug was unable to counteract psychosine toxic effect (data not shown), the combination with CoQ10 provided a partial but significant attenuation (vimentin fluorescence: 56% vs 38%; astrocytes processes: 0.60 ± 0.04 vs 1.46 ± 0.08) of the toxic-induced morphology changes. Nevertheless, SVT/CoQ10-loaded nanoparticles provided the best performance in preventing the loss of vimentin fluorescence (102.8 ± 3.1%) and astrocytes processes (Crt: 1.95 ± 0.09 vs 1.96 ± 0.13).

Vimentin staining of astrocytes incubated with the corresponding volume of blank nanoparticles showed results similar to those obtained with drugs-loaded particles (Figure 6). In fact, the fluorescence levels of vimentin were found to be around 98.3 ± 1.8 % and cells presented an average of 2.05 (± 0.11) of astrocytes extensions.

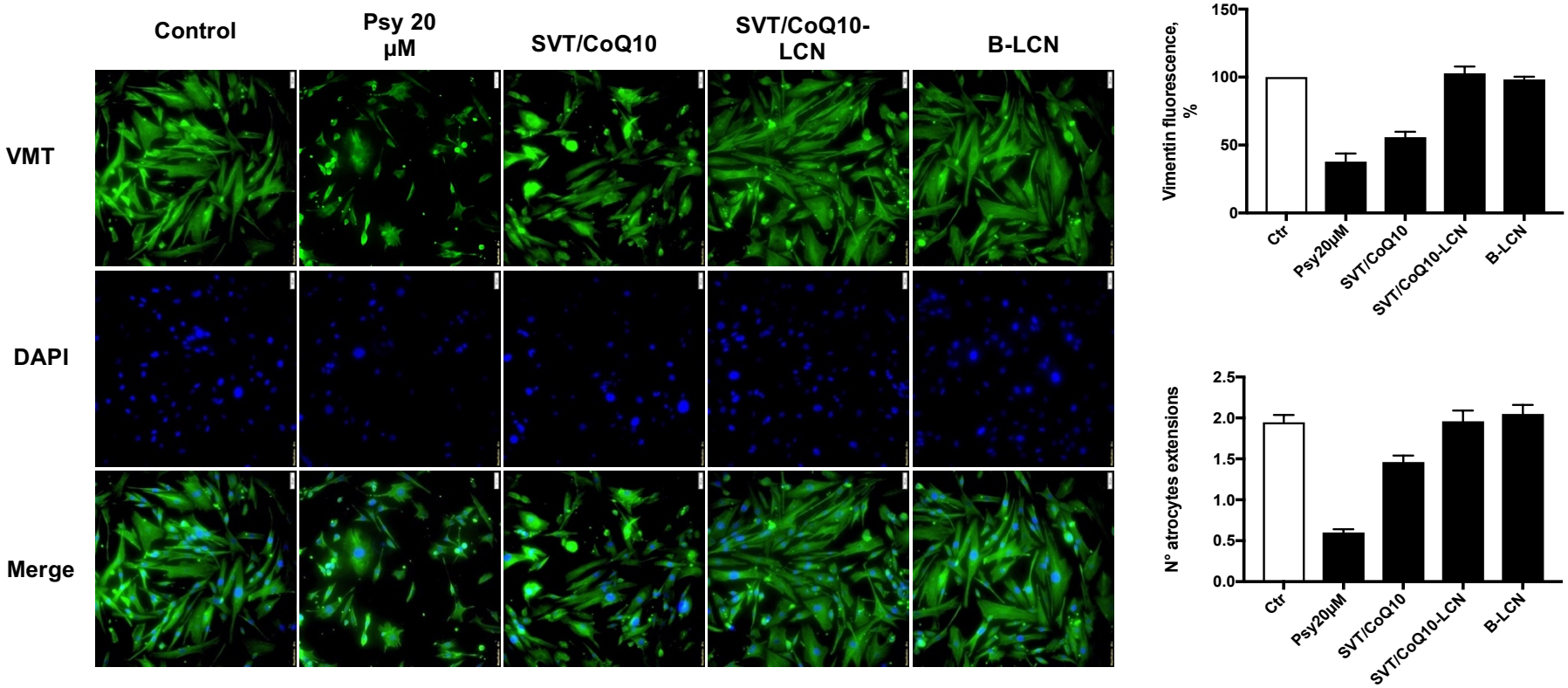

Figure 6: **Psychosine-induced decrease in vimentin marker in human astrocytes is prevented by SVT/CoQ10 nanoparticles**. Human astrocytes were seeded at $3.9x10^5$/ml density and grown for 36h. Serum preserved cells were treated for 4h with 20µM of psychosine ± 10µM SVT/CoQ10 free drugs, SVT/CoQ10-LCN or empty nanoparticles. Representative fluorescent imagines with a 20x magnification are displaying DAPI (blue) and vimentin (VMT, green) under the treatment conditions indicated on the figure. A 50µM concentric circle from cell's nucleus was drawn and the number of astrocytes extensions beyond was counted. 30 cells were counted to each condition. Fluorescence analysis was recorded using ImageJ software and expressed as percentage in a direct comparison to untreated cells control.

These results corroborate with previous finds that pyschosine-induced vimentin loss in astrocytes extensions. Moreover, the protective effect in vimentin fluorescence intensity by loaded and unloaded nanoparticles supports a role of nanoparticles in the prevention of psychosine cytotoxicity.

4.7 Simvastatin and Coenzyme Q10 Attenuate TNF-α/IL-17A-Induced Release of the Pro-Inflammatory Cytokine IL-6 from Astrocytes

To investigate the effect of SVT/CoQ10 free drugs and nanoparticles-loaded in the management of the CNS inflammation, their effect on IL-6 release from astrocytes was investigated. In a previous study, Elain and co-workers demonstrated that the co-stimulation of human astrocytes with TNF-α and IL-17 A cytokines increase the release of IL-6 within 24 hours [27]. The authors showed that human astrocytes express IL17A receptors and consequently, an *in vitro* supplement of IL-17A increases the protein levels of IL-6 in the culture medium of those cells. Moreover, this effect was enhanced in the presence of TNF-α by its induction of IL-8 mRNA over-expression.

Here, we investigated whether the TNF-α/IL-17A-mediate release of IL-6 from astrocytes occurs also in a shorter time of stimulus and if the treatment with drugs nanoformulation affects the IL-6 release. Hence, human astrocytes were treated with 10 ng/ml of TNF-α and 50 ng/ml of Il-17 A, for increasing periods of time, i.e. 2, 4 and 6 hours. As highlighted on Figure 7, stimulation of astrocytes with TNF-α and IL-17 A increased IL-6 release in a time-dependent manner. While at 2h of incubation TNF-α/IL-17A did not increase the levels of IL-6 protein released in the cell culture medium, at 4 hours and 6 hours increasing and significant levels of the cytokine were detected.

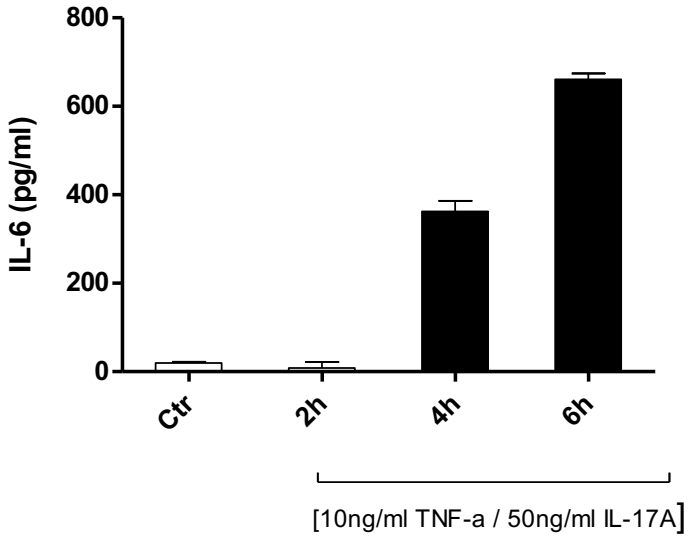

Figure 7: **TNF-α and IL-17 A increases the level of IL-6 secretion in human astrocytes.** Human astrocytes were seeded at $3.9x10^5$ cells/ml and grown for 48h, until confluent. Serum preserved cells were treated with 10 ng/ml of TNF-a and 50 ng/ml of IL-17 A for 2h, 4h and 6h. Graph shows the secretion of IL-6 over time under cytokines stimulus. Control bar represent values of untreated cells incubation. *** $p < 0.001$ compared to control.

To investigate the drugs and nanoparticles effect on the TNF-α/IL-17A-mediate increase in the IL-6 protein levels, human astrocytes were pre-treated for 1 hour simvastatin alone or in combination with CoQ10 or the two compounds co-encapsulated into nanoparticles. Afterwards, cells were co-incubated with the pro-inflammatory cytokines for further 6 hours. Controls incubation, as well as blank nanoparticles, were maintained in the same incubation conditions for all treatments.

Confirming previous findings, treatment of human astrocytes with TNF-α/IL-17A caused an increase in the levels of IL-6 within 6 hours (Figure 8). Importantly, all the treatment conditions significantly suppressed the secretion of IL-6 from astrocytes. Simvastatin drug solution reduced IL-6 secretion by 24% at the smallest drug concentration and by about 45% at 1 μM and 10 μM. In this case, empty nanoparticles did not show any effect and did not affect the release of IL-6 from astrocytes. SVT/CoQ10-LCN nanoparticles reduced TNF-α/IL-17A-induced levels of IL-6 in a concentration-dependent manner, achieving 47% of inhibition. Interesting, the best performance in the inhibition of the TNF-α/IL-17A-induced increase in the protein levels of IL-6 was presented from the association of simvastatin and CoQ10 as drugs solution. In fact, the addition of coenzyme Q10 potentiate

the effect observed for simvastatin alone (2-fold), suppressing almost 60% of IL-6 the release from TNF-α/IL-17A-stimulated astrocytes compared to positive control (Figure 8). These results confirm that both, simvastatin and coenzyme Q10, attenuate the pro-inflammatory signals of TNF-α/IL-17A in human astrocytes, decreasing IL-6 secretion.

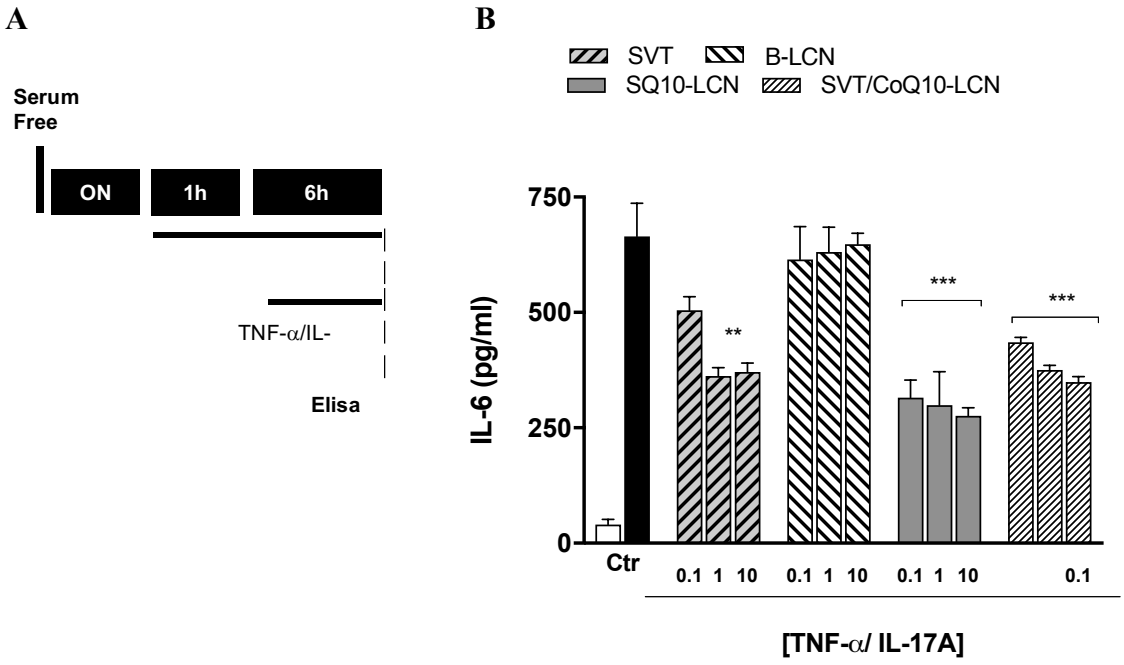

Figure 8: **TNF-α/IL-17-induced IL-6 secretion in human astrocytes is attenuated by unloaded and nanoparticles-loaded compounds**. (A) Experimental treatment diagram (B) Human astrocytes were seeded at $3.9x10^5$ cells/ml and grown for 48h, until confluent. Serum preserved cells were pre-treated with 0.1μM, 1μM and 10μM of SVT, SVT/CoQ10 and SVT/CoQ10-LCN for 1h before treatment with 10 ng/ml of TNF-a and 50 ng/ml of IL-17 for 6h. Treatment of human astrocytes with TNF-α/IL-17A showed an increase of IL-6, that was attenuated by drugs and nanoparticles treatments. $^{**}p < 0.01$ and $^{***}p < 0.001$ compared to control.

4.8 SVT/CoQ10-LCN Nanoparticles Effect on Psychosine-Induced Demyelination in Cerebellar Slices Culture: Preliminary Results

Increasing evidences have suggested the involvement of early demyelination in the establishment of a number of neurodegenerative pathogenesis, such as multiple sclerosis

(MS) [18,21,49], Krabbe's diseases (KD) [19,50] and more recently Alzheimer diseases (AD) [22,51]. Moreover, enhanced brain accumulation of psychosine has been correlated with the dysfunction on oligodendrocytes, the cells responsible for myelin formation, and mediation of demyelination process. To determine whether SVT/CoQ10-loaded nanoparticles are able to protect myelin in a condition of psychosine accumulation, cerebellar slices were exposed to psychosine (1μM) in the presence or absence of nanoparticles (1μM) for 18 hours. Slices were further treated for 30 hours with SVT/CoQ10-LCN nanoparticles or fresh medium as control.

In agreement with previous studies [28,30,48], the exposure of cerebellar slices culture to psychosine induced demyelination, as observed by the reduced expression of myelin basic protein (MBP) (Figure 9). Preliminary results showed that after 18 hours of treatment with psychosine, the fluorescence levels of MBP was significantly decreased in psychosine treated cerebellar slices (39%). It is also possible to note an increase in the protein expression of astrocytes marker glial fibrillary acid protein GFAP, expressed by the increase in fluorescence levels compared to control (155%, Figure 9 C).

Importantly, SVT/CoQ10-LCN nanoparticles (1μM) prevented the psychosine-induced decrease in MPB expression (92% vs 39%, Figure 9) and reduced psychosine activation of GFAP expression (102% vs 155%) on cerebellar slices. As already pointed out, SVT/CoQ10-LCN nanoparticles plays an important role in the inhibition of psychosine effects. These results demonstrate that nanoparticulate systems may have a protective effect on the demyelination processes of cerebellar slices culture.

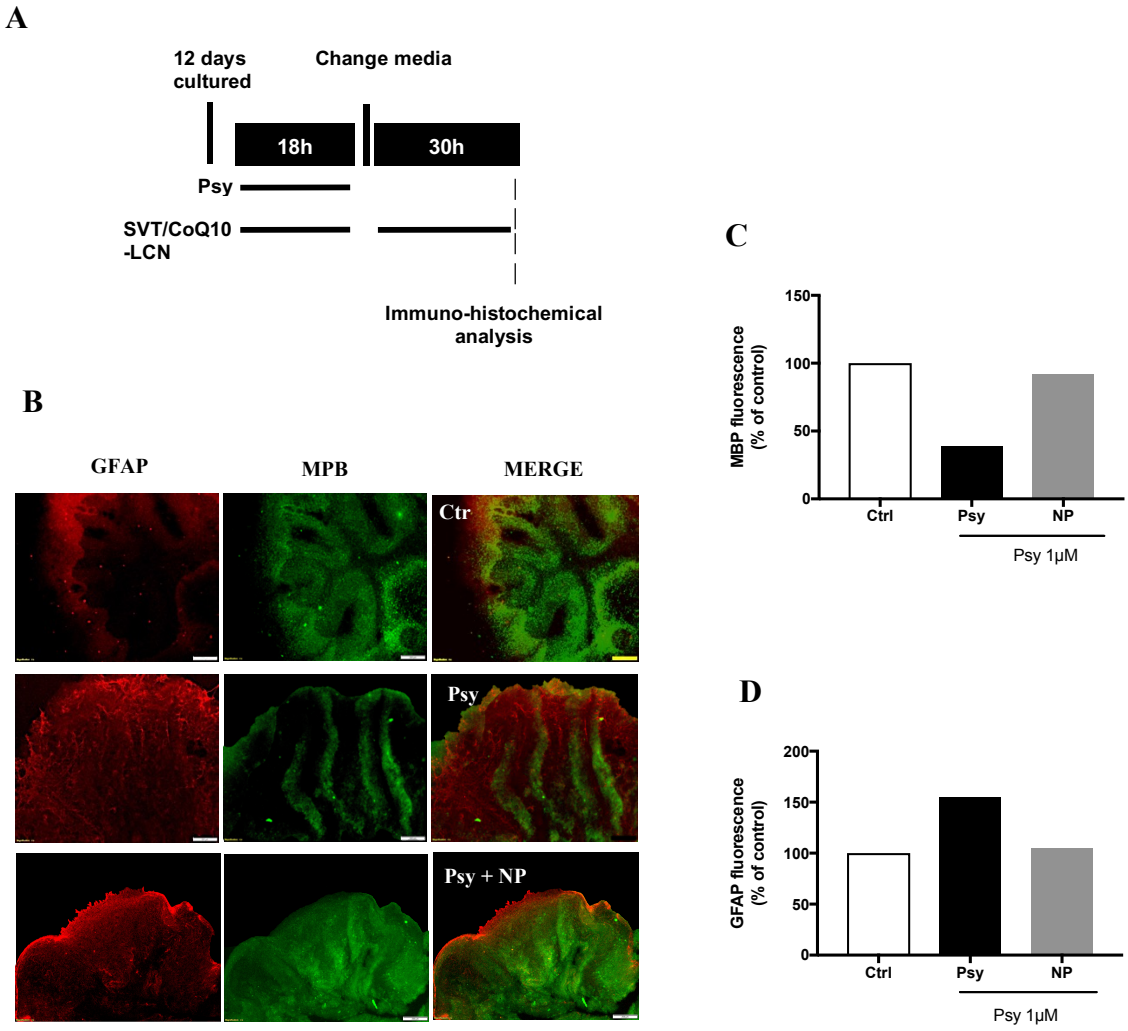

Figure 9: **SVT/CoQ10-LCN nanoparticles inhibits psychosine-induced demyelination on cerebellar slices.** (A) Experimental diagram. (B) Cerebellar cultures immunofluorescently labelled with MBP and GFAP under treatment conditions indicated. Fluorescence images captured at 10x magnification. Bar graph illustrates changes in (C) MBP and (D) GFAP staining after psychosine (1µM) and SVT/CoQ10-LCN (1µM) treatments. Fluorescence analysis was recorded using ImageJ software and expressed as percentage in a direct comparison to untreated cells control.

5 Discussion

Neurodegenerative diseases, such as multiple sclerosis, Alzheimer's and Krabbe disease, require the efficient delivery of drugs to the brain for an efficient treatment. However, such transport is considered one of the most challenging on human body due the impervious nature of the blood brain barrier (BBB), separating the systemic circulation from the CNS parenchyma[1].

It is considered that the association of the nose-to-brain administration route with nanoparticle-based delivery strategies could improve the cerebral bioavailability of many active substances [52,53]. In the past few years, our research group have proposed hybrid nanoparticles composed of natural polysaccharides and phospholipids for the delivery of many therapeutics in various diseases models [24,54–57]. Here, we proposed lecithin/chitosan nanoparticles formed by spontaneous self-assembly of the lipid and polysaccharide components, as an approach for the transport of compounds with potential neuroprotective benefits, exploiting the nose-to-brain delivery route. The main advantage of these nanoparticles is related to their biocompatibility and biodegradability [23,54]. Moreover, increasing evidences of chitosan biological activity leads to believe that this polymer represents a potential bioactive source beyond drugs transportation and targeting [58]. Chitosan biological activities already reported include, among others, antimicrobial [59–61], immunity enhancing, anti-tumour [62], hypocholesterolaemic [63–65] and anti-inflammatory effects [66,67].

In a previous work (addressed on Chapter 2), we have demonstrated the efficient accumulation of this nanoparticles in the brain of rats, following their intranasal administration [23]. This result supported the further investigation and application of this nanoparticle-based formulation for the brain delivery of neuroprotective compounds. Moreover, the possibility to deliver a combined therapy via a single administration sounds rational for neurodegenerative pathologies, whereupon this approach may be required. Simvastatin and coenzyme Q10 were selected as potential neuroprotective model drugs with multiple and complementary pharmacological properties, that could benefit from nanoparticles nose-to-brain delivery [17,34].

Nanoparticles with particles size around 230 nm were successfully obtained and showed an efficient encapsulation of both simvastatin (1 mg/ml) and coenzyme Q10 (2 mg/ml). The capability of nanoparticles to encapsulate both drugs in a stable formulation (PDI < 0.3 and ZP +39 mV ref PZ) suggests an optimal accommodation of the drugs into the hydrophobic part of the nanoparticles. Moreover, positive value of zeta potential indicates the presence of chitosan, a positively charged polymer, on the nanoparticles surface. Indeed,

SANS structural analyses evidenced in a core-shell structure for the nanoparticles produced, with a well-defined oil core containing the drugs, surrounded by a multi-layered shell alternating lecithin and chitosan.

Despite the frequent concern of the scientific community with the cytotoxicity of cationic nanoparticles, in previous studies it has been shown that the hybrid lecithin/chitosan nanoparticles are safe for human nasal (RPMI2650) and macrophage (THP-1) cell lines [23]. Moreover, viability studies carried out in this work on human astrocytes did not evidence any toxic effect for the nanoparticles carrier among overall investigated conditions. This result is significant, since a formulation intendent to target the brain should not represent any potential risk for the CNS health.

Although a toxic effect of simvastatin against astrocytes was found by Marz and co-workers [68], in the present study no significant toxic effect was observed in astrocytes viability within 6h of experiment, as supported also by other studies [39,69]. In fact, statins are potent inhibitor of the HMG-CoA reductase, the rate-limiting enzyme for cholesterol biosynthesis, and the blocking of mevalonate pathway and its metabolites may be involved in glial cells apoptosis [68]. However, it is good to emphasize that this effect was observed in a time and concentration-dependent manner, with high drugs concentrations and prolonged incubation times.

In our case, the cytotoxicity evidenced by the combination of simvastatin with CoQ10 is actually to be ascribed to the precipitation of coenzyme Q10 at high concentrations on cell surface, possibly prompting a mechanical cell damage. Indeed, coenzyme Q10 is almost insoluble in aqueous media [70], such as cell culture medium used for dilutions, and drug precipitate was clearly visible on cells surface starting from 10 μM. On the contrary, no toxic effect was observed when the materials where co-encapsulated into nanoparticles, since nanoparticles increased the apparent aqueous solubility of CoQ10 (~ 2000-fold), avoiding the formation of drug precipitate on the astrocytes surface.

Alterations in astrocytes functions has gained recognition as an important factor contributing to the onset and development of a substantial number of neurological pathologies [71]. As previously mentioned, it has been suggested that astrocytes play an important role in the exacerbation of inflammation in the CNS [27,72]. In addition, results from animal studies report astrocytes involvement in myelin damage pathways, indicating that astrocytes may participate also in the pathogenesis of demyelinating disorders [20,73]. Many studies from the research group of the Professor Dev have shown that psychosine causes dysfunctions in astrocytes cells and how it could be strictly linked with Krabbe diseases pathogenesis [28,30,48].

To support those finds, we investigated the effect of psychosine on astrocyte viability and observed morphological changes through the astrocytes cytoskeleton marker vimentin. In agreement with the current literature, experiments confirmed that psychosine induces astrocytes death in a concentration-dependent manner (Figure 2). Moreover, dysregulation on cell cytoskeleton, observed by the reduction of vimentin from cells processes (Figure 6), may precede psychosine-mediate astrocytes death. The attenuation of psychosine-induced astrocytes death and vimentin loss by obtained using the combination of CoQ10 and simvastatin may involve mitochondrial response (Figure 3(C)). For instance, O'Sullivan and Dev [30] showed that psychosine alters astrocytes mitochondrial function and electron transport, suggesting that psychosine-induced cell death may occurs via apoptosis. Coenzyme Q10, also known as ubiquinone, is present in the mitochondrial respiratory chain as a mobile electron transporter, acting as a powerful antioxidant and preventing oxidative stress damages [74]. An external supplementation of CoQ10 sounds as an effective contrast to psychosine mitochondrial damages.

Interesting, although SVT/CoQ10-LCN nanoparticles prevented psychosine-induced astrocytes vimentin loss and cellular death, a similar result was found also for the blank nanoparticles. Thus, it is possible to assume that nanoparticles structure probably play a role in the inhibition of psychosine action on astrocytes. In a physico-chemical characterization study, it has been reported the formation of spherical structures, like micelles or vesicles (15-23 nm) when psychosine is introduced in aqueous medium at pH 4.5. However, at neutral pH (7.1), the spherical structures change to heterogeneous particle populations ranging from few nm to irregularly shaped rectangular structures with more than 100 nm [75]. Similarly, when psychosine was dispersed in DME-F/12 we found a heterogeneous particle size distribution (PDI ~0.3) with average particle diameter around 300 nm (Table 1). Moreover, in presence of nanoparticles an increase in average particle diameter and decrease of the electrical surface charge was observed, suggesting an adsorption of the sphingolipid on nanoparticles surface. Actually, when investigating the hypocholesterolaemic effect of chitosan, Zhou et al., 2006 demonstrated through FTIR analyses and SEM imagines that chitosan can bind cholesterol molecules by electrostatic adsorption [65]. Thus, it has been hypothesized that the formation of nanoparticles-psychosine aggregates may prevent psychosine to interact with astrocytes membrane and/or permeate the cells by physical sequestration. The formation of those aggregates could involve also the structural hiding of psychosine-amino group, mediator of the galactosylsphigosine toxicity.

We speculate also the possibility of a competition between nanoparticles and psychosine for the astrocytes phospholipase A2 (PLA2). Misslin and co-workers (2017) investigated the effect of psychosine in the activation of PLA2. Psychosine-activation of

PLA2 leads to the formation of arachidonic acid metabolites, involved in inflammation processes, cellular oxidative stress and apoptosis. Activation of PLA2 by psychosine may have a role in astrocytes death [48]. We have demonstrated in previous studies that lecithin, the main component of the nanoparticles presented in this work, is a substrate of PLA2 [54,76,77]. A competitive inhibition of PLA2 by nanoparticles could also be associated with the attenuation of psychosine toxicity. However, this hypothesis must be thoroughly investigated and demonstrated in full.

Recent data pointed out that local brain immune activation has the capacity to facilitate and trigger the pathological physiology modifications in neurodegenerative diseases. In particular, it has been shown that astrocytes play an important role in the management of inflammation in neurodegenerative pathologies [78]. Apparently, astrocytes secrete and respond to a vast array of signalling molecules, producing elevated amounts of chemokines (CCL2 and CXCL1) and cytokines (IL-6, TNF-α and IL-1-b) [27]. Moreover, elevated levels of IL-6 in the serum and cerebrum spinal fluid has been detected in patients suffering from AD and MS diseases and it seems to play the major role in the response of brain injury [79]. In agreement with previous studies [27], data here showed that co-treatment with TNF-α and IL-17A induced a high release of IL-6 from human astrocytes. Simvastatin and coenzyme Q10 compounds could attenuate the TNF-αIL-17A-induced increase in levels of IL-6 in human astrocytes. Beyond the lipid-lowering effect, many pleiotropic effects have been attributed to statins thanks to their inhibition of mevalonic acid pathway and the formation of isoprenoids intermediates [35,80]. In fact, statins modulate inflammatory responses by I) inhibiting signal transduction pathways activating pro-inflammatory transcription factors, such as nuclear factor (NF) κB; II) by activating PPARa receptors and the anti-inflammatory activity; III) and affecting the expression of MHC II histocompatibility complex [81,82]. The anti-inflammatory results are even more relevant in the presence of CoQ10. In addition to the inhibition of ROS formation, CoQ10 anti-inflammatory effects may occurs also via gene expression [16]. Finally, anti-inflammatory activity detected for SVT/CoQ10-LCN nanoparticles is to be attributed to the drug released by nanoparticles or by the direct uptake of nanoparticles by the cells, since empty nanoparticles did not present any effect in the release of IL-6 from astrocytes. As nanoparticles degradation and/or drug release are time dependent, an apparent “reduced effect” is observed in comparison to the free drugs. The synergetic effect of the co-encapsulation of two anti-inflammatory compounds associated to nanoparticles carrier capable to deliver drugs directly from the nose to the brain constitute an innovative and promising strategy in treatment of neurodegenerative diseases.

Profound demyelination and extensively loss in microglia cells represent the major particulars in the prevalence of Krabbe's disease and multiple sclerosis [19,83]. Recently,

several studies have demonstrated also a significant association of Alzheimer's disease pathogenesis and progression with early demyelination and oligodendrocytes dysfunction [22,51,84].

It is widely accepted that supra-physiological levels of psychosine result in profound cerebellar demyelination in Krabbe's disease patients [19,45,47]. Even if the mechanisms involving psychosine demyelination are not completely elucidated, it is now clear that psychosine and glial cells death are strictly connected. Considering that psychosine toxic mechanisms overlap many neurodegenerative diseases common pathological manifestations, cerebellar demyelination induced by psychosine was adopted as a multifocal *ex vivo* model of neurodegeneration. Therefore, in this preliminary study, 10 days old mouse organotypic cerebellar slices were used to investigate the effect of SVT/CoQ10-loaded nanoparticles in the psychosine-induced cerebellar demyelination.

In agreement with the current literature, psychosine induced cerebellar demyelination as expressed by the decrease in oligodendrocytes marker (MBP) fluorescence levels. Treatment of cerebellar slices with nanoparticles prevented the psychosine-induced decrease of MBP (Figure 9(C)), maintaining myelin expression levels close to control values. Turning the attention to astrocytes in the cerebellar slices, psychosine-induced increase in astrocytes marker *Glial Fibrillary Acid Protein*, GFAP. In the injured CNS, astrocytes undergo morphological and functional modifications and activated astrocytes exhibit increase in the expression of the GFAP [85]. Similarly to myeloid cells, astrocytes processes closely surround Aβ amyloid plaques and several studies have shown that reactive astrocytes cells take up and degrade the amyloid peptide [20,71]. We have shown that psychosine-induced astrocytes activation can be attenuated through the addition of SVT/CoQ10-loaded nanoparticles as expressed by the increase in GFAP levels.

Taken together the current finds, the multimodal effects of psychosine on oligodendrocytes and astrocytes cells may induce demyelination in organotypic mouse cerebellar slices. Moreover, the reduction of astrocytes activation by nanoparticles may be an important factor for the protective effect observed in the demyelination of cerebellar slices. Although further studies are still needed, data presented on this preliminary study suggest that brain targeting of lecithin/chitosan nanoparticles loading neuroprotective compounds may be useful in treatment of demyelinating illnesses.

6 Conclusion

Hybrid nanoparticles designed for the co-encapsulation of two models of lipophilic drugs with neuroprotective potential were successfully obtained, with desirable physico-chemical features and efficient drug encapsulation. In this study, for the first time, we demonstrated the protection of nanoparticles formulation against psychosine-induced toxicity on astrocytes and cerebellar slices culture. Coenzyme Q10 association resulted in an amelioration of the anti-apoptotic and anti-inflammatory effects of simvastatin, presenting an interesting strategy to potentiate pharmacological action of neuroprotective compounds. Preliminary *ex vivo* study demonstrated that nanoparticles-loading simvastatin and coenzyme Q10 prevent demyelination induced by psychosine, suggesting that this nanoparticles technology may be useful in a range of demyelinating diseases, such as multiple sclerosis, Alzheimer’s disease and Krabbe's disease.

References

1. Mistry, A., Stolnik, S. & Illum, L. Nanoparticles for direct nose-to-brain delivery of drugs. *International Journal of Pharmaceutics* **379,** 146–157 (2009).

2. Misra, A., Ganesh, S., Shahiwala, A. & Shah, S. P. Drug delivery to the central nervous system: A review. *Journal of Pharmacy and Pharmaceutical Sciences* **6,** 252–273 (2003).

3. Taki, H., Kanazawa, T., Akiyama, F., Takashima, Y. & Okada, H. Intranasal delivery of camptothecin-loaded tat-modified nanomicells for treatment of intracranial brain tumors. *Pharmaceuticals* **5,** 1092–1102 (2012).

4. Giuliani, A. *et al.* In vivo nose-to-brain delivery of the hydrophilic antiviral ribavirin by microparticle agglomerates. *Drug Deliv.* **25,** 376–387 (2018).

5. S., C. *et al.* Effects of Regular and Long-Acting Insulin on Cognition and Alzheimer's Disease Biomarkers: A Pilot Clinical Trial. *J. Alzheimer's Dis.* **57,** 1325–1334 (2017).

6. Piazza, J. *et al.* Haloperidol-loaded intranasally administered lectin functionalized poly(ethylene glycol)-block-poly(D,L)-lactic-co-glycolic acid (PEG-PLGA) nanoparticles for the treatment of schizophrenia. *Eur. J. Pharm. Biopharm.* **87,** 30–39 (2014).

7. Sonvico, F., Zimetti, F., Pohlmann, A. R. & Guterres, S. S. Drug delivery to the brain: how can nanoencapsulated statins be used in the clinic? *Ther. Deliv.* **8,** 625–631 (2017).

8. Saraiva, C. *et al.* Nanoparticle-mediated brain drug delivery: Overcoming blood-brain barrier to treat neurodegenerative diseases. *Journal of Controlled Release* **235,** 34–47 (2016).

9. Grabrucker, A. M. *et al.* Nanoparticle transport across the blood brain barrier. *Tissue Barriers* **4,** (2016).

10. Illum, L. Transport of drugs from the nasal cavity to the central nervous system. *European Journal of Pharmaceutical Sciences* **11,** 1–18 (2000).

11. Sonvico, F. *et al.* Surface-modified nanocarriers for nose-to-brain delivery: From bioadhesion to targeting. *Pharmaceutics* **10,** (2018).

12. Romana, B., Batger, M., Prestidge, C. a, Colombo, G. & Sonvico, F. Expanding The Therapeutic Potential Of Statins By Means Of Nanotechnology Enabled Drug Delivery Systems. *Curr.Top.Med.Chem.* 1182–1193 (2014).

13. Desai, C. S., Martin, S. S. & Blumenthal, R. S. Non-cardiovascular effects associated with statins. *BMJ* **349,** (2014).

14. du Souich, P., Roederer, G. & Dufour, R. Myotoxicity of statins: Mechanism of action. *Pharmacology and Therapeutics* **175,** (2017).

15. Banach, M. *et al.* Effects of coenzyme Q10 on statin-induced myopathy: A meta-analysis of randomized controlled trials. *Mayo Clin. Proc.* **90,** 24–34 (2015).

16. Schmelzer, C. *et al.* Functions of coenzyme Q10 in inflammation and gene expression. *Biofactors* **32,** 179–183 (2008).

17. Beal, M. F. Coenzyme Q10 as a possible treatment for neurodegenerative diseases. *Free Radic. Res.* **36,** 455–460 (2002).

18. Lucchinetti, C. F. *et al.* Inflammatory Cortical Demyelination in Early Multiple Sclerosis. *N. Engl. J. Med.* **365,** 2188–2197 (2011).

19. Suzuki, K. Globoid cell leukodystrophy (Krabbe's disease): Update. *J. Child Neurol.* **18,** 595–603 (2003).

20. Heppner, F. L., Ransohoff, R. M. & Becher, B. Immune attack: The role of inflammation in Alzheimer disease. *Nature Reviews Neuroscience* **16,** 358–372 (2015).

21. Lubetzki, C. & Stankoff, B. Demyelination in multiple sclerosis. *Handb. Clin. Neurol.* **122,** 89–99 (2014).

22. Dong, Y. X. *et al.* Association between Alzheimer's disease pathogenesis and early demyelination and oligodendrocyte dysfunction. *Neural Regen. Res.* **13,** 908–914 (2018).

23. Clementino, A. *et al.* The nasal delivery of nanoencapsulated statins – An approach for brain delivery. *Int. J. Nanomedicine* **11,** 6575–6590 (2016).

24. Clementino, A. & Sonvico, F. Development and validation of a RP-HPLC method for the simultaneous detection and quantification of simvastatin's isoforms and coenzyme Q10 in lecithin/chitosan nanoparticles. *J. Pharm. Biomed. Anal.* **155,** (2018).

25. Di Bari, M. T. *et al.* Dynamics of lipid-saccharide nanoparticles by quasielastic neutron scattering. *Chem. Phys.* **345,** 239–244 (2008).

26. O'Sullivan, S. A., O'Sullivan, C., Healy, L. M., Dev, K. K. & Sheridan, G. K. Sphingosine 1-phosphate receptors regulate TLR4-induced CXCL5 release from astrocytes and microglia. *J. Neurochem.* **144,** 736–747 (2018).

27. Elain, G., Jeanneau, K., Rutkowska, A., Mir, A. K. & Dev, K. K. The selective anti-IL17A monoclonal antibody secukinumab (AIN457) attenuates IL17A-induced levels of IL6 in human astrocytes. *Glia* **62,** 725–735 (2014).

28. O'Sullivan, C., Schubart, A., Mir, A. K. & Dev, K. K. The dual S1PR1/S1PR5 drug BAF312 (Siponimod) attenuates demyelination in organotypic slice cultures. *J. Neuroinflammation* **13,** (2016).

29. O'Sullivan, S. A. & Dev, K. K. The chemokine fractalkine (CX3CL1) attenuates H2O2-induced demyelination in cerebellar slices. *J. Neuroinflammation* **14,** (2017).

30. O'Sullivan, C. & Dev, K. K. Galactosylsphingosine (psychosine)-induced demyelination is attenuated by sphingosine 1-phosphate signalling. *J. Cell Sci.* **128,** 3878–3887 (2015).

31. Sheridan, G. K. & Dev, K. K. S1P1 receptor subtype inhibits demyelination and regulates chemokine release in cerebellar slice cultures. *Glia* **60,** 382–392 (2012).

32. Zhang, Q. Z. *et al.* The brain targeting efficiency following nasally applied MPEG-PLA nanoparticles in rats. *J. Drug Target.* **14,** 281–290 (2006).

33. Mantuano, E. *et al.* Simvastatin and fluvastatin reduce interleukin-6 and interleukin-8 lipopolysaccharide (LPS) stimulated production by isolated human monocytes from chronic kidney disease patients. *Biomed. Pharmacother.* **61,** 360–365 (2007).

34. Wang, Q. *et al.* Statins: Multiple neuroprotective mechanisms in neurodegenerative diseases. *Experimental Neurology* **230,** 27–34 (2011).

35. Paoletti, R., Bolego, C. & Cignarella, A. Lipid and non-lipid effects of statins. *Handb. Exp. Pharmacol.* **170,** 365–388 (2005).

36. Yang, X., Dai, G., Li, G. & Yang, E. S. Coenzyme Q10 reduces beta-amyloid plaque in an APP/PS1 transgenic mouse model of Alzheimer's disease. *J. Mol. Neurosci.* **41,** 110–3 (2010).

37. Gerelli, Y. *et al.* Structure and organization of phospholipid/polysaccharide nanoparticles. *J. Phys. Condens. Matter* **20,** (2008).

38. Ghavami, S. *et al.* Statin-triggered cell death in primary human lung mesenchymal cells involves p53-PUMA and release of Smac and Omi but not cytochrome c. *Biochim. Biophys. Acta - Mol. Cell Res.* **1803,** 452–467 (2010).

39. Kim, M. L., Sung, K. R., Shin, J. A., Young Yoon, J. & Jang, J. Statins reduce TGF-beta2-modulation of the extracellular matrix in cultured astrocytes of the human optic nerve head. *Exp. Eye Res.* **164,** 55–63 (2017).

40. Gopalan, A., Yu, W., Sanders, B. G. & Kline, K. Simvastatin inhibition of mevalonate pathway induces apoptosis in human breast cancer cells via activation of JNK/CHOP/DR5 signaling pathway. *Cancer Lett.* **329,** 9–16 (2013).

41. Hongtau Wu,, Hao Jiang, Dunyue Lu, Ye Xiong, C. & Qu, Dong Zhao, Asim Mahmood, and M. C. Effect of Simvastatin on Glioma Cell Proliferation, Migration and Apoptosis. *Neurosurgery* **65,** 1087–1097 (2009).

42. Loh, J. W., Yeoh, G., Saunders, M. & Lim, L.-Y. Uptake and cytotoxicity of chitosan nanoparticles in human liver cells. *Toxicol. Appl. Pharmacol.* **249,** 148–157 (2010).

43. Mukherjee, S. P., Lyng, F. M., Garcia, A., Davoren, M. & Byrne, H. J. Mechanistic studies of in vitro cytotoxicity of poly(amidoamine) dendrimers in mammalian cells. *Toxicol. Appl. Pharmacol.* **248,** 259–268 (2010).

44. Fröhlich, E. The role of surface charge in cellular uptake and cytotoxicity of medical nanoparticles. *International Journal of Nanomedicine* **7,** 5577–5591 (2012).

45. Won, J. S., Kim, J., Paintlia, M. K., Singh, I. & Singh, A. K. Role of endogenous psychosine accumulation in oligodendrocyte differentiation and survival: Implication for Krabbe disease. *Brain Res.* **1508,** 44–52 (2013).

46. Giri, S., Khan, M., Nath, N., Singh, I. & Singh, A. K. The role of AMPK in psychosine mediated effects on oligodendrocytes and astrocytes: Implication for Krabbe disease. *J. Neurochem.* **105,** 1820–1833 (2008).

47. Giri, S., Khan, M., Rattan, R., Singh, I. & Singh, A. K. Krabbe disease: psychosine-mediated activation of phospholipase A2 in oligodendrocyte cell death. *J. Lipid Res.* **47,** 1478–1492 (2006).

48. Misslin, C., Velasco-Estevez, M., Albert, M., O'Sullivan, S. A. & Dev, K. K. Phospholipase A2 is involved in galactosylsphingosine-induced astrocyte toxicity, neuronal damage and demyelination. *PLoS One* **12,** (2017).

49. Bø, L., Vedeler, C. A., Nyland, H. I., Trapp, B. D. & Mørk, S. J. Subpial demyelination in the cerebral cortex of multiple sclerosis patients. *J. Neuropathol. Exp. Neurol.* **62,** 723–732 (2003).

50. K.K., D. The role of S1P receptors in myelination state. *Glia* **59,** S136 (2011).

51. Carmeli, C. *et al.* Demyelination in Mild Cognitive Impairment Suggests Progression Path to Alzheimer's Disease. *PLoS One* **8,** (2013).

52. Illum, L. Nasal drug delivery - Possibilities, problems and solutions. *J. Control. Release* **87,** 187–198 (2003).

53. Illum, L. Nasal drug delivery: New developments and strategies. *Drug Discov. Today* **7,** 1184–1189 (2002).

54. Barbieri, S. *et al.* Lecithin/chitosan controlled release nanopreparations of tamoxifen citrate: Loading, enzyme-trigger release and cell uptake. *J. Control. Release* **167,** 276–283 (2013).

55. Pereira, G. G. *et al.* Hyaluronate nanoparticles included in polymer films for the prolonged release of vitamin E for the management of skin wounds. *Eur. J. Pharm. Sci.* **83,** 203–211 (2016).

56. Sonvico, F. *et al.* Formation of self-organized nanoparticles by lecithin/chitosan ionic interaction. *Int. J. Pharm.* **324,** 67–73 (2006).

57. Şenyiğit, T. *et al.* In vivo assessment of clobetasol propionate-loaded lecithin-chitosan nanoparticles for skin delivery. *Int. J. Mol. Sci.* **18,** (2017).

58. Xia, W., Liu, P., Zhang, J. & Chen, J. Biological activities of chitosan and chitooligosaccharides. *Food Hydrocoll.* **25,** 170–179 (2011).

59. No, H. K., Young Park, N., Ho Lee, S. & Meyers, S. P. Antibacterial activity of chitosans and chitosan oligomers with different molecular weights. *Int. J. Food Microbiol.* **74,** 65–72 (2002).

60. Zhong, Z. *et al.* Synthesis of acyl thiourea derivatives of chitosan and their antimicrobial activities in vitro. *Carbohydr. Res.* **343,** 566–570 (2008).

61. Hernández-Lauzardo, A. N. *et al.* Antifungal effects of chitosan with different molecular weights on in vitro development of Rhizopus stolonifer (Ehrenb.:Fr.) Vuill. *Carbohydr. Polym.* **73,** 541–547 (2008).

62. Azuma, K., Osaki, T., Minami, S. & Okamoto, Y. Anticancer and Anti-Inflammatory Properties of Chitin and Chitosan Oligosaccharides. *J. Funct. Biomater.* **6,** 33–49 (2015).

63. Liu, J., Zhang, J. & Xia, W. Hypocholesterolaemic effects of different chitosan samples in vitro and in vivo. *Food Chem.* **107,** 419–425 (2008).

64. Cho, Y. I., No, H. K. & Meyers, S. P. Physicochemical Characteristics and Functional Properties of Various Commercial Chitin and Chitosan Products. *J. Agric. Food Chem.* **46,**

3839–3843 (1998).

65. Zhou, K., Xia, W., Zhang, C. & (Lucy) Yu, L. In vitro binding of bile acids and triglycerides by selected chitosan preparations and their physico-chemical properties. *LWT - Food Sci. Technol.* **39,** 1087–1092 (2006).

66. Bruyere, O. & Reginster, J.-Y. Glucosamine and Chondroitin Sulfate as Therapeutic Agents for Knee and Hip. *Drugs and Aging* **24,** 573–580 (2007).

67. Bruyere, O. *et al.* Glucosamine sulfate reduces osteoarthritis progression in postmenopausal women with knee osteoarthritis: Evidence from two 3-year studies. *Menopause* **11,** 138–143 (2004).

68. März, P., Otten, U. & Miserez, A. R. Statins induce differentiation and cell death in neurons and astroglia. *Glia* **55,** 1–12 (2007).

69. Dong, W., Vuletic, S. & Albers, J. J. Differential effects of simvastatin and pravastatin on expression of Alzheimer's disease-related genes in human astrocytes and neuronal cells. *J. Lipid Res.* **50,** 2095–2102 (2009).

70. Nepal, P. R., Han, H. K. & Choi, H. K. Enhancement of solubility and dissolution of Coenzyme Q10 using solid dispersion formulation. *Int. J. Pharm.* **383,** 147–153 (2010).

71. Claycomb, K. I., Johnson, K. M., Winokur, P. N., Sacino, A. V. & Crocker, S. J. Astrocyte regulation of CNS inflammation and remyelination. *Brain Sciences* **3,** 1109–1127 (2013).

72. Sharma, R. *et al.* Inflammation induced by innate immunity in the central nervous system leads to primary astrocyte dysfunction followed by demyelination. *Acta Neuropathol.* **120,** 223–236 (2010).

73. Kondo, Y., Wenger, D. A., Gallo, V. & Duncan, I. D. Galactocerebrosidase-deficient oligodendrocytes maintain stable central myelin by exogenous replacement of the missing enzyme in mice. *Proc. Natl. Acad. Sci. U. S. A.* **102,** 18670–5 (2005).

74. Potgieter, M., Pretorius, E. & Pepper, M. S. Primary and secondary coenzyme Q10 deficiency: The role of therapeutic supplementation. *Nutrition Reviews* **71,** (2013).

75. Orfi, L., Larive, C. K. & LeVine, S. M. Physicochemical characterization of psychosine by 1H nuclear magnetic resonance and electron microscopy. *Lipids* **32,** 1035–40 (1997).

76. Barbieri, S. *et al.* Ex vivo permeation of tamoxifen and its 4-OH metabolite through rat intestine from lecithin/chitosan nanoparticles. *Int. J. Pharm.* **491,** 99–104 (2015).

77. Clementino, A., Pozzoli, M., Botti, E. & Sonvico, F. Lecithin / Chitosan-based Nanoparticles for the Nasal Delivery of Statins : Enzyme-Trigger Controlled Release and Cellular Transport. *Rdd 2018* 589–594 (2018).

78. Hennessy, E., Griffin, E. W. & Cunningham, C. Astrocytes Are Primed by Chronic Neurodegeneration to Produce Exaggerated Chemokine and Cell Infiltration Responses to Acute Stimulation with the Cytokines IL-1 and TNF- . *J. Neurosci.* **35,** 8411–8422 (2015).

79. Erta, M., Quintana, A. & Hidalgo, J. Interleukin-6, a major cytokine in the central nervous system. *International Journal of Biological Sciences* **8,** 1254–1266 (2012).

80. Bedi, O., Dhawan, V., Sharma, P. L. & Kumar, P. Pleiotropic effects of statins: new therapeutic targets in drug design. *Naunyn. Schmiedebergs. Arch. Pharmacol.* **389,** 695–712 (2016).

81. Paumelle, R. *et al.* Acute antiinflammatory properties of statins involve peroxisome proliferator-activated receptor-alpha via inhibition of the protein kinase C signaling pathway. *Circ. Res.* **98,** 361–9 (2006).

82. McFarland, A. J. *et al.* Molecular mechanisms underlying the effects of statins in the central nervous system. *International Journal of Molecular Sciences* **15,** 20607–20637 (2014).

83. Kutzelnigg, A. *et al.* Cortical demyelination and diffuse white matter injury in multiple sclerosis. *Brain* **128,** 2705–2712 (2005).

84. Fornari, E., Maeder, P., Meuli, R., Ghika, J. & Knyazeva, M. G. Demyelination of superficial white matter in early Alzheimer's disease: A magnetization transfer imaging study. *Neurobiol. Aging* **33,** (2012).

85. Liu, Z. *et al.* Beneficial effects of gfap/vimentin reactive astrocytes for axonal remodeling and motor behavioral recovery in mice after stroke. *Glia* **62,** 2022–2033 (2014).

GENERAL CONCLUSION

The overall aim of this thesis was to demonstrate the potential of nanoparticles in exploiting the nose-to-brain route to deliver drugs therapeutically relevant for the treatment of neurodegenerative diseases.

The principal strategy adopted was the design of hybrid nanoparticles composed of natural, biocompatible and biodegradable phospholipids and polysaccharides able to encapsulate lipophilic drugs. Exploiting the electrostatic interactions between negative charges of lecithin with the positively charged chitosan, nanoparticles were formed in a dependable and robust self-assembly process liable to scale up.

Several formulations have been produced to optimize the encapsulation efficient of simvastatin, a lipophilic statin, using different pharmaceutical-grade oils to compose nanoparticle oil-core. The optimized nanoparticles formulation, i.e., the one with glycerol monolinoleate and medium chain triglyceride forming their oil-core, presents several features helpful for the nasal delivery of lipophilic drugs like simvastatin. Among nanoparticles desirable physico-chemical properties are small particles diameter, narrow particle size distribution, high positive surface charge and high drug encapsulation efficiency. Moreover, nanoparticles encapsulating simvastatin were physically and chemically stable for over 3 months of storage at room temperature.

Regarding to nanoparticles structure, hybrid lecithin/chitosan nanoparticles can be defined self-assembled multilayered emulsosomes, with a well-defined oil core surrounded by stratified layers alternating the lipid and the polysaccharide components, with chitosan covering nanoparticles surface.

Optimized hybrid lecithin/chitosan nanoparticles loading simvastatin were characterized in terms of nanoparticles interaction with an *in vitro* nasal mucus model containing physiologic antibacterial enzymes to simulate closely the intranasal conditions. We verified that the mucus can imprison nanoparticles in the mucins network and delays drug release. Notwithstanding, the presence of the physiological enzymes improves drug release by disassembling nanoparticles structure and increasing simvastatin availability.

Nanoparticles effects as enhancing drug permeation carrier was evaluated across two different models of nasal mucosa based on cultured human nasal epithelial RPMI2650 cells and the mucosal epithelium excised from the nose of rabbits. It has been proven that simvastatin as a suspension is not able to permeate the nasal epithelium in significant quantities. Nanoparticles instead, enable simvastatin permeation across both the cell monolayer and the intact nasal tissue.

Preliminary *in vivo* experiments of biodistribution using γ-scintigraphy highlighted that the proposed formulation presents the potential to improve brain accumulation of lipophilic drugs formulated in hybrid lecithin/chitosan nanoparticles.

Finally, nanoparticles co-encapsulating two potential neuroprotective compounds, i.e., simvastatin and coenzyme Q10, have been studied for their pharmacological activity in a multifactorial model of neurodegeneration. Preliminary data acquired in a demyelination model of cerebellar mice slices suggested that hybrid nanoparticles may be useful for a range of demyelinating neurodegenerative diseases. Moreover, coenzyme Q10 association resulted in an amelioration of pleiotropic effects of statins in the contention of brain cellular inflammation and death in an apoptotic and pro-inflammatory model of neurodegeneration using astrocytes cells.

Concluding, hybrid lecithin/chitosan nanoparticles represent a novel, safe and promising strategy to guarantee drugs access to the cerebral parenchyma, exploiting an easy and non-invasive administering route, aiming the innovative treatment of several neurodegenerative diseases.